# Role of PARP-1 in Colitis-associated Colorectal Cancer Induced by Alkylating *N*-nitroso compounds

Dissertation
zur Erlangung des Grades
"Doktor der Naturwissenschaften"

am Fachbereich Biologie
der Johannes Gutenberg-Universität
in Mainz

vorgelegt von
**Bastian Dörsam**
geb. in Weinheim

Mainz, 2016

Dekan: [redacted]

1. Berichterstatter: [redacted]

2. Berichterstatter: [redacted]

Tag der mündlichen Prüfung: 18.05.2017[1]

[1] Die vorliegende Arbeit wurde in der Zeit von April 2013 bis November 201 am Institut für Toxikologie der Universitätsmedizin Mainz angefertigt und am Fachbereich Biologie der Johannes Gutenberg Universität (D77) eingereicht.

# CONTRIBUTIONS

Animals experiments were performed under the supervision of Bastian Dörsam. [redacted] supported the execution of important steps including anaesthesia, colonoscopy and necropsy.

**Chapters 4.2 and 4.4.1:** Mini endoscopy and evaluation of mucosal inflammation was kindly performed [redacted]

**Chapter 4.3.1:** Determination of PAR levels in mouse colon tissue was performed in the lab of [redacted]

**Chapter 4.3.2:** [redacted] executed the alkaline comet assay with isolated liver cells.

**Chapter 4.3.3:** [redacted] performed the γH2X western blot analysis of WT colon and liver tissue [redacted]

**Chapter 4.3.4:** Analysis of $O^6$-MeG levels in WT colon tissue was [redacted] responsible for assessment of MGMT activity in snap frozen colon and liver tissue. The WT data was recently published by our group (Fahrer *et al.* 2015).

**Chapter 4.4.3.4:** The qPCR from isolated mouse colon cDNA was performed [redacted]

# ZUSAMMENFASSUNG

Das Enzym Poly(ADP-ribose)-Polymerase-1 (PARP-1) katalysiert die Synthese von Poly(ADP-ribose) und ist darüber hinaus an einer Vielzahl zellulärer Prozesse wie Remodellierung des Chromatins und DNA-Reparatur beteiligt. PARP-1 fördert die Basenexzisionsreparatur, einen evolutionär konservierten DNA-Reparaturmechanismus, der Basenmodifikationen wie Alkylierungen entfernt. DNA-Alkylierungen können durch *N*-Nitrosoverbindungen (NOCs) hervorgerufen werden, die dafür bekannt sind, Darmkrebs zu verursachen. Es ist beschrieben, dass PARP-1-defiziente Mäuse empfindlich gegenüber den toxischen Wirkungen von NOCs sind.

In dieser Arbeit wurde die Rolle von PARP-1 in der entzündungsvermittelten Darmkrebsentstehung nach Induktion mit NOCs untersucht. Hierzu wurden PARP-1-profiziente (PARP-$1^{+/+}$) und PARP-1-defiziente (PARP-$1^{-/-}$) Mäuse zuerst mit dem kolonotrop Tumorinitiator Azoxymethan (AOM) und danach mit der kolitisauslösenden Substanz Dextran-Natriumsulfat (DSS) behandelt. Die Tumorentstehung wurde mittels nichtinvasiver Miniendoskopie überprüft. PARP-$1^{+/+}$ Mäuse zeigten in Abhängigkeit von der AOM-Dosis eine signifikant erhöhte Tumoranzahl und Tumorscore im Vergleich zu PARP-$1^{-/-}$ Tieren. Ausgehend von diesem Befund wurde im Folgenden die DNA-Schadensinduktion untersucht.

Die Analyse der durch AOM ausgelösten initialen DNA-Schäden in beiden Genotypen zeigte eine höhere Anzahl an DNA-Strangbrüchen in den PARP-1-defizienten Tieren, wohingegen das Niveau der *O*$^6$-Methylguanin (*O*$^6$-MeG) DNA-Addukte in beiden Stämmen vergleichbar war. *O*$^6$-MeG ist die Läsion, die hauptsächlich für die Entstehung von durch NOCs ausgelöstem Dickdarmkrebs verantwortlich ist. In Übereinstimmung damit kam es zu einer Depletion der Aktivität der *O*$^6$-Methylguanin-DNA-Methyltransferase (MGMT), die für die Reparatur von *O*$^6$-MeG DNA-Addukten verantwortlich ist, in Leber- und Kolongewebe von WT und PARP-1-defizienten Tieren. Außerdem konnten weder Unterschiede in der basalen Proliferationsrate noch Zelltodinduktion durch AOM im Kolongewebe beider Mausstämme festgestellt werden.

Da PARP-1 ein wichtiger Coregulator des entzündungsfördernden Transkriptionsfaktors *nuclear factor 'kappa-light-chain-enhancer' of activated B-cells* (NF-κB) ist, wurde die durch DSS ausgelöste Kolitis mittels Miniendoskopie beurteilt. PARP-$1^{+/+}$ Mäuse zeigten eine signifikant stärker ausgeprägte Dickdarmentzündung als PARP-$1^{-/-}$ Mause nach Behandlung mit AOM/DSS, die mit einer stärkeren Induktion der NF-κB-induzierten Cyclooxygenase-2 (COX-2) einherging. Mittels Immunhistochemie und konfokaler Mikroskopie wurde eine deutlich reduzierte Anzahl an Makrophagen und Monozyten im Kolongewebe der PARP-$1^{-/-}$ Tiere festgestellt. Dementsprechend konnte eine signifikant verringerte Expression des Zytokins *high mobility group box 1* (HMBG1), was in engem Zusammenhang mit Entzündungsprozessen steht, im Kolon von PARP-1-defizienten Mäusen beobachtet werden. Die Anzahl der *cluster of differentiation 3* (CD3)-positiven T-Zellen, die ein wesentlicher Bestandteil der spezifischen Immunantwort sind, war hingegen in beiden Genotypen vergleichbar.

Unsere Gruppe demonstrierte kürzlich die hohe Empfindlichkeit von MGMT k.o. Mäusen gegenüber NOC-induziertem ausgelösten Dickdarmkrebs (Fahrer *et al.* 2015). Daher wurde die entzündungsvermittelte Tumorpromotion weiter in PARP-1-defizienten Tieren analysiert, die mit dem MGMT-Hemmer *O*$^6$-Benzylguanin (*O*$^6$-BG) vorbehandelt wurden. Die Hemmung von MGMT

verursachte einen deutlichen Anstieg von Tumoranzahl und Tumorscore, was vermutlich auf die stärkere Induktion von mutagenen $O^6$-MeG DNA Addukten in Abwesenheit von MGMT zurückzuführen ist. Dies wurde im Detail mithilfe eines PARP-$1^{-/-}$/$MGMT^{-/-}$ Doppel-*Knockout*-(DKO) Stamms untersucht. Interessanterweise wiesen DKO-Mäuse eine höhere Tumoranzahl, aber geringere mittlere Tumorgröße als $MGMT^{-/-}$ Tiere auf.

Zusammenfassend lässt sich aus den Experimenten ableiten, dass der Verlust von PARP-1 eine Resistenz gegenüber entzündungsvermitteltem Dickdarmkrebs verleiht, die größtenteils auf die verminderte Entzündungsantwort im Kolon zurückgeführt werden kann. Die verminderte Tumorentstehung kann durch die Hemmung von MGMT reviertiert werden. Die erhöhte Tumoranzahl in den DKO-Tieren weist auf die schützende Wirkung von PARP-1 während der Tumorinitiation hin, wohingegen die geringere mittlere Tumorgröße die Rolle der Entzündung bei der Tumorpromotion bestätigt. Diese Arbeit lässt wichtige Schlussfolgerungen auf die Entstehung und Therapie von Colitis-assoziiertem Dickdarmkrebs zu.

# SUMMARY

Poly(ADP-ribose) polymerase-1 (PARP-1), which catalyses the synthesis of poly(ADP-ribose), is implicated in a variety of cellular processes, such as chromatin remodelling and DNA repair. PARP-1 is well-known to promote base excision repair, a conserved pathway that removes DNA base modifications, including alkylated DNA bases. These lesions are induced by *N*-nitroso compounds (NOCs) that are tightly linked to the aetiology of colorectal cancer (CRC). It is further known that PARP-1-deficient mice display an enhanced sensitivity against alkylating agents in terms of toxicity and genomic instability.

The objective of this work was to assess the influence of PARP-1 on colitis-associated CRC induced by NOCs. PARP-1-proficient (WT) and PARP-1-deficient (PARP-1$^{-/-}$) mice were treated with the colonotropic tumour initiator azoxymethane (AOM) followed by dextran sodium sulphate (DSS), which triggers colitis. Tumour formation was monitored by non-invasive mini endoscopy. WT mice displayed a significantly higher tumour number and tumour score compared to PARP-1$^{-/-}$ animals, which correlated with the AOM dose.

Analysis of initial DNA damage induction in both genotypes revealed an increased number of DNA strand breaks in PARP-1$^{-/-}$ animals, but comparable levels of *O*$^6$-methylguanine (*O*$^6$-MeG) DNA adducts in both genotypes. The latter is the critical lesion driving NOC-induced CRC. In line with this, the activity of *O*$^6$-methylguanin-DNA methyltransferase (MGMT), which is responsible for the repair of *O*$^6$-MeG DNA adducts, was depleted in both mouse strains in liver and colon. PARP-1-proficient and PARP-1-deficient mice did not display differences in basal cell proliferation or AOM-induced cell death in colorectal tissue.

As PARP-1 is a known coregulator of the pro-inflammatory transcription factor nuclear factor 'kappa-light-chain-enhancer' of activated B-cells (NF-κB), the acute DSS-induced inflammation was assessed in WT and PARP-1$^{-/-}$ mice by mini endoscopy. WT animals exhibited significantly stronger colitis in response to AOM/DSS, which is in line with a higher abundance of the NF-kB-inducible cyclooxygenase-2 (COX-2). IHC and confocal microscopy showed strongly decreased numbers of monocytes and macrophages in colon tissue of PARP-1$^{-/-}$ animals. Accordingly, expression of the cytokine high mobility group box 1 (HMBG1), which is tightly linked to inflammation, was reduced in PARP-1 k.o. mice. The number of cluster of differentiation 3 (CD3)-positive T-cells, associated with the adaptive immune response, was similar in both genotypes.

Our group recently demonstrated the high sensitivity of MGMT k.o. animals to NOC-induced CRC (Fahrer *et al.* 2015). Therefore, the role of inflammation driven tumour promotion was dissected in PARP-1 k.o. animals treated with the MGMT inhibitor *O*$^6$-benzylguanine (*O*$^6$-BG) prior to the AOM/DSS protocol. Inhibition of MGMT caused a clear increase in both tumour score and number, likely attributable to a higher induction of mutagenic *O*$^6$-MeG DNA adducts in absence of MGMT. This was further studied with the help of a PARP-1$^{-/-}$/MGMT$^{-/-}$ double knock out (DKO) strain. Interestingly, DKO mice displayed a higher tumour number but lower mean tumour size compared to MGMT-deficient animals.

Collectively, this work demonstrates that PARP-1 deficiency confers resistance to colitis-associated CRC, which is largely attributable to an attenuated inflammatory response in the colorectum. The lower tumour induction can be reversed by MGMT depletion. The increased tumour number in DKO animals suggests a protective function of PARP-1 during NOC-mediated tumour initiation, whereas the smaller mean tumour size supports the notion that PARP-1 plays a critical role during inflammatory promotion of tumour growth. This study bears significant implications for the aetiology and therapy of colitis-associated CRC.

# TABLE OF CONTENTS

# 1 INTRODUCTION

## 1.1 COLORECTAL CANCER

Cancer is one of the leading causes of death worldwide. Here, colorectal cancer (CRC), which is localised in colon and rectum, has an outstanding role. About 1,360,000 new diagnoses and 694,000 mortalities are recorded annually for CRC. CRC is stated as the second or third (for female or male, respectively) leading cause of cancer-related death worldwide. Almost 55 % of incidents are diagnosed in first world countries, with Europe and Japan leading in both incidence and mortality (Ferlay *et al.* 2015). Although number of deaths caused by CRC was decreased since the 1990s, the disease-specific mortality rate averages at almost 33 %. Early detection methods and regular check-ups positively influence the prognosis for the patients. Most of tumours arise sporadically above an age of 50 years (Cunningham *et al.* 2010; Sameer 2013; Watson, Collins 2011) with genetic predispositions and lifestyle representing the main risks. The latter is dependent on nutrition, consumption of alcohol and tobacco, physical activity, and obesity (Giovannucci 2002; Gonzalez 2006; Roon *et al.* 2007).

### 1.1.1 ANATOMY OF THE COLON

The large intestine is the last part of the gastrointestinal tract (GIT) in vertebrates in which water is absorbed and waste material excreted as faeces. The large intestine is composed of cecum, colon, rectum, and anus. The colon is divided in the five following sections: ascending colon (including cecum and appendix), transverse colon (including colic flexures and transverse mesocolon), descending colon, sigmoid colon, and rectum.

The cecum is the first part of the colon and, in contrast to the appendix, involved in digestion. The appendix is an embryonically developed structure, which is suggested to be part of the lymphoid tissue in the gut. The ascending colon, which is the first of the large intestines sections, is connected to the small intestine via the cecum. It progresses upwards through the abdominal cavity for about 20 cm. A major function of the colon is the resorption of water and nutrients from the stool, which is moved towards the distal part of the colon by the intestinal peristalsis. The subsequent transverse colon is attached to the stomach by the so called greater omentum, a part of the peritoneum, and the posterior abdominal wall by the transverse mesocolon. In contrast to the other parts of the colon, the transverse colon is mobile. The descending colon begins at the splenic flexure (Fried *et al.* 2013; Standring, Ananad 2016). It should be noted that 60 % of CRCs are situated at or distal of the splenic flexure (Cunningham *et al.* 2010; Hamilton *et al.* 2005). Faeces are stored in the descending colon and subsequently emptied into the rectum. The sigmoid colon is localised between descending colon and rectum. Its Strong muscular walls allow the sigmoid colon to increase pressure inside the colon and thereby moving the stool into the rectum. The last part of the colon is called rectum, which holds the faeces before defecation.

The gastrointestinal wall surrounding the lumen of the colon is built up of the mucosa, submucosa, muscularis, and serosa (**Figure 1**).

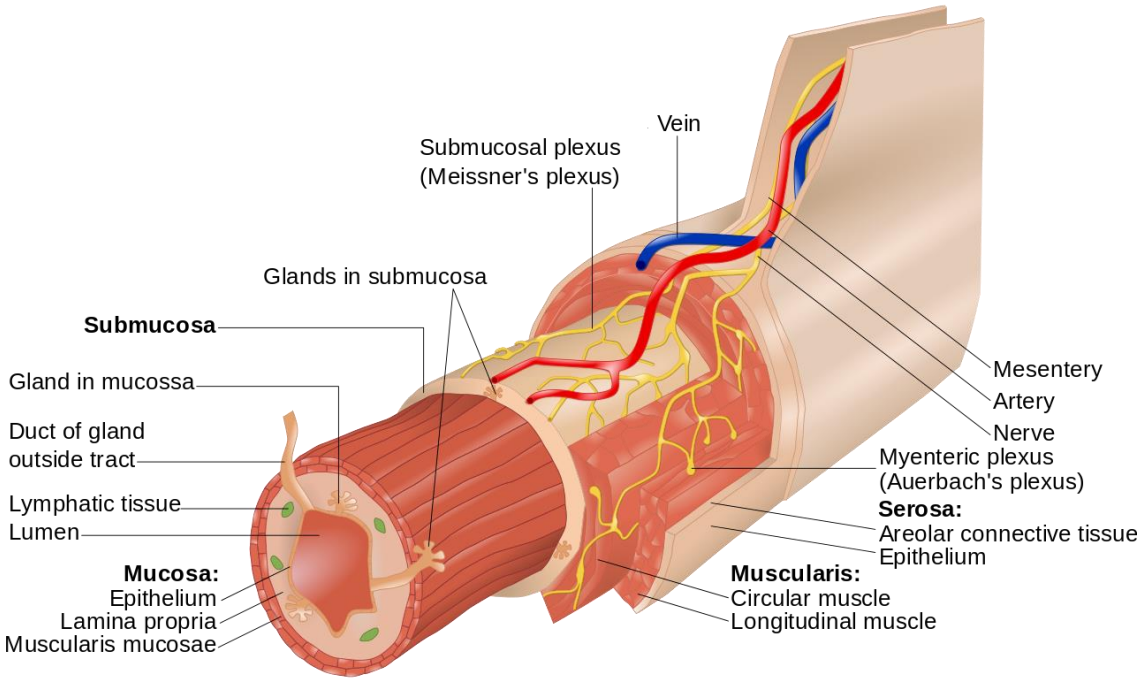


**Figure 1: Anatomy of the gastrointestinal wall (Goran tek 2014).** See text for details.

The innermost layer of the large intestine is the mucosa, which surrounds the lumen and has direct contact with the digested food respectively stool. The mucosa itself comprises three layers, starting with the epithelium on the lumen site. Here, most of the digestive, absorptive, and secretory processes take place. Localised within the mucosa, lamina propria is a layer of connective tissue. The lamina propria is surrounded by the muscularis mucosae, a layer of smooth muscle tissue. The epithelium in the large intestine is organised in simple columnar invaginations, the colon crypts. The submucosa consists of connective tissue containing blood vessels, lymphatic vessels, and nerves. The following layer is called muscularis, built of an inner muscle layer and an outer muscle layer. The inner layer is organised in circular rings around the GIT, whereas the outer layer orientated longitudinally. The muscle layers are responsible for the intestinal peristalsis controlled by the myenteric plexus. The serosa is the outermost layer of the GIT, which consists of several layers of connective tissue (Fried *et al.* 2013; Standring, Ananad 2016).

### 1.1.2 GENESIS OF CRC

In 1988, Bert Vogelstein described the model of sporadic colorectal carcinogenesis as a multistep process, in which genesis of cancer is determined by molecular gatekeepers and caretakers (Vogelstein *et al.* 1988). Genesis of CRC is characterised by an adenoma-carcinoma sequence, in which aberrant crypt foci (ACF) are described as the earliest precursor of CRC. ACF progress to colorectal polyps and

later to adenomas followed by invasive carcinomas (Chen, Huang 2009; Fearon, Vogelstein 1990; Markowitz, Bertagnolli 2009).

Tumours are initiated by deoxyribonucleic acid (DNA) damage caused by chemicals, ionising radiation, or other insults, which is translated into mutations. Activation of the Wnt signalling pathway is described as initiating event in CRC. The oncoprotein β-catenin binds to nuclear targets and creates a transcription factor that modulates genes involved in cellular activation (Fearon 2011; Vogelstein, Kinzler 2002). β-catenin levels are controlled by the β-catenin degradation complex. The tumour suppressor adenomatous polyposis coli (APC) is an essential part of this complex (Markowitz, Bertagnolli 2009). Mutations inactivating APC are the most common in CRC and cause constitutively activation of Wnt signalling (Lynch *et al.* 2008; Vogelstein, Kinzler 2002). APC mutations are present in both sporadic CRC and the inherited disorder familial adenomatous polyposis (FAP) (Morin *et al.* 1997). In the next step, activation of several oncogenes, *e.g.* K-ras and B-raf, plays a central role in the promotion of CRC by activation of the mitogen-activated protein kinase (MAPK), which leads to multiplication of the initiated cells. Permanently irritating processes (*e.g.* chronic inflammation) are considered as the main promotors. Ulcerative colitis and Chron's disease, summarised as inflammatory bowel disease, account for about 2/3 of CRC incidences (Eaden *et al.* 2001; Roon *et al.* 2007), and risk correlates with both duration and severity of inflammation (Itzkowitz, Harpaz 2004). During tumour progression, mutated cells acquire features including self-sufficiency in growth signals, insensitivity to inhibitory growth signals, limitless replicative potential, evasion of apoptosis, sustained angiogenesis, invasion of tissues, and metastasis (Hanahan, Weinberg 2011) (**Figure 2**).

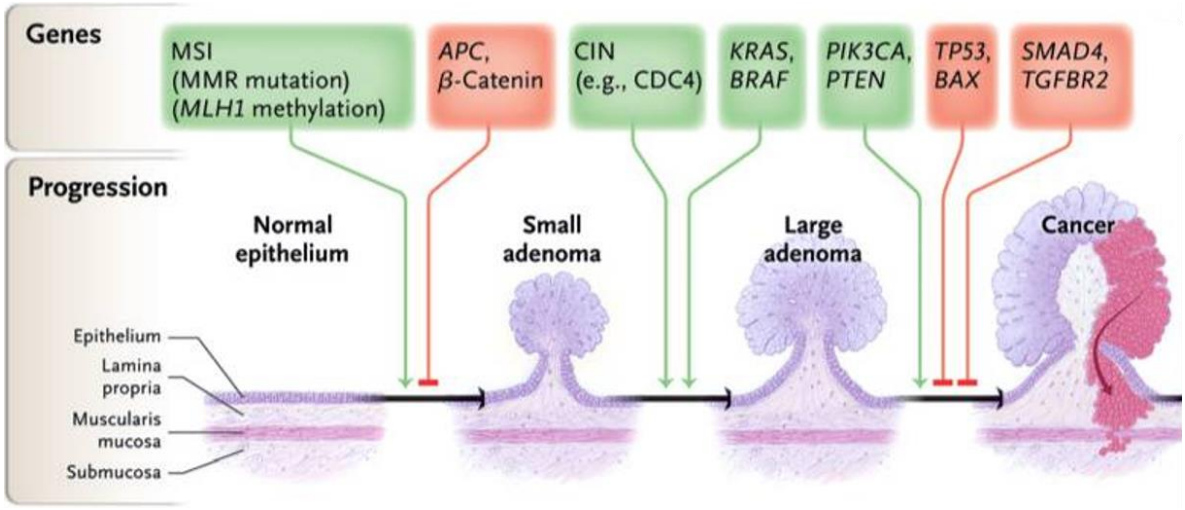


**Figure 2: Genes involved in CRC aetiology.** Green marks oncogenes that are activated in CRC, red denotes inhibitory factors that are lost during progression (Markowitz und Bertagnolli 2009), modified.

On a molecular level, tumour progression goes in line with inactivation of tumour suppressor gene like *p53*, *BCL-2-associated X* (*BAX*), and *transforming growth factor β receptor II* (*TGFBR2*). Molecular analysis of tumours allows classification into different molecular pathways, depending on different cancer-related alterations: chromosomal instability pathway, mismatch repair pathway, and serrated pathway. Majority (about 85 %) of sporadic incidences show chromosomal instability, allelic imbalance, chromosome amplification, and translocation, which all contribute to tumour aneuploidy. Chromosomal

aberrations mainly affect loci 5q, 8p, 17p, and 18q, leading to loss of genes encoding crucial tumour suppressors (*e.g.* APC and p53) or activation of oncogenes. (Lengauer *et al.* 1998; Lothe *et al.* 1993; Vogelstein *et al.* 1988; Vogelstein *et al.* 1989). A minor part (15 %) of sporadic tumours carry microsatellite instability, frameshift mutations, and base pair substitutions in microsatellite tracts (Aaltonen *et al.* 1993; Ionov *et al.* 1993). Microsatellite instability is a consequence of acquired or inherited alteration of the DNA mismatch repair (MMR) (Peltomaki 2003). MMR is a system for the repair of faulty insertions, deletions, and mis-incorporation of bases in the genome arising during DNA replication as well as the correction of DNA damage, thus maintaining genomic integrity (Iyer *et al.* 2006). Furthermore, aberrations in DNA methylation patterns can cause a downregulation of critical genes (often the MMR gene *MLH1*) on an epigenetic level (Cunningham *et al.* 1998; Markowitz, Bertagnolli 2009). CpG (5'-C-phosphate-G-3') sites are located in the promoter region of genes. The cytosine of the dinucleotides can be methylated to 5-methylcytosine, which can epigenetically silence expression of the subsequent gene (Issa 2004). The serrated pathway includes serrated polyps and adenomas usually arising in the right colon, which differ in their progression from the classic adenoma-carcinoma sequence (Noffsinger 2009). Molecular classification of the three different pathways is summarised in **Figure 3**.

| | **Chromosomal instability pathway** | **Mismatch repair pathway** | **Serrated pathway** | |
|---|---|---|---|---|
| | Hereditary and sporadic | Hereditary | Hereditary | Sporadic |
| CIMP status | Negative | Negative | High | .. |
| MSI status | MSS | MSI-H | MSI-H | MSI-L |
| Chromosomal instability | +++ | --- | --- | --- |
| *KRAS* mutation | +++ | +/- | --- | --- |
| *BRAF* mutation | --- | --- | +++ | +++ |
| *MLH1* status | Normal | Mutation | Methylated | Partial methylation |

Adapted from Noffsinger.[3] CIMP=CpG island methylator phenotype. MSS=microsatellite stability. MSI=microsatellite instability. MSI-H=high-level microsatellite instability. MSI-L=low-level microsatellite instability. +++=present. +/-=might or might not be present. ---=absent.

**Figure 3: Molecular classification of colorectal carcinoma (Cunningham et al. 2010).**

Hereditary CRC syndromes account for almost 6 % of CRC cases. 3 % are linked with the Lynch syndrome, also known as hereditary non-polposis colorectal cancer (HNPCC). The Lynch syndrome is characterised by a defective MMR leading to microsatellite stability. Here, a variety of MMR related genes can be affected. 2 % are caused by FAP (as mentioned above), and about 1 % constitute of other syndromes including deletion of *TACSTD1*, which encodes Epithelial cell adhesion molecule (EpCAM) (Cunningham *et al.* 2010).

### 1.1.3 SCREENING, DIAGNOSIS, AND THERAPY

To ensure early detection of CRC, a screening is recommended in an interval of 2 years, as CRC tends to arise 2 – 3 years before patients experience symptoms. Common screening methods are stool DNA analysis and faecal occult blood test (Cunningham *et al.* 2010). Colonoscopy should be performed only if the prior mentioned screening methods show a positive result (Benson *et al.* 2008). Sigmoidoscopy examines rectum and sigmoid colon; removal of small adenomas is possible. This can be performed on a regular basis (every 5 years) above an age of 50 years (Pignone *et al.* 2002) or once above an age of 60 years (Atkin *et al.* 2001). Due to possible complications and severity, complete colonoscopies without indication are only performed every 10 years. According to Amsterdam criteria (Llor *et al.* 2005) and revised Bethesda guidelines (Umar *et al.* 2004), genetic screenings are advised in patients with inherited disease (*e.g.* Lynch syndrome).

CRC is diagnosed via colonoscopy or sigmoidoscopy in combination with tumour biopsy. Metastasis in chest, abdomen, and pelvis are screened with the help of computed tomography (CT). Additionally, CT colonography supports surgical approaches to remove tumours (Mauchley *et al.* 2005). Diseases are classified into 4 stages, called the Duke's stages of bowl cancer (Dukes A – D) (DUKES 1959; Sameer 2013) by the Union for International Cancer Control (UICC) respective to the therapeutically opportunities and in due consideration of the TNM (tumour, node, metastases) system (Sobin, Fleming 1997). Stages I and II (Dukes A and B respectively) are still localised within the bowel and do not penetrate its outer lining. Neither affected lymph nodes nor metastasis are visible, and they are curable with surgery. Stage III (Dukes C) has already penetrated the outer lining of the bowel and affect regional lymph nodes. Therapy involves resection of the tumour in combination with adjuvant chemotherapy based on fluorouracil and oxaliplatin. Radiotherapy is an additional option for treatment of rectal cancer. CRC at stage IV (Dukes D) is fatal and goes in line with distant metastasis, particularly in liver (Markowitz *et al.* 2002; Markowitz, Bertagnolli 2009).

## 1.2 *N*-NITROSO COMPOUNDS

As already stated in 1.1, nutrition and lifestyle are the major factors influencing the aetiology of CRC. The intake of fibre and physical activity protect against CRC, whereas consumption of red and processed meat, fat, tobacco, and alcohol increase risk (Cunningham *et al.* 2010; Gonzalez 2006; Watson, Collins 2011). Procession of meat and subsequent cooking gives rise to food-borne carcinogens (Sugimura 2000) including polycyclic aromatic hydrocarbons (PAHs), heterocyclic aromatic amines (HCAs), and *N*-nitroso compounds (NOCs), which cause DNA damage after metabolic activation (Fahrer, Kaina 2016). HCAs arise during procession of meat at high temperatures and can be separated in two classes: amino-imidazoarenes and pyrolytic HCAs.

NOC, *e.g.* emerge from reaction of nitrite or nitrous gases with secondary amines, arising notably in beer, processed meat, and cheese (Lijinsky 1999) but also in cosmetics (*e.g. N*-nitrosodiethanolamine) (Schothorst, Somers 2005) and tobacco smoke (*e.g.* 4-(methylnitrosamino)-1-(3-pyridyl)-1-butanone, 4-(methylnitrosamino)-1-(3-pyridyl)-1-butanol, and *N*-nitrosonornicotine) (Hecht 1999). Additionally, NOC, *e.g. N*-nitrosamines, can be formed endogenously by transformation of amino acids (AAs) to *N*-alkynitrosamines in the stomach and the large intestine. First, AAs are decarboxylated by bacteria and subsequently nitrosylated to alkyl-nitrosamines (Lundberg, Weitzberg 2013) with the help of endogenous NO (Fahrer, Kaina 2013). Moreover, the consumption of haem or haem-containing red meat stimulates the generation of NOC (Joosen, Annemiek M C P *et al.* 2009; Kuhnle *et al.* 2007) (**Figure 4**).

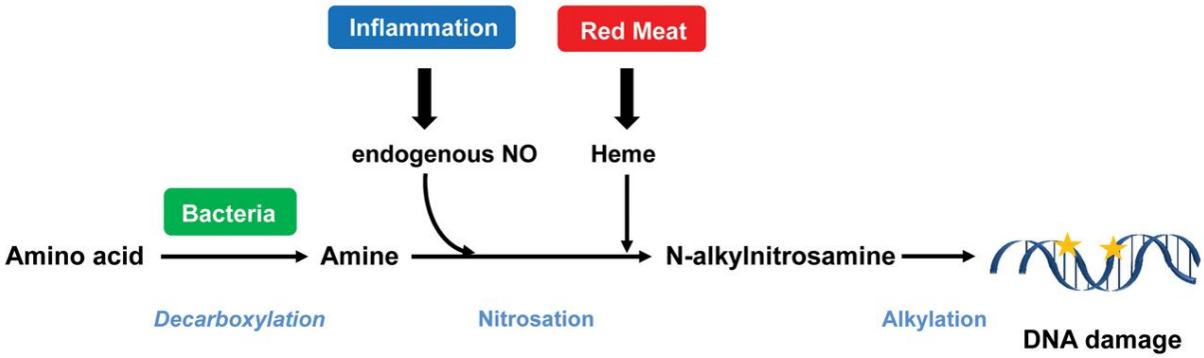


**Figure 4: Endogenous formation of NOC in the large intestine (Fahrer, Kaina 2013).** See text for details.

Upon metabolic activation, NOCs can alkylate the DNA bases being responsible for at least 12 different DNA adducts. For example, the NOC *N*-nitrosodimethylamine is *N*-hydroxylated at the α-C-atom by CYP2E1, a well-known member of the Cytochrome P450 superfamily, to *N*-nitroso(hydroxymethyl) methylamine (Yang *et al.* 1990). In the next step, *N*-nitroso(hydroxymethyl) methylamine rearranges into an intermediate methyldiazonium ion, which goes in line with elimination of an aldehyde and water. The instable methyldiazonium ion decomposes spontaneously to a methylcarbocation, which attacks the DNA. This ultimate carcinogen induces alkylation damage via nucleophilic $S_N1$ substitution at nitrogen or oxygen atoms of DNA bases, creating cytotoxic and mutagenic lesions (Fu *et al.* 2012). Approximately 75 % of the induced lesions are *N* methyl purines and $O^6$-methylguanine ($O^6$-MeG), the latter contributes to about 8 % to alkylated DNA adducts (Beranek 1990). Species of induced DNA lesions depend on reactive groups of the alkylating agent, position of alkylation, and DNA substrate (Shrivastav *et al.* 2010). Due to their cytotoxic properties, alkylating agents are used in chemotherapy, *e.g.* temozolomide (TMZ), as treatment for *Glioblastoma multiforme* (Fu *et al.* 2012).

### 1.2.1 NOC INDUCED DNA DAMAGE AND REPAIR OF THE LESIONS

DNA methylation is a special form of DNA alkylation concerning transfer of a $CH_3$ group onto nitrogen atoms of the ring structure as well as extra circular oxygen atoms of DNA bases. About 75 % of the NOC induced lesions are *N*-methylations, whereas only 8 % are *O*-methylations (Beranek 1990; Drablos *et al.* 2004).

*N*-alkylations can be further differentiated in *N*7-methylguanine (*N*7-MeG, 65–70 %) and *N*3-methyladenine (*N*3-MeA, 8–9%), both exerting their strong cytotoxic potential by inhibition of polymerases during DNA synthesis (Drablos *et al.* 2004). Majority of the methylated DNA adducts is repaired by the base excision repair (BER) (Huang *et al.* 1994), where the glycosylase 3-alkyladenine DNA glycosylase (AAG), also known as *N*-methylpurine DNA glycosylase (MPG), plays a pivotal role (Fu *et al.* 2012) (**Figure 5**). The process of BER and its role in CRC formation are described in detail in (1.2.3). Transgenic $AAG^{-/-}$ mice are prone to alkylation-induced CRC as compared to AAG proficient wild type (WT) mice (Wirtz *et al.* 2010) and the formation of dysplastic adenomas following chronic gut inflammation (Meira *et al.* 2008).

The DNA adducts *N*1-methyladenine (*N*1-MeA) and *N*3-methylcytosine (*N*3-MeC) contribute to a minor part (1.5%) to all methylation damage. The AlkB homologues ALKBH2 and ALKBH3 are responsible for the repair of these lesions (Aas *et al.* 2003). The AlkB protein is part of the adaptive response and direct reversal of alkylation damage in *Escherichia coli* (Duncan *et al.* 2002). Yet, nine human AlkB homologues have been identified, forming the ALKBH family (Gerken *et al.* 2007; Kurowski *et al.* 2003). ALKBH2 and ALKBH3 (**Figure 5**) are part of an α-ketoglutarate $Fe^{2+}$-dependent dioxygenase superfamily (Aas *et al.* 2003). Both enzymes remove DNA adducts in a two-step reaction where a hydroxylated intermediate spontaneously reacts to formaldehyde (Trewick *et al.* 2002). ALKBH2-deficient mice are prone to methylation-induced CRC compared to WT animals (Calvo *et al.* 2012).

Albeit *O*-alkylations represent only a minor part of the lesions, they bear higher mutagenic and genotoxic potential than the rather cytotoxic *N*-alkylations (Christmann *et al.* 2003). A pre-mutagenic DNA lesion is $O^6$-MeG which, together with other $O^6$-alkyl guanine adducts, is repaired by $O^6$-methylguanin-DNA methyltransferase (MGMT) (Fahrer, Kaina 2013, 2016) (**Figure 5**). The suicide DNA repair protein MGMT catalyses the transfer of the methyl group of $O^6$-MeG onto a cysteine residue in its catalytic cleft (Daniels *et al.* 2004; Guengerich *et al.* 2003), thereby reverting the damage on the guanine base. This reaction leads to inactivation of MGMT, which is subsequently degraded via the ubiquitin/proteasome pathway (Christmann, Kaina 2013). Since one MGMT only removes one lesion, the cells repair capacity for $O^6$-MeG and other $O^6$-alkyl guanine lesions directly correlates with the amount of MGMT proteins (Kaina *et al.* 2007). A special form of $O^6$-alkylation DNA damage is the nitrosated bile acid DNA lesion $O^6$-carboxymethylguanine ($O^6$-CMG), which is frequently present in DNA of humans with a high consumption of red meat and therefore suspected to be a causative factor for colorectal carcinogenesis. The lesion is probably caused by the *N*-nitrosation of glycocholic acid, a component of the bile (Lewin *et al.* 2006). In contrast to prior studies (Shuker, Margison 1997), a recent article, published by Senthong and colleagues, reported that synthetic oligodeoxyribonucleotides containing $O^6$-CMG inactivated MGMT *in vitro*. The inactivation went in line with transfer of the $O^6$-alkyl group onto a cysteine residue in the active site of MGMT. The authors conclude that $O^6$-CMG is a substrate for MGMT, and the suicide protein is likely to protect against $O^6$-CMG induced CRC formation (Senthong *et al.* 2013).

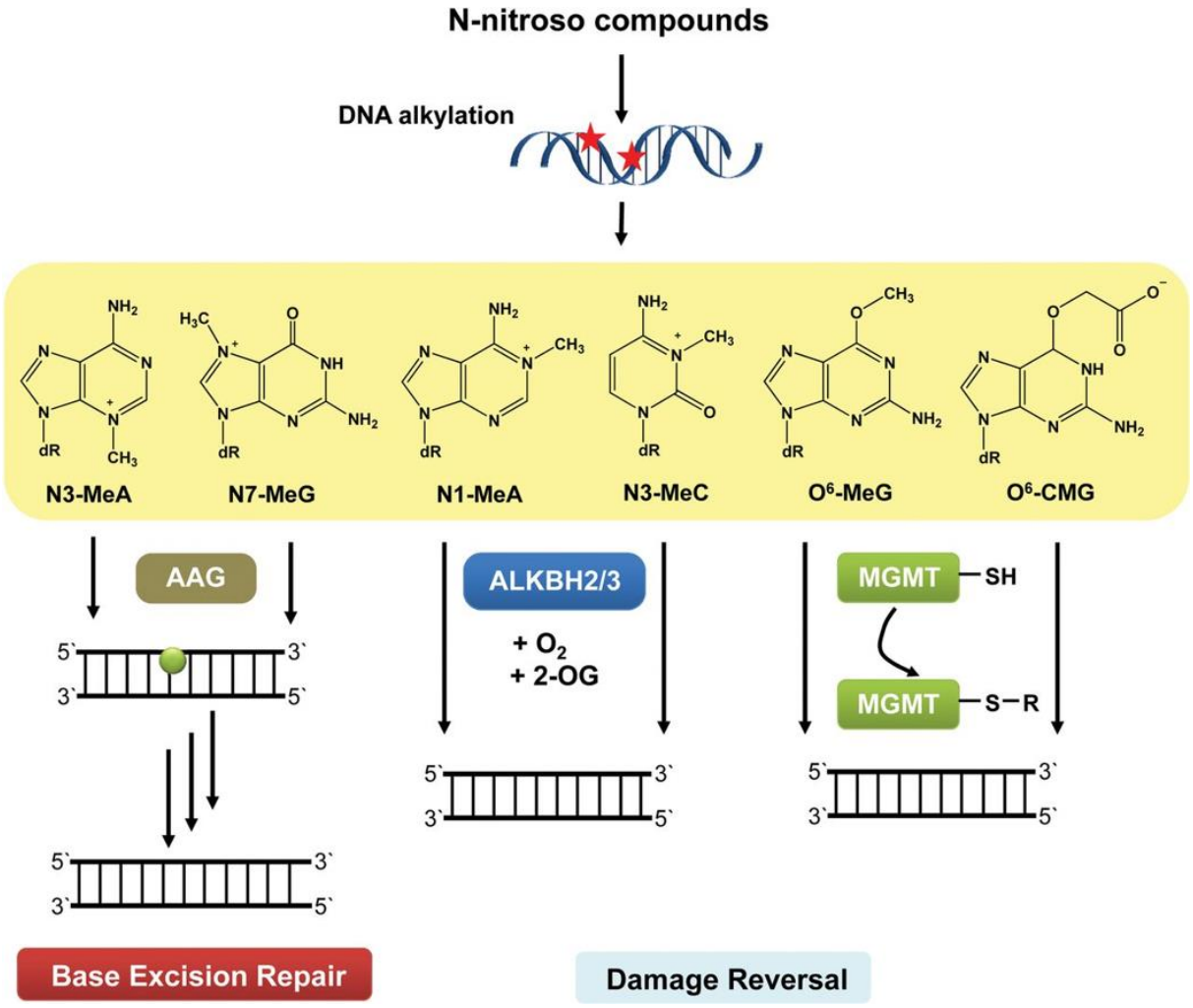


**Figure 5: Repair of NOC-induced DNA damage**. NOCs alkylate the DNA, yielding at least 12 different adducts. Majority of adducts (*N*3-MeA and *N*7-MeG) is repaired by the BER pathway. *N*1-MeA and *N*3-MeC DNA adducts are removed by AlkB homolog proteins (ALKBH2 and ALKBH3). $O^6$-MeG and other $O^6$-alkyl guanine adducts are reverted by MGMT (Fahrer und Kaina 2013).

Persistence of $O^6$-MeG adducts has dramatic consequences for the cell including cytotoxicity, mutagenicity, and cancerogenicity. $O^6$-MeG mispairs with thymidine during the first replication cycle and leads to a G:C to A:T transition mutation in the following replication cycle. The $O^6$-MeG:T mismatch is recognised by the MMR and the mispaired thymidine removed. This causes aberrant MMR cycles which generate nuclease sensitive sites (*e.g.* single-strand gaps), which finally result in DNA double strand breaks (DSBs) due to the block of the replication fork (Kaina *et al.* 2007; Lips, Kaina 2001) (**Figure 6**).

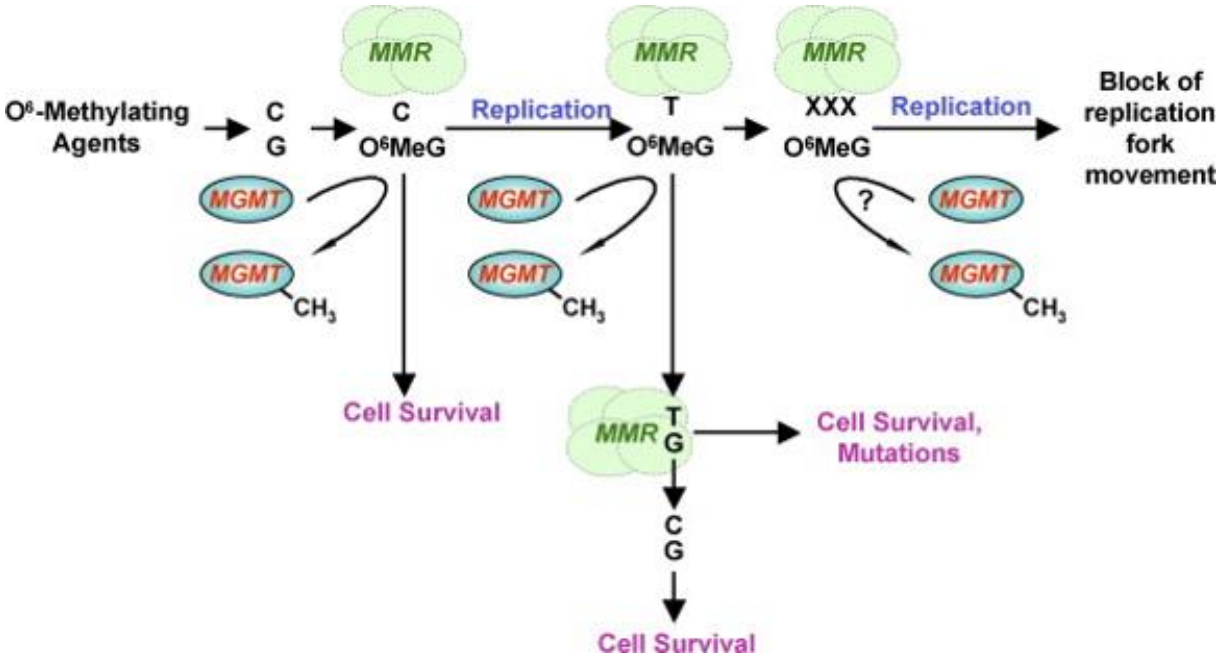


**Figure 6: Repair of *O*$^6$-MeG DNA methylation damage by MGMT and involvement of MMR (Kaina et al. 2007).** See text for further details.

The arising DSBs are highly cytotoxic, triggering apoptosis and causing chromosomal aberrations (Margison, Santibanez-Koref 2002), hence they activate DNA damage response (DDR) (Yoshioka *et al.* 2006). *In vitro* studies revealed that a defective MMR system (*e.g.* loss of MLH1) mediates resistance to *O*$^6$-MeG:T mispairings in terms of cytotoxicity (Roos, Kaina 2013) but enhances formation of G:C to A:T point mutations (Karran, Bignami 1994).

### 1.2.2 INVOLVEMENT OF MGMT IN GENESIS OF NOC-INDUCED CRC

The carcinogenesis of alkylating agents was studied using transgenic mice with altered MGMT expression. Therefore, animal strains overexpressing (Zaidi *et al.* 1995) and lacking MGMT (Sakumi *et al.* 1997; Wali 1999) were established. The studies revealed an enhanced sensitivity of MGMT k.o. animals towards lethal effects of NOCs like methylnitrosurea (MNU) in line with higher tumour formation compared to WT animals (Sakumi *et al.* 1997). MGMT plays an important role in colorectal carcinogenesis mediated by the alkylating agent azoxymethane (AOM). Upon treatment with AOM, animals overexpressing MGMT exhibit less ACF, a precursor of CRC, than WT animals (Zaidi *et al.* 1995). In contrast, MGMT-deficient animals show a higher number of ACF and increased apoptosis induction (Bugni *et al.* 2009) in line with higher tumour rate (Wirtz *et al.* 2010). Inhibition of MGMT with *O*$^6$-benzylguanine (*O*$^6$-BG) *in vivo* resulted in an increased tumour formation compared to animals with unaffected MGMT (Wali 1999). Recently, our group performed a study in which both MGMT k.o. and BER-deficient AAG k.o. animals were challenged with the AOM/dextran sodium sulfate (DSS) model of colorectal carcinogenesis. MGMT was identified as crucial barrier against CRC formation at low alkylation damage load, whereas AAG was only relevant at high alkylation damage levels (Fahrer *et al.* 2015). The MGMT repair capacity is correlating with its activity which differs along the colon with highest

activity in the rectal region. Furthermore, MGMT activity is heterogeneous between individuals (Povey *et al.* 2000) and varies within tumours (Lees *et al.* 2002). Apart from animal studies, there is evidence linking MGMT to the aetiology of human CRC. Studies revealed that methylation of CpG sites in the MGMT promotor cause a reduction of MGMT protein expression, which can result in a complete loss of MGMT function (Herfarth *et al.* 1999). MGMT promotor methylation is especially important for sporadic CRC (Lind *et al.* 2004), whereas it is less prevalent in inflammation-associated disease (Matsumura *et al.* 2003). In addition, promotor hyper-methylation of MGMT was observed even in sporadic dysplastic ACF (Chan *et al.* 2002; Nagasaka *et al.* 2008), a precursor lesion of CRC. This is an early alteration, predisposing the mucosa to alkylating agents like NOC and thereby shortening the latency of CRC formation. The loss of MGMT by promotor hyper-methylation increases the frequency of G:C to A:T mutations of *K-ras* (Esteller *et al.* 2000; Nagasaka *et al.* 2008; Vogel *et al.* 2009). The dietary intake of haem-iron is associated with the already mentioned transition mutations in *K-ras* and increased risk for CRC (Gilsing *et al.* 2013). In summary, attenuated MGMT activity, often caused by promotor hyper-methylation, increases the risk for a *K-ras* mutation which benefits tumour progression (Fahrer, Kaina 2013, 2016).

### 1.2.3 BER PATHWAY AND ITS RELATION TO NOC-INDUCED CRC

DNA bases can be chemically damaged by a variety of mechanisms (*e.g*. exogenous and endogenous DNA reactive molecules). The most common lesions, which are repaired by the BER pathway, include apurinic/apurimidinic sites (AP sites) due to spontaneous hydrolysis of DNA bases, base oxidations, base alkylations, deaminated bases, and inappropriately incorporated uracil (Lindahl 1993). These lesions cause mutations, disrupt genomic integrity, interfere with the cell metabolism, resulting in premature aging and degenerative diseases such as cancer (Lombard *et al.* 2005). The damaged DNA base can be either removed by a monofunctional DNA glycosylase, resulting in an AP site or a bifunctional DNA glycosylase, which also holds AP lyase activity creating a DNA single strand break (SSB) by cleavage of the phosphodiester bond of the DNA. In the context of NOC induced lesions, BER is responsible for repair of *N*3-MeA und *N*7-MeG adducts. The damaged base is recognised and removed by the DNA glycosylase AAG, which cleavages the glyosidic bond connecting the base and the deoxyribose sugar of the DNA backbone (1.2.1). The AP site is processed by an AP endonuclease (APE) into a SSB, which is subsequently recognised by the poly(ADP-ribose) polymerase-1 (PARP-1) (1.3) and stimulates its catalytic activity (Mangerich, Bürkle 2012; Masson *et al.* 1998; Noren Hooten *et al.* 2011). PARP-1 recruits the scaffolding factor XRCC1 and other major BER factors, including DNA polymerase-β and DNA ligase III, forming a multiprotein complex responsible for repair (Audebert *et al.* 2004; Caldecott *et al.* 1996; Confer *et al.* 2004; Leppard *et al.* 2003; Noren Hooten *et al.* 2011).

Yet, little is known about the role of BER during colorectal carcinogenesis. Studies showed the protective role of AAG against NOC-induced CRC (Calvo *et al.* 2012; Fahrer *et al.* 2015; Meira *et al.* 2008; Wirtz *et al.* 2010). Our group recently reported that AAG protects against NOC-induced CRC in the AOM/DSS model at high alkylation damage levels, whereas MGMT protects the animals from CRC at low alkylation damage levels, mediating a carcinogenic threshold (Fahrer *et al.* 2015). Other studies revealed a reduction of colon length caused by repeated chemically induced colitis and higher number

of tumours induced by alkylating agents in AAG$^{-/-}$ animals (Calvo *et al.* 2012). AAG has no influence on the initiation response to NOCs. AAG$^{-/-}$ animals show a comparable amount of ACF in response to AOM alone. In addition, AAG was reported to suppress tumorigenesis after treatment with multiple cycles of 2.5 % DSS (in absence of AOM) (Meira *et al.* 2008). Studies addressing the role of AAG in human CRC are still lacking, which is likely to relate to the fact that high levels of DNA *N*-alkylation are only found in humans during chemotherapy with alkylating agents (Fahrer, Kaina 2016). Interestingly, AAG expression is increased in inflamed tissue of patients suffering from ulcerative colitis, which might contribute to microsatellite instability (Hofseth *et al.* 2003).

## 1.3 POLY(ADP-RIBOSE) POLYMERASE

In 1963, a novel nicotinamide mononucleotide (NMN)-dependent enzyme synthesising a poly(A) polymer was characterised by Chambon and colleagues (Chambon *et al.* 1963). Later, the pol(A) polymer was identified as poly(ADP)ribose (PAR) synthesised by the enzyme poly(ADP-ribose) polymerase (PARP). The following chapter provides an overview over PARPs, in particular PARP-1, and their function.

### 1.3.1 POLY(ADP-RIBOSE) POLYMERASE-1

PARP-1 is the funding member of the PARP family, which includes 17 members with different cellular functions (Hakme *et al.* 2008). PARP-1 catalyses the synthesis of PAR in a nicotinamide adenine dinucleotide ($NAD^+$)-dependent manner. It's activity accounts for 90 % of the stress-induced nuclear poly(ADP-ribosly)ation (PARylation) (Kim *et al.* 2005). The 113 kDa human protein PARP-1 comprises the following three structural domains (**Figure 7**):

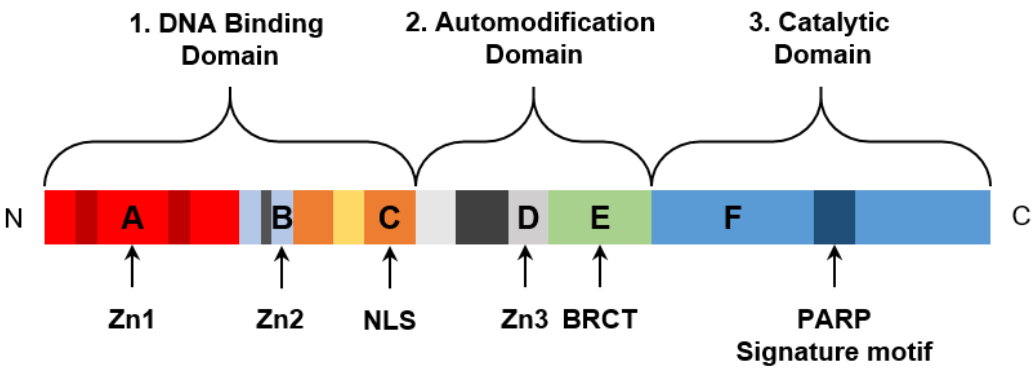


**Figure 7: Structure of human PARP-1.** The enzyme is organised in DNA-binding domain, automodification domain, and catalytic domain. The PARP signature motif is a conserved sequence designating members of the PARP family. Zn2 and Zn2: Zinc-finger motifs, Zn3: Zinc ribbon domain, NLS: nuclear localization signal, BRCT: BRCA1 carboxy terminus (Megnin-Chanet et al. 2010).

The N-terminal DNA binding domain (DBD) consists of two zinc-fingers (Zn1 and Zn2) responsible for recognition and binding of damaged DNA structures (A) (Lonskaya *et al.* 2005; Petrucco, Percudani 2008), a nuclear localization signal (NLS) and a caspase-3 cleavage site (B), another zinc-finger domain (Zn3), modulating DNA-dependent activation and coordination of DNA binding (C) (Hoffman *et al.* 2008; Langelier *et al.* 2008; Langelier *et al.* 2010). The automodification domain (AD), accommodating a BRCT fold (BRCA1-C terminus), is important for protein: protein interaction (Loeffler *et al.* 2011) and the site of autoPARylation (D) (D'Amours *et al.* 1999), a tryptophane-, glycine-and arginine-rich WGR domain (E) (Hakme *et al.* 2008). The C-terminal catalytic domain (CD) is composed of a helical subdomain (HD) and an ADP-ribosyl transferase (ART) subdomain. The latter is conserved among ARTs and known to be important for catalysis as well as binding of $NAD^+$. Furthermore, a PARP signature motif, designating members of the PARP family, is localised in this domain (F) (Megnin-Chanet *et al.* 2010; Ruf *et al.* 1996; Ruf *et al.* 1998). Besides being primarily activated by DSBs, PARP-1 can

also be stimulated by posttranslational proteins modification and protein:protein interactions (Mangerich, Bürkle 2012). Activation of PARP-1 involves formation of a homodimer or heterodimer with PARP-2 (Mendoza-Alvarez, Alvarez-Gonzalez 1993; Pion *et al.* 2003) (1.3.2). The detailed mechanism of PARP activation upon DNA damage and especially participation of the structural domains remains poorly understood. Recently, a new model of PARP-1 activation was proposed by Langelier and colleagues, which is based on the crystal structure analysis of PARP-1 in complex with a DSB:

In absence of DNA, PARP-1 is organised in an open "beads-on-a-string" conformation. The native structure of the HD domain holds the ART domain in an idle state with low basal level of catalytic activity. Upon binding of a monomer to DNA, the WGR domain, Zn1, and Zn3 form the DNA-binding site. This conformational change alters flexibility and dynamics of the ART domain and leads to catalytic activation of PARP-1. In this compact confirmation, the AD domain is close to the catalytic site, establishing PARP-1's high automodification potential. PARP-1's conformational flexibility is crucial for a multi-step enzymatic reactions like poly(ADP-ribosyl)ation reaction. Here, initial PARylation of a protein side chain, multiple cycles of $NAD^+$ hydrolysis, and repositioning of the arising polymer are necessary (Langelier *et al.* 2012).

Albeit Langelier and colleagues can explain the role of the WGR domain and intramolecular PARylation, one must consider the fact, that crystal structure analysis of a truncated protein was the basis for the proposed model. Contrary models were formerly described in the literature, in which PARP1 dimerizes with contribution of both PARP molecules to binding of damaged DNA being essential (Ali *et al.* 2012; Coquelle, Glover 2012). PARP-1's catalytic site is comprised of α-loop-β-α structural motif with three amino acids crucial for its activity. Lysine-893 and aspartate-993 are relevant for binding of the initial ADP-ribose molecule (Simonin *et al.* 1993), and glutamate-988 is essential for polymer extension. Furthermore, tyrosine-986 is pivotal for branching of the PAR chain (Marsischky *et al.* 1995).

## 1.3.2 OTHER MEMBERS OF THE PARP FAMILY

Based on the catalytic domain of PARP-1, 16 related proteins have already been identified, forming the PARP protein family (Ame *et al.* 2004). Six of them have been reported to exhibit PARylation activity; however, the other members of the PARP family are presumably mono-ADP-ribosyltransferases or possess no catalytic activity (Hottiger *et al.* 2010) (**Figure 8**).

| PARP family member | Alternative name | Transferase name* | Subclass | Size (aa)‡ | Subcellular localization | Triad motif | Enzymatic activity§ | Key functional motifs and domains‖ |
|---|---|---|---|---|---|---|---|---|
| PARP1 | | ARTD1 | DNA-dependent | 1,014 | Nuclear | H-Y-E | P and B | WGR, zinc-fingers and BRCT |
| PARP2 | | ARTD2 | DNA-dependent | 570 | Nuclear | H-Y-E | P and B | WGR |
| PARP3 | | ARTD3 | DNA-dependent | 540 | Nuclear | H-Y-E | M (P predicted) | WGR |
| PARP4 | vPARP | ARTD4 | | 1,724 | Cytosolic (vault particle) | H-Y-E | P (predicted) | BRCT |
| PARP5A | Tankyrase 1 | ARTD5 | Tankyrase | 1,327 | Nuclear and cytosolic | H-Y-E | P and O | Ankyrin repeat |
| PARP5B | Tankyrase 2 and PARP6¶ | ARTD6 | Tankyrase | 1,166 | Nuclear and cytosolic | H-Y-E | P and O | Ankyrin repeat |
| PARP6¶ | | ARTD17 | | 322 | ND | H-Y-Y | M (predicted) | |
| PARP7 | TIPARP and RM1 | ARTD14 | CCCH PARP | 657 | ND | H-Y-I | M (predicted) | Zinc-fingers and WWE |
| PARP8 | | ARTD16 | | 854 | ND | H-Y-I | M (predicted) | |
| PARP9 | BAL1 | ARTD9 | macroPARP | 854 | ND | Q-Y-T | M (predicted) | Macrodomain |
| PARP10 | | ARTD10 | | 1,025 | Nuclear and cytosolic | H-Y-I | M | |
| PARP11 | | ARTD11 | | 331 | ND | H-Y-I | M (predicted) | WWE |
| PARP12 | ZC3HDC1 | ARTD12 | CCCH PARP | 701 | Cytosolic (stress granules) | H-Y-I | M (predicted) | Zinc-fingers and WWE |
| PARP13 | ZC3HAV1 and ZAP1 | ARTD13 | CCCH PARP | 902 | Cytosolic (stress granules) | H-Y-V | M (predicted) | Zinc-fingers and WWE |
| PARP14 | BAL2 and COAST6 | ARTD8 | macroPARP | 1,801 | Cytosolic (stress granules) | H-Y-L | M | Macrodomain and WWE |
| PARP15 | BAL3 | ARTD7 | macroPARP | 444 | Cytosolic (stress granules) | H-Y-L | M (predicted) | Macrodomain |
| PARP16 | | ARTD15 | | 630 | ND | H-Y-I | M (predicted) | |

**Figure 8: Table of PARP family members and their properties.** aa: amino acid, ARTD: ADP-ribosyl transferase, BAL: B-aggressive lymphoma protein: COAST6: collaborator of signal transducer and activator of transcription 6,, ND: not determined, PARP: poly(ADP-ribose) polymerase, vPARP: vault PARP, ZAP1: zinc-finger antiviral protein 1, ZC3HAV1: zinc-finger CCCH-type antiviral protein 1, ZC3HDC1: zinc-finger CCCH domain-containing protein 1. * Based on the revised nomenclature (Hottiger et al. 2010). ‡ Size of the human protein in amino acids. § Known or predicted enzymatic activity: mono- (M), oligo- (O) or poly(ADP-ribosyl)ation (P), or branching (B) (Gibson, Kraus 2012).

Study of knock out (k.o.) mice revealed that animals lacking either PARP-1 or PARP-2 are viable. In contrast, loss of both enzymes leads to embryonic lethality, suggesting redundancy in their function (Menissier de Murcia *et al.* 2003). In agreement with this assumption, PARP-2 is also activated upon DNA damage. Furthermore, PARP-$2^{-/-}$ animals show the same enhanced sensitivity to ionizing radiation and alkylating agents, and display increased genomic instability like PARP-$1^{-/-}$ animals. Despite the redundancy, loss of PARP-2 leads to impaired spermatogenesis, adipogenesis, and T-cell development, indicating some exclusive functions of PARP-2 (Yelamos *et al.* 2008). In a similar manner, mice deficient either for tankyrase-1 (TNKS-1)/PARP5A or tankyrase-2 (TNKS-2)/PARP5B are viable, while absence of both tankyrase-1 and tankyrase-2 results in early embryonic lethality. TNKS-1 and TNKS-2 are redundant in their function but essential for embryonic development (Chiang *et al.* 2008). Both enzymes bear PARP-activity and post-translationally modify proteins participating in maintenance of telomere length, sister telomere association, glucose metabolism (Hsiao, Smith 2008), and organisation of the

mitotic spindle apparatus (Chang *et al.* 2005). Moreover, TNKS-1 is involved in separation of sister telomeres (Canudas *et al.* 2007) and control of axis inhibition protein 1 *(*Axin), a tumour suppressor and negative regulator of the Wnt/β-catenin signaling pathway (Morrone *et al.* 2012).

## 1.3.3 POLY(ADP-RIBOSYL)ATION

This chapter is a summary of the reaction catalysed by PARP, the so called PARylation. The $NAD^+$ metabolism is briefly elucidated for better understanding.

### 1.3.3.1 NAD METABOLISM

First of all, a closer look on $NAD^+$ and its metabolism is necessary to better understand PARylation, since the reaction is dependent on $NAD^+$ as cosubstrate. The dinucleotide $NAD^+$ is crucial for the metabolism of all living cells. It consists of two nucleotides connected on their phosphate groups. In the cell, $NAD^+$ is prevalent in its oxidized form $NAD^+$ and reduced form NADH, respectively, forming a potent redox couple. Generally, $NAD^+$ is involved in redox reactions, accepting or donating electrons. NAD can be synthesised *de novo* from tryptophan or aspartic acid. In an alternate fashion, $NAD^+$ can be obtained from vitamin $B_3$ (niacin) and nucleosides containing a pyridine group. The mutual step in $NAD^+$ generation is arising from the dinucleotide consisting of AMP and a pyridine nucleotide. Key enzyme in this reaction is the NMN adenyltransferase (NMNAT) transferring the adenyl group of ATP on the mononucleotide. Under excess of ATP, $NAD^+$ is mostly synthesised from pyridine mononucleotides originating from exogenous sources. Beside its role in redox reactions, $NAD^+$ can be phosphorylated by NAD kinase, converting $NAD^+$ to $NADP^+$. Latter is important for defence of reactive oxygen species (ROS), biosynthesis or detoxification reactions, and the oxidative burst during immune responses. A great moiety of $NAD^+$ consuming processes are involved in the cells signalling, summarized as ADP-ribose transfer reactions, which include ADP-ribose cyclization, deacetylation of proteins by the sirtuin family, mono(ADP-ribosyl)ation associated with cell signalling, and of course PARylation. PARylation consumes a major part of the cell's $NAD^+$ pool and is therefore critical for maintenance of the energy balance (Chiarugi *et al.* 2012). Intense activation of PARP-1 causes depletion of $NAD^+$, and ATP stocks in the cell. As a consequence, necrotic cell death is triggered by energy loss (Ha, Snyder 1999). This is of particular importance for pathogenesis, such as ischemia reperfusion injury and myocardial infarction (Ebrahimkhani *et al.* 2014; Pacher, Szabo 2007).

### 1.3.3.2 POLY(ADP-RIBOSYL)ATION

PARylation is a posttranslational protein modification in which ADP-ribose units are transferred from $NAD^+$ molecules onto glutamate, aspartate (D'Amours *et al.* 1999), and lysine residues of target proteins (Altmeyer *et al.* 2009). This results in the formation of a linear or branched polymer of PAR with unique 1''–2' ribose-ribose glycosidic linkages and 5'–5'' pyrophosphate linkages (Doly, Mandel 1967; Miwa *et al.* 1979; Miwa, Sugimura 1982; Nishizuka *et al.* 1967; Reeder *et al.* 1967; Sugimura, Fujimura 1967),

whereas branches are connected via 1'''–2'' ribose-ribose glycosidic bonds (Juarez-Salinas *et al.* 1982; Juarez-Salinas *et al.* 1983) (**Figure 9**).

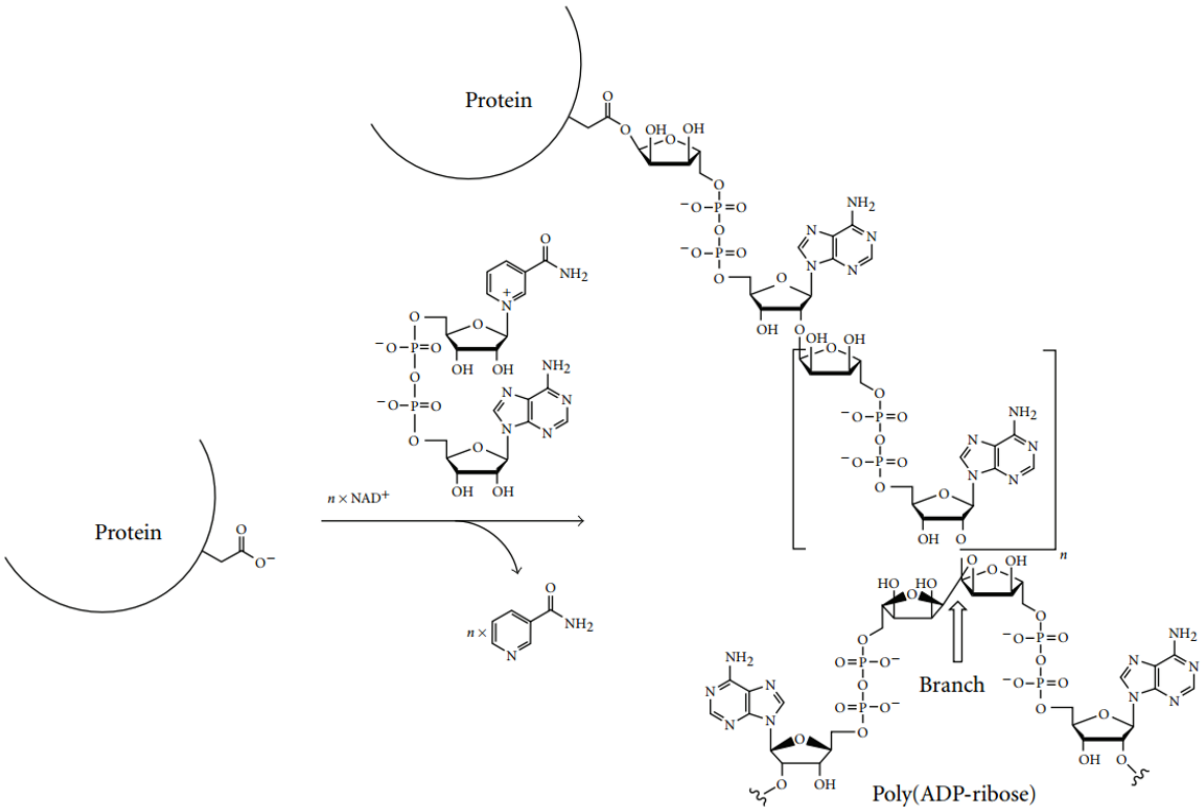


**Figure 9: Structure of the PAR polymer.** PARP-1 cleaves the glycosidic bond connecting the nicotinamide and ribose moiety of the $NAD^+$ molecule and covalently attaches an initial ADP-ribosyl unit to the acceptor protein. Subsequently, the enzyme catalyses elongation of the linear PAR chain with its characteristic ribose-ribose-phosphate-phosphate backbone. Branches are attached via 1'''-2'' glycosidic linkages to the linear polymer (Mangerich, Bürkle 2012).

The length of the PAR chain can reach up to 200 molecules (Bürkle 2005). About 90 % of the PAR is synthesised by the nuclear enzyme PARP-1 in the cell (Kim *et al.* 2005). The tertiary structure of PAR is yet unclear. Due to its nucleic acid-like attributes, a helical formation of the polymer, stabilised through hydrogen bonds, was assumed, although nuclear magnetic resonance (NMR) analysis was not able to confirm this theory (Schultheisz *et al.* 2009). The assembly of the PAR polymer can be differentiated in the following steps:

I. initiation: the initial ADP-ribose moiety is attached to the acceptor protein
II. elongation: further ADP-ribose molecules are linked via 2'-1'' glycosidic bonds
III. branching: branches are attached via 2''-1''' glycosidic bonds on the carbon of the parental chain (Alvarez-Gonzalez, Mendoza-Alvarez 1995).

PARP-1 is the predominant target of PARylation, 90 % of PAR is found on PARP-1 itself (Huletsky *et al.* 1989). AutoPARylation can occur in different patterns. For one thing, an extensive amount of ADP-ribose chains with >200 units can be added to PARP-1 by itself, otherwise a single molecule (monoPARylation) or small chains up to 20 units in length (oligoPARylation) (D'Amours *et al.* 1999; Mendoza-Alvarez, Alvarez-Gonzalez 1999). Substantial autoPARylation of PARP-1 leads to

suppression of its DNA binding and catalytic activity (D'Amours *et al.* 1999). *In vitro* analysis confirmed PARP-1's release from chromatin after activation and autoPARylation (Kim *et al.* 2004; Petesch, Lis 2008; Tulin, Spradling 2003; Wacker *et al.* 2007). In contrast, the impact of minor autoPARylation of PARP-1 is still unclear. This might be a mechanism to alter PARP-1's function (Krishnakumar, Kraus 2010b). Over 40 target proteins for covalent PARylation have been identified in the past, playing important roles in the following processes: modulation of chromatin structure (*e.g.* histones, topoisomerases (Althaus, Richter 1987; D'Amours *et al.* 1999) and DEK (Fahrer *et al.* 2010; Kappes *et al.* 2008)), DNA synthesis (*e.g.* DNA ligases and DNA polymerases), transcription (*e.g.* RNA polymerases and HMG proteins), and cell cycle (*e.g.* p53 and of proliferating cell nuclear antigen (PCNA)) (Althaus, Richter 1987; D'Amours *et al.* 1999).

Numerous proteins can interact with PAR in a non-covalent manner (Krietsch *et al.* 2013), yet with high affinity and specificity depending on PAR chain length (Fahrer *et al.* 2007). A special sequence of AAs is suggested to be responsible for non-covalent interactions. Four different motifs respectively domains have been reported in the past. The so called PAR-binding motif (PBM) is present in many proteins involved in DNA repair, chromatin remodelling, and ribonucleic acid (RNA) processing (Gagne *et al.* 2008). The PBM is characterised by a N-terminal sequence of basic AAs $(HKR]_1$-$X_2$-$X_3$-$[AIQVY]_4$-$[KR]_5$-$[KR]_6$-$[AILV]_7$-$[FILPV]_8$), which carries several Lys-Arg clusters interrupted by hydrophobic AAs (Pleschke *et al.* 2000). It is likely that the basic and hydrophilic residues of this motif cooperate to recognise PAR. Variations in the sequence of PBMs might indicate a general affinity to charged polymers including PAR, RNA, or DNA (Huambachano *et al.* 2011). The PAR-binding zinc finger (PBZ) represents the second motif that is able to bind PAR. The small and unstructured PBZ are related to singe stranded RNA (ssRNA)-binding zinc fingers. They are present in proteins participating in DNA damage response and check point control proteins. Alterations of the binding motif go in line with functional losses (Ahel *et al.* 2008; Eustermann *et al.* 2010; Isogai *et al.* 2010). A zinc-coordinated fold in the binding motif, which promotes interactions with one or two adenine residues of a PAR unit and the charcacteristic 1''–2' ribose-ribose glycosidic linkage of PAR, is responsible for the specificity for PAR polymers (Gibson, Kraus 2012). Another motif that binds to PAR is the so called macrodomain, which is found, among others, in histone macro H2A (Nusinow *et al.* 2007; Ouararhni *et al.* 2006) and members of the macroPARP family (Oberoi *et al.* 2010). The macrodomain shows affinity for the ADP-ribose units of the PAR polymer and, moreover, for other $NAD^+$ metabolites (*e.g.* ADP-ribose and O-acetyl-ADP-ribose) (Karras *et al.* 2005; Neuvonen, Ahola 2009). The WWE domain is the fourth known PAR binding motif, which is present in ligases including E3 ubiquitin-protein ligase RNF146 (Zhang *et al.* 2011), and interacts with iso-ADP ribose (e.g. the ADP-ribose monomer) (Aravind 2001; Wang *et al.* 2012).

### 1.3.4 DEGRADATION OF PAR

PARylation is a transient process with rapid turnover and responsive temporal regulation of target proteins. A variety of enzymes play a role in PAR catabolism, from which poly(ADPribose) glycohydrolase (PARG) is the most prominent. PARG exists in five posttranscriptionally modified variants, which all exhibit endo- as well as exoglycohydrolase activity. The enzyme is localised in

different compartments of the cell, including nucleus, cytoplasm and mitochondria (Meyer *et al.* 2007; Meyer-Ficca *et al.* 2004; Niere *et al.* 2008; Niere *et al.* 2012). A further important PAR degrading enzyme is the ADP-ribosylhydrolase 3 (ARH3), which hydrolyses the polymer but is, in contrast to PARG, not competent to cleave the terminal ADP-ribose unit directly mounted to the target protein (Niere *et al.* 2012).

### 1.3.5 ROLE OF PARP-1 IN DNA REPAIR

DNA strand breaks initiate recruitment of PARP-1 to the site of damage where its activity dramatically increases (up to 500-fold) (Jacobson, Jacobson 1976). The formed polymer disrupts the function of modified proteins, including PARP-1 itself, with its large negative charge density. This leads to reduced affinity of PARP-1 to negatively charged DNA by electrostatic repulsion. Furthermore, PARylation of histones leads to decondensation and relaxation of the chromatin, which renders the DNA accessible to repair proteins recruited by PARP-1 respectively PARylation (Althaus 1992). The absence of PARP-1 has been associated with sensitivity towards the geno- and cytotoxic effects of alkylating agents and ionising radiation *in vitro* and *in vivo* (Mangerich, Bürkle 2012; Murcia *et al.* 1997).

PARP-1's involvement in BER and the repair pathway are described in 1.2.3.

Beside its crucial role in BER, studies revealed the contribution of PARP-1 to other repair pathways. The nucleotide excision repair (NER) removes bulky helix-distorting DNA adducts evoked by UV radiation and endogenous metabolites (Hoeijmakers 2001). Here, DNA-dependent ATPase Cockayne syndrome group B (CSB) (Flohr *et al.* 2003; Thorslund *et al.* 2005), damage specific DNA binding protein 2 (DDB2) (Pines *et al.* 2012), and DNA damage recognition and repair factor xeroderma pigmentosus (XPA) (Fahrer *et al.* 2007; Garinis *et al.* 2008; King *et al.* 2012; Pleschke *et al.* 2000) have been reported to interact with PARP-1. Additionally, *in vitro* studies confirmed PARP1 activation upon exposure to UV irradiation (King *et al.* 2012).

DSBs represent the most critical and cytotoxic type of DNA damage caused by ionizing radiation, free radicals, chemicals, or disruption of the replication fork. Two mechanisms can repair DSBs: the error free homologous recombination repair (HRR) and the error prone non-homologous end-joining (NHEJ). Shrivastav and colleagues suggested that PARP-1 acts as a DNA-damage-detecting molecule activating the appropriate DSB repair pathway (Shrivastav *et al.* 2008). HRR requires a sister chromatid as template for repair of the DSB and can therefore only succeed in S and $G_2$ phases (Christmann *et al.* 2003). At initial steps, PARP-1 contributes by interaction with the DSB sensing MRE11/Rad50/NBS1 (MRN) complex potentially guiding them to the site of damage and competes with them for binding at free DNA ends (Haince *et al.* 2008). Additionally, PARP-1 cooperates with the phosphatidyl inositol 3-like protein kinase (PIKK) ataxia telangiectasia mutated (ATM), which is essential for DSB damage signalling (Aguilar-Quesada *et al.* 2007; Haince *et al.* 2007). In contrast, NHEJ joins the free ends of the DNA strand without a template, which is likely to result in insertions or deletions and frame-shift mutations (Christmann *et al.* 2003). PARP-1 recruits Ku70/80 at the DSB, thereby initiating the repair process. Moreover, PARP-1 competes with Ku70/80 for binding at free DNA ends (Wang *et al.* 2006) and interacts with the PIKK DNA-dependent protein kinase catalytic subunit (DNA-PKcs),

which, in association with Ku70/80, processes the DSB (Ruscetti *et al.* 1998; Spagnolo *et al.* 2012). An alternative end joining pathway, backup non-homologous end-joining (B-NHEJ), is activated when the HRR (Soni *et al.* 2014) and the classical DNA-PK-dependent NHEJ fails (Iliakis 2009). Failure of HRR and NHEJ can result from loss of an essential factor (*e.g*. by mutation) or failures in repair of individual DSBs (*e.g.* malfunctioning assembly of repair machinery or lacking key factors) (Schipler, Iliakis 2013). Multiple studies successfully confirmed the dependency of B-NHEJ on PARP-1 (Audebert *et al.* 2004; Schipler, Iliakis 2013; Soni *et al.* 2014; Wang *et al.* 2006).

## 1.3.6 PARP-1 AND IMMUNE RESPONSE

A brief summary of the immune response is presented to put the processes in which PARP-1 takes part in a broader context.

### 1.3.6.1 THE INNATE IMMUNE RESPONSE

The unspecific innate immune defence responds to microorganisms and pathogens in an universal way (Litman *et al.* 2005) and does not confer a persisting immunity against a specific pathogen. However, it is the dominant host defence mechanism in most organisms. Inflammation represents the frontline response to infection or irritation driven by chemical factors, which are secreted by harmed cells (Alberts 2002; Matzinger 2002; Medzhitov 2007). Inflammation establishes a physical barrier preventing a spreading of the infection and facilitates healing of damaged tissue after elimination of pathogens. Acute inflammation is initiated by immune cells resident in the tissue: macrophages, dendritic cells, histiocytes, Kupffer cells, and mastocytes. The immune cells are equipped with pattern recognition receptors (PRRs) competent for recognition of pathogen-associated molecular patterns (PAMPs). PAMPs are specific pathogens-related molecules including bacterial lipopolysaccharides or proteins and nucleic acids of viruses. Toll-like receptors (TLRs) are a class of PRRs, playing a key role in the innate immune response. TLRs are expressed on the surface of sentinel cells (*e.g.* macrophages and dendritic cells) which promote the subsequent adaptive immune response upon recognition of a PAMP. Inflammatory mediators causing the clinical characteristics of inflammation are released by activated immune cells. These pro-inflammatory factors (histamine, bradykinin, serotonin, leukotrienes, and prostaglandins) promote sensitisation of pain receptors, local vasodilatation, and attraction of phagocytes (Stvrtinová *et al.* 1995). A major part of the phagocytes is constituted of neutrophils, which trigger further parts of the immune system by secretion of factors attracting leukocytes and lymphocytes. Leukocytes of the innate immune system include: natural killer cells, mast cells, eosinophils, basophils, and phagocytic cells. Phagocytic cells can be further distinguished into macrophages, neutrophils, and dendritic cells (Janeway 2005). Cytokines produced by cells of the innate immune system, especially macrophages, maintain the inflammatory response. Important cytokines are high mobility group box 1 protein (HMGB1), interleukin-1 (IL-1), and the tumour necrosis factor superfamily (TNF) (Lotze, Tracey 2005), which are all reported to participate in the activation of the inflammatory master regulator nuclear factor '*kappa*-light-chain-enhancer' of activated B-cells (NF-κB) (Ebrahimkhani *et al.* 2014; Fitzgerald *et al.*

2007; Luan *et al.* 2010; Renard *et al.* 1997). Additionally, ROS, produced by macrophages, are also important for pro-inflammatory signalling (Hargrave *et al.* 2003).

#### 1.3.6.2 THE ADAPTIVE IMMUNE RESPONSE

The adaptive immune system facilitates a stronger immune response and, in contrast to the innate immune system, even an immunological memory. Adaptive immune response works in an antigen-specific manner and requires identification of pathogen-exclusive antigens for the so-called antigen presentation. This response is slower than the innate immune response but allows a particular response only targeting pathogens or infected cells. Specific memory cells can easily eradicate a pathogen in case of repeated infection (Pancer, Cooper 2006). A subpopulation of leukocytes, the lymphocytes, which derive from hematopoietic stem cells, constitute the adaptive immune system. The major cell types are the B-cells being responsible for the humoral immune response and T-cells that are responsible for cell-mediated response. Both cell types are equipped with receptor molecules to identify specific targets. T-cells are only able to recognise pathogens after the antigens have been presented in combination with a major histocompatibility complex (MHC) molecule. In contrast, the receptor prominent on the surface of B-cells is able to recognise whole pathogen without prior processing of antigens (Janeway 2005).

#### 1.3.6.3 ROLE OF PARP-1 IN THE INFLAMMATORY RESPONSE

Genetic studies in PARP-$1^{-/-}$ mice revealed the involvement of PARP-1 in inflammatory processes and related pathologies. PARP-1-deficient animals are protected from inflammation-associated pathologies including ischemic infarction, collagen induced arthritis, and LPS-induced septic shock (Chevanne *et al.* 2007; Hassa, Hottiger 2002). Further, loss of PARP-1 causes resistance to MPTP-induced Parkinson's disease and streptozotocin-induced diabetes mellitus (Burkart *et al.* 1999; Mandir *et al.* 1999; Masutani *et al.* 1999; Pieper *et al.* 1999). Various studies reported that PARP-1 is involved in transcriptional processes by either general chromatin remodelling or interaction and regulation of transcription factors (Braun, Anderson 2007; Kraus 2008). NF-κB is a central player regulating gene expression in response to inflammatory stimuli. The homo- or hetero-dimeric transcription factor is assembled of two Rel family members including RelA/p65, RelB, c-Rel, p50, and p52, of which p65 and p50 represent the major subunits. Inactive NF-κB is bound to inhibitor of κB (IκB) proteins in the cytoplasm, which are phosphorylated upon inflammatory stimuli by IκB kinases (IKKs). Ubiquitination and proteasomal degradation of IκBs releases NF-κB, which translocates into the nucleus. Here, NF-κB acts as a transcription factor activating preferentially inflammation-related genes (Hayden, Ghosh 2008). Posttranslational modifications and transcriptional cofactors strictly regulate NF-κB within the nucleus. Importantly, NF-κB activates the expression of genes related to aging in both mice and humans (Adler *et al.* 2008). Recent studies unveiled that hyperactive NF-κB signalling promotes premature aging in mice (Kawahara *et al.* 2009). Moreover, inhibition of NF-κB in aged mice successfully reversed several characteristics of skin aging (Adler *et al.* 2007; Adler *et al.* 2008). In line with these findings, the lifespan of Drosophila melanogaster was extended by about 15 % through pharmacological suppression of

NF κB (Moskalev, Shaposhnikov 2011). *In vitro* studies in human fibroblasts revealed an induction of NF-κB-dependent gene transcription in response to genotoxic stress and suggest a role of NF-κB in the aetiology of senescence (Rovillain *et al.* 2011). In accordance with this, NF-κB signalling contributes to the maintenance of senescence (Wang *et al.* 2009b) and is necessary for transcription of many factors of the senescence-associated secretory phenotype (SASP) (Freund *et al.* 2010; Ohanna *et al.* 2011). Taken together, there is a growing body of evidence for the crucial role of NF-κB in aging and related diseases (Tilstra *et al.* 2011).

PARP-1 and NF-κB show very similar activation and expression patterns in many tissues (Mangerich, Bürkle 2012). This notion was supported by the discovery that PARP-1$^{-/-}$ mice exhibit changes in expression of NF-κB-dependent pro-inflammatory mediators including TNFα, IL6, E-selectin, ICAM-1 and nitric oxide synthase (NOS) (Haddad *et al.* 2006; Hassa, Hottiger 2002; Jijon *et al.* 2000; Naura *et al.* 2009; Oliver *et al.* 1999). PARP-1 was found to interact with the p65 and p50 subunits of NF-κB (Hassa, Hottiger 2002). Inflammatory stimuli facilitate the interaction of PARP-1 with histone acetyl-transferases p300 and CREB-binding protein (CBP) to activate NF-κB-dependent gene expression in a synergistic manner. The acetylation of PARP-1 by p300/CBP is necessary for the interaction of PARP-1 with p50, enhancement of p300–p50 interaction, and coactivation of NF-κB-mediated gene expression (Hassa *et al.* 2003; Hoesel, Schmid 2013). The subsequent expression of pro-inflammatory mediators leads to the generation of reactive chemicals, which themselves cause additional DNA damage, thereby establishing a positive feedback mechanism of PARP-1 activation. In this context, neither DNA binding nor catalytic activity of PARP-1 was required for activation of NF-κB (Hassa *et al.* 2001). However, PARP-1 acts as a trigger for translocation of NF-κB to the nucleus (Stilmann *et al.* 2009), while inhibition of PARP's catalytic activity is enough to reduce the expression of the pro-inflammatory mediators mentioned above *in vitro* and *in vivo* (Haddad *et al.* 2006; Hottiger, Altmeyer 2009; Jijon *et al.* 2000). A model presented by Mangerich and Bürkle in 2012 describes the recruitment of PARP-1 to DNA strand breaks followed by autoPARylation. Automodified PARP-1 dissociates from the DNA strand and then recruits further factors (including SUMO1 ligase PIASy, IKKγ (NEMO), and ATM) to form a signalosome. The complex is stabilised by protein:protein interactions of the recruited factors together with the binding of PIASy and ATM to the PAR polymer via specific binding motifs. In the next step, destabilisation of the signalosome by PARG results in the SUMOylation of IKKγ, followed by its translocation to the cytoplasm, phosphorylation of IκB proteins and thereby NF-kB activation. This signalling mechanism connects the role of PARP-1 in DNA damage signalling directly to the NF-κB mediated inflammatory response (Mangerich, Bürkle 2012) (**Figure 10**).

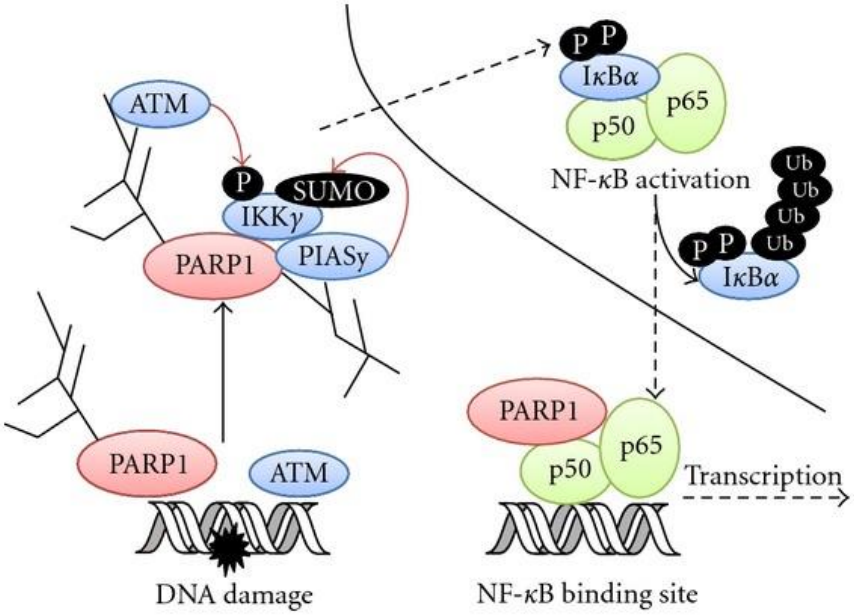


**Figure 10: PARP-1 mediated activation of NF-κB.** PARP-1 activation through DNA damage includes formation of a signalosome which causes NF-κB activation (Mangerich, Bürkle 2012).

Beside the important role of NF-κB in the acute immune response, it is also involved in the elimination of degenerated and potentially cancerous cells. However, the activation of pro-inflammatory factors by PARP-1-NF-κB signalling might contribute to a low-level chronic inflammation, promoting tumour formation and aging (Ohanna *et al.* 2011). A disturbed regulation of the NF-κB signalling pathway was found in several types of cancer including breast, prostate, and head and neck cancer (Gilmore *et al.* 2002). PARP inhibition might also alleviate adverse effects of anti-cancer drugs, suggesting a positive effect of inhibitors in multidrug regimens (Korkmaz *et al.* 2008). In addition, inhibition of the NF-κB signalling pathway is reported to disturb angiogenesis and metastasis (Huang *et al.* 2001; Ohanna *et al.* 2011). Surprisingly, HRR proficient human epidermal growth factor receptor 2 (HER2)-positive breast cancer cells are reported to show sensitivity towards PARP inhibition through suppression of NF-κB-mediated signalling (Nowsheen *et al.* 2012). Challenge with a PARP inhibitor caused reduction of IKKα expression levels and phosphorylated p65 with increasing IkBα, which together result in attenuated NF-κB transcriptional activity in HER2-positive breast cancer cells, while HER2-negative cells remain unaffected (Nowsheen *et al.* 2012). Overexpression of HER2 alone mediates sensitivity to PARP inhibition, indicating synthetic lethality with PARP inhibition in HER2 overexpressing cancer cells via NF-κB-related signal pathways (Weaver, Yang 2013). A recent work studied the innate inflammatory response in PARP-1-deficient mice after challenge with DSS only. The resistance to chemically induced colitis of PARP-$1^{-/-}$ animals goes in line with reduced expression of pro-inflammatory cytokines including interferon-γ (IFNγ) and tumour necrosis factor alpha (TNFα), a transcriptional reprogramming of the colon, and modulation of the microbial flora in the gut (Larmonier *et al.* 2016).

## 1.3.7 OTHER FUNCTIONS OF PARP-1

### 1.3.7.1 TRANSCRIPTION

Electrostatic repulsion between the PAR polymer and the DNA also influences transcriptional processes. PARylation of transcription factors abrogates their DNA binding and thus activation of target genes (Mendoza-Alvarez, Alvarez-Gonzalez 2001; Oei *et al.* 1997; Wesierska-Gadek *et al.* 1996b). Formation of the pre-initiation complex is inhibited by PARylation of the TATA-binding protein (Oei *et al.* 1998b; Oei *et al.* 1998a). Notably, PARylation of histones, leading to remodelling of chromosomes and relaxation of chromatin, renders DNA sequences accessible and thereby allows transcription (Beneke 2012). DNA methylation is another important mechanism, influencing the transcription of genes. The methylation of CpG sites in the promoter region of genes can reduce their expression (Herfarth *et al.* 1999). The cytosine bases in the CpG sites are transformed to 5-methylcytosine by an enzyme called DNA methyltransferase (DNMT) (Bird 2002), which harbours two PBMs (Reale *et al.* 2005). Studies demonstrated a hypermethylation of DNA caused by inhibition of PARP-1 (Capoa *et al.* 1999; Zardo *et al.* 1999) and alteration of DNA methylation patterns in case of PARP-1 over-activation (Guastafierro *et al.* 2008). PAR is suggested to compete with DNA for binding of DMNT, thus inhibiting DNA methylation (Zampieri *et al.* 2009). In a more specific manner, PARP-1 can promote the activity of RNA polymerase II at promoters through a histone demethylase KDM5B-dependent way (Krishnakumar, Kraus 2010a), enhancement of the RNA polymerase II mediator complex by PARylation of repressing factors (Gamble, Fisher 2007), and formation of a scaffold structure to support RNA polymerase II (Zobeck *et al.* 2010).

### 1.3.7.2 TELOMER STABILITY

PARP-1 is involved in the protection of the telomeres. The repetitive sequences at the end of the chromosomes are vulnerable to degradation during replication (Blasco 2005; Liu *et al.* 2004). According to the literature, few works revealed a loss of almost 1/3 of telomeric DNA in PARP-1$^{-/-}$ mice (Di d'Adda Fagagna *et al.* 1999; Tong *et al.* 2001), while other groups reported no effect (Espejel *et al.* 2004; Samper *et al.* 2001). However, inhibition of PARP-1 leads to the decrease of telomere length in line with the fact that reconstitution of PARP-1 activity allows regain in telomeric length (Beneke *et al.* 2008). PARP-1 is sporadically localised at normal telomeres, whereas it is abundant at eroded telomeres, preventing fusion of chromosomes and genomic instability (Gomez *et al.* 2006). Further, PARP-1 is known to interact with the Werner syndrome RecQ like helicase (WRN), which is also involved in telomeric maintenance (Rossi *et al.* 2010). Mutation of WRN causes the so called Werner syndrome, a disorder which causes premature aging of the patients (Mangerich, Bürkle 2012).

### 1.3.7.3 DNA REPLICATION, CELL CYCLE AND MITOSIS

During replication, the DNA is vulnerable to critical events like stalling replication forks from which cytotoxic DSBs can arise. Checkpoint pathways are important to maintain genomic integrity (Branzei, Foiani 2005, 2007). Upon detection of a stalled or collapsed replication fork, PARP-1 attracts the MRN complex, which is needed for processing of the DNA ends. Subsequently, the intermediate single-stranded DNA (ssDNA) is coated with replication protein A (RPA). HRR is then started by

replacement of RPA with RAD51 (Bryant *et al.* 2009; Jones, Petermann 2012). The topoisomerase I inhibitor camptothecin slows the replication fork and induces unusual structures like a "reversed fork". The DNA polymerase extends the new DNA strand in reversed direction, giving rise to a trident shaped structure. PARP-1 is necessary for the successful repair of the degenerated fork and prevention DSB (Ray Chaudhuri *et al.* 2012). Mitosis is another process that is critical for genomic integrity (Scholey *et al.* 2003). The PARP family member TNKS1 (1.3.2) acts as a key regulator for assembly of the mitotic spindle, and also PARP-3 was recently reported to contribute to this event (Boehler *et al.* 2011). Moreover, PARP-1 and PARP-2 interact with the centromere proteins Cenpa, Cenpb and the spindle check point protein Bub3 (Kanai *et al.* 2000; Kanai *et al.* 2003; Kanai *et al.* 2007; Saxena *et al.* 2002a; Saxena *et al.* 2002b).

#### 1.3.7.4 p53 TUMOUR SUPPRESSOR PROTEIN

The tumour suppressor p53 has a central function in genomic maintenance (Gomez-Lazaro *et al.* 2004; Romer *et al.* 2006). Upon DNA damage, p53 either halts the cell cycle to allow DNA repair or, in case of severe damage, triggers apoptosis (Reinhardt, Schumacher 2012). Studies revealed lower p53 levels in PARP-1-deficient cells and demonstrated direct interaction of the two proteins *in vitro* as well as *in vivo* (Wesierska-Gadek *et al.* 1996a; Wesierska-Gadek *et al.* 1996b; Wesierska-Gadek *et al.* 2003a, 2003b). p53 holds three PBMs, which facilitate a differential response to PAR formation induced by DNA damage (Malanga 1998). Low PAR levels obstruct the association of p53 with ssDNA and favour its transcriptional activity. In contrast, high PAR levels prevent the association of p53 with double-stranded DNA (dsDNA), thereby promoting its transcriptional activity. Moreover, excessive PARP-1 activation in line with massive consumption of $NAD^+$ is suggested to inhibit p53 activities and thus contributing to initiation of apoptosis (Alano *et al.* 2004; Malanga, Althaus 2005; Yu *et al.* 2002). High PAR levels induced by DNA damage are reported to mask the nuclear export sequence of p53, resulting in an accumulation in the nucleus. Accumulation of p53 in the nucleus leads to subsequent activation of its transactivational functions including the induction of cell cycle arrest and apoptosis (Kanai *et al.* 2007; Malanga, Althaus 2005).

#### 1.3.7.5 CELL DEATH

PARP-1 is involved in several cell death pathways. Depending on its activity, PARP-1 consumes a large portion of the cellular $NAD^+$ stock (Berger, Berger 1986; Carson *et al.* 1988; Juarez-Salinas *et al.* 1979). The result of PARP-1 hyperactivation is depletion of cellular energy resources ($NAD^+$ and ATP) upon DNA damage, triggering necrosis (Huang *et al.* 2009; Zong *et al.* 2004). The degradation of PAR by PARG creates a huge amount of ADP-ribose, which is further hydrolysed to phosphoribose and AMP by the pyrophosphohydrolases NUDIX, NUDT5 and NUTD9 (Formentini *et al.* 2009). The altered AMP:ATP ratio triggers autophagy via inhibition of the TORC1 signal pathway (Ethier *et al.* 2012). Moreover, PARP-1 is able to induce cell death through modulation of p53 (Beneke *et al.* 2000; Kumari *et al.* 1998). PARP-1 is cleaved by caspase-3/7 in a small (24 kDa) and a large (89 kDA) fragment in

order to inactivate the catalytic activity of the enzyme and prevent depletion of the cellular energy resources during apoptosis (Germain *et al.* 1999; Koh *et al.* 2005).

PARP-1 regulates the c-Jun N-terminal kinase (JNK)-mediated necrotic cell death (Chen *et al.* 2001; Yang *et al.* 2004). MAP kinase phosphatase MKP-1 expression and Akt/protein kinase B, which both activate JNK, are inhibited by PARP-1 (Racz *et al.* 2010; Szanto *et al.* 2009). Furthermore, PARP-1 triggers a caspase-independent pathway of cell death named “Parthanatos” (Andrabi *et al.* 2006; David *et al.* 2009). PAR, either as free polymer or protein-associated, translocates from the nucleus into the cytosol leading to the release of apoptotic inducing factor (AIF) from the mitochondria. Subsequently, AIF shifts into the nucleus to promote cell death (Andrabi *et al.* 2008; Chiu *et al.* 2011).

### 1.3.8 INFLUENCE OF PARP-1 ON TUMOURIGENESIS

Beyond its contribution to DNA repair, inflammation, genomic maintenance, and the other processes presented previously in this work, PARP-1 influences the activity of JNK and extracellular-signal regulated kinases (ERK) in a positive manner, thus promoting MAPK-dependent growth signalling (Chiarugi *et al.* 2012; Racz *et al.* 2010), which has been identified as a driver of tumour development and treatment response in many cancers (Chen *et al.* 2001; Yang *et al.* 2004). Beside cell death, ERK facilitates tumour progression, angiogenesis, and metastasis. The activation of ERK contributes to the survival of cancer cells by the induction of anti-apoptotic proteins and suppression of caspase activity (Boucher *et al.* 2000). Disruption of the ERK signal pathway has been linked to the suppression of tumour growth (Kandala *et al.* 2012), reduced metastatic potential (Kim *et al.* 2012), and sensitivity to cytotoxic agents (Kohno *et al.* 2011).

PARP-1 is involved in a plethora of cellular functions, including both DNA-repair related (1.2.3 and 1.3.5) and unrelated (1.3.6 and 1.3.7) processes, making it a worthwhile target for prevention and even therapy of cancer. A recent review summarised the DNA repair-independent functions and related them to the "hallmarks of cancer" proposed by Hanahan and Weinberg (Weaver, Yang 2013) (**Figure 11**).

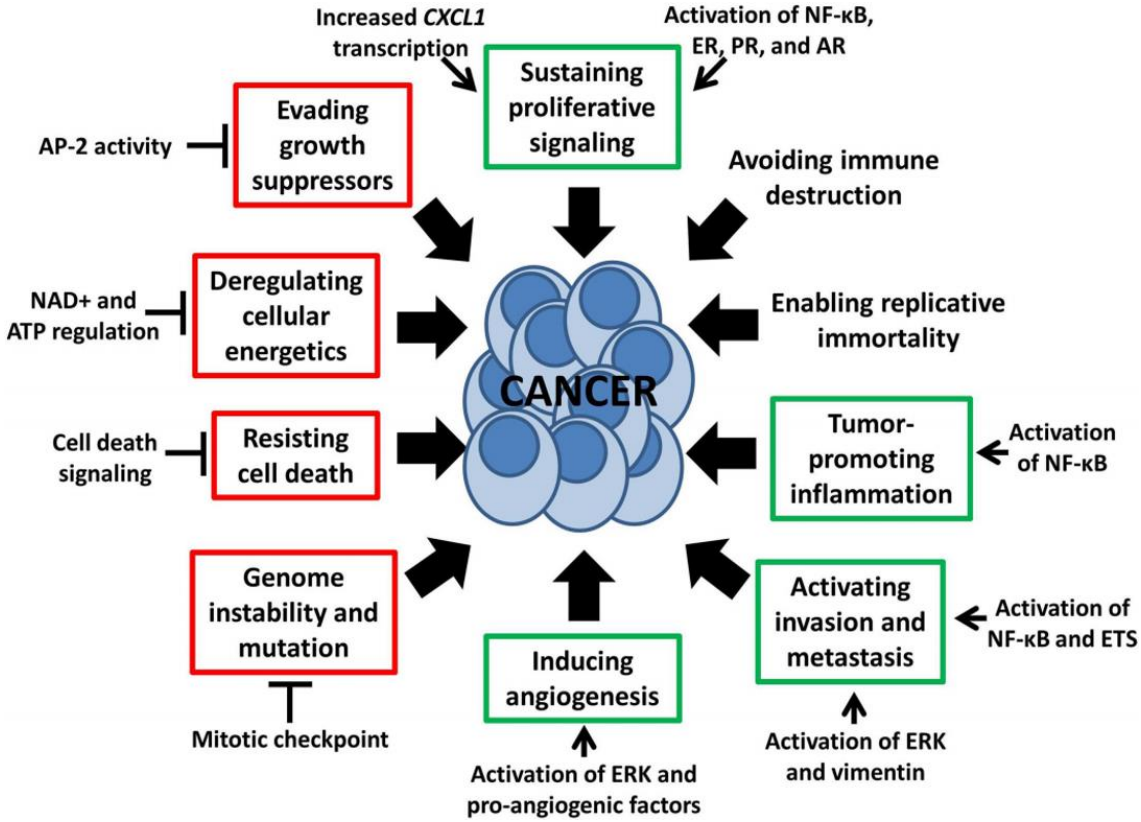


**Figure 11: DNA repair-unrelated functions of PARP-1 influencing the "hallmarks of cancer" (Hanahan, Weinberg 2011).** The figure summarises PARP-1-dependent processes which either suppress (red box) or stimulate (green box) the "hallmarks of cancer", proposed by Hanahan and Weinberg (Weaver, Yang 2013). See chapters 1.3.6.3 , and 1.3.7 for details.

#### 1.3.8.1 PARP INHIBITORS AND CANCER THERAPY

Lately, PARP-1 inhibitors gained great attention for their use in cancer therapy, either alone or in combination with other anti-cancer drugs. Studies of PARP-1 inhibitors for possible anticancer treatment exploit a mechanism called synthetic lethality. Inhibition of PARP-1 is cytotoxic in cells with defective HRR, whereas HRR proficient cells show no sensitivity. This includes cancers cells lacking BRCA2 (Bryant *et al.* 2005), tumour cells deficient for ATM (Weston *et al.* 2010), microsatellite unstable CRC cells lacking functional MRE11 (Vilar *et al.* 2011), and RAD51C-deficient cancer cells (Min *et al.* 2013). Meanwhile, the initial model has been challenged by several reports (Helleday 2011). The initial model suggests that the inhibition of PARP-1 causes the persistence of SSBs, which lead to collapse of the replication fork and the formation of one-ended DSBs. DSB-induction would be selectively toxic in BRCA-deficient cells lacking HRR (Bryant *et al.* 2005). In the second model, PARP-1 inhibitors are expected to trap PARP-1 onto SSBs, which are formed spontaneously or as intermediate during BER. This might create an obstacle for the replication machinery, which requires HRR to bypass (Strom *et al.* 2011). The third model proposes that PARP and HRR are activated in case of stalling of the replication fork due to the absence of replication factors or obstacles. This activates distinct pathways to restart the replication fork, including Mre11-dependent replication restart by HRR (Bryant *et al.* 2009). Additionally, PARP-1 activity plays a role in regulation of NEHJ in HRR-deficient cells and beyond that deregulation of NEHJ plays a central role in synthetic lethality (Patel *et al.* 2011). Further, studies reported that the deprivation of PARP-1 can inhibit the expression of the HRR key factors BRCA1 and RAD51 (Hegan *et al.* 2010).

PARP inhibitors are divided in six classes, according to their chemical structure (Mangerich, Bürkle 2011; Southan, Szabo 2003):

I. Benzamide analogues: A class with low potency and specificity, members are Nicotinamide, 3-aminobenzamide, and iniparib, which reached a phase III clinical trial. Unfortunately, a recent *in vitro* study could not confirm the inhibition of PARP by iniparib (Patel *et al.* 2012).
II. Isoquinolinones and dihydroisoquinolinones: This class is more effective compared to members of the first class. 3, 4-dihydroisoquinolin-1(2H)-ones and isoquinolin-1(2H)-ones.
III. Benzimidazoles, indoles, and related compounds: Members of this class, such as benzimidazole-4-carboxamides, are characterised by an $IC_{50}$ in the nanomolar range. A promising member, ABT-888 (also known as veliparib), was reported to enhance irinotecan treatment of CRC cell lines (Davidson *et al.* 2013) and has lately entered phase II clinical trials. It is applied for the treatment of solid tumors and together with TMZ in the treatment of glioblastoma (Kummar *et al.* 2011; Kummar *et al.* 2012).
IV. Phthalazin-1(2H)-ones and quinazolinones: This class exhibits good efficacy and pharmacokinetics. AZD2281 (also known as olaparib) is used in clinical trials for the treatment of solid tumours (Marchetti, Imperiale et al. 2012). Notably, olaparib was applied after failure of the standard therapy of colorectal cancer but lacked activity regardless of the tumour's microsatellite status (Leichman *et al.* 2016).
V. Isoindolinones: A class with good potency that is used in experimental studies.
VI. Phenanthridinones: Members of this class are also limited to the use in research.

#### 1.3.8.2 ROLE OF PARP-1 IN THE AETHIOLOGY OF CRC

Several studies confirmed increased PARP-1 mRNA and protein levels in human CRC (Idogawa *et al.* 2005; Nosho *et al.* 2006; Sulzyc-Bielicka *et al.* 2012), which is associated with localisation and stage of the tumour. PARP-1 expression was higher in colonic tumours compared to rectal tumours and also higher in Duke's B compared to Duke's C (Sulzyc-Bielicka *et al.* 2012).

PARP-1 was identified as coactivator of the β-catenin/T-cell factor(TCF)-4 complex (Idogawa *et al.* 2005), which plays a crucial role in the initiation of intestinal carcinogenesis (Giles *et al.* 2003). As described in (1.1.2), loss of *APC*, a common alteration during early genesis of human CRC, results in cytoplasmic accumulation of β-catenin (Vogelstein, Kinzler 2002). β-catenin forms a complex with the TCF-4, which only activates its target genes upon binding to β-catenin (Idogawa *et al.* 2005). In intestinal epithelial cells, TCF-4 regulates genes involved in growth and differentiation (*e.g. cyclin D1* and *c-myc*). Moreover, PARP-1 was reported to be a target of the cellular myelocytomatosis oncogene (c-Myc) (Shiio *et al.* 2002), which is regulated by the β-catenin/TCF-4 complex (He *et al.* 1998), indicating an indirect regulation of PARP-1 by the β-catenin/TCF-4 complex (Idogawa *et al.* 2005). A study analysing the expression levels of *PARP-1*, *β-catenin*, c-*myc* and *cyclin D1* in human CRC confirmed increased mRNA levels in early stage of CRC. Further, overexpression of PARP-1 is associated with β-catenin overexpression. Idogawa and colleagues reported a competitive regulation of the β-catenin/TCF-4-mediated gene activation by Ku70, which is part of the NHEJ and PARP-1. This finding indicates a potential linkage between DNA damage recognition and the Wnt signalling pathway (Idogawa *et al.* 2007).

About 440 single-nucleotide polymorphisms (SNPs) of PARP-1 have been reported in the last years. The Val762Ala SNP is the best known alteration and the only one associated with increased cancer risk (Yu *et al.* 2012; Zaremba *et al.* 2009). The mutation is a result of a base substitution in the PARP signature motif of the catalytic domain, which changes the enzymes catalytic activity by 30–40 % (Cottet *et al.* 2000) and possibly impairs the BER repair pathway (Wang *et al.* 2007). Noteworthy, the association of the Val762Ala SNP is heterogeneous among populations. An increased risk for cancer was observed in Chinese, whereas Caucasians showed decreased risk (Yu *et al.* 2012) and Saudi population (Alshammari *et al.* 2014) no change in risk. The Met129Thr genotype, which was only discovered in a single patient, located in one of PARP-1's zinc finger motifs (Shiokawa *et al.* 2005), might change the interaction with the DNA strand (Alshammari *et al.* 2014), as the zinc finger motifs play a role in DNA binding of PARP-1 (Ali *et al.* 2012; Langelier *et al.* 2012; Shiokawa *et al.* 2005). Alshammari and colleagues identified two further mutations, which had an impact on CRC risk in the studied Saudi population. The mutations Lys933Asn and Lys945Asn, both located in the PARP-1 CD, are also suspected to impact the enzyme's catalytic activity, possibly leading to its inactivation. Val762Ala and Met129Thr genotypes failed to affect cancer risk in Saudi population (Alshammari *et al.* 2014).

Taken together, alterations enhancing or disrupting the function of PARP-1 are likely to influence PARP-1-dependent processes in the cell (1.3.8), potentially leading to CRC formation.

Only few clinical trials concerning PARP inhibitors for treatment of cancer focus on CRC (Table 1).

**Table 1: Completed and current clinical trials treating CRC with PARP inhibitors (U.S. National Institutes of Health).**

| Drug | Clinical Trial Phase | Intervention | Patient risk stratification |
|---|---|---|---|
| Olaparib | Phase I | Combination | No |
| Olaparib | Phase III | Monotherapy | MSI status |
| Veliparib | Phase I | Combination | No |
| Olaparib | Phase II | Combination | No |

A recently completed clinical trial investigated the application of olaparib after failure of standard therapy of CRC but was not successful to show activity regardless of the tumour's microsatellite status (Leichman *et al.* 2016). The PARP family members TNKS1 and TNKS2 might be promising targets since they regulate the canonical Wnt/β-catenin pathway, which plays an important role during the genesis of CRC (Clevers 2006) (1.1.2). Both enzyme regulate Axin, which is the bottleneck in β-catenin degradation (Huang *et al.* 2009). A drug combination approach is suggested to enhance the potential of TNKS inhibition. This notion is supported by studies showing increased potency of agents aiming at MEK- and EGFR-pathways, combined with TNKS inhibition in *K-ras* mutated CRC cell lines (Lau *et al.* 2013) and lung cancer cell lines (Casas-Selves *et al.* 2012; Lupo, Trusolino 2014). Taken together, PARP inhibitors have failed to show an anti-cancer effect in clinical trials, yet. Future strategies exploiting specific pathways impaired in CRC, as described above, might be promising.

## 1.4 AOM/DSS PROTOCOL OF COLORECTAL CARCINOGENESIS

Laboratory animals rarely develop spontaneous colorectal tumours (Grasso, Creasey 1969). Hence, animal models utilising chemicals have been established to study CRC in rodents in the recent years. 1,2-dimethylhydrazine (DMH) and its metabolite AOM have been used to study colorectal carcinogenesis in mice and rats. DMH and AOM require several steps for metabolic activation to generate DNA-reactive molecules. After application, AOM is transported via the blood stream to the liver as first organ of contact. AOM is hydroxylated by the phase I enzyme cytochrome P450 2E1 (CYP2E1) to methylazoxymethanol (MAM) (Delker *et al.* 1998; Sohn *et al.* 1991), which is also the aglyconic derivate of glycoside cycasin occurring in cycad genera (LAQUEUR 1964; Luca *et al.* 1980). The unstable compound MAM, which has a half-life of 12 h under physiological conditions (Feinberg, Zedeck 1980; NAGASAWA *et al.* 1972), spontaneously decomposes to a highly reactive alkylating methyldiazonium ion (NAGASAWA *et al.* 1972). The methyldiazonium ion methylates macromolecules like the DNA, which results in the formation of the mutagenic lesions $O^6$-MeG, *N*7-MeG (1.2.1), and $O^4$-methylthymine (Herron, Shank 1979; Matsumoto, Higa 1966; O'Toole *et al.* 1993; Shank, Magee 1967). The oxidation of MAM to methylazoxyformaldehyde by the alcohol dehydrogenase (ADH) was first proposed by Schoental (Schoental 1973), and *in vitro* studies confirmed the ability of ADH to metabolise MAM (Feinberg, Zedeck 1980; Notman *et al.* 1982). Subsequent *in vivo* testing of the metabolic MAM activation in class I ADH-deficient deer mice in comparison with class I ADH proficient animals revealed comparable metabolic rates and levels of liver DNA alkylation in both animal strains.

These studies concluded that ADH holds the potential but is not necessary for the metabolisation of MAM (Fiala *et al.* 1984; Zheng *et al.* 1993). In contrast, later studies showed that inhibition of CYP2E1 *in vitro* prevented the oxidation of MAM (Sohn *et al.* 1991), and *in vivo* studies comparing CYP2E1 negative mice to WT animals clearly confirmed the requirement of CYP2E1 for metabolic activation of MAM (Sohn *et al.* 2001). MAM can be conjugated with glucuronic acid by the phase II UDP-glucuronosyltransferase and is excreted via the bile into the bowel. In the colon, MAM-glucuronide is hydrolysed by bacterial and mucosal β-glucuronidase and subsequently metabolised by the gut flora (Fiala 1977; Reddy *et al.* 1974). Furthermore, the expression of CYP2E1 was reported in the human gastrointestinal tract (Thorn *et al.* 2005) (**Figure 12**).

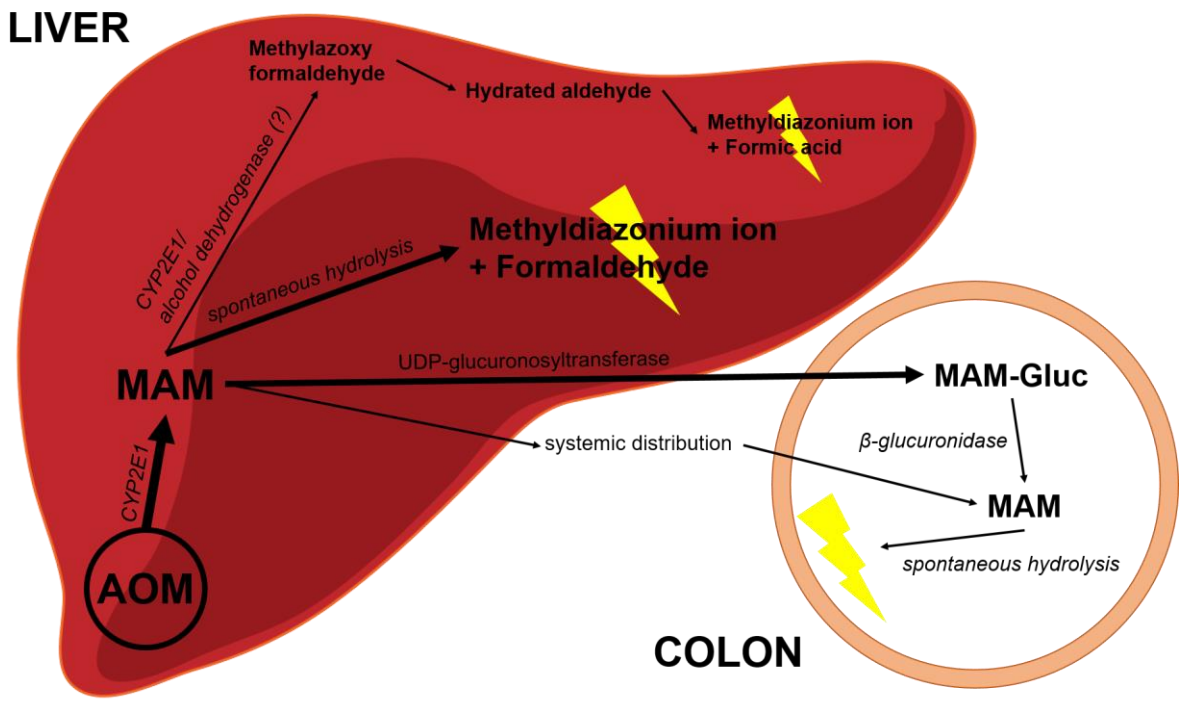


**Figure 12: Metabolism of AOM in colon and liver.** Upon transport to the liver via the blood stream, AOM is hydroxylated by the phase I enzyme CYP2E1 to MAM. MAM either hydrolyses spontaneously to a methyldiazonium ion (and formaldehyde) or can potentially be further metabolised by CYP2E1/alcohol dehydrogenase to methylazoxy formaldehyde. The latter can be transformed into a methyldiazonium (and formic acid). MAM is glucoronidated by the phase II UDP-glucuronosyltransferase and secreted via the bile into the bowel. Bacterial and mucosal β-glucuronidase activate the MAM again by cleavage of the glucuronic acid. Additionally, MAM can be systemically distributed. Scheme based on (Delker et al. 1998; Haase et al. 1973; Megaraj et al. 2014; Sohn et al. 2001).

Early studies analysing CRC formation in rodents were performed with DMH (Deschner, Long 1977; Thurnherr *et al.* 1973). Subsequently, AOM was preferred due to advantages, such as reproducibility, high potency, simple mode of application, excellent stability in solution, and low price (Neufert *et al.* 2007; Suzuki *et al.* 2006; Tanaka *et al.* 2003). The mechanism of human colorectal carcinogenesis is described as progression of healthy tissue to cancer with a sequential accumulation of mutations (1.1.2). AOM-induced tumours show many histopathological and molecular similarities with human CRC (**Figure 13**).

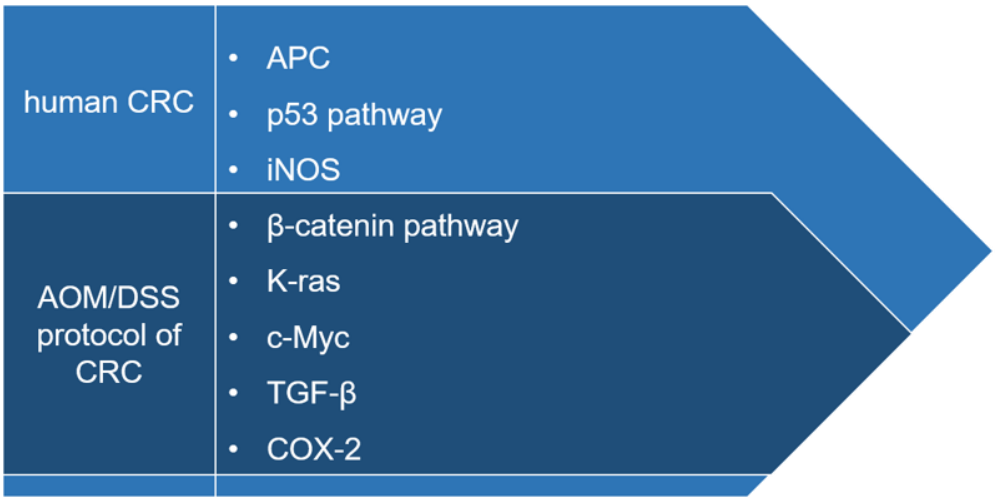


**Figure 13: Molecular features of human CRC and AOM-induced tumours in rodents.** AOM-induced tumours share alterations in the β-catenin pathway, K-ras. c-Myc, TGFβ, and COX-2 with human CRC. Mutations in APC and the p53 pathway are less common in chemically induced colorectal tumours in rodents. iNOS is potentially involved in the formation of human CRC, while it is not necessary for AOM-induced tumour formation. See text for details.

Consistent with human CRC, AOM/DSS-induced tumours have alterations in the APC/β-catenin-signalling pathway, including aberrant expression of APC as well as mutations and altered localisation patterns of β-catenin (Maltzman *et al.* 1997; Takahashi *et al.* 2000b; Vivona *et al.* 1993; Wang *et al.* 1998). However, APC mutations are less frequent in rodents, and they are less likely to metastasise (Kobaek-Larsen *et al.* 2000; Neufert *et al.* 2007). Further, *c-myc*, *cyclin D1*, and *cyclin-dependent kinase 4* (*Cdk4*), target genes of the APC/β-catenin-signalling pathway, are dysregulated (Wang *et al.* 1998). Human CRC and AOM/DSS-induced tumours share mutations in *K-ras* and increased protein levels of the inducible cyclooxygenase-2 (COX-2) as well as the nitric oxide synthase iNOS, which are involved in prostaglandin synthesis respectively nitric oxide synthesis (Takahashi *et al.* 2000b; Vivona *et al.* 1993). The mutation of β-catenin is reported as early event in both murine and human colorectal carcinogenesis. Alterations inactivating APC or activating β-catenin leading to stimulation of Wnt signalling are observed in most colon tumours in humans and rodents (Cooper *et al.* 2000; Takahashi *et al.* 2000a). AOM/DSS-induced tumours exhibit activation of the canonical Wnt pathway (Bissahoyo *et al.* 2005). Colitis-associated colonic neoplasms and tumours in both humans (Mikami *et al.* 2000) and rodents exhibit aberrant expression of β-catenin (Cooper *et al.* 2000). The gene *CTNNB1*, which encodes β-catenin, is frequently mutated at codons 33, 41, and 45 of the glycogen synthase kinase-3β (GSK-3β) phosphorylation motif in human CRC without APC mutations. AOM/DSS-induced tumours in rodents are often altered at codons 32, 33, and 34 of

*CTNNB1* (Tanaka *et al.* 2005). Sporadic colorectal tumours induced with AOM show mutations in codons 33, 34, 37, and 41 of *CTNNB1* but not at codon 32 (Cooper *et al.* 2000). Mutations in codons 37 and 41, important sites for GSK-3β phosphorylation, are associated with higher oncogenic potential (Koesters *et al.* 2001). Similar to human CRC, AOM/DSS-induced tumours show upregulation of the *Tcf-4* transcript (Svec *et al.* 2010).

A great variety of mutations activating K-ras have been reported in human carcinogenesis. The activation of K-ras stimulates cell proliferation, transformation, and differentiation (Valencia *et al.* 1991). AOM/DSS-induced tumours share the involvement of activating *K-ras* mutations in early stages of colorectal carcinogenesis with human CRC (Takahashi, Wakabayashi 2004).

The p53 pathway is an important checkpoint, altered in the aetiology of colitis-associated colonic neoplasms in both rodents and humans (Takesue *et al.* 2001). The ARF/p53 pathway, which limits proliferation and survival of cancer cells, is reported to be dysregulated in human carcinogenesis (Robertis *et al.* 2011). AOM/DSS-induced colonic dysplasia and neoplasms in rodents exhibit no aberrant expression of p53 (Tanaka *et al.* 2003). In accordance, colitis-associated tumours in rats show no mutations in p53 (Suzui *et al.* 1995). This might be attributable to the low frequency of mutations in p53 in chemically induced colorectal carcinogenesis in rodents (Robertis *et al.* 2011). Immunohistological assessment of p53 in DSS-induced colon tumours show p53 overexpression only in few tumours (Takesue *et al.* 2001). A study by Nambiar and colleagues suggested that ARF and p53 are not altered in AOM-induced CRC, but p53 shows lower potential to activate or inhibit transcription of target genes (Nambiar *et al.* 2002). It should be noted that inhibition of p53 in the absence of sequence alterations might results from altered acetylation or phosphorylation patterns (Minamoto *et al.* 2001). Yet, it is unclear if p53 is suppressed by post-translational modifications in AOM-induced tumours (Robertis *et al.* 2011).

c-Myc is known to contribute to a plethora of oncogenic processes (Knoepfler 2007). c-Myc is overexpressed in human CRC with both normal and altered Wnt/β-catenin signal pathways. It is target of the Wnt/β-catenin signalling pathway, while transforming grwoth factor-β (TGF-β) signalling is linked to inhibition of c-Myc. Multiple studies indicate that c-Myc plays a central role in the formation of human CRC (Frederick *et al.* 2004). Rodent studies revealed that decreased expression of *c-Myc* mediates resistance to colorectal carcinogenesis (Yekkala, Baudino 2007), which was confirmed by the inhibition of c-Myc in human CRC (Choi *et al.* 2008). In line with this, AOM/DSS-induced high grade carcinoma show an increased expression of c-Myc (Suzuki *et al.* 2007; Svec *et al.* 2010).

Sporadic human CRC commonly acquires resistance to TGF-β signalling and, at later stages, increased TGF-β expression facilitates invasion and metastasis (Gordon, Blobe 2008). TGF-β1-deficient mice suffer from a lethal inflammation (Kulkarni *et al.* 1993). Mice additionally lacking Rag2 have no functional B- and T-cells and survive until adulthood but develop carcinoma of caecum and colon. This indicates that inflammation combined with the loss of TGF-β1 results in a predisposition to cancer (Engle *et al.* 1999). In contrast to *Tgfb1*, *Tgfb3* is downregulated in in the colonic mucosa of AOM/DSS treated mice (Suzuki *et al.* 2007). Downregulation of TGF-β3 has been casually linked to nitric oxide (Abdelaziz *et al.*

2001). Transgenic TGF-β-receptor negative mice showed a significantly increased number of tumours after challenge with AOM/DSS compared to WT animals (Becker *et al.* 2006b).

COX-2 synthesises inflammatory mediators (prostaglandins and prostacyclins) from arachidonic acid. Increased COX-2 expression is linked with sites of inflammation and human CRC (Eberhart *et al.* 1994), and is also present in the cytoplasm of neoplastic colonic epithelial cells. In contrast, healthy cells show no expression of COX-2. An upregulation of COX-2 in line with *Apc* mutation was reported in neoplastic cells in the colon of mice treated with the AOM/DSS protocol (Sinicrope, Gill 2004). COX-2 is suspected to contribute to tumour formation by modulation of critical processes including apoptosis, angiogenesis, and invasiveness (Tsujii, DuBois 1995). The tumorigenic effect of COX-2 has been investigated in both spontaneous (Oshima *et al.* 1996) and inflammation-linked (Kim *et al.* 2008; Tanaka *et al.* 2003) tumour models.

Enhanced iNOS activity potentially plays a role in colitis-related colon carcinogenesis in humans (Chichlowski *et al.* 2010). Neoplasms and dysplasia in the large bowel of AOM/DSS treated animals show positive reactivity for iNOS. However, this is not yet confirmed on mRNA levels (Choi *et al.* 2008). Rodent studies indicate that iNOS is not necessary for colitis-associated tumour formation (Seril *et al.* 2007), although the inhibition of iNOS prevents tumour formation in mice treated with AOM/DSS (Kohno *et al.* 2006).

Upon challenge with AOM, most tumours arise in the distal part of the colon, passing through the adenoma-carcinoma sequence comparable to human CRC (1.1.2) (Takahashi, Wakabayashi 2004). Classical models are based on multiple intraperitoneal (*i.p.*) AOM injections. Combination with the inflammatory substance DSS administered via the drinking water has proven to shorten the latency for CRC induction. Multiple tumours have been reported within 10 weeks, whereas latency time for CRC formation without DSS was about 30 weeks (Neufert *et al.* 2007). DSS was found to form nanometre sized vesicles with medium-chain-length fatty acids, such as dodecanoate, which fuse with colonocyte membranes. A study suggests that the internalisation of the vesicles activates inflammatory signalling pathways. Moreover, the DSS moieties show inflammatory activity (Laroui *et al.* 2012). DSS promotes CRC formation by chronic inflammation and enhanced cell proliferation in the colon of rodents. Furthermore, the AOM/DSS protocol is also suitable to dissect inflammation-driven tumour progression as in inflammatory bowel disease (Neufert *et al.* 2007; Okayasu *et al.* 1990). A detailed description of the AOM/DSS protocol applied in the present work is provided in chapter 3.2.3.

# 2 OBJECTIVE

CRC is the third most common type of cancer and the fourth leading cause of cancer-related deaths worldwide (Ferlay *et al.* 2015). Beside life style related factors and genetic predispositions, inflammatory bowel diseases are associated with an increased risk for CRC (Roon et al. 2007; Eaden et al. 2001). Previous *in vivo* studies demonstrated the protective role of DNA repair mechanisms against NOC-induced CRC (Wirtz *et al.* 2010). Our group recently reported the protective role of the DNA repair protein MGMT and the BER-related DNA glycosylase AAG protects against NOC-induced CRC in the AOM/DSS model. Of note, MGMT caused a carcinogenic threshold at low alkylation damage levels, whereas AAG was only relevant at high alkylation damage levels (Fahrer *et al.* 2015). The nuclear enzyme PARP-1 is of paramount relevance for a plethora of cellular functions including DNA repair, especially BER (Caldecott *et al.* 1996) and DNA strand break repair (Wang *et al.* 2006), and genomic maintenance (Mangerich, Bürkle 2012). Moreover, PARP-1 is a coactivator of the inflammatory master key regulator NF-kB and thereby contributes to tumour-promoting inflammatory processes (Hassa, Hottiger 2002). Furthermore, analysis of human biopsies revealed an increased expression of PARP-1 in intestinal adenomas of patients with FAP (Idogawa *et al.* 2005), suggesting a role of PARP-1 in CRC aetiology.

The objective of this work is to dissect the role of PARP-1 in the aetiology of CRC using the murine AOM/DSS protocol of colorectal carcinogenesis. First, the formation CRC shall be compared between PARP-1-proficient WT and PARP-1-deficient animals via non-invasive mini endoscopy. Next, the basal and AOM-induced formation of PAR shall be analysed via HPLC-coupled tandem mass spectrometry (LC-MS/MS) in WT and PARP-1$^{-/-}$ animals. Subsequently, it is planned to study differences in the tumour initiating primary DNA damage induction between both mouse strains with western blot and alkaline comet assay. Then, the formation of mutagenic $O^6$-MeG DNA adducts and MGMT activity shall be compared in colon and liver tissue of both genotypes by means of slot blot and MGMT activity assay. IHC and confocal microscopy shall be utilised to detail the impact of PARP-1 on basal cell proliferation and AOM-induced cell death in colon tissue. The second part of this work shall address the role of PARP-1 in the tumour promoting inflammatory response after challenge with AOM/DSS. Therefore, the MEICS, as indicator for colitis severity, shall be evaluated via mini endoscopy and compared between WT and PARP-1$^{-/-}$ animals. It is planned to assess the invasion of macrophages and monocytes, important cells of the innate immune response, via IHC and confocal microscopy in colon tissue of WT and PARP-1$^{-/-}$ animals. Furthermore, the expression of pro-inflammatory cytokines, *e.g.* HMGB1, and other inflammatory markers including COX-2. Subsequently, the expression of selected NF-kB target genes shall be studied with qPCR. Finally, the generation of a PARP-1$^{-/-}$/MGMT$^{-/-}$ strain is envisaged to dissect the influence of PARP-1 during both tumour initiating DNA damage formation and tumour promoting inflammatory processes in animals susceptible to primary NOC-induced DNA damage.

# 3 MATERIAL AND METHODS

## 3.1 MATERIAL

### 3.1.1 DEVICES

**Table 2: Devices**

| | |
|---|---|
| AB Applied Biosystems StepOnePlus Real-Time PCR-System | Thermo Fisher Scientific, Inc., Massachusetts, USA |
| Autoclave VX-150 | Systec GmbH, Wetternberg, Germany |
| Automated tissue-processing machine Sakura Tissue Tek VIP | Vogel GmbH & Co. KG, Gießen, Germany |
| Benchtop centrifuge Spectrafuge Mini C1301 | Labnet International, Inc., Woodbridge, USA |
| Electrophoresis chamber | Bio-Rad Laboratories GmbH, München, Germany |
| Gel imaging system Ingenius | Syngene, Cambridge, UK |
| Glas plates | Bio-Rad Laboratories GmbH, München, Germany |
| Ice machine AF30 | Scotsman Ice Srl, Milan, Italy |
| Incubator | Heraeus GmbH, Hanau, Germany |
| Laboratory oven | Memmert GmbH + Co. KG, Schwabach, Germany |
| Laboratory vacuum pump Vacusafe | IBS Integra Biosciences, Fernwald, Germany |
| Laminar flow hood Laminar BDK 5.13B | BDK Luft- und Reinraumtechnik, Sonnenbühl-Genkingen, Germany |
| Magnetic stirrer IKA RH Basic 2 | IKA Werke GmbH & Co. KG, Staufen, Germany |
| Microplate reader Sunrise | Tecan Schweiz AG, Männedorf, Switzerland |
| Microscope Axio Observer Z1 with LSM 710 confocal system | Carl Zeiss Jena GmbH, Jena, Germany |
| Microscope Primo Vert | Carl Zeiss Jena GmbH, Jena, Germany |
| Microtome HYAX M25 | Carl Zeiss Jena GmbH, Jena, Germany |
| Mini endoscoy system (image 1 hub, SCB xeon 175) | KARL STORZ GmbH & Co. KG, Tuttlingen, Germany |

| | |
|---|---|
| NanoDrop 2000 | Thermo Fisher Scientific, Braunschweig, Germany |
| PCR thermal cycler Thermo Cycler T100 | Bio-Rad Laboratories GmbH, München, Germany |
| pH meter Typ PH523 | WTW - a xylem brand, Weilheim, Germany |
| Pipetboy Comfort | INTEGRA Biosciences GmbH, Biebertal, Germany |
| Pipettes | Mettler-Toledo GmbH, Gießen, Germany |
| Platform shaker Domax 1030 | Heidolph Instruments Labortechnik, Schwabach, Germany |
| Power supply MODEL 200/20 | Bio-Rad Laboratories GmbH, München, Germany |
| Power supply Power Pac Basic | Bio-Rad Laboratories GmbH, München, Germany |
| Power supply Power Pac HC | Bio-Rad Laboratories GmbH, München, Germany |
| Precision scale | Sartorius Laboratory, Göttingen |
| Refrigerated centrifuge Centrifuge 5424R | Eppendorf Instrumente GmbH, Hamburg, Germany |
| Scale | Sartorius AG, Göttingen, Germany |
| Shaker Duomax 1030 | Heidolph Instruments Labortechnik, Schwabach, Germany |
| Sonifier Cell Disruptor B15 | Emerson Electric Co., St. Louis, USA |
| Steamer | Braun GmbH, Kronberg, Germany |
| ThermoMixer Comfort | Eppendorf Instrumente GmbH, Hamburg, Germany |
| Tissue embedding system Sakura Tissue Tek TEC | Vogel GmbH & Co. KG, Gießen, Germany |
| Tri-Carb 2100TR Liquid Scintillation Counter | PerkinElmer, Waltham, USA |
| Vacuum- and bagsealer | Severin Elektrogeräte, Sundern, Germany |

| | |
|---|---|
| Vortex mixer REAX 2000 | Heidolph Instruments Labortechnik, Schwabach, Germany |
| Water bath | Science Services GmbH, München, Germany |
| Water bath | Gesellschaft für Labortechnik mbH, Burgwendel, Germany |
| Wet blot chamber | Bio-Rad Laboratories GmbH, München, Germany |

### 3.1.2 CHEMICALS AND SOLUTIONS

**Table 3: Chemicals and purchasable solutions**

| | |
|---|---|
| 100 bp DNA Ladder | New England BioLabs GmbH, Frankfurt, Germany |
| Acetic acid | Carl Roth GmbH & Co. KG, Karlsruhe, Germany |
| Ammonium acetate | Carl Roth GmbH & Co. KG, Karlsruhe, Germany |
| Aprotinin | Sigma-Aldrich Produktions GmbH, Steinheim, Germany |
| Aqua (for DSS application) | B. Braun Melsungen AG, Melsungen, Germany |
| Aqua valde purificata (for injection solutions) | Fresenius Kabi Deutschland GmbH, Bad Homburg, Germany |
| Azoxymethane | Sigma-Aldrich Produktions GmbH, Steinheim, Germany |
| Bestatin | Sigma-Aldrich Produktions GmbH, Steinheim, Germany |
| Boric acid | Carl Roth GmbH & Co. KG, Karlsruhe, Germany |
| Bovine serum albumin fraction V (BSA) | Carl Roth GmbH & Co. KG, Karlsruhe, Germany |
| Bromphenol blue | AppliChem GmbH, Darmstadt, Germany |
| Complete EDTA-free Protease Inhibitor Cocktail Tablets | Roche Diagnostics GmbH, Mannheim, Germany |
| Coomassie Brilliant Blue G250 (Serva Blue G) | Serva Electrophoresis GmbH, Heidelberg |
| DAKO Protein Block | DAKO Deuschland GmbH, Hamburg |
| DAKO Target Retrieval Solution | DAKO Deuschland GmbH, Hamburg |

| | |
|---|---|
| DSS | MP Biomedicals, Illkirch, France |
| Dithiothreitol (DTT) | Carl Roth GmbH & Co. KG, Karlsruhe, Germany |
| Dimethyl sulfoxide (DMSO) | Carl Roth GmbH & Co. KG, Karlsruhe, Germany |
| Deoxyribonuclease (DNAse), RNAse-free | Thermo Fisher Scientific, Braunschweig, Germany |
| Ethylenediaminetetraacetic acid (EDTA) | Carl Roth GmbH & Co. KG, Karlsruhe, Germany |
| Eosin-G-solution (0.5 % alcoholic) | Merck KGaA, Darmstadt, Germany |
| Ethanol | Carl Roth GmbH & Co. KG, Karlsruhe, Germany |
| Gel Loading Dye Blue | New England BioLabs GmbH, Frankfurt, Germany |
| Glycerin | Carl Roth GmbH & Co. KG, Karlsruhe, Germany |
| Glycin | Carl Roth GmbH & Co. KG, Karlsruhe, Germany |
| $H_2O_2$, 30 % | Carl Roth GmbH & Co. KG, Karlsruhe, Germany |
| $H_3PO_4$ | Carl Roth GmbH & Co. KG, Karlsruhe, Germany |
| Haematoxylin solution modified acc. to Gill III | Merck KGaA, Darmstadt, Germany |
| HCl, 30 % | Carl Roth GmbH & Co. KG, Karlsruhe, Germany |
| HEPES | Carl Roth GmbH & Co. KG, Karlsruhe, Germany |
| Isopropanol | Carl Roth GmbH & Co. KG, Karlsruhe, Germany |
| Isotonic saline solution (0.9 %) | B. Braun Melsungen AG, Melsungen, Germany |
| Ketamine (Ketavet, 100 mg/ml) | Pharmica GmbH, Berlin, Germany |
| Kodak GBX developer/replenisher | Sigma-Aldrich Produktions GmbH, Steinheim, Germany |
| Kodak GBX fixer & replenisher | Sigma-Aldrich Produktions GmbH, Steinheim, Germany |
| Leupeptin | Sigma-Aldrich Produktions GmbH, Steinheim, Germany |
| Low melting point agarose | Invitrogen, Life Technologies, Darmstadt, Germany |
| Luminol | Sigma-Aldrich Produktions GmbH, Steinheim, Germany |

| | |
|---|---|
| Methanol | AppliChem GmbH, Darmstadt, Germany |
| $MgCl_2$, | Carl Roth GmbH & Co. KG, Karlsruhe, Germany |
| Milk powder Blotting Grade | Carl Roth GmbH & Co. KG, Karlsruhe, Germany |
| $Na_3VO_4$ | Sigma-Aldrich Produktions GmbH, Steinheim, Germany |
| NaCl | Carl Roth GmbH & Co. KG, Karlsruhe, Germany |
| Na-Deoxycholate | AppliChem GmbH, Darmstadt, Germany |
| NaF | Sigma-Aldrich Produktions GmbH, Steinheim, Germany |
| NaOH | Carl Roth GmbH & Co. KG, Karlsruhe, Germany |
| NP-40 | Sigma-Aldrich Produktions GmbH, Steinheim, Germany |
| $O^6$-BG | Sigma-Aldrich Produktions GmbH, Steinheim, Germany |
| PageRuler Plus Prestained Protein Ladder | Thermo Fisher Scientific, Braunschweig, Germany |
| Phosphate bufferes saline (PBS) | Dulbecco Biochrom AG, Berlin, Germany |
| Pepstatin A | Sigma-Aldrich Produktions GmbH, Steinheim, Germany |
| Phenol/Chloroform/Isoamyl alcohol (25:24:1, v/v) | Carl Roth GmbH & Co. KG, Karlsruhe, Germany |
| Phenylmethylsulfonyl fluoride (PMSF) | Sigma-Aldrich Produktions GmbH, Steinheim, Germany |
| Polyethylene glycol 400 (PEG 400) | Sigma-Aldrich Produktions GmbH, Steinheim, Germany |
| Ponceau S | Sigma-Aldrich Produktions GmbH, Steinheim, Germany |
| Propidium iodide (PI) | Sigma-Aldrich Produktions GmbH, Steinheim, Germany |
| Proteinase K | Roche Diagnostics GmbH, Mannheim, Germany |

| | |
|---|---|
| Ribonuclease A (RNAse A), DNAse and protease-free | Thermo Fisher Scientific, Braunschweig, Germany |
| Roti-Histofix 4 %, phosphate-buffered formaldehyde | Carl Roth GmbH & Co. KG, Karlsruhe, Germany |
| Roti-Histokitt mounting medium | Carl Roth GmbH & Co. KG, Karlsruhe, Germany |
| Rotiszint eco plus Scintillation Cocktail | Carl Roth GmbH & Co. KG, Karlsruhe, Germany |
| Sodium dodecyl sulfate (SDS) | Carl Roth GmbH & Co. KG, Karlsruhe, Germany |
| StarPure Agarose | Starlab International GmbH, Hamburg, Germany |
| Tetramethylethylenediamine (TEMED) | Carl Roth GmbH & Co. KG, Karlsruhe, Germany |
| TO-PRO-3 | Invitrogen, Life Technologies, Darmstadt, Germany |
| Trichloroacetic acid | Carl Roth GmbH & Co. KG, Karlsruhe, Germany |
| Tris | Carl Roth GmbH & Co. KG, Karlsruhe, Germany |
| Triton X100 | AppliChem GmbH, Darmstadt, Germany |
| Tween 20 | Carl Roth GmbH & Co. KG, Karlsruhe, Germany |
| Vectashield Mounting Medium with Dapi | Linaris Biologische Produkte GmbH, Dossenheim, Germany |
| Western Lightning Enhanced Luminol Reagent Plus | PerkinElmer, Waltham, USA |
| Western Lightning Oxidizing Reagent Plus | PerkinElmer, Waltham, USA |
| Xylazine (Rompun 2 %, 20 mg/ml) | Bayer Vital GmbH, Leverkusen, Germany |
| Xylene | AppliChem GmbH, Darmstadt, Germany |
| β-Mercaptoethanol | Carl Roth GmbH & Co. KG, Karlsruhe, Germany |

### 3.1.3 OTHER MATERIALS

**Table 4: Other materials**

| | |
|---|---|
| 96-Well Plates | Thermo Fisher Scientific, Braunschweig, Germany |
| CELLSTAR PCR Tubes 0.5 ml | Greiner Bio-One GmbH, Frickenhausen |
| Eye ointment Bausch & Lomb Corneregel | Dr. Gerhard Mann chem.-pharm. Fabrik GmbH, Berlin, Germany |

| | |
|---|---|
| Cover slips | Carl Roth GmbH + Co. KG, Karlsruhe, Germany |
| Dako Pen | DAKO Deuschland GmbH, Hamburg |
| Falcon Cell Strainer 70 µm | Corning, Inc., New York, USA |
| Centrifuge tubes (15 ml and 50 ml) | Sigma-Aldrich Produktions GmbH, Steinheim, Germany |
| Hypodermic needles | Becton, Dickinson and Company, Franklin Lakes, USA |
| Microscope slides | Diagonal GmbH & Co. KG, Münster, Germany |
| Nylon membrane (Hybond-N+) | GE Healthcare Life Sciences, München, Germany |
| Photographic film MEDICAL Y-RAY FILM BLUE | Agfa HealthCare NV, Montsel, Belgium |
| Pipet tips | Eppendorf Instrumente GmbH, Hamburg, Germany |
| PROTRAN Pure Nitrocellulose Membrane | PerkinElmer Technologies GmbH & Co. KG, Walluf, Germany |
| Safe-Lock Tubes 1.5 ml | Eppendorf, München |
| Scintillation vials | Sigma-Aldrich Produktions GmbH, Steinheim, Germany |
| Superfrost Plus Microscope Slides | Thermo Fisher Scientific, Braunschweig, Germany |
| Syringes and hypodermic needles | B. Braun Melsungen AG, Melsungen, Germany |
| Tissue-processing embedding cassettes | Carl Roth GmbH + Co. KG, Karlsruhe |
| Underpads with cellulose fluff | PAUL HARTMANN Ltd., Heywood/Lancshire, UK |
| Whatman Cellulose Filter Paper | Sigma-Aldrich Produktions GmbH, Steinheim, Germany |

### 3.1.4 ANTIBODIES

**Table 5: Primary antibodies**

| | | |
|---|---|---|
| Anti-CD3, monoclonal rat | MCA500A488 | AbD Serotec MCA, Kidlington, UK |
| Anti-CD11b, polyclonal rabbit | NB110-89474 | Novus Biologicals Europe, Abingdon, UK |
| Anti-COX-2, monoclonal mouse | 610204 | BD Transduction Laboratories, Becton, Dickinson and Company, Franklin Lakes, USA |
| Anti-F4/80, monoclonal rat | BM4007 | OriGene Europe – Acris Antibodies, Herford, Germany |
| Anti-HMGB1, polyclonal rabbit | GTX101277 | GeneTex, Inc., Irvine, USA |
| Anti-Hsp90α/β, polyclonal rabbit | ab13495 | Abcam, Cambridge, UK |

| | | |
|---|---|---|
| Anti-$O^6$-MeG, monoclonal mouse | SQX-SQM003.1 | Axxora, Enzo Life Sciences, Inc., Farmingdale (NY), USA |
| Anti-PCNA, monoclonal mouse | sc-56 | Santa Cruz Biotechnology, Inc., Heidelberg, Germany |
| Anti-γH2AX, polyclonal rabbit | ab11174 | Abcam, Cambridge, UK |

**Table 6: Secondary antibodies**

| | | |
|---|---|---|
| Goat anti-mouse-HRP | sc-2005 | Santa Cruz Biotechnology, Inc., Heidelberg, Germany |
| Goat anti-mouse-Alexa Fluor 488 | A11001 | Invitrogen, Life Technologies, Darmstadt, Germany |
| Goat anti-rabbit-Alexa Fluor 488 | A11008 | Invitrogen, Life Technologies, Darmstadt, Germany |
| Goat anti-rabbit-HRP | Sc-2004 | Santa Cruz Biotechnology, Inc., Heidelberg, Germany |
| Goat anti-rat-Cy3 | 112-165-167 | Jackson ImmunoResearch, Inc., West Grove, USA |

### 3.1.5 BUFFERS AND SOLUTIONS

**Table 7: Buffers and solutions**

| | |
|---|---|
| 10x Reaction buffer (MGMT assay) | 700 mM Hepes-KOH, pH 7.8<br>10 mM DDT<br>50 mM EDTA |
| 10x SDS running buffer / blotting buffer | 200 mM Tris<br>1,54 M Glycin |
| 10x TBS pH 7,6 (HCl) | 100 mM Tris<br>1,5 M NaCl |
| 1x Blotting buffer | 10% 10x Blotting buffer<br>20% Methanol |
| 1x SDS running buffer | 200 mM Tris-HCl pH 6,8<br>8 % SDS<br>40 % Glycerin<br>0.08 % Bromphenol blue<br>4 % β-Mercaptoethanol |
| 5x SDS loading buffer | 200 mM Tris-HCl pH 6,8<br>8 % SDS<br>40 % Glycerin<br>0.08 % Bromphenol blue<br>4 % β-Mercaptoethanol |

| | |
|---|---|
| Ammonium acetate buffer | 2 M $NH_4Ac$ |
| Anaesthesia | 12 mg/ml Ketamine<br>1.6 mg/ml Xylazine<br>Isotonic saline solution (0.9 %) |
| Blocking solution | 5 % Milk powder or 5 % BSA in TBS-T |
| Bradford solution (100 ml) | 10 mg Coomassie Brilliant Blue G250<br>5 ml 99,8% EtOH<br>10 ml H3PO4<br>ad 100 ml ddH2O |
| DSS solution | 1 % or 2.5 % DSS in Aqua |
| Electrophoresis buffer (alkaline comer assay) | 300 mM NaOH<br>1 mM EDTA |
| Lysis buffer, pH 10 (NaOH) (alkaline comet assay) | 2.5 M NaCl<br>100 mM EDTA<br>10 mM Tris<br>1 % Triton X-100<br>10 % DMSO |
| Neutralisation buffer, pH 7.5 (alkaline comet assay) | 0.4 M Tris |
| Merchant's Medium | 0,14 M NaCl<br>1,47 mM KH2PO4<br>2.7 mM KCl<br>8,1 mM EDTA pH 7,4 |
| Ponceau S solution | 5 % Acetic acid<br>0.1 % Ponceau S |
| PI staining solution | 0.05 mg/ml PI |
| RIPA buffer | 25 mM Tris-HCl pH 7.4<br>150 mM NaCl<br>0.1 % SDS<br>1 % Na-Deoxycholate<br>1 % NP-40<br>0.2 mM Na3VO4<br>2 mM EDTA<br>50 mM NaF<br>1 mM PMSF<br>1x Complete Protease Inhibitor Cocktail |
| Sonication buffer (MGMT assay) | 20 mM Tris-EDTA pH 8.5<br>1 mM EDTA<br>1 mM β-Mercaptoehanol<br>5 % Glycerin |

| | |
|---|---|
| | Added before use:<br>10 µg/ml Aprotinin<br>10 nmol/ml Bestatin<br>10 nmol/ml Leupeptin<br>1 nmol/ml Pepstatin A<br>0.1 µmol/ml PMSF |
| Tail buffer | 100 mM Tris-HCl pH 8.5<br>5 mM EDTA<br>0.2 % SDS<br>200 mM NaCl |
| TBE buffer | 89 mM Tris<br>89 mM Boric acid<br>2 mM EDTA |
| TBS-T | 1x TBS<br>0,1% Tween 20 |
| TE buffer | 10 mM Tris pH 8.0<br>1 mM EDTA |

### 3.1.6 KITS

**Table 8: Kits**

| | |
|---|---|
| *In situ* Cell Death Detection Kit, Fluorescein | Roche Diagnostics Deutschland GmbH, Mannheim |
| NucleoSpin RNA II | MACHEREY-NAGEL GmbH & Co. KG, Düren |
| QuantiTect SYBR Green PCR Kit | Qiagen, Hilden, Germany |
| REDExtract-N-Amp Tissue PCR Kit | Sigma-Aldrich Produktions GmbH, Steinheim, Germany |
| Taq DNA Polymerase 2x Master Mix Red | Ampliqon A/S, Odense M, Denmark |
| Verso cDNA Kit | Thermo Fisher Scientific, Braunschweig, Germany |

### 3.1.7 ANIMALS

For the present work, PARP-1$^{-/-}$ and MGMT$^{-/-}$ mice with C57BL/6 background were utilised as described in prior studies (Glassner *et al.* 1999; Murcia *et al.* 1997). PARP-1$^{-/-}$ mice were obtained from Françoise Dantzer (Institut de Recherche de l'Ecole de Biotechnologie de Strasbourg, France) and MGMT$^{-/-}$ mice were obtained from Leona D. Samson (Department of Biological Engineering, Massachusetts Institute of Technology, Cambridge, MA, USA). The PARP-1$^{-/-}$/MGMT$^{-/-}$ strain was bred in the context of this work by mating PARP-1$^{-/-}$ and MGMT$^{-/-}$ animals followed by verification of the offspring's genotype via polymerase chain reaction (PCR) (3.2.1). The age of the animals was between 8 and 11 weeks for carcinogenesis studies and up to 16 weeks for other experiments. Animal housing and experiments were carried out according to guidelines of the European Communities Council Directive as of 24$^{th}$ November 1986 (80/609/EEC) and approved by the Animal Care and Use Committee of the University of Mainz. A maximum of five mice was kept in one cage, access to food and drinking water was unrestricted, the atmospheric environment was steady at 22 °C and 60–70% humidity.

### 3.1.8 SOFTWARE

Figures and diagrams, including statistical analysis, were created with GraphPad Prism 6 or Microsoft PowerPoint 2016. Other calculations were performed with Microsoft Excel 2015. Microscopic pictures were edited and analysed with ImageJ, GIMP 2 and Microsoft Image Composite Editor 2.0.3.0. Densitometric evaluation of western blots and slot blots was performed with Adobe Photoshop CS5. Word processing was realised with Microsoft Word 2016 and Citavi 5 as reference manager.

# 3.2 METHODS

## 3.2.1 GENOTYPING OF TRANSGENIC ANIMALS

Genotyping of PARP-1 was performed with the REDExtract-N-Amp Tissue PCR Kit. For this purpose, genetic material was obtained from mouse ear punchings.

Regarding MGMT$^{-/-}$ animals, DNA for genotyping was extracted from mouse-tail tips. Therefore, tissue was digested in 40 µl Tail Buffer with 2 mg/ml Proteinase K overnight at 56 °C and 400 rpm on a thermomixer. Subsequently, 300 µl double-distilled water (dd$H_2O$) were added and Proteinase K was inactivated at 95 °C for 10 min. After short centrifugation, the supernatant was used for PCR.

PCR is an exponential amplification of genetic material. Here, a DNA polymerase synthesizes multiple copies of a complementary DNA strand from a DNA template. As starting point for the DNA polymerase serve primers, small (18–30 bp) oligonucleotides, aligning upstream of the complementary sequence on the DNA template. Initially, native dsDNA is heated to 94 °C to break the hydrogen bonds and separate it into ssDNA. Afterwards, primers hybridise with template DNA in the so-called annealing step followed by the synthesis of the complementary DNA strand in the elongation step. The used PCR Master Mixes (**Table 10**, **Table 11**) already included the necessary components (polymerase, deoxynucleotides, $MgCl_2$, and reaction buffer). Only primers, dd$H_2O$, and template DNA were added according to the manufacturer's instructions.

The following primers were utilised for analysis of the target sequences (**Table 9**). Components for the PCR premix are listed in **Table 10** as well as **Table 11**. **Table 12** shows the programme of the thermocycler.

**Table 9: Primers for genotyping.**

| | | |
|---|---|---|
| **PARP-1**<br>Wild type allele: 200 bp (P-A & P-B)<br>Mutated allele: 700 bp (P-A & P-C) | Primer P-A | 5′-TTGATGGCCGGGAGCTGCTTCTT-3′ |
| | Primer P-B | 5′-GGCCAGATGCGCCTGTCCAAGAAG-3′ |
| | Primer P-C | 5′-GGCGAGGATCTCGTCGTGACCCATG-3′ |
| **MGMT**<br>Wild type allele: 542 bp (M-A & M-C)<br>Mutated allele: 409 bp (M-A & M-B) | Primer M-A | 5'-GGCATCTTCCTCCTAAACCTGGA-3' |
| | Primer M-B | 5'-GGTGGGATTAGATAAATGCCTGCT-3' |
| | Primer M-C | 5'-CCCCAGGACACTTGCAGCTCT-3' |

**Table 10: Components of PCR mix for PARP-1 genotyping.**

| **Component** | **Volume [µl]** |
|---|---|
| REDExtract-N-Amp PCR ReadyMix | 7,5 |
| Primer A and B (each primer) | 0.12 |
| **OR:** primer A and C (each primer) | 0.12 |
| dd$H_2O$ | 4.26 |
| DNA template | 3 |
| Σ | 15 |

**Table 11: Components of PCR mix for MGMT genotyping.**

| Component | Volume [µl] |
|---|---|
| Taq DNA Polymerase 2x Master Mix Red | 7 |
| Primer (each) | 1 |
| $ddH_2O$ | 4 |
| DNA template | 1 |
| Σ | 15 |

**Table 12: PCR program for PARP-1 and MGMT genotyping.**

| Gene | PARP-1 | | MGMT | |
|---|---|---|---|---|
| **Lid** | 105 °C | | 105 °C | |
| **Step** | **Temperature** | **Duration** | **Temperature** | **Duration** |
| **1** | 94 °C | 2 min | 94 °C | 4 min |
| **2** | 94 °C | 40 sec | 94 °C | 1 min |
| **3** | 61 °C | 45 sec | 62 °C | 1 min |
| **4** | 72 °C | 1 min | 72 °C | 1 min |
| **5** | GOTO 2 (30 cycles) | | GOTO 2 (30 cycles) | |
| **6** | 72 °C | 8 min | 72 °C | 8 min |
| **7** | 4 °C | ∞ | 4 °C | ∞ |

PCR products were loaded onto a 1.5 % agarose gel with ethidium bromide for gel electrophoretic separation. In an electric field, negatively charged DNA migrates towards the cathode. Small fragments move faster through the gel matrix than large fragments. In order to estimate the size of the DNA samples, 5 µl of 100 bp DNA ladder (New England Biolabs) were added to the gel. DNA samples were separated at 100 V for 1 h in an electrophoresis chamber and PCR products were visualised with UV light and compared to the defined size of the marker bands.

### 3.2.2 PREPARATION OF AOM FOR INTRAPERITONEAL INJECTION

The following scheme was applied for all experiments (short-term treatment, analysis of inflammation and carcinogenesis studies). One day before injection, the mice were grouped, marked via ear punching, and weighted. Based on to animals' weight and treatment, the necessary volume of AOM stock solution was calculated and adjusted with PBS to a total injection volume of 500 µl. AOM stock solution was stored at a concentration of 10 mg/ml at –80 °C. Before injection, AOM stock solution was thawed on ice to prevent hydrolysis. AOM stock solution was then mixed with sterile 10x PBS and $ddH_2O$ to produce a 1 mg/ml AOM working solution in PBS. The calculated AOM volume for each animal was transferred in a 1.5 ml reaction tube already containing the calculated volume of 1x PBS (500 µl in total). Reaction tubes were shortly centrifuged, put on ice, and the AOM solution *i.p.* injected. One needle was used for five injections, and syringes were only used for the same AOM concentrations. All works with AOM were

performed under sterile conditions. A maximum of 15 animals were injected at once to prevent AOM decomposition.

### 3.2.3 AOM/DSS MODEL OF COLORECTAL CARCINOGENESIS

The AOM/DSS model is used as a protocol to chemically induce CRC in rodents. An initiating single *i.p.* injection of the *N*-nitroso compound AOM (1.2) is followed by the exposure to the inflammatory agent DSS through the drinking water. Compared to sporadic models, the inflammation has proven to shorten the latency time for CRC formation in rodents dramatically and features the aberrant crypt foci-adenoma–carcinoma sequence, which is characteristic for sporadic human CRC formation. Due to its reproducibility and feasibility, the AOM/DSS model is a well-established procedure for studying colorectal carcinogenesis (1.4).

The housing of the animals during the experiment is stated in 3.1.7; preparation and injection of AOM is described in 3.2.2. DSS solution with sterile dd$H_2O$ was renewed after 2 – 3 days. AOM injection on day 1 was followed by two DSS cycles from day 4 to day 11 and day 25 to day 32 with a gap of two weeks in-between (**Figure 14**). After two cycles of DSS, a (mild) chronic colitis occurred.

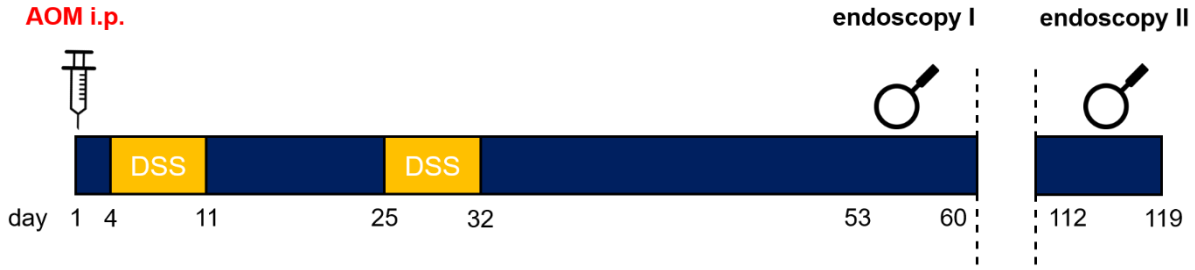


**Figure 14: Treatment scheme of the AOM/DSS model.**

For the studies of tumour induction, AOM doses up to 15 mg/kg body weight (bw) were applied in combination with 1 % DSS. In another set of experiments, a higher dose of 2.5 % DSS was only combined with 10 mg/kg bw AOM to prevent high mortality due to significantly higher colitis. Control animals received PBS.

### 3.2.4 MGMT INHIBITION WITH *O*$^6$-BG *IN VIVO*

*O*$^6$-BG, a synthetic derivate of purine base guanine, acts as a pseudo substrate for MGMT causing its inactivation and degradation.

Grouping, marking, and weighing was performed in preparation of the AOM injection on the day before (as described in 3.2.2). The *O*$^6$-BG stock solution for each experiment was freshly prepared under sterile conditions prior the first injection and stored at 4°C. *O*$^6$-BG was dissolved in a 40 % aqueous PEG 400 solution at a stock concentration of 1 mg/ml. Animals were treated with 40 mg/kg bw *O*$^6$-BG. Before each injection, the calculated amount of the *O*$^6$-BG stock solution per animal was filled up with sterile PBS to a total volume of 200 µl in separate reaction tubes. Reaction tubes were shortly centrifuged and

the inhibitor solution immediately *i.p.* injected. The $O^6$-BG injection solution was not kept on ice to prevent precipitation. The inhibitor was applied 2 h before the AOM injection and then in an interval of 12 h up to 36 h after the first injection (0 h, 12 h, 24 h and 36 h).

## 3.2.5 COLONSCOPY IN ANESTHETISED MICE

Initially, the setup of the mini endoscopy system was checked, and the endoscope was cleaned with 70 % ethanol (EtOH). Next, airflow was adjusted via the valve on the telescope to create an adequate flow. A strong airflow can harm the gastrointestinal tract of the animals, thus setting the airflow strength is a critical step. Subsequently, animals were anesthetised with an *i.p.* injection of ketamine and xylazine (7 µl/g bw) (3.1.5). The consciousness of the animals was tested before endoscopy by examination of the animals' reflexes and eye ointment was applied to prevent drying of the cornea. When the animal was completely sedated, the endoscope was carefully inserted in the animal's rectum and introduced up to the flexure of the colon under visual control. If stool did block the colon, it was removed with a colon lavage. The endoscopy was recorded on a USB stick by the mini endoscopic system or directly with a personal computer. Tumour number and tumour respectively the murine endoscopic index of colitis severity (MEICS) were assessed either directly during mini endoscopy or later with the video record. After examination, animals were put back in their cages, and their awakening was observed.

### 3.2.5.1 TUMOUR SCORING

The colorectal carcinogenesis of the animals treated with AOM and 1 % DSS was monitored via mini endoscopy (3.2.5) after 8 and 16 weeks. Tumour score and tumour number were used to assess colorectal carcinogenesis as described (Becker *et al.* 2006a). Tumours were graded in relation to colon diameter as shown in **Figure 15**.

| Size (avg. diameter) | | Score |
|---|---|---|
| Just detectable |  | 1 |
| 1/8 |  | 2 |
| 1/4 |  | 3 |
| 1/2 |  | 4 |
| ≥ 1/2 |  | 5 |

**Figure 15: Endoscopic scoring of tumours in mice (Becker et al. 2006).**

The score of the observed tumours was summed to a total tumour score for every animal. Differences in tumour score indicate differences in tumour progression, whereas tumour number denotes the amount of induced tumours (Becker *et al.* 2006a).

Animals treated with AOM and 2.5 % DSS showed a dramatically increased tumour formation and progression. Even during the first tumour scoring after 8 weeks (3.2.3), it was not possible to introduce the endoscope in the colon of all animals because the colon was occupied by stool and tumours. Hence, the protocol was altered. The animals were sacrificed after 12 weeks and the abdominal cavity opened to remove the whole colon. Afterwards, the colon was sliced longitudinally and rinsed with pre-cooled PBS. After cleaning, the colon was flattened with the lumen facing up and recorded with the camera of the mini endoscopy system. The camera was moved slowly from the rectum to the proximal part of the colon. Afterwards, the colon tissue was stained in PBS with 0.5 % methylene blue for 30 sec, rinsed in PBS for 30 sec, and recorded in the same manner. Tumours were scored as described in **Figure 15**.

#### 3.2.5.2 COLITIS SCORING

The degree of colitis severity was estimated by the evaluation of the MEICS, developed by Becker and colleagues (Becker *et al.* 2006a). The MEICS is based on the rating of five parameters: translucency of the colon wall, changes in vascular pattern, presence of fibrin, mucosal granularity, and stool consistency (**Figure 16**). MEICS was assessed via mini endoscopy as described in 3.2.5 at the end of the first DSS cycle (3.2.3).

**A**

| | Murine endoscopic index of colitis severity (MEICS) | | | | |
|---|---|---|---|---|---|
| | 0 | 1 | 2 | 3 | Total |
| Thickening of the colon | Transparent | Moderate | Marked | Non-transparent | 0–3 |
| Changes of the vascular pattern | Normal | Moderate | Marked | Bleeding | 0–3 |
| Fibrin visible | None | Little | Marked | Extreme | 0–3 |
| Granularity of the mucosal surface | None | Moderate | Marked | Extreme | 0–3 |
| Stool consistency | Normal + solid | Still shaped | Unshaped | Spread | 0–3 |
| | | | | | Overall: 0–15 |

Endoscopic colitis score based on the observed signs of inflammation. The MEICS consisted of five parameters, as indicated.

**B**

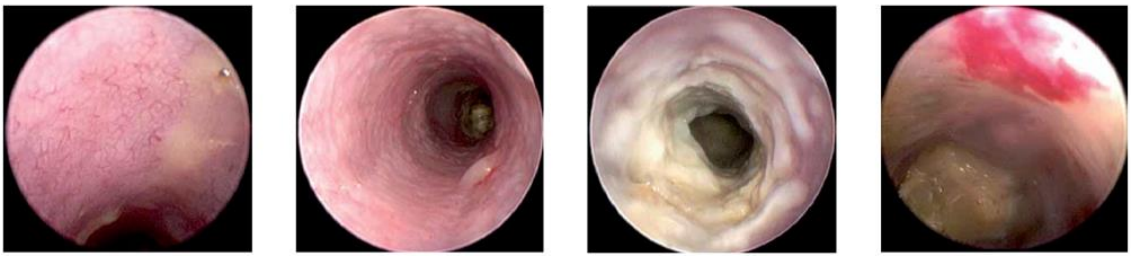

**Figure 16: Assessment of the MEICS. A** Rating of inflammation severity (MEICS). **B** Representative pictures (Becker et al. 2006).

### 3.2.6 TISSUE COLLECTION AND PROCESSING

At the end of the experiment, mice were sacrificed via cervical dislocation. Subsequently, the abdominal cavity was opened, rinsed with cold PBS and first liver and then colon removed. Organs were repeatedly rinsed with cold PBS to remove remains from blood and stool. The removed part of the bowel included rectum, distal, and proximal colon. It was fragmented in six pieces, according to **Figure 17**.

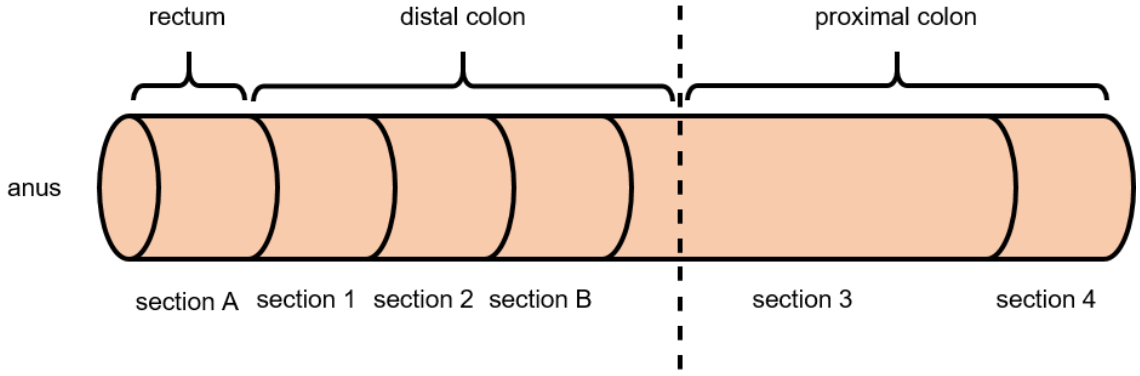


**Figure 17: Sections of the colon.** Section A and B were fixed in 4 % formaldehyde and embedded in paraffin; sections 1 – 4 were snap frozen.

Section A and B and a half liver lobe were designated for histological analysis and therefore fixed in 4 % Roti-Histofix for 6–8 h. Colon sections 1 to 4 and one liver lobe were snap frozen in liquid nitrogen and stored at –80 °C.

After fixation, colon section A and B and the liver tissue were transferred in tissue-processing embedding cassettes and processed with an automated tissue-processing machine (Sakura Tissue Tek VIP) following the programme in **Table 13**.

**Table 13: Programme of the automated tissue processing machine.**

| Step | Solution | Time | Temperature |
|---|---|---|---|
| 1 | EtOH 50 % | 30 min | 40°C |
| 2 | EtOH 70 % | 60 min | 40°C |
| 3 | EtOH 80 % | 60 min | 40°C |
| 4 | EtOH 96 % | 60 min | 40°C |
| 5 | EtOH 96 % | 60 min | 40°C |
| 6 | EtOH 100 % | 60 min | 40°C |
| 7 | EtOH 100 % | 60 min | 40°C |
| 8 | Xylene | 60 min | 40°C |
| 9 | Xylene | 60 min | 40°C |
| 10 | Xylene | 60 min | 40°C |
| 11 | Paraffin | 60 min | 60°C |
| 12 | Paraffin | 60 min | 60°C |
| 13 | Paraffin | 60 min | 60°C |
| 14 | Paraffin | 60 min | 60°C |

Processed tissue was embedded in paraffin with, help of a tissue embedding system (Sakura Tissue Tek TEC) and stored at room temperature (RT).

## 3.2.7 IMMUNOHISTOCHEMISTRY

Immunohistochemistry (IHC) is a process, in which antibodies specifically bind to the antigen of interest in fixed cells and tissues. Primary antibodies are recognised by fluorescent-coupled secondary antibodies which can be excited at specific wavelengths to visualise the target structure with a fluorescence microscope.

Paraffin embedded tissue (3.2.6) was cooled down in a -20 °C freezer for 5–10 min and sectioned with the Zeiss Rotary Microtome HM 325 in 5 µm thick slices. Sections were allowed to unfurl in a 37 °C water bath, and four sections of each sample were collected with a microscope slide. After air-drying, sections were stored at RT. Sections from colon section B (**Figure 17**) were used for IHC.

### 3.2.7.1 SAMPLE PREPARATION FOR IHC

First, slides were pre-heated at 60 °C for 30 min in a dry cabinet to liquefy the paraffin surrounding the tissue. Next, slides were incubated in xylene to remove paraffin residues, hydrated in a decreasing serial ethanol dilution, and washed in PBS (**Table 14**).

**Table 14: Deparaffinization and rehydration of colon tissue for IHC.**

| Solution | Number of steps | Duration |
|---|---|---|
| Xylene | 3 | 5 min |
| EtOH 100 % | 2 | 5 min |
| EtOH 96 % | 1 | 5 min |
| EtOH 90 % | 1 | 5 min |
| EtOH 80 % | 1 | 5 min |
| EtOH 70 % | 1 | 5 min |
| dd$H_2O$ | 2 | wash shortly |
| PBS | 1 | wash shortly |

Demasking of the target epitopes was performed by incubation of the samples with DAKO Target Retrieval Solution in a steamer for 30 min (60 min for γH2AX). Afterwards, slides were allowed to cool down at RT for 20 min and rinsed twice with PBS.

### 3.2.7.2 IMMUNOFLUORESCENCE

Two sections per sample were encircled with a water repelling DAKO Pen. Subsequently, slides were washed twice with PBS and blocked with DAKO Blocking Solution for 2 h at RT in a humid incubation chamber. Slides were shortly washed with PBS and incubated with the primary antibody at 4 °C

overnight in a humid incubation chamber. Dilutions for primary and secondary antibodies are listed in **Table 15**.

**Table 15: Antibody solutions for immunofluorescence.**

| Primary antibody | Dilution | Origin | Secondary antibody | Dilution |
|---|---|---|---|---|
| Anti-CD3 | 1:400, 2 %-BSA in PBS | Monoclonal rat | Goat-anti-Rat-Cy3 | 1:500, 2% BSA in TBS-T |
| Anti-CD11b | 1:400, 2 %-BSA in PBS | Polyclonal rabbit | Goat anti-rabbit-Alexa Fluor 488 | 1:500, 2% BSA in TBS-T |
| Anti-COX-2 | 1:400, 0.2 % Triton X100 in PBS | Monoclonal mouse | Goat anti-mouse-Alexa Fluor 488 | 1:500, PBS |
| Anti-F4/80 | 1:400, 2 %-BSA in PBS | Monoclonal rat | Goat-anti-Rat-Cy3 | 1:500, 2% BSA in TBS-T |
| Anti-HMBG1 | 1:400, 0.2% Triton X100 in PBS | Polyclonal rabbit | Goat anti-rabbit-Alexa Fluor 488 | 1:500, PBS |
| Anti-PCNA | 1:400, 1% BSA in PBS with 0,2% Triton X-100 | Polyclonal rabbit | Goat anti-rabbit-Alexa Fluor 488 | 1:500 0.2 % Triton X-100 in PBS |

Excess antibody was washed off (3 x 10 min, PBS/0.1 % Tween 20). The binding of the secondary antibody (**Table 15**) was performed for 2 h at RT in a dark and humid incubation chamber. All steps were done under exclusion of light to prevent bleaching of the dye coupled to the secondary antibody. After washing (PBS/0.1% Tween 20), sections were incubated with TO-PRO-3 (1:1000, PBS) to stain nuclei. Finally, slides were shortly washed in PBS and coated with VECTASHIELD mounting medium. Finally, samples were mounted with a coverslip and sealed with clear nail polish.

### 3.2.7.3 CONFOCAL MICROSCOPY

Samples were analysed with a Zeiss Axio Observer Z1 microscope (excitation/emission wavelengths for fluorophores: **Table 16**), which was equipped with a LSM710 confocal microscopy unit.

**Table 16: Secondary antibodies for IHC.**

| Antibody/Fluorophore | Laser wavelength | Excitation/emission wavelength |
|---|---|---|
| TO-PRO-3 | 633 nm | 640 nm/655 nm |
| Goat anti-mouse-Alexa Fluor 488 | 488 nm | 500 nm/520 nm |
| Goat anti-rabbit- Alexa Fluor 488 | 488 nm | 500 nm/520 nm |
| Goat-anti-Rat-Cy3 | 552 nm | 560 nm/565 nm |

One of the two processed sections on each slide was selected and 8-12 pictures of each sample were taken (magnifications are stated in the caption of the pictures). The intensity of the laser exciting the dye on the secondary antibody was retained within each experiment, whereas intensity of the 633 nm laser was adjusted to the TO-PRO-3 staining. Pictures were taken with the software Zeiss Zen 2009. After microscopy, mean signal intensity or positive cells were evaluated (stated in the description of the figures) and processed with the software listed in 3.1.8.

#### 3.2.7.4 TERMINAL DEOXYNUCLEOTIDYL TRANSFERASE-MEDIATED DEOXYURIDINE-TRIPHOSPHATE (DUTP) NICK END LABELING (TUNEL ASSAY)

During apoptosis, SSBs and DSBs are introduced in cells genome by DNases in order to degrade it. Free 3'-OH-groups of the single-strand breaks can be visualized with the TUNEL labelling as a marker for apoptotic cells. Terminal deoxynucleotidyl transferase serves as catalytic enzyme for the integration of fluorescein-coupled nucleotides (deoxyuridin triphosphate, dUTP) in the free 3'-OH-gropus of the fragmented DNA. Thus, apoptotic cells can be analysed with fluorescence microscopy. Here, dUTP is stimulated at a wavelength of 488 nm. The preparation of the samples was performed analogously to 3.2.7 and 3.2.7.1. Sections from colon section B (**Figure 17**) were used for TUNEL assay. Comparable to 3.2.7.2, slides were placed in a humid incubation chamber and circled with water repelling DAKO Pen. Additionally, one section on a slide was used as positive control. The positive control was incubated with DNase (1 mg/ml BSA, 1x DNase reaction buffer including $MgCl_2$, 50 U/ml DNase) for 10 min at RT to digest the contained DNA. TUNEL assay was performed with the 'In situ Cell Death Detection Kit, Fluorescein' (Roche), which contains label solution and enzyme solution. Initially, 100 µl label solution were transferred in a new reaction tube for the negative control. Then the remaining label solution was mixed with the enzyme solution (= TUNEL solution). The following steps were performed under the fume cupboard. Two sections per slide were incubated with 50 µl of the TUNEL solution in a humid incubation chamber at 37 °C for 1 h, including the positive control. In contrast, the negative control was only incubated with the label solution. After incubation, slides were washed with PBS and stained with TO-PRO-3, processed and analysed as described in 3.2.7.2 (microscopy at 488 nm and 633 nm wavelength). For evaluation, TUNEL positive cells per colonic crypt were counted.

### 3.2.8 HAEMATOXYLIN AND EOSIN STAIN

Haematoxylin and eosin stain (HE stain) is a basic stain in histology and the gold standard for pathological examination of sections and tissue samples. Hemalum is a complex composed of aluminium ions and hematein, which arises from the oxidation of haematoxylin. It colours negatively charged (basophilic) structures like the nucleus in blue colour. A staining with an alcoholic eosin solution dyes positively charged (eosinophilic) components like the cytoplasm in various shades of red.

For the HE stain, samples were collected and processed as described in 3.2.6 and **Table 17**.

**Table 17: Deparaffinisation and rehydration of paraffin sections for histology.**

| Solution | Number of steps | Duration |
|---|---|---|
| Xylene | 3 | 3 min |
| EtOH 100 % | 1 | 2 min |
| EtOH 96 % | 1 | 2 min |
| EtOH 70 % | 1 | 2 min |
| dd$H_2O$ | 1 | 2 min |

In the first step, slides were stained with haematoxylin solution modified acc. to Gill III for 1 min and rinsed with tap water until the desired colour intensity was reached. In the next step, slides were stained with Eosin G solution (0.5 % alcoholic) for 1-5 sec and dehydrated (**Table 18**).

**Table 18: Dehydration of paraffin sections for histology.**

| Solution | Number of steps | Duration |
|---|---|---|
| EtOH 70 % | 1 | Rinse |
| EtOH 96 % | 1 | Rinse |
| EtOH 100 % | 2 | 2 min |
| Xylene | 3 | 2 min |

Finally, slides were coated with mounting medium (Roti Histokitt) and capped with a cover slip. After air-drying for about 1 h, samples were ready for microscopy or storage at RT. Samples were analysed with a Zeiss Axiovert 35 microscope, which was equipped with an Olympus Colorview I camera. Pictures were recorded with the software Cell$^A$. Best samples per slide were selected and pictures taken with 10x–20x magnification. The whole colon was recorded in about 20 pictures with the software Cell$^A$ and later merged with Image Composite Editor into one picture.

### 3.2.9 PROTEIN LYSATES FROM COLON AND LIVER TISSUE

Protein lysates were produced from snap frozen colon and liver tissue. 30 mg per sample were processed according to the following protocol. All steps were performed on ice, a maximum of twelve

samples were prepared at once to prevent long handling times. Frozen tissue was put in a reaction tube with 250-300 µl RIPA lysis buffer and mortared with a small metal pestle in a 1.5 ml reaction tube. After all samples were mortared, they were homogenised via sonication with 10 pulses (20 % power, 50 % duty cycle), twice per sample, while held on ice to prevent heating of the lysates. Finally, lysates were centrifuged at 4 °C with 15,000 g for 10 min. Supernatant was aliquoted and snap frozen in small amounts to prevent numerous freezing and defrosting of the lysate and to maintain its quality and reproducibility of the experiments. Lysates were stored at –80 °C.

## 3.2.10 BRADFORD PROTEIN ASSAY

The Bradford protein assay is a spectroscopic method to determine the protein concentration in a solution. The assay is based on an absorbance change of Coomassie Brilliant Blue G-250. Hydrophobic and ionic interactions play a role in the stabilisation of the dye's blue form. The amount of the blue form of the Coomassie dye in solution, serves as an indicator for the protein concentration and can be measured by the use of a spectrophotometer.

First, the protein lysates (3.2.9) of colon tissue were diluted 1:100 in dd$H_2O$, lysates of liver tissue were diluted 1:150 in dd$H_2O$ and kept on ice. A calibration curve was created with bovine serum albumin (BSA) in dd$H_2O$ (0-250 µg/ml). 10 µl of each sample as well as BSA solutions for the calibration curve were pipetted in triplicates on a 96 well plate and incubated with 110 µl Bradford solution for 5 min at RT under exclusion of light. Absorption was measured with a plate reader (wave length: 595 nm). Protein concentrations of the samples were calculated with the equation gained from the calibration curve.

## 3.2.11 WESTERN BLOT

Western blot is an assay for detection of proteins that is based on specific antigen detection via antibodies. Proteins are extracted and separated via gel electrophoresis following transfer onto a nitrocellulose or nylon membrane. Identification of protein is realised with specific antibodies recognising antigens on the membrane. For visualisation, horseradish peroxidase (HRP)-conjugated secondary antibodies produce a chemiluminescent signal which is recorded on a photographic film.

### 3.2.11.1 SDS-POLYACRYLAMIDE GEL ELECTROPHORESIS (SDS-PAGE)

SDS-PAGE is a common method to separate proteins in a polyacrylamide gel by electrophoresis. SDS molecules are used to denature the proteins, and negatively charged complexes with a constant mass-to-charge ratio arise. Thereby, proteins migrate towards the anode in an electric field. Discontinuous polyacrylamide gels are composed of a stacking gel to concentrate the proteins and a separation gel to split the proteins according to their molecular weight.

**Table 19: Composition of the stacking gels and concentration gels.**

| Components | Stacking gel 5 % | Separation gel 15 % |
|---|---|---|
| $ddH_2O$ | 3.81 ml | 6.39 ml |
| Tris 0.625 M pH 6,8 | 1.2 ml | - |
| Tris 1.5M pH 8,8 | - | 4.5 ml |
| SDS 10 % | 120 µl | 180 µl |
| Acrylamid / Bis 40 % | 570 ml | 6.75 ml |
| APS 10 % | 60 µl | 90 µl |
| TEMED | 46 µl | 9 µl |

First, separation gel (**Table 19**) was poured between two glass plates with 1.5 mm spacer and covered with isopropanol to prevent air bubbles. After polymerisation of the separation gel, the isopropanol was completely removed and the stacking gel (**Table 19**) poured on top of it. A comb was introduced in the stacking gel to form pockets for the samples. The comb was removed after complete polymerisation of the stacking gel and the gel was installed in an electrophoresis cell filled with SDS running buffer. Concentration of protein lysates from colon section 1 and snap-frozen liver tissue (**Figure 17**, 3.2.9) was determined with a Bradford protein assay as described in 3.2.10. Volumes of the individual protein lysates were adjusted with ddH2O and mixed with the adequate volume of 5x SDS loading buffer. Afterwards, samples were denatured at 95 °C for 10 min, shortly centrifuged and loaded in the pockets of the stacking gel. Additionally, 5 µl of the PageRuler Plus Prestained protein ladder were subjected into the first pocket of every polyacrylamide gel. Electrophoresis ran at 20 mA per gel until the dye front reached the separation gel and for migration through the separation gel increased to 40–50 mA per gel.

### 3.2.11.2 IMMUNOBLOT

Following electrophoresis, proteins separated in the polyacrylamide gel were transferred onto a nitrocellulose membrane. Using a wet-blot chamber, negatively charged proteins migrate towards the anode into the nitrocellulose membrane. The polyacrylamide gel was removed from the glass plates and placed onto a blotting buffer-soaked nitrocellulose membrane. Both sides were covered with blot buffer-soaked cellulose filter paper and foam pads. Transfer was executed in an electrophoresis cell filled with blotting buffer with 400 mA for 2.5 h at 4 °C. After blotting, the transfer was verified with a Ponceau S staining. Ponceau S is a sodium salt of a diazo dye with red colour and binds reversibly to the amino groups of proteins. The membrane was incubated in Ponceau S staining solution for 1 min at RT and subsequently rinsed with $ddH_2O$ to remove the excess colouring. Next, the dye was washed off with TBS-T under light shaking.

### 3.2.11.3 IMMUNODETECTION

HRP, conjugated to the secondary antibody, catalyses the oxidation of luminol into an unstable product which emits light at a wavelength of 428 nm proportional to the amount of a specific protein targeted by

the primary antibody. A photographic film (Agfa Medical X-Ray Film Blue) is exposed to the light emissions to record the short-time signal.

After the transfer, the nitrocellulose membrane was blocked with 5 % milk powder in TBS-T for 1 h at RT. Blocking is necessary to mask reactive protein groups which could elicit unspecific antibody binding in following steps. Subsequently, the membrane was washed with TBS-T and incubated with the primary antibody according to the conditions in **Table 20** for 1 h at RT.

**Table 20: Primary antibodies and incubation conditions for immunoblot.**

| Antibody | Dilution | Origin |
|---|---|---|
| Anti-Hsp90 | 1:1000, TBS-T | Polyclonal rabbit |
| Anti-γH2AX | 1:1000, TBS-T | Monoclonal rabbit |

The membrane was washed 3 x 10 min with TBS-T after incubation with the primary antibody and then incubated with the secondary antibody for 1 h at RT (**Table 21**).

**Table 21: Secondary antibodies and incubation conditions for immunoblot.**

| Antibody | Dilution | Origin |
|---|---|---|
| Anti-Rabbit-HRP | 1:1000, 5 % milk powder in TBS-T | Goat |

Excess antibody was removed by washing in TBS-T and the membrane incubated with ECL reagent under exclusion of light in preparation of detection. Therefore, the membrane was evenly covered with a fresh mixture of both components of the ECL solution. Either self-made or commercial ECL solution was used for detection depending on the affinity of the antibody and expected intensity of chemiluminescence. Unnecessary ECL solution was removed prior to exposure, development (Kodak autoradiography developer, Sigma-Aldrich) and fixation (Kodak autoradiography fixer, Sigma-Aldrich) of the photographic film.

## 3.2.12 ALKALINE COMET ASSAY

The comet assay, also known as single cell gel electrophoresis, is a very sensitive technique to detect both SSBs and DSBs and alkali labile sites in individual cells. DNA strand breaks can be classified into direct damage triggered by radical attack of reactive molecules and secondary damage resulting from impairment of structure relevant proteins. DNA is denatured with an alkaline buffer (3.1.5) before electrophoresis. After electrophoresis, DNA is renatured with a neutral buffer to allow staining with the fluorescence dye PI. Smaller DNA fragments migrate faster through the agarose gel than intact genomic DNA, whereby a comet-like tail arises.

The following protocol was performed on ice to protect cells from unnecessary damage. Snap frozen mouse liver tissue was put through a cell strainer with 70 µM mesh size and moisturised with 0.5 ml Merchant‘s Medium (Jackson *et al.* 2013). A flat spatula was used to carefully press the tissue in a rotary movement through the mesh. Separated cells were flushed with 1.5 ml Merchant‘s Medium into

a reaction tube below the cell strainer. Collected cells were centrifuged with 3,000 rpm at 4 °C, and the supernatant was removed. 10 µl of a cell suspension with $1x10^6$ cells per ml were mixed with 120 µl 5 % low melting point agarose and subjected on agarose coated slides. Slides were copped with a coverslip and agarose could settle on ice. After the removal of the cover slips, slides were incubated for 1 h at 4 °C in lysis buffer. After lysis, samples were transferred in the electrophoresis chamber and covered with pre-cooled electrophoresis buffer. Alkaline denaturation for 25 min at 4°C under exclusion of light followed. Electrophoresis was performed for 15 min with 25 V / 30 mA. Samples were rinsed three times with neutralisation butter, fixed in EtOH and air-dried. Cells were stained with 50 µl PI solution prior to microscopy with a fluorescence microscope (Nikon Microphot-FXA with Basler scA 1300 camera). Analysis of 50 cells per sample was performed with the software Comet Assay IV (Perceptive Instruments).

### 3.2.13 QUANTIFICATION OF CELLULAR PAR LEVELS BY LC-MS/MS

The method used for quantification of cellular PAR levels is based on LC-MS/MS. PAR was TCA-precipitated, detached from proteins by alkaline treatment and subsequently digested. Next, PAR was extracted via solid-phase extraction or DHBB-affinity chromatography. The obtained PAR was hydrolysed to monomeric nucleosides, which include adenosine (Ado), ribosyladenosine (R-Ado), and diribosyladenosine ($R_2$-Ado) characteristic for the terminal, linear, or branched part of the PAR polymer. Only R-Ado and $R_2$-Ado are specific for PAR, whereas Ado can also be derived from RNA. Samples were separated by HPLC. PAR is composed to 98–99 % of R-Ado, which was subsequently analysed via mass spectrometry. The quantification limit with this method is < 50 fmol R-Ado. This method was recently published and described in detail by Martello and colleagues (Martello *et al.* 2013).

PAR levels in snap frozen tissue samples of mouse colon section 3 (**Figure 17**) and liver tissue were analysed.

### 3.2.14 MGMT ACTIVITY ASSAY

MGMT plays a crucial role in DNA repair. MGMT removes the methyl group from the mutagenic lesion $O^6$-MeG which would otherwise result in G:C to A:T point mutations and DSBs during DNA replication respectively transcription.

Animals were treated with AOM (3.2.2) and organs harvested at desired time point as described in 3.2.6. Colon section 2 (**Figure 17**), and snap frozen liver tissue was analysed with the MGMT assay. Pre-cooled sonication buffer (3.1.5) was added to the frozen tissue in a reaction tube and then homogenized with a pestle on ice. In the next step, each sample was sonicated twice with 10 impulses (intensity of 4.5, duty cycle 40%) on ice. After centrifugation for 10 min at 14,000 rpm and 4 °C, the supernatant was aliquoted and snap frozen except for a small volume used for Bradford protein assay (3.2.10). Final protein concentration of extract should be about 2-6 µg/µl. MGMT activity of the samples was measured using a radioactive assay, which was previously described by Preuss and colleagues (Preuss *et al.* 1995). The underlying principle is the transfer of tritium-labelled methyl groups from the

*O*$^6$-position of guanine in calf thymus DNA onto MGMT. Extracts from HeLA S3 cells with high MGMT expression served as positive control and extracts from MGMT-deficient HeLA MR cells as negative control. Radioactivity, as indicator for MGMT activity, was determined via scintillation counting. Samples were measured in duplicates.

### 3.2.15 DNA EXTRACTION AND DETECTION OF *O*$^6$-MeG (SLOT BLOT)

To determine the pre-mutagenic DNA lesion *O*$^6$-MeG, mice were treated as described in 3.2.2, and sacrificed according to 3.2.6. *O*$^6$-MeG DNA adduct levels of snap frozen colon section 2 (**Figure 17**) and liver were determined as described previously (Fahrer *et al.* 2015).

Snap frozen tissue was homogenised mechanically, digested in 300 µl TE buffer with RNase for 30 min at RT and afterwards with Proteinase K at 48 °C for 18 h. Proteinase K was deactivated at 95 °C and DNA extracted. For this, 700 µl phenol–chloroform was added to the samples, mixed and centrifuged at 14,000 rpm for 5 min at RT. The aqueous phase was transferred in a new reaction tube and the previous step repeated. For precipitation of the DNA, 70 % ice cold EtOH was added and mixed carefully. Samples were centrifuged, the pellet washed with 70 % EtOH, and air-dried. Subsequently, DNA was dissolved in 50 µl TE buffer and DNA concentration determined with a NanoDrop 2000. The extracted DNA was stored at – 20 °C. *O*$^6$-MeG DNA adduct levels were determined with an immune slot blot assay as formerly published (Goder *et al.* 2015). To this end, DNA is denatured, transferred on a positively charged nylon membrane via vacuum and heat-fixed. After blocking, *O*$^6$-MeG was targeted with an *O*$^6$-MeG antibody followed by incubation with an HRP-coupled secondary antibody and detected via enhanced chemiluminescence with a photographic film, analogous to immunoblot analysis (3.2.11.2, 3.2.11.3, 3.1.4).

### 3.2.16 mRNA ISOLATION, cDNA SYNTHESIS AND REAL-TIME PCR

Animals were challenged as described in 2.4.2 and samples harvested according to 2.4.6 after the first DSS cycle. mRNA was isolated from snap frozen colon section 1 (**Figure 17**). 30 mg of snap frozen colon tissue was mortared while keeping it frozen with liquid nitrogen. mRNA was isolated from the powder using the kit NucleoSpin RNA (MACHEREY-NAGEL) according to the manufacturer's protocol. Concentration and purity of the isolated mRNA were determined with a spectrophotometer. 500 ng template mRNA were transcribed with a cDNA synthesis kit into cDNA (Thermo Scientific). The cDNA was diluted 1:5 with dd$H_2O$ and stored at –20°C. The DNA intercalating dye SYBR GreenER (Qiagen) was used for qPCR. The kit contained everything apart from template cDNA and primer. Mixture for one reaction contained 1 µl cDNA, 5 µl SYBR GreenER, 3 µl dd$H_2O$ and 1 µl of the according primer (Qiagen), sequences of the primers are not available (**Table 22**). *ACTB* was used as reference gene. The dye intercalates into the synthesised DNA double strand, causing a correlation of fluorescence signal intensity with the amount of DNA.

**Table 22: Primers for qPCR analysis.**

| Gene | Locus |
|---|---|
| *ACTB* | NM_007393 |
| *COX-2* | NM_011198 |
| *CXCL2* | NM_009140 |
| *CXCR2* | NM_001168298 |
| *IL-1B* | NM_008361 |
| *IL-6* | NM_031168 |
| *IL-17A* | NM_010927 |

Real-time PCR was performed in triplicates with the StepOnePlus Real-Time PCR-System (AB Applied Biosystems). The PCR programme is described in **Table 23**.

**Table 23: PCR programme qPCR analysis.**

| Step | Temperature | Duration |
|---|---|---|
| **1** | 95 °C | 15 sec |
| **2** | 95 °C | 15 sec |
| **3** | 55 °C | 30 sec |
| **4** | 72 °C | 30 sec |
| **5** | GOTO 2 (40 cycles) | |
| **6** | 90 °C | 15 sec |
| **7** | 60 °C | 60 sec |
| **8** | 90 °C | 15 sec |

#### 3.2.16.1 ANALYSIS OF REAL-TIME PCR DATA

Data from real-time PCR were analysed with the StepOne Software v2.2 (AB Applied Biosystems). $C_t$-values were computed from triplicate measurements of each sample and normalised with the help of the reference gene *ACTB* based on the $2^{-\Delta\Delta Ct}$ method (Livak, Schmittgen 2001). The measured data is normalised to a calibrator and the reference gene. If no calibrator is choosen manually, the software refers the expression of the samples to the sample with the lowest $C_t$-value.

# 4 RESULTS

The experimental outcome is presented in the following chapter. It is separated in three parts. In the first part, the AOM/DSS-induced colorectal carcinogenesis (4.2) including the DNA damage induction upon challenge with AOM (4.3) was studied in WT and PARP-1-deficient mice. The DNA damage induced by AOM holds a strong tumour-inducing potential. The role of PARP-1 in the inflammatory response is dissected in the middle part (4.4). Here, the animals were challenged with AOM and the inflammatory agent DSS to induce a tumour-promoting gut inflammation. Finally, the tumour initiation by AOM and the chemically provoked colitis, both driving the formation of CRC and investigated separately in the two preceding parts of the results, were conjoined in a new PARP-1$^{-/-}$/MGMT$^{-/-}$ strain (4.5).

## 4.1 GENOTYPING OF K.O. MICE

Prior to the animal experiments, the genotype of the mice was confirmed via PCR as described in 3.2.1 with genetic material from mouse tail tips and ear punchings. **Figure 18** shows a representative agarose gel with the PCR products of a PARP-1 genotyping. The left site of the gel shows the products of the PCR ran with primers P-A and P-B. This primer pair amplifies a sequence of the WT *PARP-1* with a size of 200 bp. The PCR products amplified with the primers for the k.o. band (P-A and P-C) were loaded on the right site. The PARP-1 k.o. sequence has a size of 700 bp. The PARP-1 WT control sample only showed a band on the left site, whereas no band is detected on the right site. In contrast, the PARP-1 k.o. control sample only showed a band on the right site, where the k.o. sequence was amplified. Sample 3 was obtained from an animal with a homozygous PARP-1 k.o., samples 1, 2, 3 and 5 from animals carrying a WT and an k.o. allele.

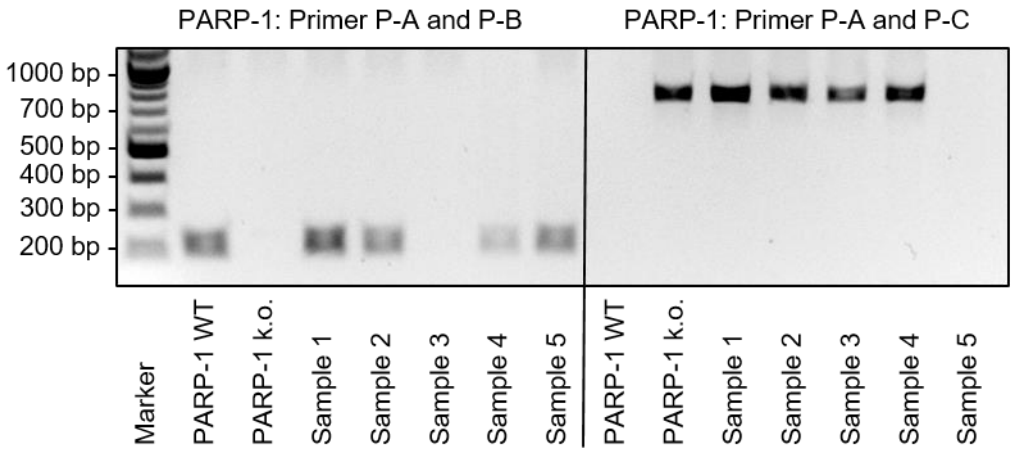


**Figure 18: Exemplary picture of PARP-1 genotyping.** Presented is a 1.5 % agarose gel including marker, PARP-1-proficient WT samples and PARP-1$^{-/-}$ samples as controls. The WT band has a size of 200 bp and the k.o. band a size of 700 bp.

MGMT genotyping was performed in a similar manner. The agarose gel presented in **Figure 19** was loaded with MGMT WT genetic material and MGMT k.o. genetic material as controls and samples from the animals mated for the PARP-1$^{-/-}$/MGMT$^{-/-}$ strain (sample 1-6). The MGMT-proficient control showed

a band at 542 bp and the MGMT-deficient control a band at 409 bp. Sample 1, 2, 4 and 5 are homozygous k.o. animals whereas sample 3 and 6 carry two *MGMT* WT alleles.

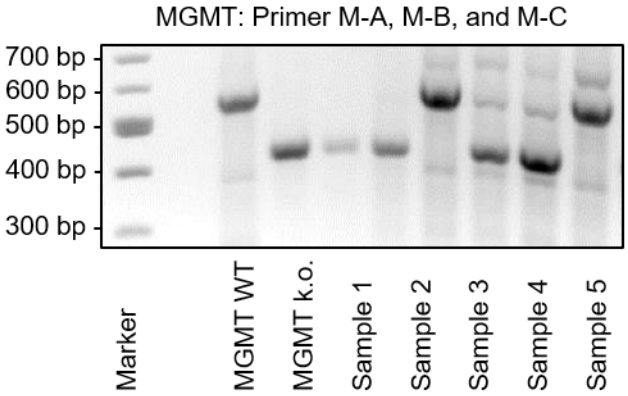


**Figure 19: Representative picture of MGMT genotyping.** Shown is a 1.5 % agarose gel containing marker, MGMT-proficient WT samples and MGMT k.o. samples as controls. The WT band has a size of 542 bp and the k.o. band a size of only 409 bp.

## 4.2 LOSS OF PARP-1 CRITICALLY INFLUENCES CRC FORMATION

To investigate the role of PARP-1 in NOC-induced CRC formation, PARP-1-proficient WT animals were compared to PARP-1-deficient animals, which were both treated with increasing doses of AOM as part of the AOM/DSS murine model of CRC (3.2.3). Tumour formation was monitored via mini endoscopy (3.2.5) and rated as described in 3.2.5.1. Mini endoscopy was kindly performed [redacted]

Mice were injected with an increasing dose series of AOM (0–15 mg/kg bw) and two subsequent cycles of 1 % DSS in the drinking water (3.2.3). **Figure 20** shows representative pictures of WT and PARP-1 k.o. animals at the end of the experiment.

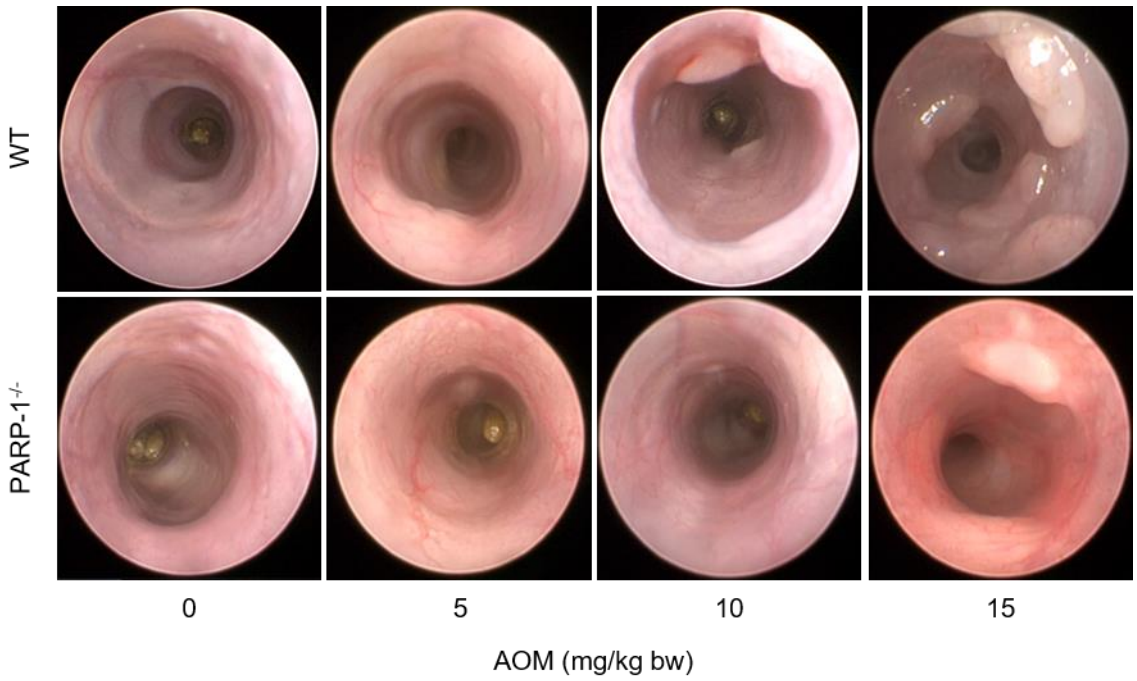


**Figure 20: Exemplary pictures of mini endoscopy.** Presented are WT and PARP-1$^{-/-}$ mouse colons after treatment with AOM (0, 10 and 15 mg/kg bw) and two cycles of 1 % DSS at the end of the experiment (after 16 weeks).

Statistical analysis showed a significant dose-dependent increase of tumour number and size in the WT animals. Here, tumour number grew to about 4 tumours per animal and the tumour score to 10, albeit tumour score showed a big standard error. In contrast, PARP-1-deficient animals displayed a different response. There was no increase in CRC formation visible, neither in tumour number nor in tumour score. PARP-1$^{-/-}$ animals exhibited a higher basal rate of tumour formation compared to WT animals (**Figure 21**).

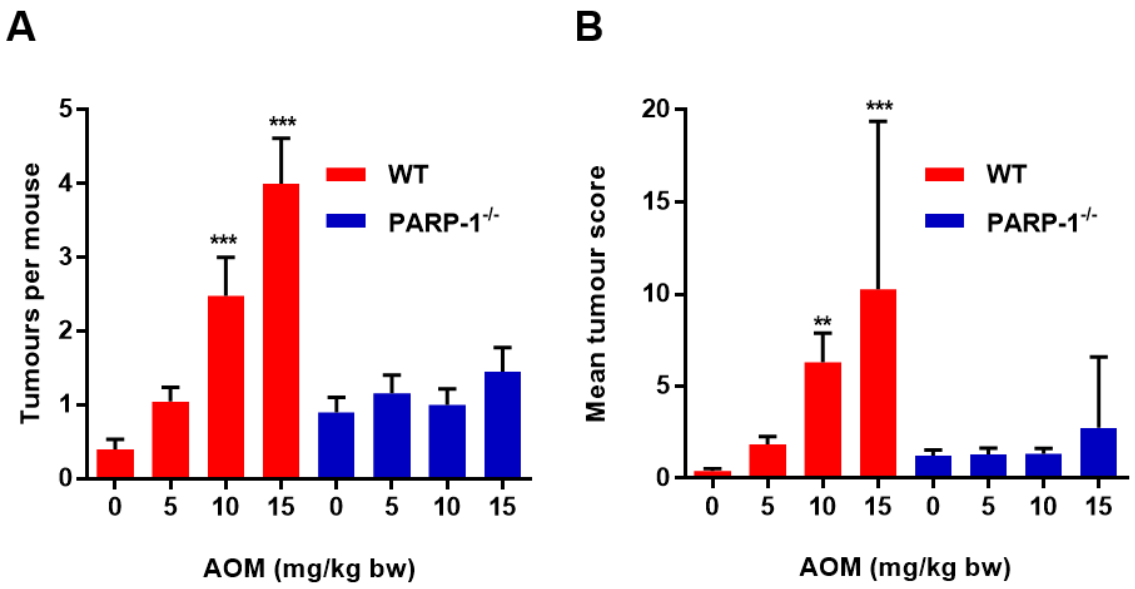


**Figure 21: Colorectal carcinogenesis in WT and PARP-1$^{-/-}$ animals after 16 weeks.** Mice received AOM and two 1 % DSS cycles. Numerical description of **A** tumour number and **B** mean tumour score per animal. Tumour score and number were assessed with the help of mini endoscopy and are presented as mean ± SEM of n ≥ 15 animals. Statistical significance was calculated to PBS treated animals for each phenotype using an one-way ANOVA with Tukey's multiple comparisons test. **p < 0.01, ***p < 0.001.

## 4.3 ROLE OF PARP-1 IN NOC-INDUCED DNA DAMAGE

After the initial finding revealing the resistance of PARP-1$^{-/-}$ mice to the AOM/DSS protocol, differences in primary DNA damage induction by AOM between WT and PARP-1 k.o. animals in colon and liver tissue were further detailed. Aim of this part of the work was to compare the primary genotoxic potential and consequences like cell death between both genotypes. DNA damage leading to mutations and loss of genomic stability is known to play in important role in tumour initiation.

### 4.3.1 LACK OF PARP-1 LEADS TO DRAMATICALLY REDUCED FORMATION OF PAR

The PARP enzyme family catalyses the formation of PAR in an $NAD^+$-dependent manner. PAPR-1 is responsible for almost 90 % of nuclear PARP activity (Shieh *et al.* 1998). Furthermore, it is known that PARP activity differs in several organs (Martello *et al.* 2013). Quantification of PAR levels in mouse tissue was performed in the lab [redacted] (3.2.13).

Basal PAR levels of colon and liver tissue were analysed in three animals per group to verify the absence of PARP-1 activity in the mice and is presented in **Figure 22**. In general, the generated data revealed significantly higher PAR levels in liver tissue than in colon tissue. For WT animals, PAR level in liver tissue (15.7 pmol/mg DNA) was twice as high as in colon (7.5 pmol/mg DNA). Similar to WT animals, PAR levels in the liver of PARP-1$^{-/-}$ animals (6 fmol/mg DNA) were also higher than in colon tissue (1.5 fmol/mg DNA). Comparison between the genotypes showed lower PAR levels in the PARP-1-deficient animals, with stronger difference in liver tissue. The measured amounts of PAR respectively R-Ado were above the detection limit of < 50 fmol for all measured samples. The residual PAR in PARP-1$^{-/-}$ animals is attributable to the catalytic activity of other members of the PARP superfamily, *e.g.* PARP-2.

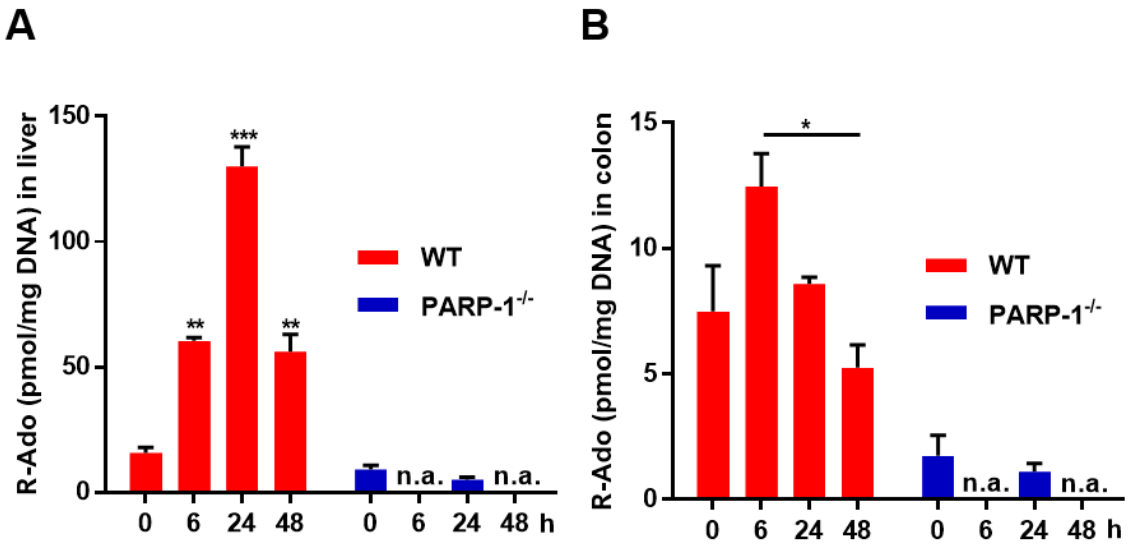


**Figure 22: PAR levels after challenge with 10 mg/kg bw AOM.** PAR levels in **A** liver and **B** colon tissue of WT and PARP-1-deficient mice was assessed up to 48 h after treatment. Statistical analysis was performed using one-way ANOVA and Tukey's multiple comparisons test. Data are shown as mean ± SEM (n = 3). Asterisks on top of the bars indicate significance to untreated control of each group. *p < 0.05, **p < 0.01, ***p < 0.001.

PARP-1 plays a crucial role in response to AOM-mediated DNA damage which leads to formation of PAR at the site of damage. Hence, PAR levels after challenge with AOM were measured. Animals were treated up to 48 h with 10 mg/kg bw AOM. **Figure 22 A** presents data of PAR analysis in liver tissue and **Figure 22 B** in colon tissue. In the PARP-1$^{-/-}$ animals, hepatic PAR levels were lower as compared to the WT. Untreated animals showed 9 pmol/mg DNA and half of the amount after 24 h, though with no statistical significance (**Figure 22 A**). PAR quantification in colon tissue of WT mice revealed only a moderate effect on the R-Ado level after 6 h, which dropped to approximately the basal level after 48 h. PARP-1$^{-/-}$ mice showed only little PAR in colon tissue. Only two time points were probed to confirm that PAR levels remain unaffected by treatment with AOM. The R-Ado level in the untreated WT liver tissue was almost twice as high as in the WT colon tissue. 24 h after AOM administration, R-Ado levels strongly increased to 130 pmol/mg DNA and then declined to 56 pmol/mg DNA after 48 h, which was still above the basal R-Ado level of about 16 pmol/mg DNA. PAR levels in WT animals showed a comparable time-dependent pattern of PAR induction upon AOM treatment in liver and colon tissue, whereas PARP-1 k.o. exhibited no induction of PAR formation (**Figure 22 B**).

In general, liver tissue held more PARP activity compared to colon tissue. In contrast to WT mice, no induction of PAR formation was visible in animals lacking PARP-1. Residual PAR was likely attributable to other members of the PARP protein family (*e.g.* PARP-2).

### 4.3.2 PARP-1-DEFICIENT ANIMALS ARE PRONE TO NOC-INDUCED DNA STRAND BREAKS

PARP-1 plays an important role in the recruitment of BER proteins including XRCC1, DNA polymerase-β and DNA ligase III (Audebert *et al.* 2004; Caldecott *et al.* 1996). During the process of BER, DNA strand breaks can arise as critical intermediate. Strand break formation in PARP-1-proficient (WT) and PARP-1-deficient animals was studied with the alkaline comet assay (3.2.12) which detects alkali-labile sites, SSBs, and DSBs.

Animals of both genotypes were treated with 5 mg/kg bw and 10 mg/kg bw AOM up to 48 h and organs were subsequently harvested (3.2.2, 3.2.6). Following experiments were only performed with cells gained from snap frozen liver. **Figure 23** shows representative pictures of analysed liver cells from animals treated with 5 mg/kg bw and 10 mg/kg bw AOM up to 48 h.

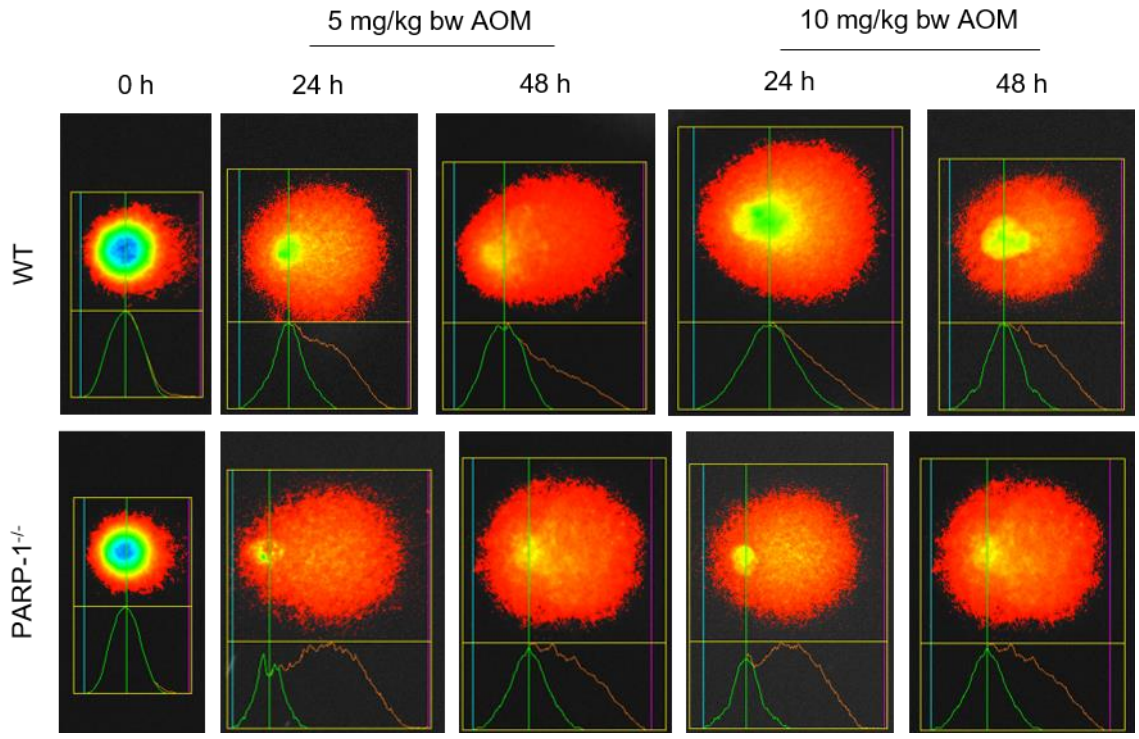


**Figure 23: Representative pictures of DNA strand breaks in liver tissue of WT and PARP-1$^{-/-}$ animals.** Alkaline comet assay was performed after treatment with 5 mg/kg bw AOM and 10 mg/kg bw AOM up to 48 h.

Statistical analysis of three animals per group is presented in **Figure 24**. After treatment of WT animals with the low AOM dose for 24 h, a strong induction of the tail intensity from 3.3 to 31 was measurable. Due to the variability in tail intensity upon administration of 5 mg/kg bw AOM, no statistical significance was reached. After 48 h, tail intensity was at 27.3. The tail intensity within this group varied strongly and the experiment failed to prove statistical significance. Basal tail intensity of 2.4 in liver cells of PARP-1$^{-/-}$ animals was significantly increased by AOM treatment after 24 h (43.6) and dropped to 23.8 after 48 h in a time-dependent manner. Challenge with 10 mg/kg bw led to a stronger increase of DNA strand breaks in WT animals to a tail intensity over 30, which was significant to untreated animals after 24 h and 48 h. Due to the strong variation within the animals treated with 5 mg/kg bw AOM, the increase lacked significance. Nevertheless, PARP-1-deficient animals displayed an increase which was significantly higher compared to the 5 mg/kg bw group. Here, a significant higher tail intensity of 55.7 after 24 h and 42.0 after 48 h was measurable compared to untreated animals (2.4).

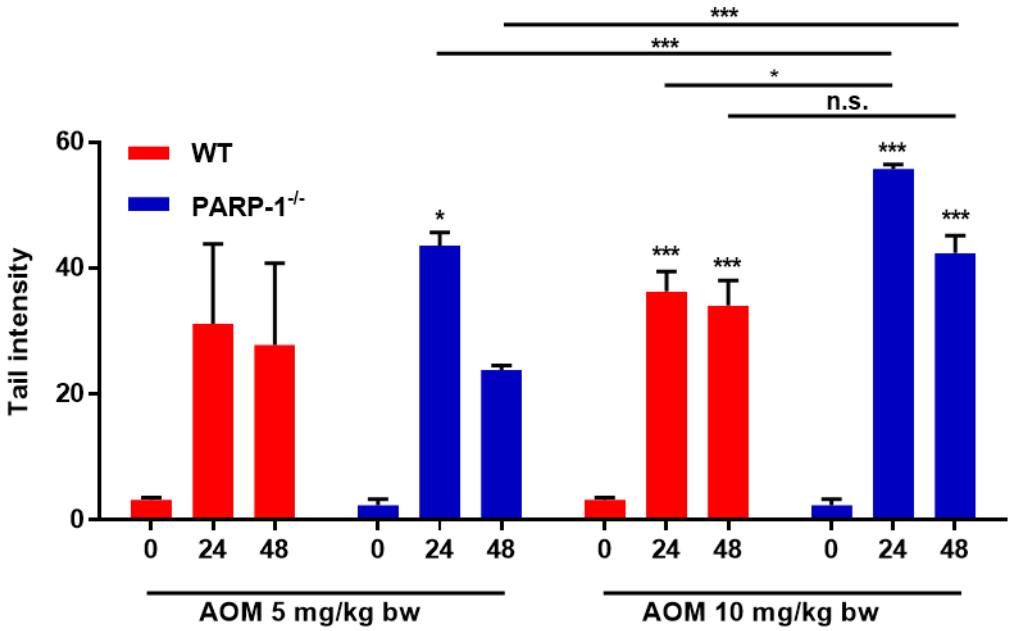


**Figure 24: Statistical evaluation of comet tail intensity in liver tissue of WT and PARP-1$^{-/-}$ animals.** Animals received 5 mg/kg bw AOM and 10 mg/kg bw AOM up to 48 h. Data are shown as mean ± SEM (n = 3). Statistical analysis was performed using two-way ANOVA and Bonferroni's multiple comparisons test. Asterisks on top of the bars indicate significance to untreated control of each group. n.s. = not significant, *p < 0.05, ***p < 0.001.

It was not possible to generate reliable data from snap frozen colon tissue. Samples from the same treatment group strongly varied and measurements were not reproducible. In conclusion, treatment with AOM increased DNA strand breaks in liver cells of WT and PARP-1 k.o. animals, which was generally stronger in PARP-1-deficient mice. Regarding both genotypes, the induced DNA damage correlated with AOM dose.

### 4.3.3 AOM-INDUCED DDR IN WT AND PARP-1$^{-/-}$ ANIMALS

To analyse the AOM-triggered DDR, phosphorylated histone H2AX (γH2AX), a well-established surrogate marker for DSB and part of the DDR induced by genotoxic stress (Kuo, Yang 2008, 2008),

was analysed via immunoblotting. Mice were treated with AOM (3.2.2) and sacrificed at the indicated time points as described in 3.2.6. Upon lysis of colon and liver tissue, protein concentration was determined with the help of the Bradford protein assay (3.2.10). Proteins were separated via SDS-PAGE and visualised via immunodetection (3.2.11).

**Figure 25 A** shows a representative time-course in WT and PARP-1$^{-/-}$ animals after challenge with 5 mg/kg bw AOM up to 48 h and **Figure 25 B** after treatment with 10 mg/kg bw AOM.

The double band of the loading control, Hsp90 primary antibody of mouse origin, in the immunoblots of WT animals should be noted (**Figure 25**). The lower band might be a degradation product which arose from tissue lysis and/or handling. Alternatively, it could be an unspecific band. To eliminate the lower band, immunoblot analysis of Hsp90 in this work was performed with a rabbit polyclonal Hsp90 primary antibody.

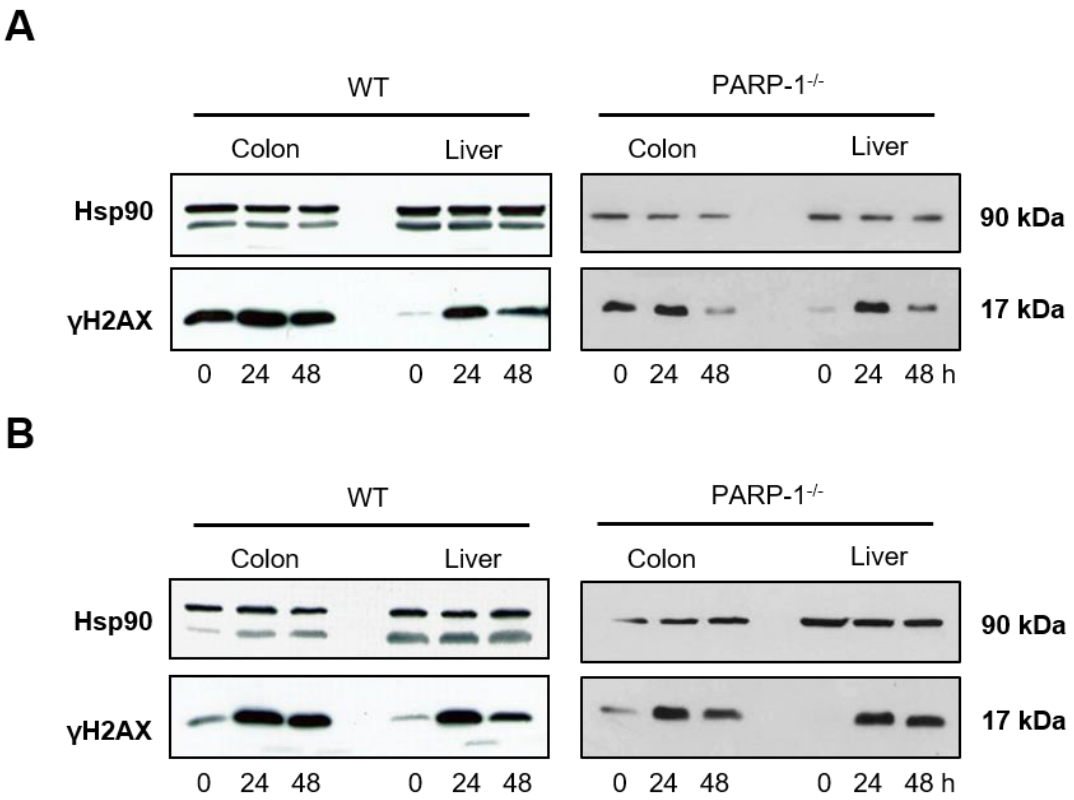


**Figure 25: Analysis of γH2AX levels in liver and colon tissue following AOM treatment.** Animals received 5 mg/kg bw AOM and 10 mg/kg bw up to 48 h. Hsp90 was visualised as loading control. Different Hsp90 antibodies were used for WT and PARP-1$^{-/-}$ samples, see text for details.

Densitometric evaluation of immunoblots from tissue of three different animals per group is presented in **Figure 26**. In WT liver, γH2AX levels were significantly induced to almost 6-fold of the untreated animals after 24 h and dropped to the 2.3-fold after 48 h. In PARP-1-deficient animals, a 3-fold increase was visible after 24 h, which lacked significance and declined to 1.4-fold of the basal γH2AX level after 48 h. A comparable but weaker time-dependent induction pattern was observable in colon tissue. Analysis of colon tissue revealed a small increase of γH2AX 24 h after AOM injection, returning to basal levels after 48 h, which both lacked statistical significance. The time-dependent induction pattern did not

differ between both genotypes. There was no statistical difference between genotypes. The basal γH2AX levels were stronger in colon tissue (**Figure 25 A**), whereas the induction was stronger in liver tissues (**Figure 26**).

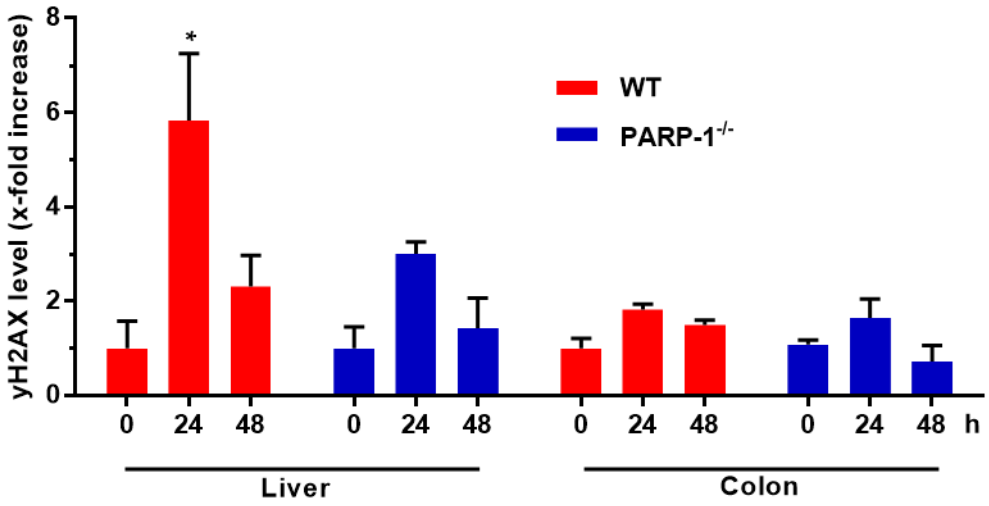


**Figure 26: Densitometric evaluation of γH2AX levels in colon and liver tissue**. WT and PARP-1-deficient animals were challenged with 5 mg/kg bw AOM up to 48 h. Data are presented as mean ± SEM (n = 3). Statistical analysis was performed using one-way ANOVA and Tukey's multiple comparisons test. Asterisks on top of the bars indicate significance to untreated control of each group. *p < 0.05. WT data was already published by our group (Fahrer *et al.* 2015).

To further investigate γH2AX induction, animals were treated with 10 mg/kg bw AOM analogous to the experiment described above. Presented is the densitometric quantification of three animals per group (**Figure 27**). In liver tissue, a significant increase of γH2AX levels to 8.7-fold in WT and 9.6-fold in PARP-1-deficient animals was measurable 24 h after challenge with the high AOM dose. After 48 h, levels dropped to 5.6-fold in WT and 5.8-fold in PARP-1 k.o. mice. In colon tissue of WT animals, a 2.6-fold increase was measurable after 24 h and declined to 2.3-fold after 48 h. A slight induction of γH2AX (about 2-fold) was visible in colon tissue of PARP-1$^{-/-}$ was visible after 48 h and only minimal induction after 24 h. In addition, there was neither a significant variation of γH2AX levels in colon tissue after treatment nor difference between both genotypes visible. Time-dependent induction did not differ between liver tissue of WT and PARP-1-deficient animals. As already described for the lower dose, basal γH2AX levels were stronger in colon tissue (**Figure 25 B**) and the induction stronger in liver tissue (**Figure 27**).

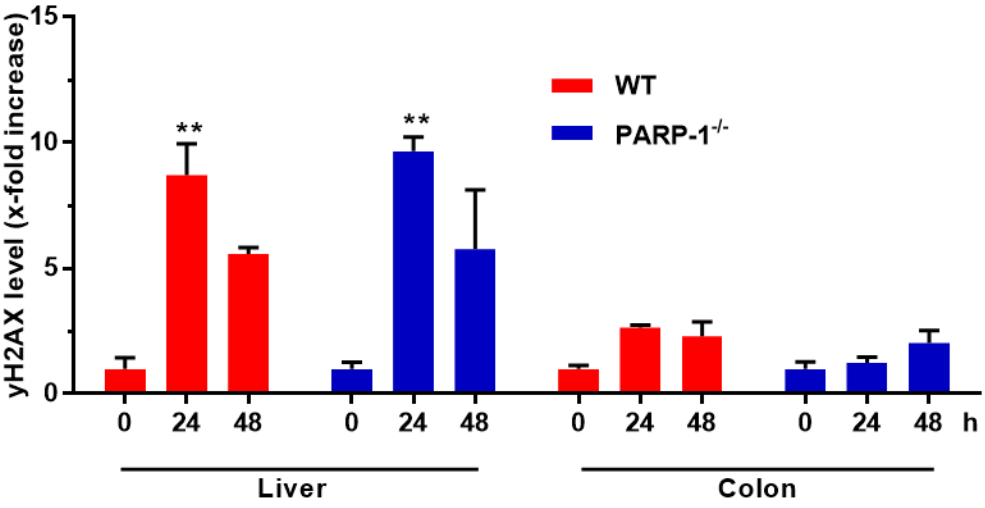


**Figure 27: Densitometric evaluation of γH2AX levels in liver and colon tissue**. WT and PARP-1-deficient animals were treated with 10 mg/kg bw AOM up to 48 h. Data are presented as mean ± SEM (n = 3). Statistical analysis was performed using one-way ANOVA and Tukey's multiple comparisons test. Asterisks on top of the bars indicate significance to the according untreated control. *p < 0.05, **p < 0.01. WT data was already published by our group (Fahrer *et al.* 2015).

In summary, a time-dependent induction of γH2AX formation was detectable in WT and PARP-1$^{-/-}$ animals after AOM treatment. The strength of induction was correlating with the applied AOM dose. In general, the basal γH2AX levels were stronger in colon but the induction was stronger in liver tissue.

### 4.3.4 PARP-1 HAS NO INFLUENCE ON FORMATION OF AOM-INDUCED *O*$^6$-MeG ADDUCTS AND MGMT ACTIVITY

NOC, such as AOM, cause DNA alkylation whereby a methyl group is transferred onto a DNA base, which can occur on nitrogen atoms within the base's circular structure and on extracircular oxygen atoms. One of the most critical pre-mutagenic methylations is *O*$^6$-MeG, which is reverted by the protein MGMT. Upon transfer of the methyl group from *O*$^6$-MeG onto MGMT, it is inactivated and proteasomally degraded (Fahrer *et al.* 2015; Kaina *et al.* 2007).

To address the question whether PARP-1 has any influence on $O^6$-MeG induction, DNA of three AOM-treated animals per group was analysed via slot blot analysis (3.2.15). Initially, DNA of WT and PARP-1 k.o. animals were compared at 24 h and 48 h after treatment with 10 mg/kg bw AOM. **Figure 28** shows representative slot blots of analysed liver DNA after treatment with 10 mg/kg bw AOM for 24 h (**A**) and 48 h (**B**). In the graph below (**Figure 28 C**), densitometric evaluation of $O^6$-MeG levels upon AOM treatment are presented. Both genotypes showed a slight increase in $O^6$-MeG levels in colon tissue (WT: 1.6-fold, PARP-1 k.o. 1.7-fold) after 24 h, which returned to control level after 48 h. The induction was stronger in liver tissue. Here, $O^6$-MeG adducts significantly rose the 7.3-fold of the basal level after 24 h and reached their maximum at 8.2-fold after 48 h, albeit with a big variation between the animals. PARP-$1^{-/-}$ mice also showed a significant induction of $O^6$-MeG adduct levels after 24 h to 10.9-fold increase followed by a drop to 5.4-fold of control level after 48 h. Means of AOM-induced $O^6$-MeG adduct levels were comparable in liver tissue of WT and PARP-$1^{-/-}$ mice.

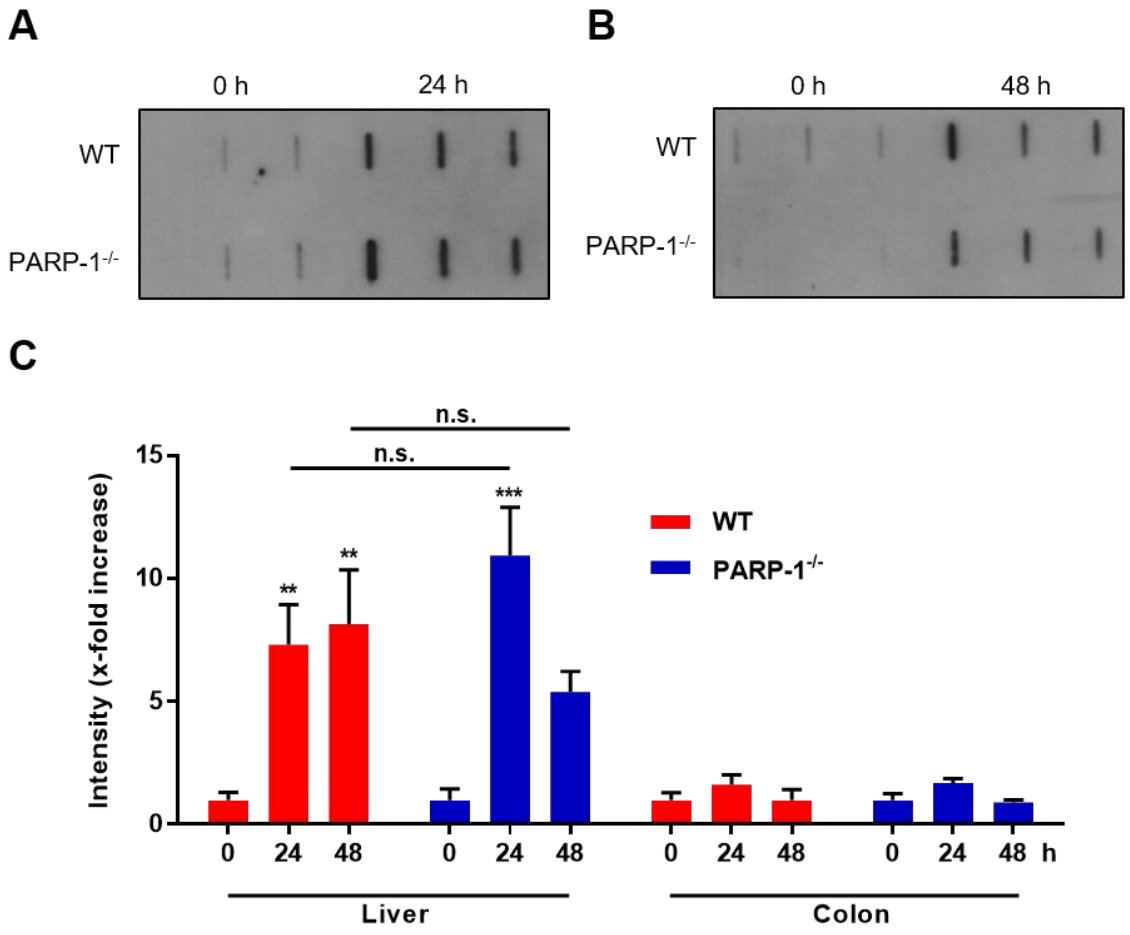


**Figure 28: Determination of $O^6$-MeG levels in liver and colon tissue of WT and PARP-1-deficient animals.** $O^6$-MeG adducts were assessed via slot blot after challenge with 10 mg/kg bw AOM up to 48 h. **A** Representative slot blot of WT and PARP-1 k.o liver DNA 24 h and **B** 48 h after treatment. **C** Statistical evaluation of band intensity. Data are shown as mean ± SEM (n = 3). Statistical analysis was performed using one-way ANOVA and Tukey's multiple comparisons test. Asterisks on top of the bars indicate significance to the related untreated control. **p < 0.01, ***p < 0.001. WT data was already published by our group (Fahrer *et al.* 2015).

Furthermore, MGMT activity (according to 3.2.14) in both genotypes was compared in a time-dependent manner (three animals per group). **Figure 29 A** presents the time-dependent activity of MGMT in WT and PARP-1-deficient animals after treatment with 5 mg/kg bw AOM up to 48 h. Analysis of WT animals revealed a reduction of MGMT activity with strongest depletion at 48 h. In contrast, PARP-1 k.o. animals showed a reduction of activity after 24 h to almost 50 % of basal levels and recovery after 48 h. Differences between genotypes were not statistically significant. The MGMT depletion pattern is alike in liver tissue of both genotypes. After 24 h, MGMT was almost completely depleted and activity restored to over 50 % after 48 h. Next, a higher AOM dose (10 mg/kg bw) was administered (**Figure 29 B**). The depletion of MGMT was strikingly increased in all samples.

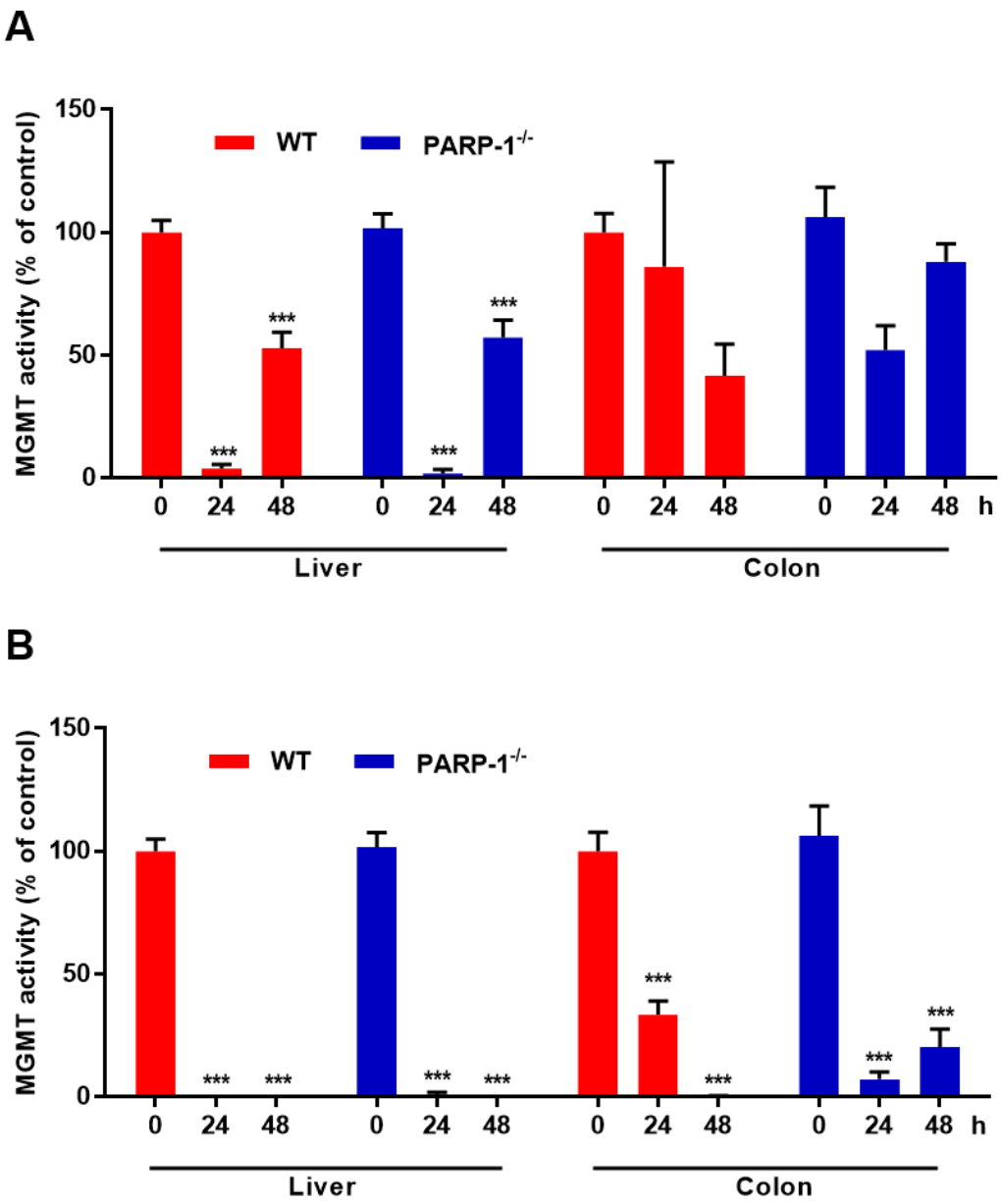


**Figure 29: Analysis of MGMT activity in colon and liver tissue of WT and PARP-1 k.o. mice.** Animals were challenged with **A** 5 mg/kg bw AOM and **B** 10 mg/kg bw AOM up to 48 h. Data are displayed as mean ± SEM (n = 3). Statistical analysis was performed using two-way ANOVA and Bonferroni's multiple comparisons test. Asterisks on top of the bars indicate significance to untreated control of each group. ***p < 0.001. WT data was already published by our group (Fahrer *et al.* 2015).

Consistent with the results of the low dose (**Figure 29 A**), MGMT activity in colon tissue was different in both genotypes upon AOM treatment. WT animals experienced a significant drop of MGMT activity to 34 % of control after 24 h with complete depletion after 48 h. In PARP-$1^{-/-}$ colon tissue, a decline of MGMT activity to 7 % after 24 h with recovery to 20 % of basal levels was measurable. As observed before, differences were not significant between both genotypes. The high AOM dose led to a complete depletion of MGMT activity in the liver of WT and PARP-1-deficient animals up to 48 h.

Taken together, AOM-induced *O*$^6$-MeG adducts in both genotypes were strikingly stronger in liver tissue. In line with these results, MGMT activity was reduced after challenge with AOM in liver and colon tissue of WT and PARP-1 k.o. animals. Here, a recovery of MGMT activity was visible in animals treated with a low AOM dose. However, the higher AOM dose provoked stronger and longer persisting deprivation of MGMT.

### 4.3.5 CELL PROLIFERATION AND APOPTOSIS INDUCTION ARE NOT INFLUENCED BY PARP-1

Since PARP-1 plays an important role in a plethora of cellular mechanisms, including regulation of the cell cycle (Mangerich, Bürkle 2012), the question whether loss of PARP-1 results in an altered cell proliferation, thereby influencing the response to DNA damage, was addressed. In this regard, the PCNA was analysed as marker for cell proliferation via immunolocalisation (3.2.7). The 36 kD nuclear protein acts as cofactor of DNA polymerase δ during DNA synthesis and is therefore an established indicator for cell proliferation (Hall *et al.* 1990).

PCNA abundance and localisation in colon sections of untreated WT and PARP-1 k.o. animals were compared by IHC staining and confocal microscopy (3.2.7). Selected captures of stained colon slices are presented in **Figure 30 A**. PCNA expressing cells were localised in the proliferative zone of the crypts with decreasing signal towards the differentiation zone in the villi. Statistical analysis of three untreated animals per genotype confirmed similar average cell proliferation in the colon crypts of both PARP-1-proficient and PARP-1-deficient animals (**Figure 30 B**).

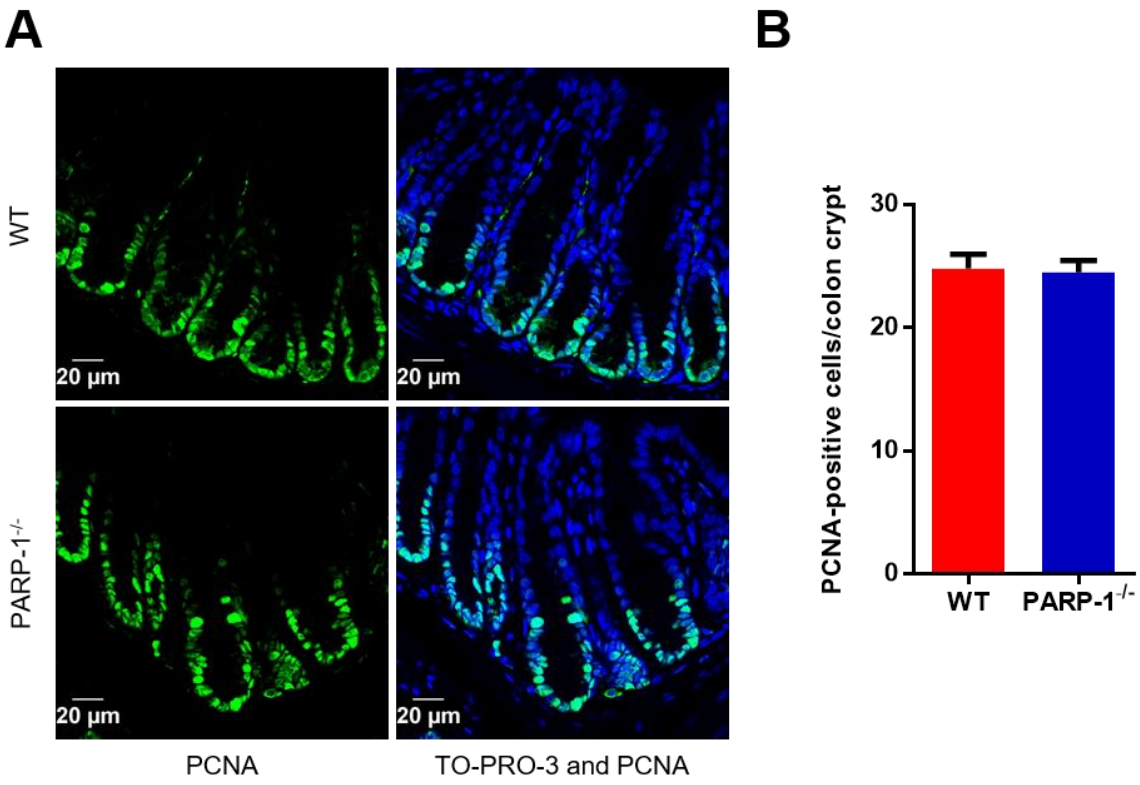


**Figure 30: Basal cell proliferation in untreated WT and PARP-1-deficient animals**. **A** Representative pictures of PCNA-stained colon sections: nuclei were stained with TO-PRO-3 (blue) and PCNA (green). Samples were observed via confocal microscopy at 40x magnification (scan zoom 1.0). **B** Statistical evaluation of basal cell proliferation was performed using student's t-test. Data are displayed as mean ± SEM (n = 3).

AOM-mediated DNA lesions lead to DNA strand break induction and base adducts, which can result in the induction of cell death if the lesions persist or repair malfunctions (Fu *et al.* 2012; Roos, Kaina 2006). AOM-induced cell death in colon tissue was analysed via TUNEL staining (3.2.7.4). This assay is based

on the incorporation of fluorescein-coupled nucleotides at free 3'-OH-groups of DNA strand breaks, which are then visualised with fluorescence microscopy.

Groups of three animals per genotype were treated with 5 mg/kg bw AOM and 10 mg/kg bw AOM for 48 h (3.2.2) and sacrificed (3.2.6). **Figure 31** shows representative pictures of the stained colon sections after challenge with 10 mg/kg bw AOM. A work published by our group (Fahrer *et al.* 2015) reported a strong induction of apoptosis in MGMT$^{-/-}$ animals after challenge with AOM. Therefore, MGMT-deficient animals treated with 10 mg/kg bw AOM for 48 h were used as positive control.

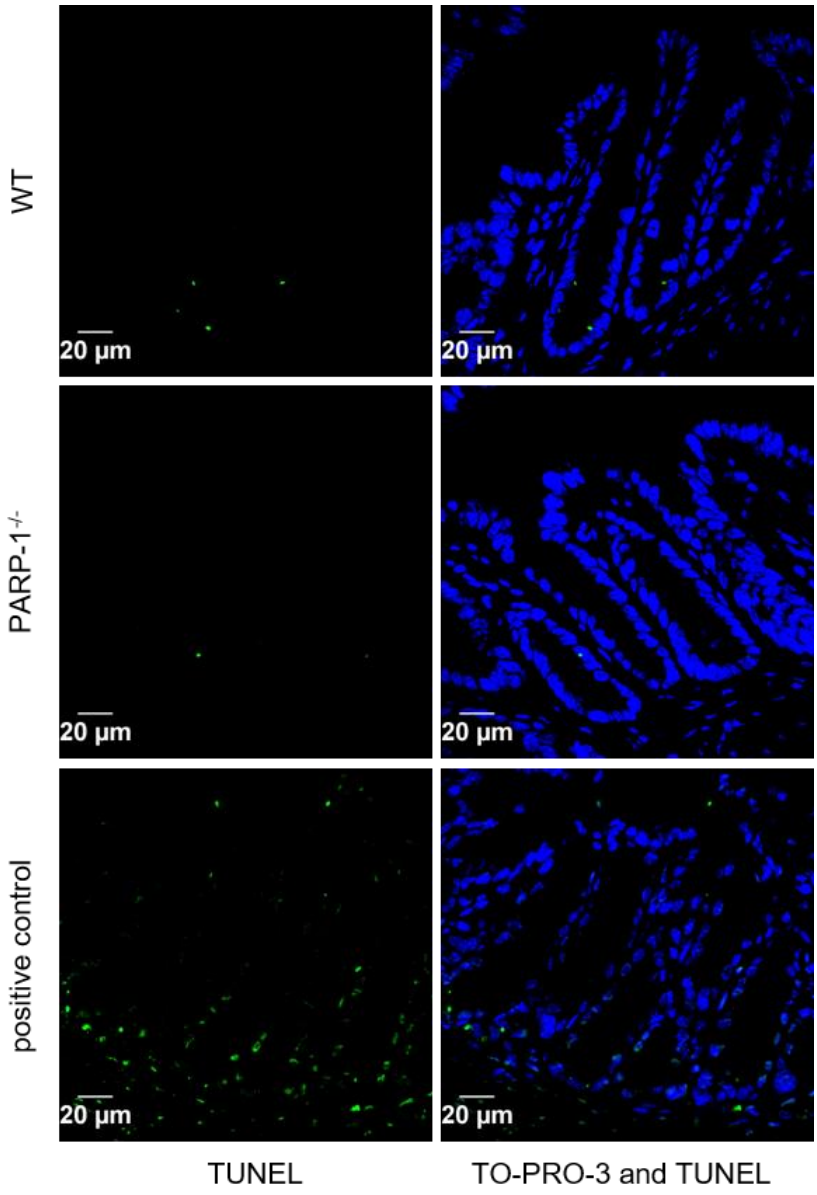


**Figure 31: TUNEL-positive cells in the colon crypts of WT and PARP-1-deficient animals.** Representative pictures of TUNEL-stained colon sections after challenge with 10 mg/kg bw AOM for 48 h. Colon sections of MGMT-deficient mice treated with 10 mg/kg bw AOM for 48 h were used as positive control. Nuclei are stained with TO-PRO-3 (blue). Samples were analysed with confocal microscopy at 40x magnification (scan zoom 1.0).

Statistical evaluation of the TUNEL staining (**Figure 32**) revealed that WT animals exhibited about 0.17 positive cells per colonic crypt after treatment with 5 mg/kg bw AOM and 0.34 positive cells per colonic crypt after treatment with the twofold dose. However, the difference was not statistically significant. A significant increase from 0.13 positive cells at 5 mg/kg bw AOM to 0.36 positive cells at 10 mg/kg bw AOM was visible for PARP-1 k.o. animals. Comparison of both genotypes revealed lower apoptosis induction in the colon of PARP-1-deficient animals without statistical significance. Apoptosis induction at 10 mg/kg bw AOM was comparable in both genotypes.

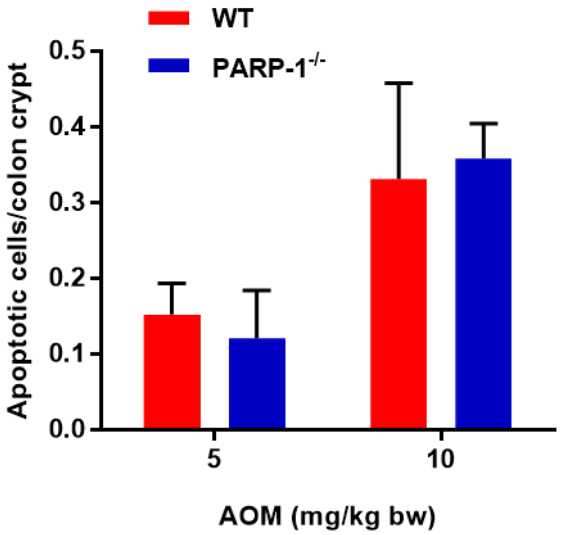


**Figure 32: Statistical evaluation of TUNEL-stained colon sections.** Animals were challenged with 5 mg/kg bw or 10 mg/kg bw AOM for 48 h. Data are presented as mean ± SEM (n = 3). Statistical analysis was performed with two-way ANOVA and Tukey's multiple comparisons test.

Altogether, these experiments confirmed that the absence of PARP-1 has neither an influence on basal cell proliferation nor induction of DNA damage-induced apoptosis.

### 4.3.6 SUMMARY: ROLE OF PARP-1 IN NOC-INDUCED DNA DAMAGE

The results of the experiments presented in this chapter are summarised in **Table 24**.

**Table 24: Results presented in chapter 4.3 Role of PARP-1 in NOC-induced DNA Damage.**

| **Dramatically Reduced PAR Formation in Absence of PARP-1** |
|---|
| • higher basal and induced PAR levels in liver tissue compared to colon tissue<br>• time-dependent induction of PAR formation in liver and colon tissue of WT animals but not in PARP-1 k.o. animals<br>• residual PAR formation in PARP-1-deficient animals (likely attributable to PARP-2) |
| **PARP-1 k.o. Animals are Sensitive to NOC-induced DNA Strand Breaks** |
| • AOM-induced DNA strand breaks in liver cells of WT and PARP-1 k.o. animals<br>- stronger induction in PARP-1-deficient mice<br>• comparable induction of γH2AX in WT and PARP-1$^{-/-}$ animals after AOM treatment<br>- stronger γH2AX-induction in liver tissue compared to colon tissue<br>- higher basal γH2AX levels in colon but induction stronger in liver tissue |
| **No Impact of PARP-1 on *O*$^6$-MeG DNA Adduct Formation or MGMT Activity** |
| • induction of *O*$^6$-MeG DNA adducts after treatment with AOM in both genotypes<br>- adduct formation was stronger in liver tissue than in colon tissue<br>• reduced MGMT activity after challenge with AOM in liver and colon tissue<br>- recovery of MGMT activity visible after treatment with low AOM dose<br>- higher AOM dose caused stronger and persistent depletion of MGMT |
| **Lack of PARP-1 has no Influence on Basal Cell Proliferation and NOC-Induced Apoptosis in Colon Crypts** |
| • lack of PARP-1 has neither an influence on basal cell proliferation nor induction of apoptosis upon challenge with AOM |

## 4.4 ROLE OF PARP-1 IN INFLAMMATORY RESPONSE

Besides its important role in DNA damage repair, PARP-1 is a crucial player of the inflammatory response, in which it functions as activator of the inflammatory master regulator NF-κB (Hassa *et al.* 2003). Considering that inflammation promotes the malignant transformation of initiated cells and promotes carcinogenesis, the inflammatory process induced by DSS was further investigated in WT and PARP-1-deficient animals.

### 4.4.1 PARP-1-DEFICIENT ANIMALS ARE PROTECTED AGAINST DSS-INDUCED COLITIS

AOM/DSS-induced colitis severity was assessed by evaluation of the MEICS (Becker *et al.* 2006a). Therefore, the strength of the animals' colitis was studied after the first DSS cycle (**Figure 14**) via mini endoscopy (3.2.5.2). Mini endoscopy and scoring of mucosal inflammation was kindly [redacted]

PARP-1-proficient (WT) and PARP-1$^{-/-}$ animals were challenged with 1 % and 2.5 % DSS. The AOM dose was reduced from 15 mg/kg bw to 10 mg/kg bw for the animals treated with 2.5 % DSS to prevent increased mortality. **Figure 33** shows selected pictures of the mini endoscopy supplemented with HE-stained colon sections and statistical evaluation of the obtained MEICS. After challenge with 1 % DSS, WT animals showed a significantly higher MEICS (1.5) compared to PARP-1 k.o. animals (0.8) (**Figure 33 A & B**). The assessed MEICS in animals treated with 1 % DSS was still within a range (0-3) which can be found in healthy animals (Becker *et al.* 2006a). The DSS dose was increased to 2.5% to reach a clearly pathological colitis and strengthen differences between the mouse strains (**Figure 33 C & D**). The MEICS in WT animals rose to 8.8 and PARP-1-deficient mice exhibited a significantly lower MEICS of 2.4. For both genotypes, inflammation was significantly increased within the higher DSS dose of 2.5 %. As visible in **Figure 33 D**, the mucosa was dull. Furthermore, vascular patterns disappeared and fibrin deposits started to form. HE staining of samples obtained after the first DSS cycle revealed hyperplastic tissue (red arrow, right panel in **Figure 33 C**) in the colon of WT animals and loss of the crypt architecture. These findings are possible predictors for tumour formation.

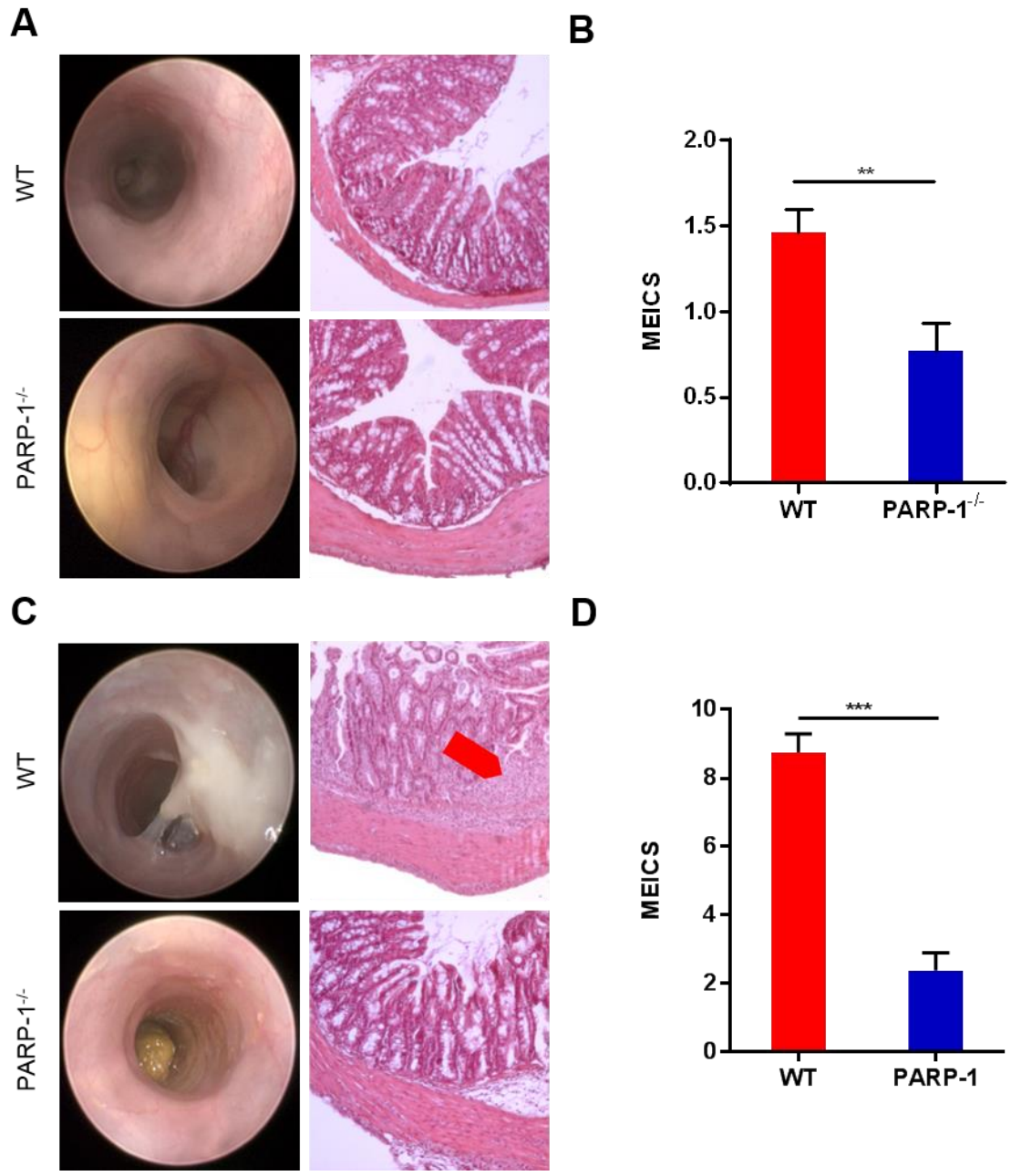


**Figure 33: Analysis of mucosal inflammation in WT and PARP-1-deficient animals.** The mice were challenged with **A & B** 15 mg/kg bw AOM/1 % DSS and **C & D** 10 mg/kg bw AOM/2.5 % DSS. The MEICS was assessed at the end of the first DSS cycle. **A & C** Representative pictures of colon mucosa during mini endoscopy and HE-stained colon sections of animals treated with the high DSS dose. The red arrow marks hyperplastic tissue. **B & D** Statistical evaluation of the MEICS. Data are presented as mean ± SEM (n ≥ 14). Statistical analysis was performed using student's t-test. **p < 0.01, ***p < 0.001.

In summary, WT animals showed higher gut inflammation and already hyperplastic lesions, which may progress to tumours later. In contrast, PARP-1-deficient animals are protected from colitis induction in the AOM/DSS model of CRC.

### 4.4.2 INFLUENCE OF PARP-1 ON THE ABUNDANCE OF THE INDUCIBLE CYCLOOXYGENASE COX-2

Additionally, molecular markers were investigated to confirm the macroscopic observation. The cyclooxygenase COX-2 is selectively induced at the site of inflammation by the inflammatory master key regulator NF-κB and pro-inflammatory mediators (*e.g.* interleukin-1 beta (IL-1b)). COX-2 was analysed as molecular marker for the inflammation observed via mini endoscopy (4.4.1). Samples for immunohistochemical analysis of the inflammation marker COX-2 originated from the animals which were studied to assess the MEICS. Only animals challenged with 10 mg/kg bw AOM and 2.5 % DSS were examined.

First, one colon section of untreated animals of each genotype was qualitatively compared to assess the basal COX-2 levels (**Figure 34**). Only low intensity of COX-2 signal was visible in untreated animals.

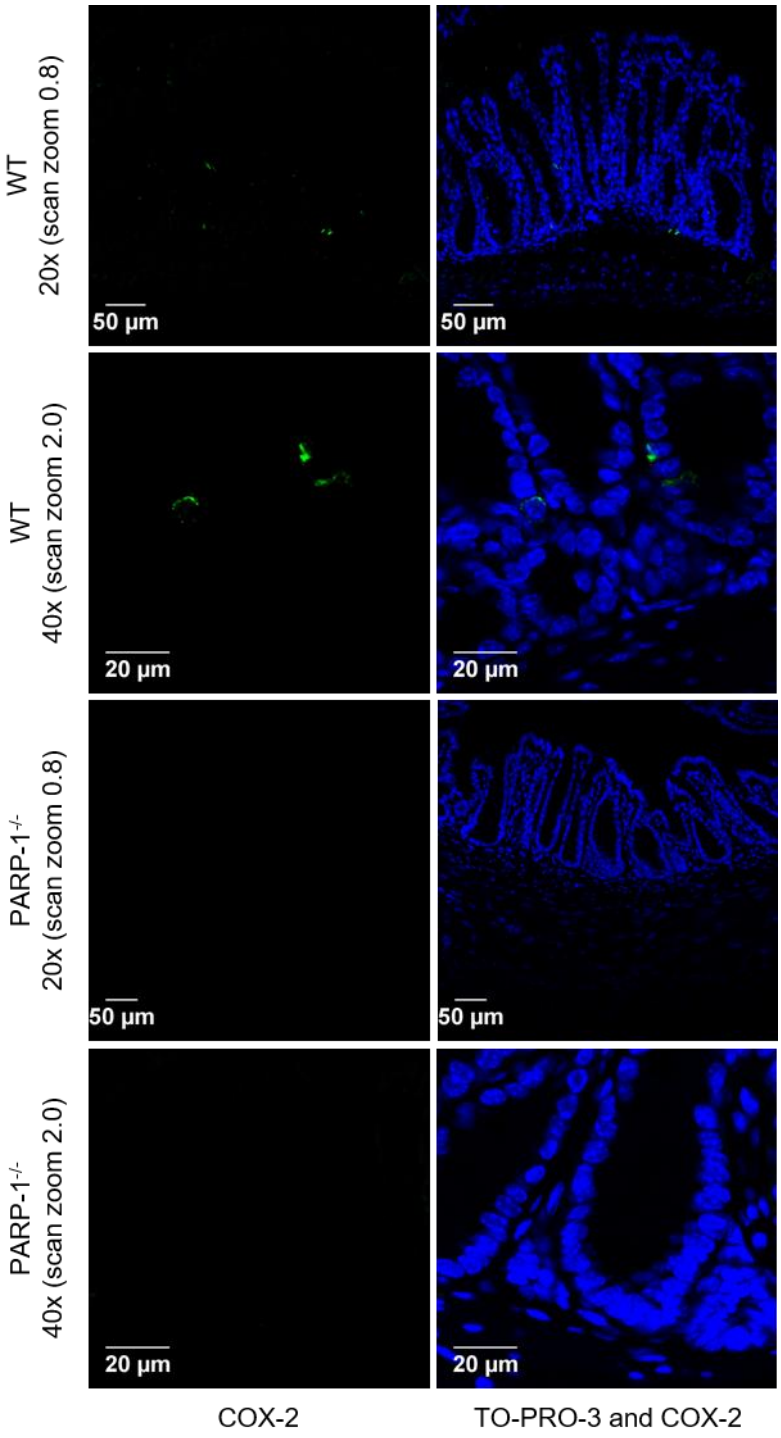


**Figure 34: COX-2 abundance in untreated animals.** Overview and detail pictures of colon sections of untreated animals. Nuclei were stained with TO-PRO-3 (blue); green signal shows COX-2. Samples were analysed with confocal microscopy; magnifications (20x (scan zoom 0.8) and 40x (scan zoom 2.0)) are indicated in the figure.

Next, COX-2 intensity in three treated animals per genotype was recorded. **Figure 35** shows detailed pictures of the analysed samples.

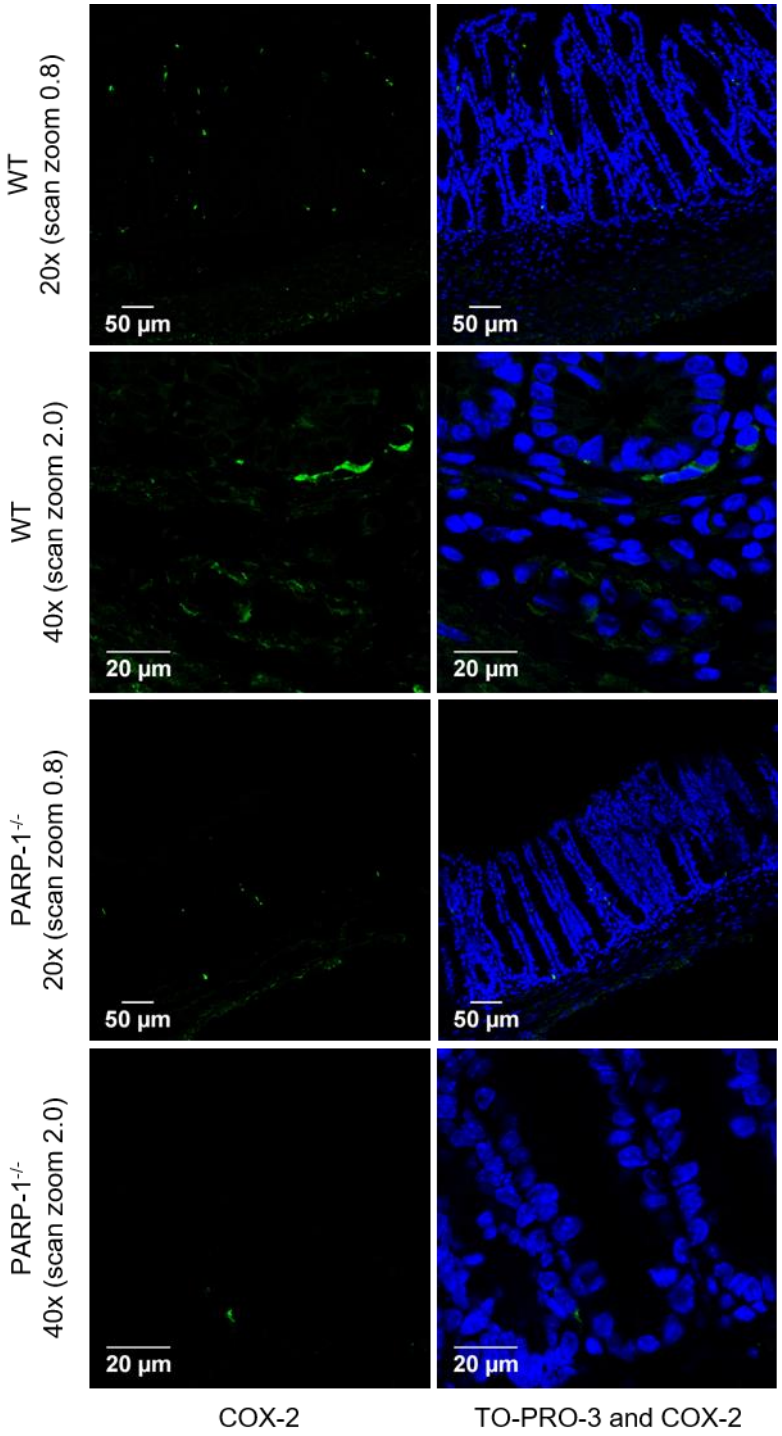


**Figure 35: COX-2 signal intensity in colon sections after the first DSS cycle.** WT and PARP-1-deficient animals were challenged with 10 mg/kg bw AOM and one 2.5 % DSS cycle. Nuclei were stained with TO-PRO-3 (blue); green signal shows COX-2. Samples were analysed with confocal microscopy; magnifications (20x (scan zoom 0.8) and 40x (scan zoom 2.0)) are indicated in the figure.

After the first DSS cycle, the mean COX-2 intensity in PARP-1$^{-/-}$ samples was about 60 % reduced compared to WT colon sections (**Figure 36**).

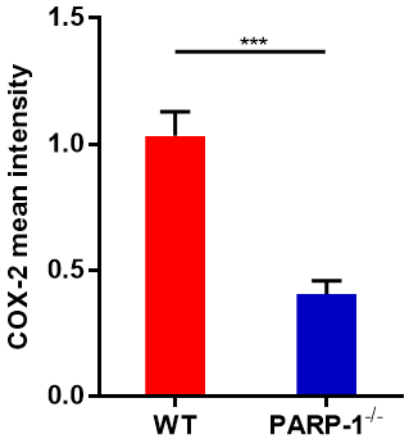


**Figure 36: Statistical evaluation of COX-2 mean intensity.** WT and PARP-1-deficient animals received 10 mg/kg bw AOM followed by one cycle of 2.5 % DSS. Statistical analysis was performed using student's t-test. Data are displayed as mean ± SEM (n = 3). ***p < 0.001.

Qualitative assessment of COX-2 abundance via IHC and confocal microscopy in untreated WT and PARP-1$^{-/-}$ animals showed slightly lower signal in absence of PARP-1. Statistical analysis of COX-2 in colon sections of animals after the first DSS cycle revealed a significantly lower abundance of the pro-inflammatory protein in PARP-1 k.o. mice. This supports the endoscopic analysis of gut inflammation (4.4.1), which already showed that PARP-1$^{-/-}$ mice exhibit a lower mucosal inflammation after treatment with AOM and one DSS cycle.

## 4.4.3 PARP-1 MEDIATES INVASION OF IMMUNE CELLS OF THE INNATE IMMUNE RESPONSE AND CYTOKINE SECRETION

### 4.4.3.1 DECREASED INNATE IMMUNE RESONSE FOLLOWING DSS TREATMENT IN PARP-1-DEFICIENT ANIMALS

During inflammation, immune cells invade the site of inflammation. In the following chapter the presence macrophages and monocytes, which are part of the innate immune response, was analysed in colon tissue. In subsequent experiments, CD3-positive T-cells, which are part of the adaptive immune system, were studied. IHC (3.2.7) and confocal microscopy were used to visualise the immune cells after the first DSS cycle. Animals treated with the high DSS dose (10 mg/kg bw AOM and 2.5 % DSS) showed a stronger inflammatory response. To restrict the number of used animals, experiments were performed with the high DSS dose only.

First, the integrin cluster differentiation molecule 11b (CD11b), a widely-used marker for murine monocytes (Lai *et al.* 1998), was assessed via IHC and confocal microscopy in colon sections of three WT and PARP-1$^{-/-}$ mice. Selected pictures of colon sections of WT and PARP-1-deficient mice are presented in **Figure 37**. CD11b signal was visible in submucosa, muscularis, and serosa with stronger intensity in WT animals.

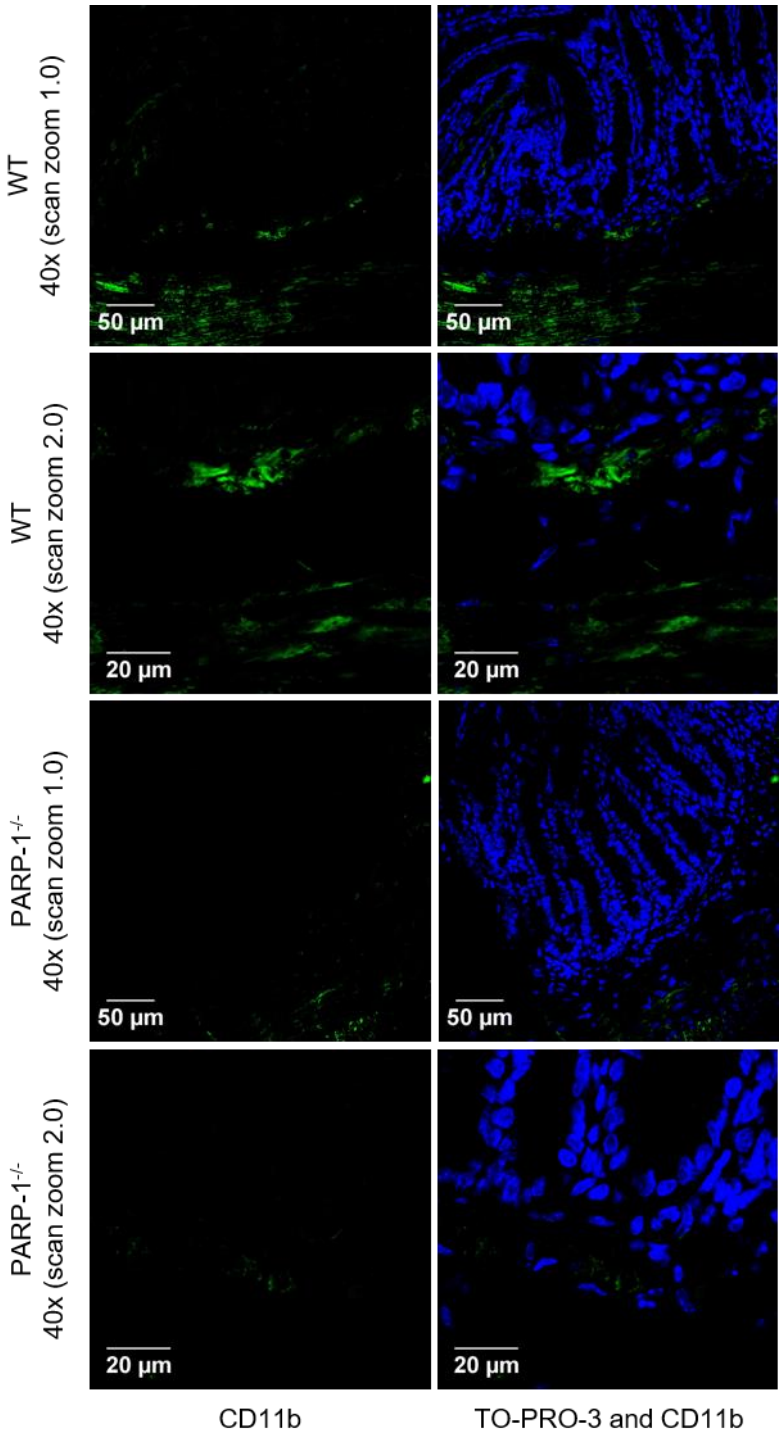


**Figure 37: CD11b-positive cells in WT and PARP-1$^{-/-}$ colon sections after the first DSS cycle.** Selected pictures of the CD11b stained colon sections analysed with confocal microscopy. Animals were challenged with 10 mg/kg bw AOM and 2.5 % DSS. Nuclei were stained with TO-PRO-3 (blue); green signal shows CD11b. Magnifications (40x (scan zoom 1.0 and scan zoom 2.0) are indicated in the figure.

Further statistical evaluation of the mean CD11b signal intensity per optical section is given in **Figure 38**. Presented mean intensity of the CD11b signal was 1.2 for WT animals and 0.45 for PARP-1$^{-/-}$ animals. However, difference between the genotypes was not statistically significant due to variation of the CD11b signal intensity within the genotypes.

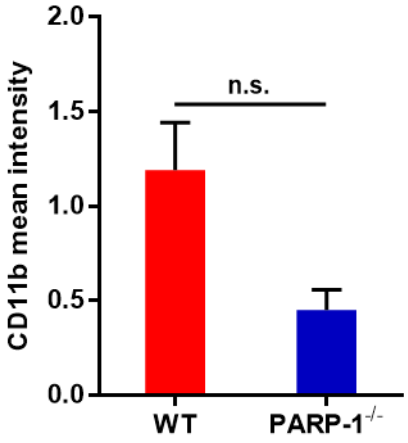


**Figure 38: Statistical analysis of CD11b staining**. Animals were challenged with a single exposure to 10 mg/kg bw AOM and one 2.5 % DSS cycle. Data are presented as mean ± SEM (n = 3). Statistical analysis was performed with student's t-test. n.s. = not significant.

Upon migration from blood vessels into the inflamed tissue, monocytes differentiate to macrophages. Thus, F4/80 was analysed via IHC as marker for murine macrophages (Austyn, Gordon 1981). Groups of three animals per genotype were challenged with 10 mg/kg bw AOM a subsequent 2.5 % DSS cycle.

**Figure 39** presents selected detail pictures of F4/80 stained colon sections at 20x and 40x magnification, statistical evaluation was based on the latter. In contrast to the localisation of the CD11b signal (**Figure 37**), murine macrophages were localised in the lamina propria of the animal's colon and not in the tissue layers underneath.

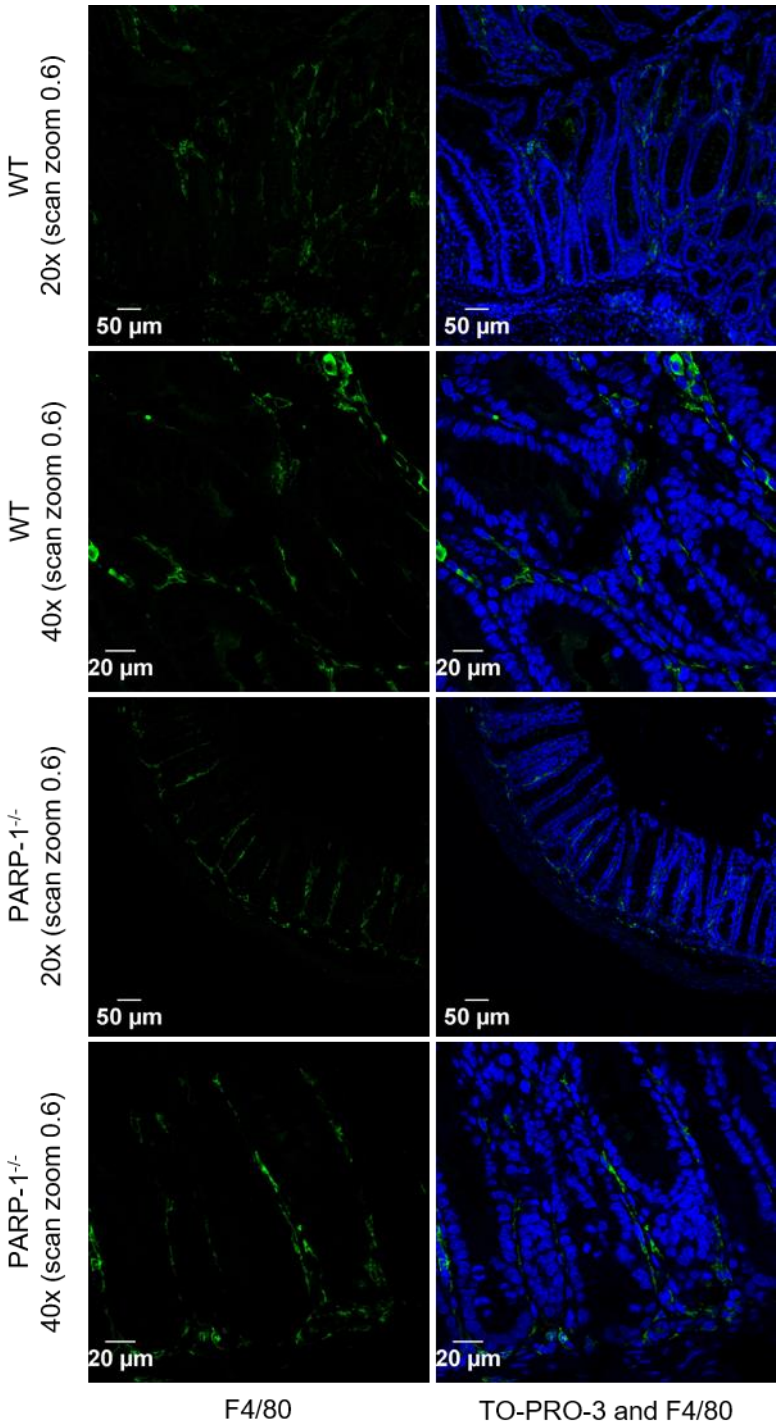


**Figure 39: Microscopy pictures of F4/80 stained WT and PARP-1$^{-/-}$ animals after first DSS cycle.** Mice received 10 mg/kg bw AOM and one 2.5 % DSS cycle. Pictures were analysed via confocal microscopy and recorded at 20x, (scan zoom 0.6) and 40x (scan zoom 0.6) magnification, as indicated in the figure. Nuclei were stained with TO-PRO-3 (blue); green signal visualised F4/80.

Statistical analysis of the microscopic assessment is given in **Figure 40**. AOM/DSS treatment led to an average of 17.4 F4/80-positive cells per crypt. PARP-1 k.o. animals showed a significantly lower number of 9.3 positive cells per crypt. Furthermore, increase of DSS dose raised the number of F4/80-positive cells significantly within the genotypes.

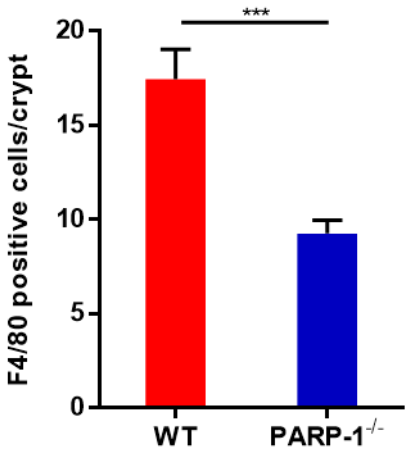


**Figure 40: Statistical analysis of F4/80 staining.** Animals were challenged with 10 mg/kg bw AOM and one 2.5 % DSS cycle. Data are presented as mean ± SEM (n = 3). Statistical analysis was performed via student's t-test. ***p < 0.01.

IHC revealed a stronger invasion of monocytes and macrophages into the inflamed colon tissue of WT animals. PARP-1-deficient animals showed a similar pattern of immune cell invasion of monocytes and macrophages in response to the DSS-induced colitis, but in an attenuated manner. Differences between WT and PARP-1 k.o animals were noticeable, but without statistical significance for monocyte attraction and significant for macrophages localised in the lamina propria. Results obtained from analysis of immune cell infiltration correlated with the mucosal inflammation (**Figure 33**).

#### 4.4.3.2 RESPONSE OF THE ADAPTIVE IMMUNE SYSTEM FOLLOWING AOM/DSS TREATMENT

Besides the unspecific innate immune response, the immune system is equipped with a slower but more specific adaptive response. The so called adaptive or acquired immune system is activated, when a pathogen-specific antigen activates dendritic cells. T-cells are part of the specific immune response and express the membrane-associated receptor CD3, which associates with the T-cell receptor (Smith-Garvin *et al.* 2009). Therefore, CD3 served as marker for T-cells of the adaptive immune system.

Animals were treated with 10 mg/kg bw AOM followed by one cycle 2.5 % DSS and the presence of CD3-positive cells in paraffin-embedded PFA-fixed colon sections was analysed via IHC and confocal microscopy (3.2.7). **Figure 41** shows qualitative CD3-stained colon sections of untreated animals Both genotypes exhibited a comparable CD3 signal.

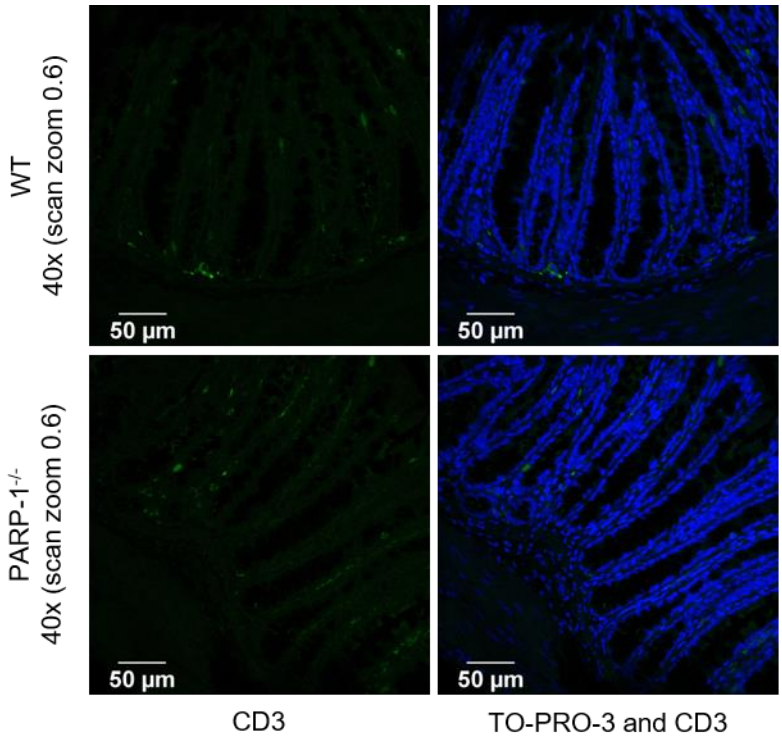


**Figure 41: Pictures of untreated WT and PARP-1$^{-/-}$ colon sections.** Samples were stained via IHC and analysed by confocal microscopy at a magnification of 40x (scan zoom 0.6). Nuclei were stained with TO-PRO-3 (blue) and green signal visualises CD3.

The presence of CD3-positive cells was studied in three animals per group via IHC and confocal microscopy. AOM/DSS treatment did not increase the number of CD3-positive cells. Counting of CD3-positive cells per optical section (**Figure 42 A**) and subsequent statistical evaluation confirmed a similar amount of CD3 T-cells in colon of both genotypes after treatment (**Figure 42 B**). A mean of 6.6 CD3-positive cells was found in WT animals compared to 6.3 in PARP-1$^{-/-}$ animals.

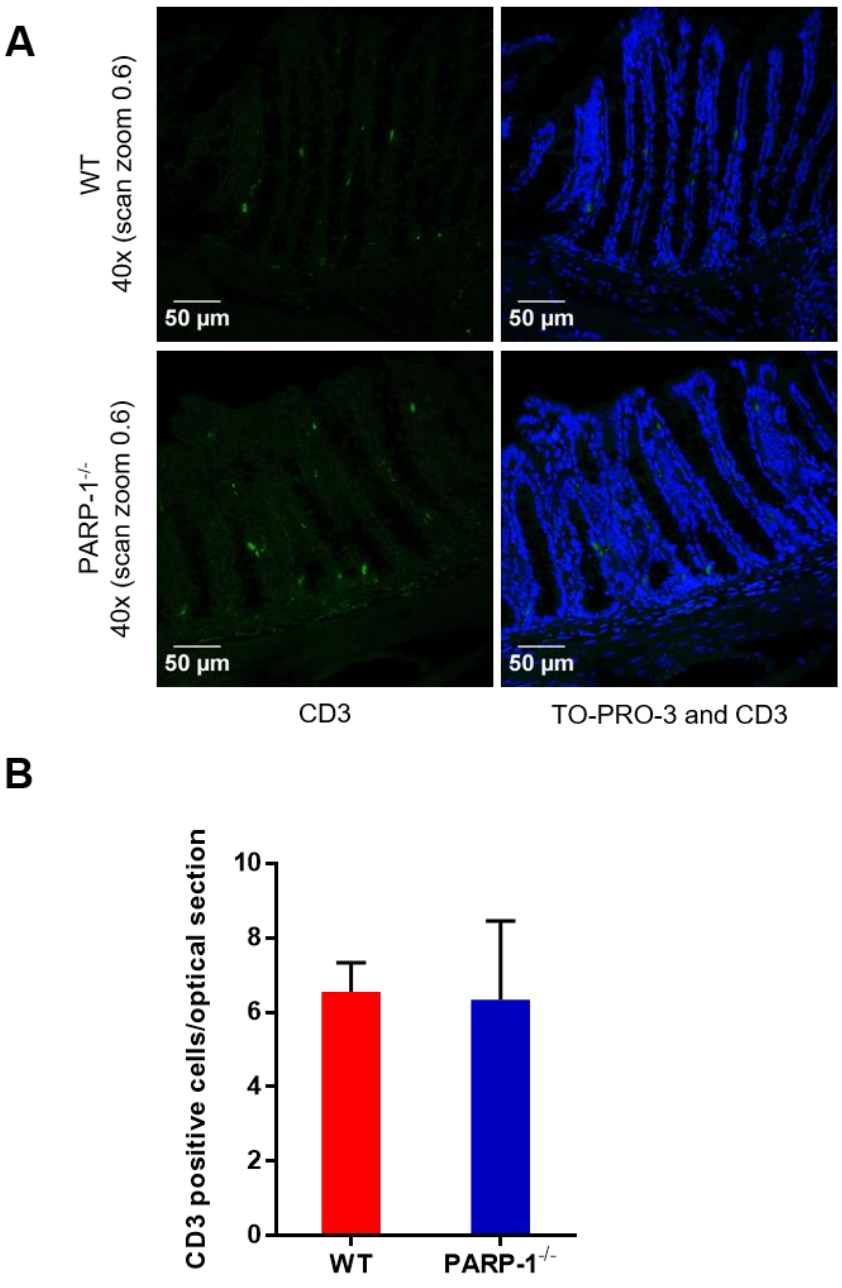


**Figure 42: Analysis of CD3-positive cells in WT and PARP-1$^{-/-}$ colon sections after challenge with AOM/DSS.** Animals received 10 mg/kg bw AOM and one subsequent DSS cycle (2.5 %). **A** Confocal microscopy was used to analyse the samples and record pictures with 40x magnification (scan zoom 0.6). Nuclei were stained with TO-PRO-3 (blue) and the green signal represents CD3. **B** Statistical analysis of CD3-positive cells in mouse colon sections. Data are expressed as mean ± SEM (n = 3). Statistical analysis was performed with student's t-test.

Analysis of CD3 as marker for T-cells of the adaptive immune system failed to show a difference between the genotypes. Moreover, there was no clear induction of CD3-positive cells in the colon of the animals after treatment.

#### 4.4.3.3 CYTOKINE SECRETION

Cytokines are secreted by invading immune cells and lead to activation of processes crucial for inflammation like invasion of immune cells and activation of inflammatory proteins. In this context, HMGB1 was studied due to its important role in the innate inflammatory response. The transcription factor HMGB1 is mainly secreted by macrophages and monocytes invading the inflamed tissue (Klune, JR *et al.* 2008). As described above, both cell populations were found in colon tissue of animals challenged with AOM and DSS, but more pronounced in WT animals. Additionally, HMGB1 is highly expressed in inflamed tissue. Upon activation of PARP-1, nuclear HMGB1 is PARylated and secreted by the cells after translocation into the cytoplasm (Ditsworth *et al.* 2007). To make use of IHC and confocal microscopy (3.2.7), colon sections of WT and PARP-1$^{-/-}$ animals were tested for their HMGB1 abundance in terms of intensity and localisation. Untreated animals were analysed to determine basal HMGB1 levels and compared to animals of both genotypes treated with 10 mg/kg bw AOM and 2.5 % DSS. Samples were, as in previous inflammation-related experiments, harvested after the first DSS cycle.

**Figure 43** shows selected pictures of untreated animals. Almost no signal was discernible in untreated animals of both genotypes.

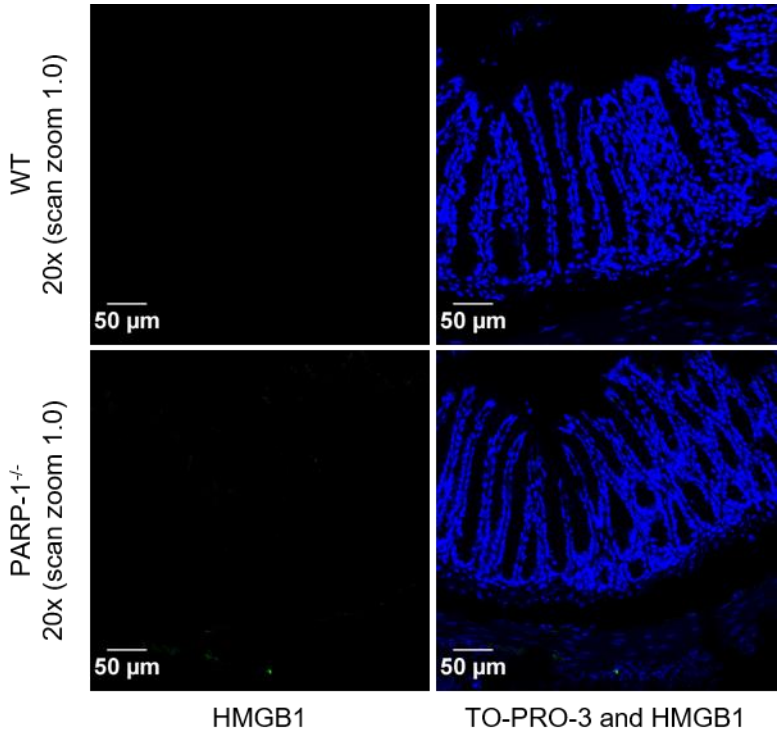


**Figure 43: IHC analysis of HMBG1 abundance in untreated WT and PARP-1 k.o. animals.** IHC-stained colon sections were studied with confocal microscopy and pictures recorded at 20x magnification (scan zoom 1.0). Nuclei were stained with TO-PRO-3 (blue) and HMGB1 is represented by the green signal.

Detailed microscopy pictures of colon tissue after treatment, taken with 20x and 63x magnification, are presented in **Figure 44**. As it can be seen on the pictures with the lower magnification, HMBG1 was distributed all over the cells and parts of the colon and not locally limited like the invading immune cells.

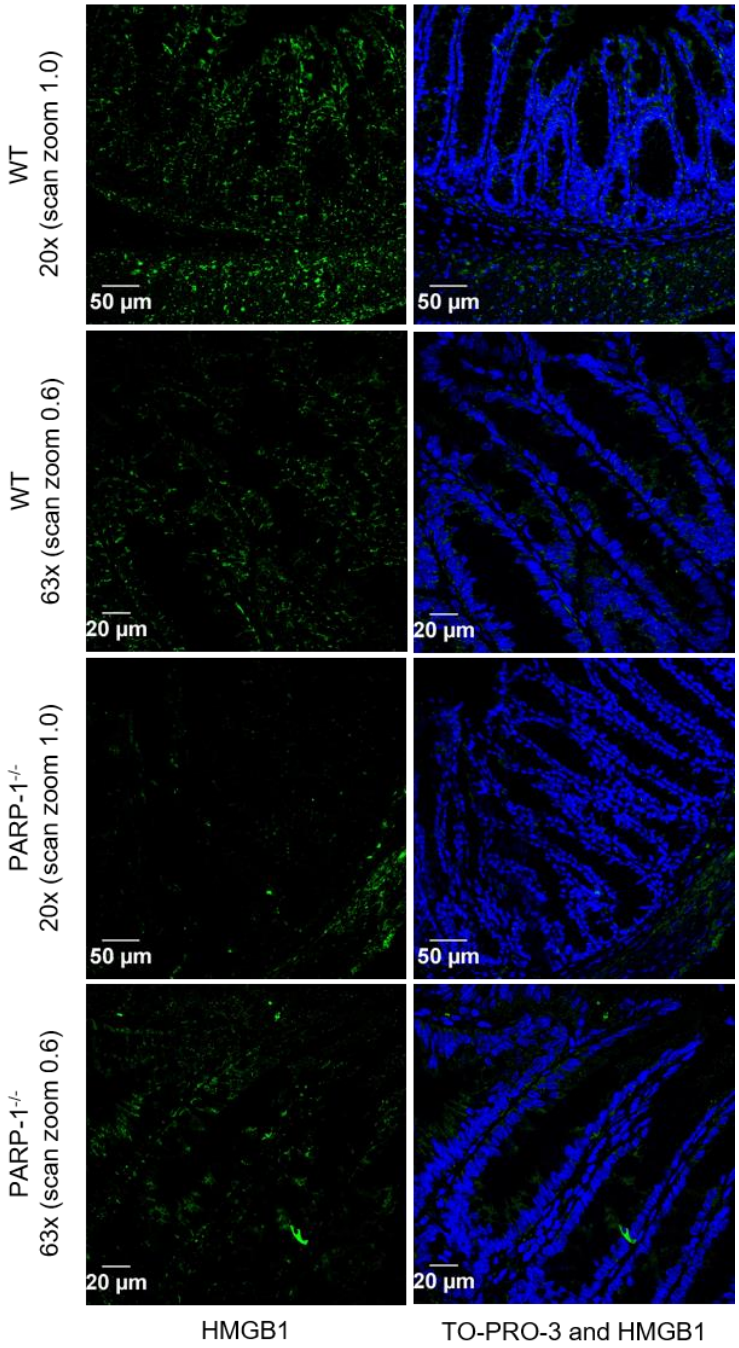


**Figure 44: Representative pictures of abundance of HMBG1 in colon sections after AOM/DSS treatment.** WT and PARP-1 k.o. animals were challenged with 10 mg/kg bw AOM and one 2.5 % DSS cycle. Pictures were recorded with confocal microscopy at a magnification of 20x (scan zoom 1.0) and 63x (scan zoom 0.6). Nuclei were stained with TO-PRO-3 (blue); HMGB1 is displayed as green signal.

Statistical appraisal of mean HMGB1 intensity in treated animals (three per group) revealed a significant difference of HMGB1 levels of both genotypes in response to inflammation. While WT showed a mean HMGB1 signal intensity of 6.6, PARP-1 k.o. samples had a significantly lower intensity of 3.5 (**Figure 45**).

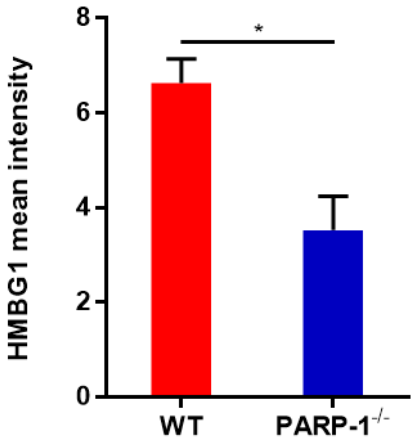


**Figure 45: Evaluation of HMBG1 abundance in WT and PARP-1 k.o. animals after treatment.** Animals received 10 mg/kg bw AOM and 2.5 % DSS. Data are presented as mean ± SEM (n = 3). Statistical analysis was performed with student's t-test. *p < 0.05.

HMBG1 mean intensity was significantly lower in PARP-1-deficient mice at the end of the first DSS cycle. This finding fits to the results presented in the previous chapters, in which data indicated less infiltration of monocytes and macrophages in PARP-1 k.o. mice (4.4.3.1).

#### 4.4.3.4 EXPRESSION OF INFLAMMATION-RELATED GENES IS ATTENUATED IN PARP-1 K.O. ANIMALS

After the first DSS cycle (10 mg/kg bw AOM and 2.5 % DSS), mRNA expression of selected NF-κB target genes was further investigated with the help of qPCR. mRNA of three animals per group was isolated from colon section 1 (**Figure 17**) and transcribed into cDNA. Expression was normalised to the WT (x-fold). The qPCR was performed [redacted]

Consistent with IHC analysis (**Figure 36**), mRNA expression levels of *COX*-2 trended to be lower in PARP-1$^{-/-}$ animals (0.7-fold). The small cytokine *chemokine (C-X-C motif) ligand 2* (*CXCL2*), produced by macrophages and monocytes, and its receptor *C-X-C motif chemokine receptor 2* (*CXCR2*) had a tendency to be decreased to 0.8-fold in the PARP-1-deficient mouse strain. The pro-inflammatory pyrogen *IL-1b* is expressed *e.g.* in macrophages and monocytes. In accordance with IHC of macrophages and monocytes in colon sections, *IL-1b* mRNA levels trended be lower expressed (0.42-fold) in animals lacking PARP-1. Expression of *interleukin-6* (*IL-6*) is stimulated by IL-1b (Luo *et al.* 2003). Almost no *IL-6* expression was visible in the PARP-1 k.o. genotype. Last, *iNOS*, which is expressed as direct consequence of inflammatory processes, was studied. The mRNA expression levels in PARP-1$^{-/-}$ colon tissue had a tendency to be lower compared to the WT.

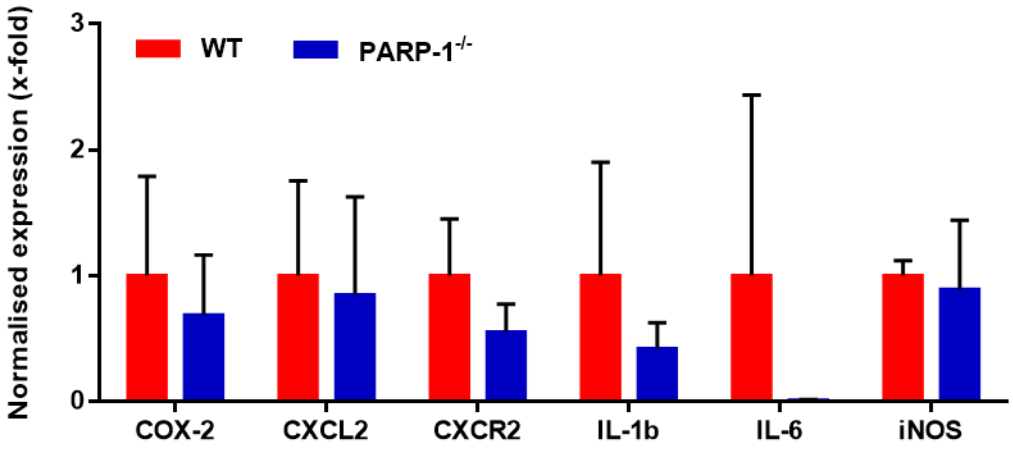


**Figure 46: Relative mRNA expression in WT and PARP-1$^{-/-}$ colon tissue of NF-κB target genes.** Expression is displayed normalised to the WT (x-fold). Samples were harvested after the first DSS cycle (10 mg/kg bw AOM and 2.5 % DSS). Data are presented as mean ± SEM (n = 3). Statistical analysis was performed via one-way ANOVA and Tukey's multiple comparison test.

In general, expression levels of all examined genes tended to be reduced in PARP-1-deficient animals compared to the proficient WT. This tendency goes in line with the findings from the previous experiments analysing the inflammatory response (4.4).

### 4.4.4 TUMOUR FORMATION INCREASES WITH STONGER INFLAMMATORY STIMULUS

Tumour formation was assessed in animals treated with the high DSS dose. Treatment scheme is described in 3.2.3 and tumour number as well as tumour score were determined as described in 3.2.5.1.

**Figure 47** shows selected pictures of WT and PARP-1 k.o. animals after 12 weeks. Both genotypes showed increased CRC formation in the distal part of the colon (compared to **Figure 20**). Data of the distal colon is comparable to the tumour data assessed via mini endoscopy. Since the proximal part of the colon cannot be examined with the rigid telescope, tumour data presented for this part of the colon cannot be compared with the results presented in 4.2.

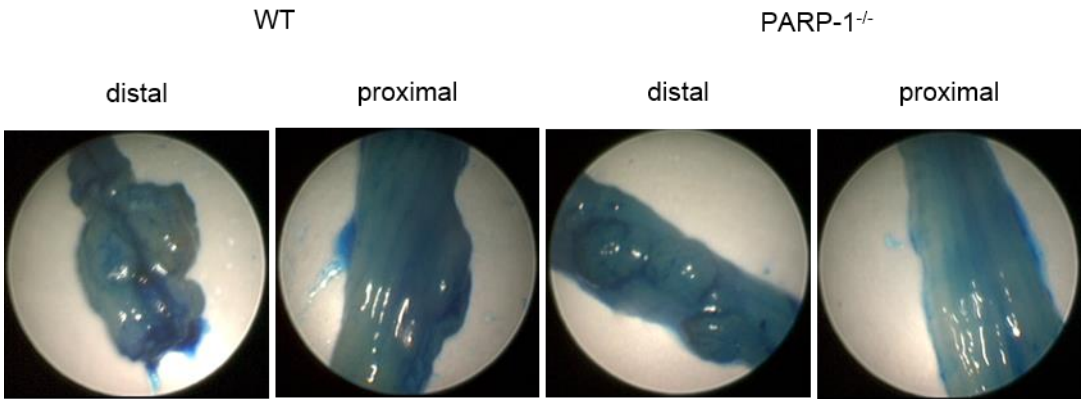


**Figure 47: Exemplary pictures of explanted and flattened colon of WT and PARP-1$^{-/-}$ mice**. Animals were treated with 10 mg/kg bw AOM and two cycles of 2.5 % DSS via the drinking water. Tumour formation was assessed after 12 weeks and pictures recorded with the camera of the mini endoscopy system. Colons were stained with 0.5 % methylene blue.

Statistical evaluation of tumour number and tumour score was done separately for the distal and proximal part of the colon. Here, mean tumour number in the distal colon of WT animals (6.6) is slightly higher than the PARP-1 k.o. animals (5.2), but lacked significant difference (**Figure 48 A**). Accordingly, PARP-1$^{-/-}$ animals (15.4) showed a significantly lower tumour score compared to WT animals (22.5) (**Figure 48 B**). In contrast to the distal colon section, there was a lower tumour formation in the proximal part of the animal's colon visible. A mean of 2.1 tumours was observed in WT animals and a significantly lower number of 0.4 tumours in PARP-1$^{-/-}$ mice (**Figure 48 C**). In line with tumour number, mean tumour score in PARP-1-deficient animals (0.7) was significantly reduced compared to the PARP-1-proficient WT (4.6) (**Figure 48 D**).

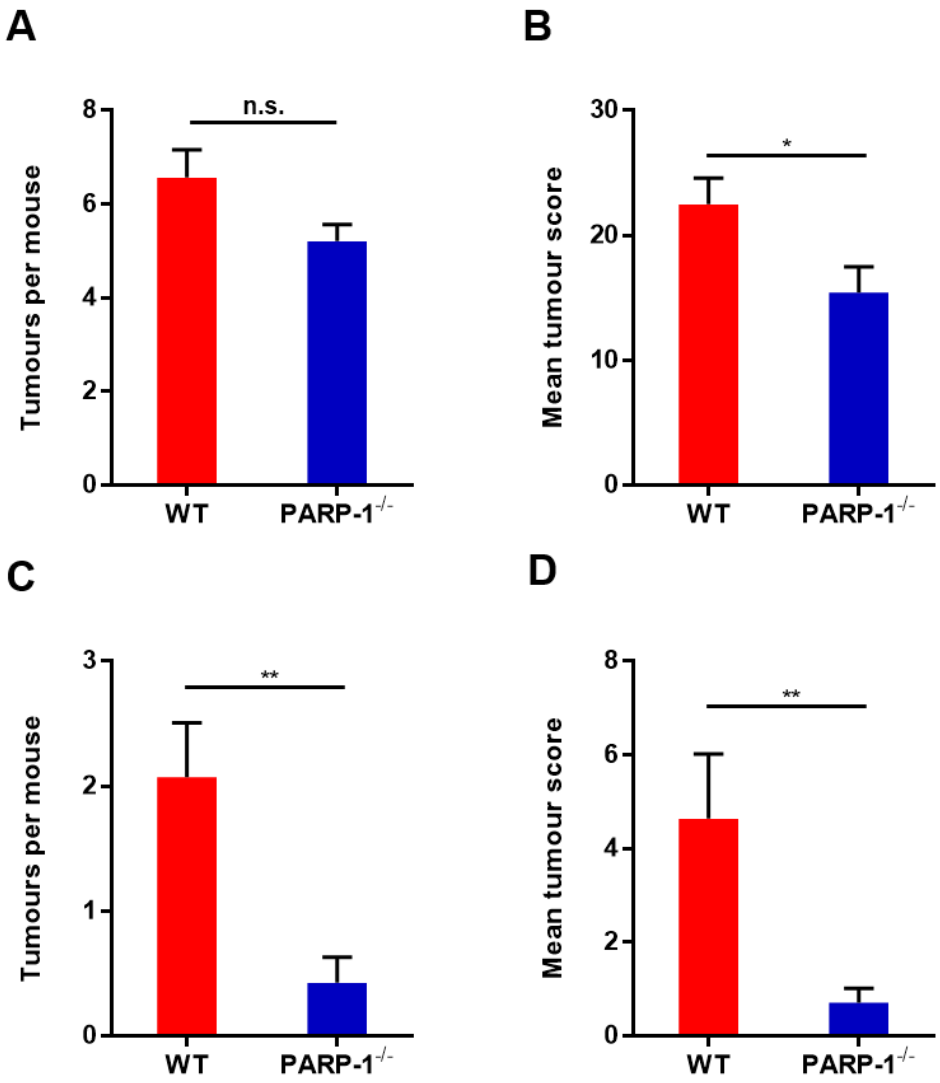


**Figure 48: Statistical analysis of tumours in WT and PARP-1$^{-/-}$ animals after 12 weeks.** Animals were treated with 10 mg/kg bw AOM and received two cycles of 2.5 % DSS via the drinking water. **A** Tumour number and **B** tumour score of distal colon sections of both genotypes. **C** Mean tumour number and **D** tumour score of the proximal part of the animal's colon. Data was collected after 12 weeks and is presented as mean ± SEM (n ≥ 14). Statistical analysis was performed using a student's t-test. n.s. = not significant, *p < 0.05; **p < 0.01.

Compared to animals challenged with 1 % DSS (4.2), CRC formation in the distal colon increased with the administered DSS dose. Challenge with 1 % DSS in combination with AOM caused no increase of

CRC formation in PARP-1$^{-/-}$ animals. whereas it caused a concentation-dependent increase in WT animals (**Figure 21**). The data cannot be directly compared, since the experiments investigating colorectal carcinogenesis after challenge with the high DSS dose was terminated 4 weeks earlier. Due to the different techniques used to assess tumour formation, the proximal colon was not studied in animals treated with AOM and 1% DSS. Tumour number and score in the proximal colon of WT animals was significantly higher as in PARP-1$^{-/-}$ mice after challenge with 10 mg/kg bw AOM and two cycles of 2.5 DSS. In general, tumour formation was lower in the proximal colon.

## 4.4.5 SUMMARY: ROLE OF PARP-1 IN INFLAMMATION

**Table 25** summarises the results presented in this chapter, which addressed the tumour-promoting inflammatory response in PARP-1-proficient WT animals and PARP-1-deficient animals.

**Table 25: Summary of chapter 4.4 Role of PARP-1 in Inflammatory Response.**

| |
|---|
| **PARP-1 k.o. Animals are Resistant to AOM/DSS-induced Colitis** |
| • significantly lower gut inflammation in PARP-1$^{-/-}$ animals<br>  - strength of gut inflammation correlated with the DSS dose<br>  - loss of colon crypt structure and hyperplastic tissue in WT animals<br>• |
| **Lack of PARP-1 is Linked with Lower Abundance of COX-2 in Colon Tissue** |
| • lower COX-2 signal in colon sections of PARP-1-deficient animals compared to WT animals after the first DSS cycle |
| **Attenuated Innate Immune Response in PARP-1$^{-/-}$ Animals** |
| • higher abundance of CD11b in WT animals in the outer layers of the colon<br>• higher level of F4/80 in the lamina propria of WT animals<br>• no evidence for invation of CD3-positive T-cells in both genotypes |
| **Lower Expression of Cytokines in PARP-1-deficient animals** |
| • significantly reduced abundance of HMGB1 in absence of PARP-1<br>• tendency for lower expression of NF-κB target genes in colon tissue of PARP-1-deficient mice |
| **CRC Formation Correlates with DSS Dose** |
| • treatment with two cycles of 2.5 % DSS caused an increase of tumour number and tumour size in both genotypes<br>• tumour formation was lower in the proximal colon and significantly reduced in PARP-1 k.o. animals compared to WT animals<br>• |

## 4.5 PARP-1 FACILITATES TUMOUR PROGRESSION

Thus far, this work addressed the role of PARP-1 in the context of initiating DNA damage induction and repair as well as the impact on chronic inflammation promoting tumourigenesis. The prior results confirm the initial observation: absence of PARP-1 mediates resistance to colitis-associated CRC in the murine AOM/DSS model (4.2), although the animals are prone to NOC-induced DNA damage (4.3.1). The lower tumour formation went in line with an attenuated inflammatory response (4.4). A dramatically increased sensitivity of MGMT-deficient mice challenged with the AOM/DSS model was recently reported by our group. Absence of MGMT led to an increased formation of $O^6$-MeG adducts upon challenge with AOM, resulting in a higher tumour formation compared to WT animals. $MGMT^{-/-}$ animals showed a linear dose-dependent increase in tumour formation, which correlated with the initial DNA damage induction (Fahrer *et al.* 2015). A PARP-1/MGMT DKO strain was bred to further differentiate the role of tumour-promoting chronic inflammatory processes in combination with a high level of tumour-initiating primary DNA damage.

### 4.5.1 INHIBITION OF MGMT LEADS TO INCREASED CRC FORMATION IN PARP-1$^{-/-}$ ANIMALS

Ahead of the experiments analysing the DKO mouse strain, an experiment with the MGMT inhibitor *O*$^6$-BG was performed in PARP-1$^{-/-}$ mice. The inhibitor was applied *i.p.* before AOM injection and refreshed every 12 h up to 36 h to ensure stable MGMT inhibition during the time AOM respectively its alkylating metabolites were active (3.2.4). AOM was injected 2 h upon the first dose of 40 mg/kg bw *O*$^6$-BG according to the AOM/DSS model described in 3.2.3. Animals received 10 mg/kg bw AOM and two cycles of 1 % DSS via the drinking water. Tumour number and score were assessed after 16 weeks as described in 3.2.5.1.

Statistical evaluation of colorectal tumours is presented in **Figure 49**. Inhibition of MGMT in PARP-1 k.o. animals resulted in a mean tumour number of 3 and a tumour score of 6.9. Tumour number and tumour score were significantly increased versus MGMT-proficient PARP-1$^{-/-}$ mice, which showed a tumour number of 1 and tumour score of 1.4. WT animals challenged with 10 mg/kg bw AOM and 1 % DSS exhibited a tumour number of 2.5 and tumour score of 6.3, both comparable to the tumour formation in PARP-1 k.o. animals.

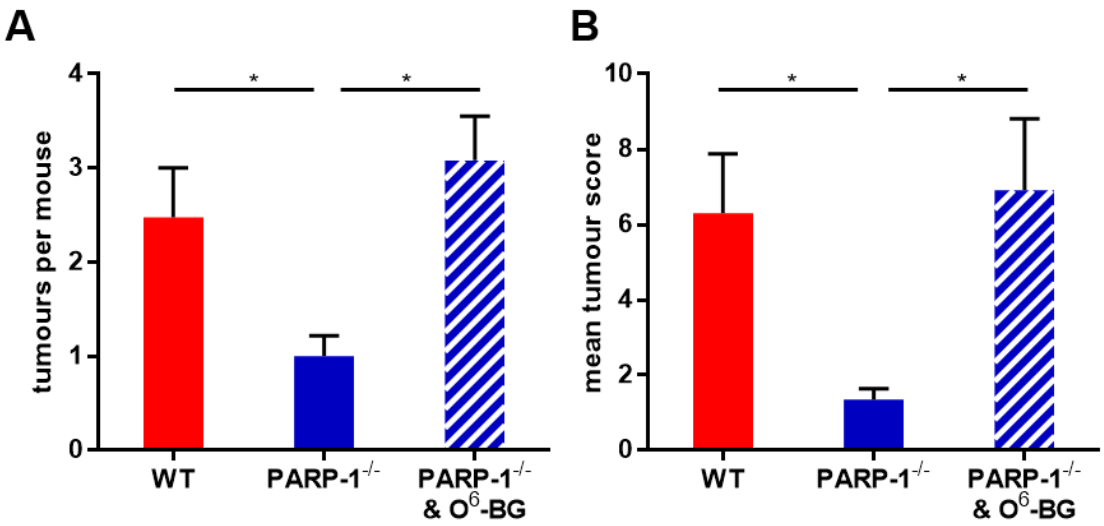


**Figure 49: Colorectal carcinogenesis in WT, PARP-1$^{-/-}$ and PARP-1$^{-/-}$ animals pretreated with *O*$^6$-BG.** Colorectal carcinogenesis was assessed after 16 weeks via mini endoscopy. Animals received one initial injection of 10 mg/kg bw AOM followed by two 1 % DSS cycles. Numerical description of **A** tumour number and **B** mean tumour score per animal. Data are presented as mean ± SEM of n ≥ 15 animals. Statistical significance was calculated with a one-way ANOVA and Bonferroni's multiple comparisons test. *p < 05.

### 4.5.2 PARP-1/MGMT DOUBLE KNOCK OUT ANIMALS ARE PRONE TO AOM-INDUCED TUMOURS BUT SHOW ATTENUATED TUMOUR PROMOTION

DKO mice were challenged with the AOM/DSS protocol (10 mg/kg bw AOM and two cycles of 1 % DSS) and tumour formation was assessed after 16 weeks via mini endoscopy (3.2.5.1). The DKO strain showed outstanding sensitivity to the lethal effects of the AOM/DSS protocol during the first DSS cycle. Hence, animals were only challenged with 1 mg/kg bw AOM and 3 mg/kg bw AOM to prevent excessive toxicity and death of animals. PARP-1$^{-/-}$ mice experienced no increase in tumour formation after challenge with AOM/DSS in the previous experiments (**Figure 21**). Thus, colorectal carcinogenesis was not studied in doses of 1 mg/kg bw and 3 mg/kg bw AOM during this work in order to keep the number of animals low. Results of CRC formation in MGMT$^{-/-}$ and PARP-1$^{-/-}$/MGMT$^{-/-}$ animals were correlated to the PARP-1-deficient genotype treated with the lowest AOM dose (5 mg/kg bw). PARP-1 k.o. animals in this group displayed a mean tumour number of 1.2 and tumour score of 1.3.

Tumour number and tumour score observed in DKO animals was significantly higher after challenge with AOM/DSS compared to WT animals and MGMT-deficient animals (**Figure 50**). Tumour number in WT (0.5) and MGMT k.o. animals (0.7) differed only slightly, whereas the tumour number in DKO animals was significantly increased compared to the other genotypes (3.2). Treatment with 3 mg/kg bw AOM resulted in 0.5 tumours in WT animals, which was significantly lower compared to MGMT$^{-/-}$ (1.5) and DKO mice (3.8). The difference between MGMT-deficient and DKO animals was significant (**Figure 50 A**). The tumour score assessed after exposure to 1 mg/kg bw AOM and two cycles of 1 % DSS in WT mice (0.5) was lower compared to MGMT-deficient mice (1.85). DKO animals showed a significantly increased tumour score compared to WT and MGMT k.o. animals. The WT group receiving the high AOM dose displayed a tumour score of 0.5, which was significantly lower compared to the other genotypes. The tumour score of MGMT$^{-/-}$ animals (4.5) was significantly higher than in WT animals and only slightly lower compared to the DKO group (4.9) challenged with the high AOM dose. Moreover, only MGMT-deficient animals showed a dose-dependent increase of the tumour score (**Figure 50 B**).

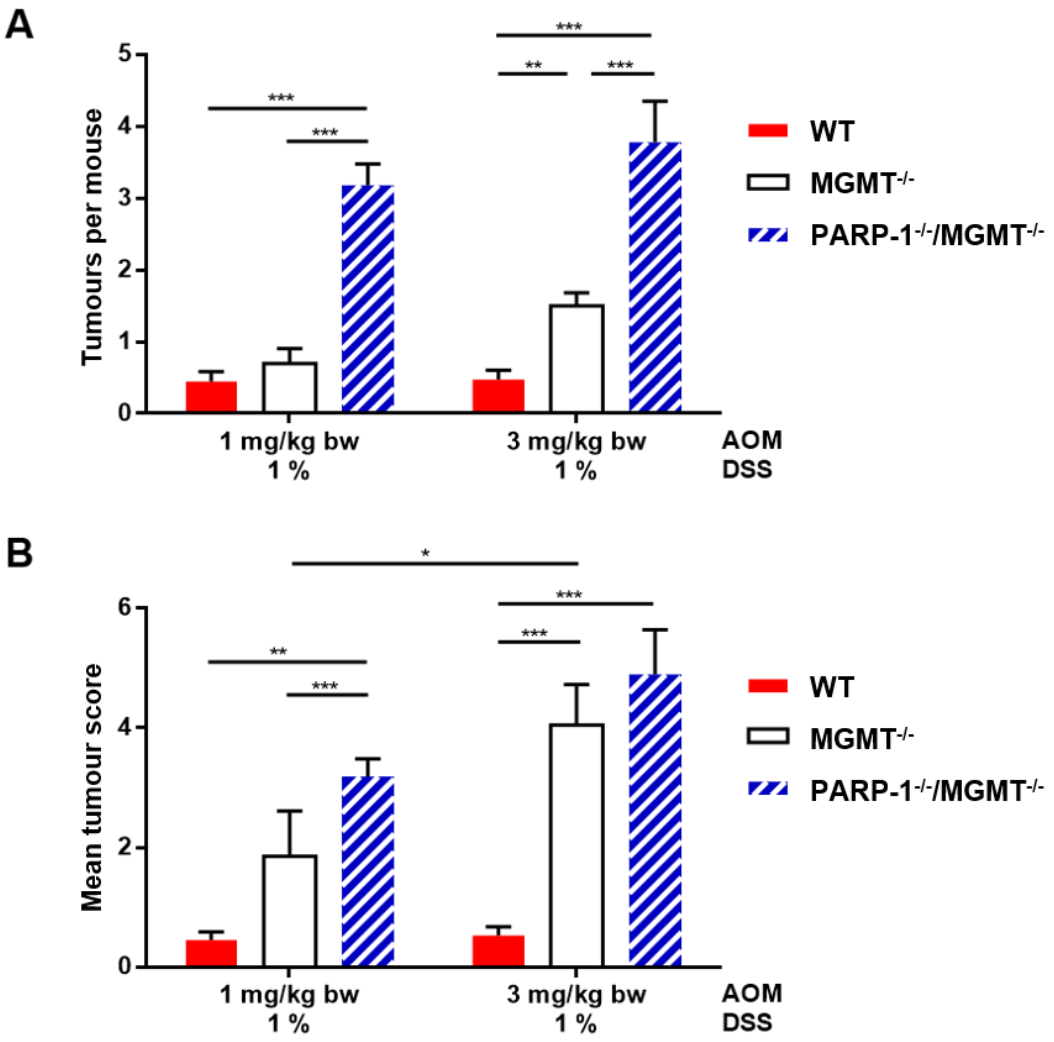


**Figure 50: CRC formation in WT, MGMT k.o. and PARP-1/MGMT dko animals after 16 weeks.** Animals received 1 or 3 mg/kg bw AOM and two subsequent 1 % DSS cycles. Presented are **A** tumour number and **B** mean tumour score assessed by mini endoscopy. Data are shown as mean ± SEM of n ≥ 13 animals. Statistical significance was calculated by two-way ANOVA with Bonferroni's multiple comparisons test. *p < 0.5, **p < 0.01, ***p < 0.001.

Additionally, the mean tumour size of the genotypes was compared (**Figure 51**). After challenge with the low AOM dose, the mean tumour size in WT animals (0.48) was significantly lower compared to MGMT$^{-/-}$ animals and DKO animals. MGMT k.o animals showed the highest mean tumour size of 2.6, which was significantly higher than the mean tumour size found in DKO animals (1.0). Treatment with 3 mg/kg bw AOM and two 1 % DSS cycles did not increase the mean tumour sizes. Similar to the low AOM dose, WT animals exhibited the lowest mean tumour size (0.6), which was significantly lower compared to the other genotypes. The highest mean tumour size was found in MGMT-deficient animals (2.7), which was significantly higher as in DKO animals (1.2).

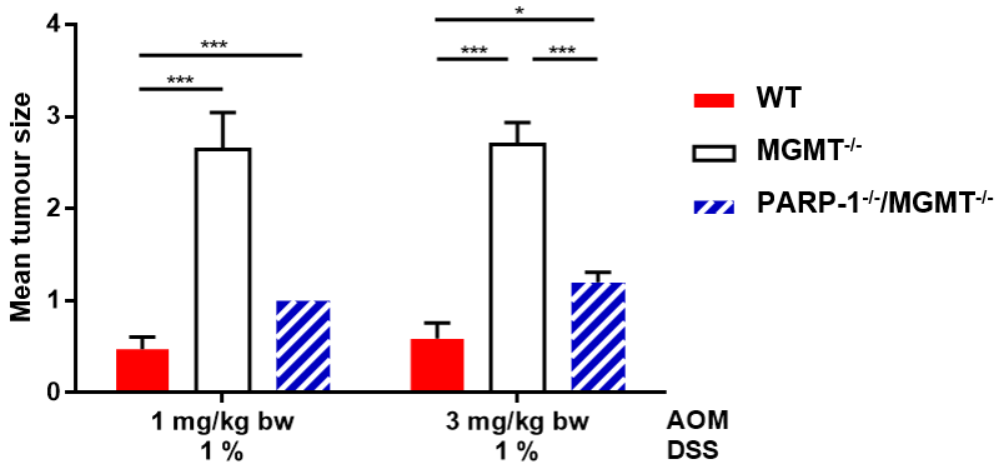


**Figure 51: Mean tumour size of WT, MGMT k.o. and PARP-1/MGMT dko animals after 16 weeks.** Treatment and assessment of data was performed as described in **Figure 50**. Data are presented as mean ± SEM of n ≥ 13 animals. Statistical significance was calculated by two-way ANOVA with Bonferroni's multiple comparisons test. *p<0.5, ***p < 0.001.

Collectively, the mean tumour size in DKO animals was significantly lower compared to MGMT k.o. animals, whereas DKO animals displayed more tumours. This finding suggests a higher initiation of tumours in DKO mice but attenuated tumour progression.

### 4.5.3 DKO ANIMALS ARE SENSITIVE TO AOM/DSS-INDUCED COLITIS

Mucosal inflammation severity in MGMT$^{-/-}$ and PARP-1$^{-/-}$/MGMT$^{-/-}$ mice, which received 3 mg/kg bw AOM and one subsequent cycle of 1 % DSS, was assessed via mini endoscopy (3.2.5.2). **Figure 52 A** shows representative pictures of the mini endoscopy and **Figure 52 B** the statistical analysis. MGMT-deficient mice showed a MEICS of 8.9 and DKO animals a slightly higher MEICS of 10.8. It should be noted that the gut inflammation of WT and PARP-1$^{-/-}$ mice was only studied at an AOM concentration of 10 mg/kg bw and one DSS cycle of 1 %. WT animals exhibited a MEICS of 1.5 and the PARP-1$^{-/-}$ mice a MEICS of 0.8 (**Figure 33**). Comparison with the WT and PARP-1-deficient animals confirmed that the additional loss of MGMT strongly increased sensitivity to the induced colitis.

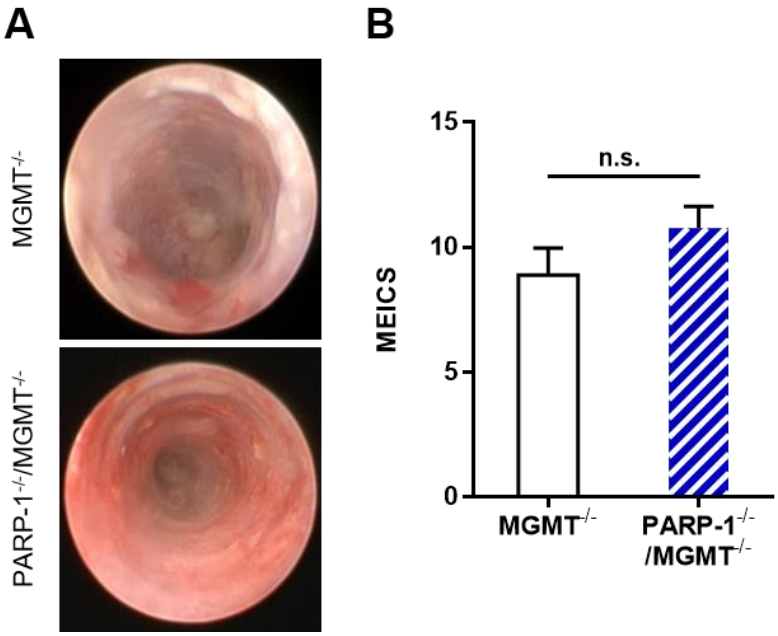


**Figure 52: Mucosal inflammation in MGMT$^{-/-}$ and PARP-1$^{-/-}$/MGMT$^{-/-}$ animals after the first DSS cycle.** Gut inflammation was assessed via mini endoscopy after challenge with 3 mg/kg bw AOM and one cycle of 1 % DSS. **A** Representative pictures of the mini endoscopy and **B** statistical evaluation of the MEICS. Presented are mean ± SEM of n ≥ 11 animals. Statistical significance was calculated using a student's t-test. n.s. = not significant.

DKO animals displayed outstanding sensitivity towards the AOM/DSS-induced colitis, which was even slightly higher compared to the sensitive MGMT$^{-/-}$ genotype.

### 4.5.4 SUMMARY: PARP-1 FACILITATES TUMOUR PROGRESSION

The results which are presented in this chapter are resumed in **Table 26**.

**Table 26: Results presented in chapter 4.5 PARP-1 Facilitates Tumour Progression.**

| **MGMT Inhibition Increases CRC formation in PARP-1 k.o. Mice** |
|---|
| • inhibition of MGMT with *O*$^6$-BG in PARP-1 k.o. animals significantly increases tumour formation |
| **DKO Animals Display Higher Tumour Initiation but Slower Tumour Progression** |
| • significantly higher number of tumours in DKO animals compared to WT and MGMT-deficient animals<br>• smaller mean tumour size in DKO animals compared to MGMT k.o. animals |
| **DKO Animals Show Outstanding Sensitivity to AOM/DSS-induced Colitis** |
| • DKO animals are slightly more sensitive than MGMT$^{-/-}$ to AOM/DSS-induced colitis<br>• notably higher MEICS in DKO mice compared to WT and PARP-1 k.o. mice |

# 5 DISCUSSION

## 5.1 LOSS OF PARP-1 CRITICALLY INFLUENCES CRC FORMATION

Assessment of CRC formation upon challenge with AOM/DSS revealed a strong dose-dependent induction of colorectal tumours in WT animals, whereas colorectal carcinogenesis in PARP-1-deficient mice did not increase (**Figure 21**). The resistance of PARP-1$^{-/-}$ towards AOM/DSS-induced CRC was surprising, as prior studies reported increased susceptibility of PARP-1 k.o. animals to the alkylating agent MNU and ionizing radiation. Mortality of PARP-1-deficient mice was significantly higher compared to WT animals upon challenge with single MNU injections of 25 mg/kg bw and 75 mg/kg bw and mortality correlated with the administered dose. Treatment with the high MNU dose lead to death of all PARP-1$^{-/-}$ animals, whereas only 43 % of the WT animals died after 4 weeks. In line with this, all PARP-1$^{-/-}$ animals died within 9 days after irradiation with 8 Gy of γ-radiation whereas 50 % of WT animals survived until day 15 post-irradiation. PARP-1$^{-/-}$ animals receiving with a single dose of MNU showed a dramatically increased rate of sister chromatid exchanges and slightly more chromosome breaks compared to WT animals. Challenge of mouse embryonic fibroblasts (MEFs), derived from PARP-1 k.o animals, with MNU caused a cell cycle arrest in $G_2$/M, whereas cell cycle distribution in WT cells was hardly affected. (Murcia *et al.* 1997). Exposure of PARP-1$^{-/-}$ MEFs to methylmethanesulfonate (MMS) caused a severe decrease in growth rate as well as viability and confirmed a transient NOC-induced cell cycle arrest in $G_2$/M after 24 h. Of note, alkaline comet assay revealed a severe BER deficiency in PARP-1$^{-/-}$ MEFs (Trucco *et al.* 1998). An BER deficiency of PARP-1$^{-/-}$ animals was also observed in an *in vitro* study investigating the interaction of PARP-1$^{-/-}$ MEF extracts with a DNA substrate holding an abastic site. Long-patch BER was markedly delayed, whereas short-patch repair was only partly affected (Dantzer *et al.* 1999). Prior studies of AOM/DSS-induced CRC formation in DNA repair deficient mice confirmed the important role of DNA repair mechanisms in protection against NOC-induced CRC (Wirtz *et al.* 2010). A recent study performed by in our lab demonstrated the sensitivity of MGMT$^{-/-}$ and the BER-deficient AAG$^{-/-}$ animals towards AOM/DSS-induced CRC (Fahrer *et al.* 2015). Since PARP-1 facilitates DNA repair, especially BER (Caldecott *et al.* 1996) and DNA strand break repair (Wang *et al.* 2006), a sensitivity of PARP-1-deficient animals towards AOM and the AOM/DSS protocol was expected.

Apart from that, PARP-1 is known as crucial coactivator of NF-kB. This transcription factor is a central mediator of the inflammatory response, which facilitates tumour-promoting inflammatory processes. PARP-1$^{-/-}$ mice display an impaired activation of NF-kB and target genes (Hassa, Hottiger 2002; Oliver *et al.* 1999). Therefore, the attenuated inflammatory response might be responsible for the lower tumour promotion in PARP-1 k.o. animals, which was addressed in 4.4. This suggestion is supported by a study of Greten and colleagues: Mice with a deletion of IKKβ, which is necessary for the activation of NF-κB, displayed a lower tumour formation after challenge with the AOM/DSS protocol. Interestingly, the authors did not link this to an attenuated inflammatory response but suggested an increased epithelial apoptosis during tumour promotion (Greten *et al.* 2004), which disagrees with the findings of this work.

Another aspect, which might explain the lower tumour formation in PARP-1 k.o. animals, is the association of PARP-1 with the aetiology of CRC. Most human CRCs and precursors (*e.g.* intestinal

adenomas) display increased PARP-1 mRNA and protein levels (Idogawa *et al.* 2005; Nosho *et al.* 2006; Sulzyc-Bielicka *et al.* 2012), which is dependent on the tumour's localisation and stage (Sulzyc-Bielicka *et al.* 2012). Furthermore, PARP-1 acts as coactivator of the β-catenin/TCF-4 complex (Idogawa *et al.* 2005). The β-catenin/TCF-4 complex regulates genes involved in growth and differentiation (*e.g. cyclin D1* and *c-myc*) and, thus, promotes the initiation of intestinal tumours (1.3.8.2).

Animals of the control groups received no AOM but two cycles of 1 % DSS. PARP-$1^{-/-}$ control animals displayed a higher tumour number and score compared to the WT control group (**Figure 21**). Inflammatory processes are linked with the generation of reactive oxygen and nitrogen species (RONS). RONS induce DNA damage; *e.g.* DNA base oxidation, DNA base deamination, DNA base alkylation via lipid peroxidation (LPO), and etheno-modified bases by reaction of DNA with a LPO products. The RONS-induced DNA base damage is repaired by BER (Meira *et al.* 2008). As already mentioned above, PARP-1-deficient mice display a severe BER deficiency (Trucco *et al.* 1998), which might explain a higher tumour formation induced by the DSS-induced colitis without AOM. The higher tumour formation in the PARP-1 k.o. group could be further examined by comparison of basal tumour formation in untreated PARP-$1^{-/-}$ animals to the PARP-1-deficient control animals.

In conclusion, assessment of tumour formation revealed a decreased tumour number and tumour score in PARP-1 k.o. animals compared to WT animals.

## 5.2 ROLE OF PARP-1 IN NOC-INDUCED DNA DAMAGE

Upon arrival of the *i.p.* applied AOM in the liver, it is hydroxylated by CYP2E1 to MAM (Delker *et al.* 1998; Sohn *et al.* 1991), which spontaneously decomposes to a highly reactive alkylating methyldiazonium ion (NAGASAWA *et al.* 1972). Moreover, MAM can be conjugated with glucuronic acid by the phase II enzyme UDP-glucuronosyltransferase and the arising MAM-glucuronide is transported via the bile into the colon. The MAM-glucuronide is hydrolysed by bacterial and mucosal β-glucuronidase to MAM, which is subsequently metabolised by the gut flora (Fiala 1977; Reddy *et al.* 1974) or gastrointestinal CYP2E1 to the alkylating methyldiazonium ion (Thorn *et al.* 2005). Due to the specific activation of the ultimate carcinogen in liver and colon, DNA damage induction was analysed in both organs.

### 5.2.1 LACK OF PARP-1 LEADS TO DRAMATICALLY REDUCED FORMATION OF PAR

First, cellular PAR levels were determined via LC-MS/MS. As expected, absence of PARP-1 led to significantly decreased basal PAR formation in liver and colon (**Figure 22**). Residual PAR levels are likely attributable to other PARP species (*e.g*. PARP-2). Second, there was a big difference between PAR formation in liver and colon tissue with significantly lower levels in the latter. This goes in line with a recent publication of Rita Martello and colleagues (Martello *et al.* 2013), in which the variability of PAR levels in different mouse organs was assessed. Here, PAR levels of 7.5 pmol/mg R-Ado/DNA in mouse

liver tissue were reported; colon tissue was not analysed. This is about half of the basal R-Ado amount (15.7 pmol/mg R-Ado/DNA) observed in the liver of WT animals used in this work (**Figure 22 A**). Reason for the variance might be the fact that Martello analysed tissue from SJL mice, whereas this work is based on mice with C57BL/6 background. Challenge of WT animals with AOM caused a striking increase of R-Ado/DNA in liver tissue up to 24 h and subsequent decline. In contrast, PARP-1 k.o. animals displayed no increase in PAR levels (**Figure 22 A**). Analysis of colon tissue revealed a slight increase of R-Ado/DNA levels in WT animals after 6 h, which reached basal levels after 24 h. Comparable to liver tissue, no AOM-induced increase of R-Ado/DNA was visible in PARP-1-deficient animals after 24 h (**Figure 22 B**). The transient formation of PAR upon challenge with AOM was previously demonstrated by Ethier and colleagues: The group analysed PAR formation in HeLa cells and HEK293 upon treatment with the alkylating agent methylnitronitrosoguanidine. Western blot analysis revealed a quick and transient PAR-induction after 5 min, which remained stable for 30 min and then gradually declined on control levels over a time of 3 h. Additionally, inhibition of PARP-1 with the PARP inhibitor PJ34 prevented PARP-1 overactivation and concomitant cell death (Ethier *et al.* 2007; Ethier *et al.* 2012). This goes in line with absence of PAR induction in PARP-1$^{-/-}$ animals upon challenge with AOM.

In contrast to our expectation, the highest PAR formation in liver tissue was 24 h after AOM injection compared to 6 h in colon tissue. Due to the pharmacokinetics of AOM activation, we expected a delayed PAR formation in colon tissue. However, AOM-induced PAR formation in colon tissue was not significant. It is possible, that the amount of AOM metabolites activated in the liver to the DNA damaging methyldiazonium ion is not sufficient to induce a significant amount of PARP-1. This notion is supported by the analysis of γH2AX induction as marker for DSBs (**Figure 26** and **Figure 27**) and *O*$^6$-MeG adduct formation (**Figure 28**). Both γH2AX and *O*$^6$-MeG adducts were stronger induced in liver tissue compared to colon tissue of both genotypes.

Collectively, the determination of PAR levels revealed higher basal PAR formation in WT animals and a clear time-dependent induction upon challenge with AOM, whereas PARP-1-deficient animals showed only low basal PAR levels and no induction upon exposure to AOM.

### 5.2.2 PARP-1-DEFICIENT ANIMALS ARE PRONE TO NOC-INDUCED DNA STRAND BREAKS

DNA strand break induction was analysed with the alkaline comet assay up to 48 h after exposure to AOM. Challenge with 5 mg/kg bw AOM induced DNA strand breaks in liver tissue after 24 h and 48 h. Due to the strong variation between the analysed animals, statistical significance was not reached. PARP-1$^{-/-}$ animals experienced a significant increase of DNA strand breaks after 24 h, followed by a reduction of about 40 % after 48 h. Differences between the genotypes did not reach statistical significance. Following, animals were challenged with 10 mg/kg AOM, which caused a significant time-dependent induction of DNA strand breaks in both genotypes after 24 h and slight decrease after 48 h. The tail moment in PARP-1-deficient animals was significantly higher after 24 h and still slightly increased after 48 h, compared to WT mice. Moreover, DNA strand break induction in PARP-1 k.o. liver

tissue correlated with the AOM dose (**Figure 24**). Trucco and colleagues studied MSS-induced DNA strand breaks in WT and PARP-1$^{-/-}$ MEFs via alkaline comet assay and interpreted a delayed reduction of the tail moment compared in PARP-1$^{-/-}$ cells as BER deficiency (Trucco *et al.* 1998). Due to the standard errors of the analysed WT liver cells obtained from animals challenged with 5 mg/kg bw AOM, no save conclusion is possible. However, there is a higher DNA strand break induction in liver cells of PARP-1$^{-/-}$ mice after challenge with 10 mg/kg bw AOM. It should be noted, that the alkaline comet assay detects both SSBs and DSBs and alkali labile sites. Therefore, one should be careful to interpret this as sole effect of BER. Both MMS (Beranek 1990) and AOM induce DSBs, which are also detected by the alkaline comet assay. There is strong evidence for PARP-1's important role during DNA strand break repair as DNA-damage-detecting molecule activating the appropriate DSB repair pathway (Shrivastav *et al.* 2008). PARP-1 interacts with the factors of HRR (MRN complex (Haince *et al.* 2008) and ATM (Aguilar-Quesada *et al.* 2007; Haince *et al.* 2007)), NHEJ (Ku70/80 (Wang *et al.* 2006) and DNA-PKcs (Ruscetti *et al.* 1998; Spagnolo *et al.* 2012)) and B-NHEJ (Iliakis 2009; Soni *et al.* 2014). Althought induction of γH2X induction upon AOM treatment was comparable in both genotypes (**Figure 26** and **Figure 27**), further experiments necessary. DSB formation could be studied with the neutral comet assay, which only detects DBSs, and compared to the alkaline comet assay to determine the amount of SSBs and alkali labile sites. Additionally, a repair assays with liver and colon cell lysates could support a conclusion.

Another important point, which must be discussed, is the alkaline comet assay itself. The alkaline comet assay is an assay prone variations. It was not possible to analyse all samples at once and slight variations might have critically influenced the assay. Apart from that, the sample material was snap frozen tissue obtained from *in vivo* experiments. It is possible that small differences in sample preparation might have caused DNA strand breaks during organ harvest or cell separation before performing the alkaline comet assay. A higher animal number might be suitable to reduce error bars and variations between single experiments. Unfortunately, it was not possible generate reproducible data from snap frozen colon tissue. This can be ascribable to inappropriate single cell separation from colon tissue. In contrast to liver, the colon tissue is more rigid containing several layers of muscle tissue (1.1.1). As discussed above (5.2.1), the results from the experiments analysing γH2AX induction and formation of $O^6$-MeG adducts indicate, that the AOM-induced DNA damage in colon tissue is lower in colon tissue compared to liver tissue. Thus, the DNA strand break induction might range below the detection limit of the assay or stays below basal levels.

In summary, PARP-1 k.o. animals are prone to AOM-induced DNA strand breaks. As already mentioned above, further experiments are necessary to determine whether this is due to a delay in BER.

### 5.2.3 AOM-INDUCED DDR IN WT AND PARP-1$^{-/-}$ ANIMALS

After detection of a DSB by the DNA damage sensing MRN complex, histone H2AX is phosphorylated on Ser139 by members of the PIKK family (ATM, ATR, DNA-PK). The phosphorylated histone H2AX, also known as γH2AX, is a well described marker for DSBs (Kuo, Yang 2008).

It should be noted, that γH2AX levels of WT and PARP-1 k.o. animals were not assessed in one experiment. Different exposure times of the photographic films might have negatively influenced the comparability of γH2AX induction in WT and PARP-1$^{-/-}$ animals.

AOM-induced formation of γH2AX was analysed in liver and colon tissue of WT and PARP-1$^{-/-}$ animals via western blot. Animals were challenged with 5 mg/kg bw AOM or 10 mg/kg bw AOM up to 48 h. For both concentrations, induced γH2AX levels were higher in liver tissue, whereas higher basal levels were observed in colon tissue (**Figure 25**). This goes in line with a study of Wang and colleagues, which reports a frequency of 8.4 ± 1.7 % γH2AX foci-positive cells in hepatocytes, whereas colon crypts displayed a frequency of 26.7 ± 1.9 % γH2AX foci-positive cells (Wang *et al.* 2009a). The difference in basal γH2AX levels of colon and lifer tissue is explainable by their span of life and exposure to exogenic noxae. Liver hepatocyte cells have a turnover time of 0.5-1 year compared to a life span of 3-4 days of gastrointestinal colon crypt cells (Rogakou *et al.* 2000).

Surprisingly, the induction of γH2AX after 24 h and 48 h in WT liver tissue was stronger compared to PARP-1 k.o., but the differences missed statistical significance. Treatment with 5 mg/kg bw led to quite similar moderate induction of γH2AX in colon tissue of both genotypes after 24 h, which subsequently declined to almost basal level. (**Figure 26**). Based on the stated higher sensitivity of PARP-1-deficient models *in vitro* and *in vivo*, an increased induction of γH2AX was expected (Murcia *et al.* 1997; Trucco *et al.* 1998). The involvement of PARP-1 in DSB repair was already mentioned above and is outlined in chapter 1.3.5. PARP-1 promotes DNA strand break repair by its function as DNA-damage-detecting molecule (Shrivastav *et al.* 2008) and interacts with important players of the subsequent DNA repair pathways (Haince *et al.* 2007; Haince *et al.* 2008; Soni *et al.* 2014; Spagnolo *et al.* 2012). Aguilar-Quesada and colleagues studied the interaction of PARP-1 and ATM in detail: The group found a defective ATM-kinase activity concomitant with reduced γH2AX foci formation in PARP-1-deficient cells after γ-irradiation (Aguilar-Quesada *et al.* 2007). This might be an explanation for the lower induction of γH2AX in PARP-1$^{-/-}$ liver tissue. Consequently, γH2AX might not be a suitable endpoint for the assessment of NOC-induced DSBs in a PARP-1-deficient model. The alkaline comet assay is a method which directly assesses the formation of induced DNA strand breaks and is therefore not influenced by the activity of PARP-1. The lower γH2AX formation in colon tissue fits to the lower NOC-induced formation of PAR (**Figure 22**) and $O^6$-MeG adducts (**Figure 28**).

The high AOM dose (10 mg/kg bw AOM) led to a significant induction of γH2AX levels after 24 h and subsequent decrease after 48 h in liver tissue. The time-dependent induction was comparable in both genotypes and furthermore, γH2AX-induction in liver tissue correlated with the AOM dose. The γH2AX levels observed in colon tissue of both genotypes were comparable to the levels assessed after challenge with 5 mg/kg bw AOM (**Figure 27**). The DNA damage induced by the high AOM dose might have exceeded the capacity of the PIKK family proteins and therefore, differences in strand break induction might not be correctly assessed by analysis γH2AX. The neutral comet assay might represent a more appropriate endpoint.

Assessment of AOM-induced γH2AX induction was comparable in both genotypes. The experiments should be repeated and γH2AX induction of WT and PARP-1-deficient animals directly compared on

the same western blot. Further experiments, *e.g.* neutral comet assay, should be performed to elucidate, if phosphorylation of H2AX is an appropriate endpoint for DSB formation in absence of PARP-1.

### 5.2.4 PARP-1 HAS NO INFLUENCE ON FORMATION OF AOM-INDUCED *O*$^6$-MeG ADDUCTS AND MGMT ACTIVITY

Treatment with AOM induces *O*$^6$-MeG adducts, which were formed in a time-dependent manner in tissue of both genotypes. The amount of induced *O*$^6$-MeG adducts was significantly higher in live tissue (**Figure 28**), in accordance with NOC-induced PAR formation (**Figure 22**) and γH2AX levels (**Figure 26** and **Figure 27**). As stated before, the suggested amount of ultimate carcinogen reaching the colon might be lower, which is reflected by these findings. Since there is no known connection between PARP-1 and MGMT, the strong variation of *O*$^6$-MeG adducts in liver tissue of both genotypes is explainable by variation of the MGMT expression within the probed individuals/organs. Interindividual variation of MGMT expression in liver and colon of healthy individuals was already reported in the literature (Gerson *et al.* 1986; Grafstrom *et al.* 1984) as well as longitudinal variation along the colon (Lees *et al.* 2002; Lees *et al.* 2007).

Next, the activity of MGMT, which is exclusively responsible for the reversal *O*$^6$-MeG DNA adducts, was assessed. During repair, the methyl group is transferred from *O*$^6$-MeG onto MGMT, which leads to its inactivation and subsequent proteasomal degradation (Fahrer *et al.* 2015; Kaina *et al.* 2007). Analysis of liver tissue revealed a comparable pattern of MGMT activity in PARP-1-proficient and PARP-1-deficient animals. 24 h after AOM injection, MGMT was almost completely depleted. Animals receiving the low AOM dose showed a recovery of MGMT activity after 48 h to about 50 %, whereas the depletion persisted in mice challenged with the high AOM dose (**Figure 29**). The low AOM dose (5 mg/kg bw AOM) led to a time-dependent reduction in WT colon tissue below 50 % after 48 h, whereas a recovery of MGMT activity was visible in PARP-1 k.o animals after 48 h (**Figure 29 A**). The high AOM dose (10 mg/kg bw) caused a complete depletion of MGMT activity in both animal strains after 48 h and, in line with the previous results, a small recovery in PARP-1-deficient animals at the same time point (**Figure 29 B**). The variation of MGMT activity in colon tissue between the mouse strains might be due to the different interindividual expression of MGMT within the colon (Gerson *et al.* 1986; Grafstrom *et al.* 1984; Lees *et al.* 2002).

The reduction of MGMT activity and formation of *O*$^6$-MeG DNA adducts was stronger in liver tissue and correlated with the AOM dose. This confirms the results obtained from analysis of AOM-induced PAR and γH2AX formation. Further, the time-dependency of *O*$^6$-MeG adduct formation and depletion of MGMT activity after challenge with AOM was observed in prior studies published by our group (Fahrer *et al.* 2015).

Collectively, WT and PARP-1-deficient animals showed a comparable trend of time-dependent induction of *O*$^6$-MeG adducts and depletion of MGMT activity after exposure to AOM.

### 5.2.5 CELL PROLIFERATION AND APOPTOSIS INDUCTION ARE NOT INFLUENCED BY PARP-1

Besides DNA repair, PARP-1 is involved in a plethora of cellular processes like cell cycle and cell death (1.3.7). The S-phase related protein PCNA, a well-established marker for colonic cell proliferation (Kubben *et al.* 1994), was analysed with the help of IHC. Untreated colon samples of both genotypes displayed a similar amount of PCNA-positive cells (**Figure 30**). This result goes in line with a study of Trucco and colleagues, which reports a comparable cell cycle distribution of PARP-1-deficient MEFs to WT MEFs in absence of DNA damage (Trucco *et al.* 1998). However, PARP-1 detects stalled or collapsed replication forks arising during replication and facilitates subsequent repair by interaction with the MRN complex (Bryant *et al.* 2009; Jones, Petermann 2012). Both PARP-1 and PARP-2 are known to interact with the centromere proteins and the spindle check points (Kanai *et al.* 2000; Kanai *et al.* 2003; Kanai *et al.* 2007; Saxena *et al.* 2002a; Saxena *et al.* 2002b). Therefore, an altered proliferation rate of colon cells in PARP-1$^{-/-}$ mice was expected to be possible. PARP-1$^{-/-}$ MEFs show a cell cycle arrest in $G_2$/M upon exposure to MMS (Trucco *et al.* 1998). Analysis of PCNA-positive cells after treatment with AOM might reveal a decreased proliferation in colonic crypts of PARP-1 k.o. animals.

AOM-dependent induction of apoptosis in colon tissue was assessed via TUNEL staining 48 h after injection (**Figure 31**). Contrasting to the expectations, WT and PARP-1$^{-/-}$ animals exhibited comparable levels of apoptotic cells in colonic crypts (**Figure 32**). In line with the previous results, the induction of apoptosis was correlating with the applied AOM dose. Prior studies showed the sensitivity of PARP-1$^{-/-}$ MEFs towards the cytotoxic effects of the NOCs NMU and MMS (Murcia *et al.* 1997; Trucco *et al.* 1998). Compared to WT animals, a higher apoptosis induction in PARP-1$^{-/-}$ splenocytes was observed 2-6 h after MNU treatment. This was concomitant with a rapid accumulation of p53. The authors suggested an increased p53 and cell death induction due to delayed DNA repair (Murcia *et al.* 1997). The comparison of WT MEFs to PARP-1$^{-/-}$ MEFs upon exposure to MMS revealed a significant decrease in doubling time, dose-dependent decrease in viability and cell cycle arrest in $G_2$/M (Trucco *et al.* 1998). As already discussed previously, the AOM-induced damage in colon tissue was relatively low compared to liver tissue. The chosen assay might not be sensitive enough to detect differences in colon tissue. TUNEL analysis of liver tissue could reveal differences in cell death induction. Additionally, cell death induction in colon tissue could be studied via flow cytometry (*e.g.* Annexin V/PI). This would also allow evaluation of the cell cycle distribution after challenge with AOM.

PARP-1-proficient WT and PARP-1-deficient mice displayed a comparable basal cell proliferation and AOM-induced cell death in colon crypts. The latter should be detailed with additional experiments; *e.g.* Annexin V/PI staining or analysis of cell cycle distribution via flow cytometry.

## 5.3 ROLE OF PARP-1 IN INFLAMMATORY RESPONSE

### 5.3.1 PARP-1-DEFICIENT ANIMALS ARE PROTECTED AGAINST DSS-INDUCED COLITIS

Mini endoscopic assessment of the MEICS after the first DSS cycle (1 %) of mice receiving 15 mg/kg bw AOM unveiled a significantly attenuated level of inflammation in PARP-1-deficient animals compared to the WT (**Figure 33 A & B**). Further histological analysis with the help of HE staining did not show a difference between the colonic tissue of both genotypes (**Figure 33 A**). According to Becker and colleagues, the MEICS observed in animals treated with 1 % DSS was within a range (0-3) which can be found in healthy animals (Becker *et al.* 2006a). Thus, the DSS dose was increased to 2.5% to provoke a clearly pathological colitis (**Figure 33 C & D**). Of note, the AOM dose was reduced to 10 mg/kg bw to ensure survival of the mice. As expected, the MEICS in WT animals dramatically increased, whereas PARP-$1^{-/-}$ animals displayed a moderate rise.

The attenuated inflammation in absence of PARP-1 confirms the results from prior studies: PARP-1-deficient animals are immune to inflammation-related pathologies such as ischemic infarction, collagen induced arthritis, and LPS-induced septic shock (Chevanne *et al.* 2007; Hassa, Hottiger 2002). *In vivo* studies investigated the effect of PARP inhibitors (3-Aminobenzamide and 1,5-Dihydroxyisoquinoline) on a trinitrobenzene sulfonic acid (TNBS)-induced colitis in Wistar rats. Colitis-induction with TNBS is characterised by activation of NF-κB, infiltration of immune cells, synthesis of prostaglandins, expression of COX-1 and COX-2 and mucosal damage (Sanchez-Fidalgo *et al.* 2007; Zingarelli *et al.* 2003). Hence, the TNBS-induced colitis shares features with the DSS-induced colitis (1.4). Inhibition of PARP successfully reduced theTNBS-mediated muscosal damage. Importantly, the DNA binding of NF-κB in colon cells was reduced. This went in line with reduced activity and abundance of inflammatory targets (*e.g.* prostaglandins and COX-2) (Sanchez-Fidalgo *et al.* 2007; Zingarelli *et al.* 2003). These results confirm the role of PARP-1 as critical driver of NF-κB-mediated colitis, which was studied in this thesis. Moreover, inflammatory bowel disease (ulcerative colitis and Crohn's disease) is an important driver of human colorectal carcinogenesis (Eaden *et al.* 2001; Roon *et al.* 2007). Both duration and inflammation severity correlate with risk for CRC (Itzkowitz, Harpaz 2004).

The profound inflammation in WT mice went in line with hyperplastic cell growth and loss of the crypt structure in colon tissue (**Figure 33 C**). Hyperplastic tissue is likely to progress into neoplastic lesions (Cooper 1992). Distortion of the colonic crypts was also observed in other studies utilising the murine AOM/DSS model (Paradisi *et al.* 2009; Tanaka *et al.* 2003).

In conclusion, lack of PARP-1 resulted in an attenuated mucosal inflammation after treatment with the AOM/DSS protocol.

### 5.3.2 INFLUENCE OF PARP-1 ON THE ABUNDANCE OF THE INDUCIBLE CYCLOOXYGENASE COX-2

The DSS-mediated colitis was further investigated via IHC staining of colon sections. First, the inducible COX-2 was analysed as downstream target of the inflammation cascade. COX-2 is specifically induced by inflammatory cytokines and chemokines (Kuwano *et al.* 2004). Comparison of untreated mice indicated a slightly higher abundance of COX-2 in PARP-1-proficient WT animals (**Figure 34**). COX-2 was localised in the cytoplasm of the colonic cells. Quantitative evaluation of WT and PARP-1 k.o. animals, which received 10 mg/kg bw AOM and one cycle with 2.5 % DSS, revealed a significantly lower abundance of COX-2 in PARP-$1^{-/-}$ mice (**Figure 36**). Similar to the COX-2 localisation in untreated samples, COX-2 was primarily found in the cytoplasm of the colonic cells.

As induction of COX-2 is often implicated in inflammatory pathologies including inflammatory bowel disease and CRC (Wang, DuBois 2010), the higher induction of COX-2 in the animals with higher mucosal inflammation confirmed our expectation. In the context of colitis, the cytokines IL-1b and TNFα secreted by immune cells as well as the proto-oncogenes Ras promote COX-2 expression (DuBois *et al.* 1998; Wang *et al.* 2005). Among others, the inflammatory master key regulator NF-κB can induce COX-2 on the transcriptional level (Young *et al.* 2009). The involvement of NF-κB indicates the link between PARP-1, which plays an important role in its activation, and COX-2. On the other hand, genetic studies showed that COX-2 deficiency increases the sensitivity towards DSS-induced colitis in a mouse model implying a central role of COX-2 in the defence of the colonic mucosa (Morteau *et al.* 2000). Furthermore, loss of COX-2 is linked with lower tumour formation in an $Apc^{Min/+}$ model of CRC (Chulada *et al.* 2000) as well as in $Apc^{\Delta 716}$ mice (Oshima *et al.* 1996). Overexpression of COX-2 in transgenic mice did not influence the rate of spontaneous tumour formation but was sufficient to enhance tumour promotion upon challenge with AOM compared to WT mice (Al-Salihi *et al.* 2009). The decreased abundance of COX-2 in absence of PARP-1 was also observed in *In vivo* studies investigating the effect of PARP inhibitors on a TNBS-induced colitis model (Sanchez-Fidalgo *et al.* 2007; Zingarelli *et al.* 2003). A large body of evidence confirms a significantly decreased risk for colorectal carcinogenesis in humans through permanent inhibition of COX-2 (Chan *et al.* 2008; Flossmann, Rothwell 2007; Rostom *et al.* 2007) and improves overall survival in CRC patients whose tumours overexpress COX-2 (Chan *et al.* 2009).

In summary, the lower abundanceof COX-2 in PARP-$1^{-/-}$ animals can be linked to an attenuated NF-κB-mediated inflammatory response. This suggestion could be further strengthened by analysis of NF-κB activation via IHC or western blot analysis. Another experimental approach could focus on the inhibitory IκB proteins, which prevent the translocalisation of NF-κB into the nucleus. The lower induction of COX-2 is likely contributing to lower CRC formation and tumour progression.

## 5.3.3 PARP-1 MEDIATES INVASION OF IMMUNE CELLS OF THE INNATE IMMUNE RESPONSE AND CYTOKINE SECRETION

### 5.3.3.1 DECREASED INNATE IMMUNE RESONSE FOLLOWING DSS TREATMENT IN PARP-1-DEFICIENT ANIMALS

The innate immune system is the first line of defence against pathogens. Immune cells invading the site of inflammation secrete chemo- and cytokines thus modulating the subsequent response (Janeway 2005). IHC analysis of CD11b, an established marker for murine monocytes (Lai *et al.* 1998), in colon sections of animals treated with 10 mg/kg bw AOM after the first cycle with 2.5 % DSS confirmed a dramatically reduced invasion of CD11b positive cells. Monocytes were located in submucosa, muscularis, and serosa (**Figure 38**).

F4/80, a marker for murine macrophages (Austyn, Gordon 1981), was examined after treatment with 10 mg/kg bw AOM and 2.5 % DSS at the same time point as the experiments described previously. In accordance with the CB11b analysis, PARP-1$^{-/-}$ animals displayed a lower level of F4/80-positive cells in the colonic crypts (**Figure 40**).

Prior studies of the innate immune response with the AOM/DSS protocol reported signs of diffuse inflammation in line with high numbers of inflammatory cells in the colonic mucosa (Paradisi *et al.* 2009; Tanaka *et al.* 2003). Colitis-induction with DSS in mice is associated with invasion of macrophages in the colonic mucosa (Okayasu *et al.* 1990). Yet, the role of PARP-1 in the innate immune response is poorly understood. First evidence confirming the involvement of PARP-1 in the innate immune response and immune-mediated diseases was obtained from murine rheumatoid arthritis model. In contrast to WT mice, PARP-1-deficient mice experienced only a mild rheumatoid arthritis concomitant with lower expression of IL-1b and monocyte chemoattractant protein 1 in arthritic joints (Garcia *et al.* 2006). Moreover, PARP-1 is required for the expression of chemoattractant chemokines (IL-8, macrophage inflammatory proteins 1 and 2, monocyte chemoattractant protein 1), inhibition or gene knock down of PARP-1 results in a weakened migration of immune cells to inflammatory sites (Sharp *et al.* 2001; Ullrich *et al.* 2001; Zingarelli *et al.* 1998). *In vivo* studies using a TNBS-induced colitis model in rats also reported an attenuated inflammatory response after inhibition of PARP compared to animals which received no inhibitor (Sanchez-Fidalgo *et al.* 2007; Zingarelli *et al.* 2003).

In accordance with the literature and the prior experiments performed during this work and the literature, the response of the innate immune system to AOM/DSS-induced colitis is weaker in the PARP-1-deficient mouse strain.

### 5.3.3.2 RESPONSE OF THE ADAPTIVE IMMUNE SYSTEM FOLLOWING AOM/DSS TREATMENT

The adaptive immune system is a slower but more specific response which involves T-cells targeting pathogens and infected cells (Janeway 2005). CD3 was used as marker for T-cells. As expected, untreated colon sections of both WT and PARP-1 k.o. animals exhibited only little CD3 signal (**Figure 41**). Surprisingly, signal intensity did not increase after exposure to 10 mg/kg bw AOM and one cycle

with 2.5 % DSS (**Figure 42**). Statistical evaluation of treated animals did not reveal any difference between the two genotypes.

An elevated level of CD3 positive T-cells was suggested, as DSS-induced colitis in rats leads to an increase of activated T-cells in colon tissue (Shintani *et al.* 1997; Takizawa *et al.* 2004). It is possible, that the adaptive immune response had not reached their full potential at the time of necropsy. The adaptive immune system is known to take up to 7 days to develop its full potential (Janeway 2005). During the experimental procedure, it was observed that the colitis did develop a few days after first DSS administration and samples were taken 7 days after first administration of the colitogen DSS. Therefore, a later time point (probably 10 days after start of the DSS cycle) might reveal a stronger response of the adaptive immune system.

Investigation of the adaptive immune response upon challenge with AOM/DSS in WT and PARP-1 k.o. animals showed no difference between the genotypes, later time point should be studied in other experiments.

#### 5.3.3.3 CYTOKINE SECRETION

During the inflammatory immune response, cytokines are secreted by the diseased tissue and immune cells. The chemokine HMGB1 is secreted by leukocytes (Klune, JR *et al.* 2008), especially macrophages and monocytes (Tang *et al.* 2007), and the inflamed tissue (Ditsworth *et al.* 2007). First, the basal HMGB1 levels in untreated colon tissue of WT and PARP-1 k.o. animals were studied. Almost no HMGB1 signal was observed with the help of qualitative IHC analysis in both animal strains (**Figure 43**). After the first 2.5 % DSS cycle, HMGB1 was clearly visible in colon tissue of both mouse strains. Statistical evaluation confirmed a significantly lower level of HMGB1 in the animals lacking PARP-1 (**Figure 45**). This goes perfectly in line with the literature. HMGB1 translocates from the nucleus into the cytoplasm and is secreted into the surrounding tissue to attract immune cells (Zhang *et al.* 2013). HMGB1 translocation correlates with PARP-1 activation (Ebrahimkhani *et al.* 2014). Recent publications link HMGB1 expression to aging (Huang *et al.* 2015) and inflammation-associated diseases (Andersson, Tracey 2011; Harris *et al.* 2012). The pro-inflammatory function of HMGB1 is mediated by receptors, *e.g.* receptors for advanced glycation end products (RAGE) (Hori *et al.* 1995), TLRs (Park *et al.* 2004; Tian *et al.* 2007), as well as endocytic HMGB1 uptake (Kang *et al.* 2014; Xu *et al.* 2014). The master key regulator NF-κB, interferon regulatory factor-3, and PI3K are activated by HMGB1 (Lotze, Tracey 2005). Although the mechanisms regulating HMGB1 release and activity vary depending on context, experimental studies suggest that oxidative stress is likely involved in modulation of HMGB1 (Green *et al.* 2009; Linkermann *et al.* 2014; Tang *et al.* 2011).

The increase in PAR polymer formation through BER activation goes in line with extracellular release of HMGB1 (Ebrahimkhani *et al.* 2014). Interestingly, this finding supports the notion that HMGB1 is involved in DNA repair and primary damage induction. Of note, an impaired BER by loss of AAG is associated with an attenuated PARP-1 activation and HMGB1 release (Ebrahimkhani *et al.* 2014). A co-staining of HMGB1 and PARP-1 or PAR might allow further insight in the interplay between HMGB1 and PARP-1. Beside its role in inflammation, the nuclear factor HMGB1 sustains chromosomal stability.

Absence of HMGB1 results in genomic instability (Giavara *et al.* 2005), abnormal gene transcription (Rowell *et al.* 2012), impaired DNA damage response (Lange *et al.* 2008) and genome chromatinisation (Celona *et al.* 2011). In this context, the interaction of PARP-1 and HMGB1 could be further investigated. Analysis of HMBG1 abundance/localisation upon challenge with AOM alone might reveal valuable details of the DNA damage-induced activation of HMGB1.

Assessment of HMGB1 in colon sections confirmed a lower intensity in PARP-1$^{-/-}$ animals, which is likely to result from absence of PARP-1. The interplay of PARP-1 and HMGB1 should be further investigated in the context of NOC-induced DNA damage and AOM/DSS-induced colitis.

#### 5.3.3.4 EXPRESSION OF INFLAMMATION-RELATED GENES IS ATTENUATED IN PARP-1 K.O. ANIMALS

The expression of pro-inflammatory NF-κB target genes was compared between WT and PARP-1$^{-/-}$ animals via qPCR (**Figure 46**). In line with the results from IHC analysis of COX-2 expression (**Figure 36**), mRNA expression levels of *COX-2* tended to be lower expressed in PARP-1-deficient animals. Expression of the small cytokine *CXCL2*, which is produced by macrophages and monocytes, as well as expression of the related receptor *CXCR2* had a tendency to be decreased in absence of PARP-1. Expression levels of the pyrogen *IL-1b*, which is secreted by macrophages and monocytes, showed a trend to be reduced in PARP-1$^{-/-}$ animals. Expression of *IL-6* , which is stimulated by IL-1b (Luo *et al.* 2003), was almost not present in absence of PARP-1. mRNA levels of *iNOS*, expressed as direct consequence of inflammatory processes, trended to be lower in PARP-1$^{-/-}$ colon tissue compared to WT colon tissue. Expression levels of all examined genes had a tendency to be were lower in PARP-1 k.o. animals but the differences did not reach statistical significance. A higher number of analysed animals might reduce the variation of the expression levels and thus statistical difference between the genotypes might be reached.

Larmonier and colleagues compared the mRNA expression levels of pro-inflammatory genes between WT and PARP-1-deficient mice. The latter displayed significantly reduced expression of *TNFα*, *interferon gamma* (*IFNγ*) and *IL-17* (Larmonier *et al.* 2016). NF-κB promotes the expression of *TNFα* and IFNγ (Rovetto *et al.* 1975), IL-17 is able stimulate the inflammatory response via NF-κB (Hata *et al.* 2002). TNFα, which is mainly secreted by monocytes/macrophages, and IFNγ, which is secreted by leukocytes, are critically involved in the aetiology of human CRC (Slattery *et al.* 2011; Stanilov *et al.* 2014). Interestingly, IL-17 is produced by T-helper cells (Miossec *et al.* 2009). This supports the notion, that the adaptive immune response in involved in DSS-induced inflammatory processes. In addition, Basilia and colleagues observed a decreased DNA binding of NF-κB after inhibition of PARP in a TNBS-induced colitis model (Zingarelli *et al.* 2003).

Analysis of mRNA expression levels of pro-inflammatory genes provided further evidence of the involvement of PARP-1 in the activation of the tumour-promoting NF-κB-mediated inflammatory response.

### 5.3.4 TUMOUR FORMATION INCREASES WITH STONGER INFLAMMATORY STIMULUS

In addition, colorectal carcinogenesis was studied after challenge with 10 mg/kg bw AOM and two cycles of 2.5 % DSS. The dramatically increased size and number of the arising colorectal tumours blocked the colon. Thus, tumour data was assessed with a new methodical approach. The experiment was terminated after 12 weeks due to the strong tumour formation and health of the animals. The colon was harvested, longitudinally opened and tumours recorded with the camera of the mini endoscopy system (3.2.5.1). In contrast to mini endoscopy, this altered experimental setup allowed to investigate tumour formation in the whole colon, not only the distal part. Confirming previous studies concerning the AOM/DSS protocol of colorectal carcinogenesis (Robertis *et al.* 2011), majority of tumours was located in the distal colon. Statistical evaluation of tumour formation in the distal colon revealed a slightly lower tumour number (**Figure 48 A**) and significantly decreased tumour score (**Figure 48 B**) in PARP-1$^{-/-}$ mice compared to the WT. Besides the generally lower CRC formation in the proximal colon on both animal strains, tumour number (**Figure 48 C)** and score (**Figure 48 D**) were significantly lower in this colon part of PARP-1 k.o. animals.

Tumour number and tumour size of distal colon tumours correlated with the administered DSS dose but were still attenuated in PARP-1-deficient mice compared to the WT. In line with the literature, the tumour formation was significantly lower in the proximal part of the colon.

## 5.4 PARP-1 FACILITATES TUMOUR PROGRESSION

The last part of this thesis addressed the particular impact of primary damage induction and the tumour promoting inflammatory processes on the genesis of CRC in the used murine AOM/DSS model. As confirmed by the initial experiments, absence of PARP-1 is linked with an attenuated inflammatory response (4.4) and lower tumour formation (4.2). Our group recently reported the sensitivity of DNA repair-deficient MGMT$^{-/-}$ mice to the AOM/DSS protocol. Compared to the WT, MGMT-deficient animals were prone to primary AOM-induced DNA damage and showed a dramatically increased tumour formation (Fahrer *et al.* 2015). Therefore, a PARP-1/MGMT DKO strain was generated in the context of this work to study the role of inflammatory tumour promotion in combination with high primary DNA damage induction.

### 5.4.1 INHIBITION OF MGMT LEADS TO INCREASED CRC FORMATION IN PARP-1$^{-/-}$ ANIMALS

Prior to experiments with DKO animals, PARP-1$^{-/-}$ mice were *i.p.* injected with $O^6$-BG to deplete MGMT repair activity. Subsequently, animals were challenged with the AOM/DSS protocol and the tumour formation assessed via mini endoscopy after 16 weeks. The AOM-metabolite MAM is reported to possess a maximum half-life of 12 h under physiological conditions (Feinberg, Zedeck 1980), therefore MGMT inhibition with $O^6$-BG was maintained for at least 48 h after AOM injection. The adequate $O^6$-BG

concentration and injection intervals to maintain MGMT inhibition over the desired time-period were tested in advance with a small group of animals (data not presented). As expected, inhibition of MGMT lead to an increase of colorectal tumours in PARP-1$^{-/-}$ animals. Tumour number and tumour size in the PARP-1-deficient mice dramatically increased after inhibition of MGMT with $O^6$-BG (**Figure 49**).

This interesting result confirms the critical impact of primary DNA damage induction on the risk for CRC.

### 5.4.2 PARP-1/MGMT DOUBLE KNOCK OUT ANIMALS ARE PRONE TO AOM-INDUCED TUMOURS BUT SHOW ATTENUATED TUMOUR PROMOTION

The newly generated genotype lacking both PARP-1 and MGMT was treated with an initial dose of 1 mg/kg bw AOM and 3 mg/kg bw AOM and two subsequent cycles of 1 % DSS. Unfortunately, it was not possible to treat the mice with a higher AOM dose. Application of higher doses caused death in almost all animals during the first DSS cycle. Notably, experiments with the PARP-1 k.o. animals were only performed with doses of 5 mg/kg bw AOM and above due to their insensitivity to the AOM/DSS protocol. Colorectal tumour formation in DKO animals was assessed after 16 weeks and compared to WT as well as MGMT$^{-/-}$ animals. For both AOM doses, the mean tumour number was dramatically higher in the DKO animals with clear statistical significance (**Figure 50 A**). Also, the tumour score was increased in DKO animals compared to WT and MGMT-deficient animals. The difference between DKO and MGMT k.o. mice did not reach statistical significance (**Figure 50 B**). Of note, the mean tumour size in DKO animals was significantly smaller compared to MGMT$^{-/-}$ animals (**Figure 51**).

The findings, especially the reduced mean tumour size, indicate a lower tumour progression in DKO animals compared to the MGMT$^{-/-}$ genotype due to the attenuated inflammatory response. However, the number of induced tumours was significantly higher in DKO animals compared to the other genotypes. Considering the literature, the increased number of tumours in DKO animals might be attributable to the higher susceptibility to AOM-induced DNA damage in absence of PARP-1 (4.3.1). Sensitivity to the genotoxic effects of NOCs in absence of PARP-1 was also reported by previous *in vitro* and *in vivo* studies (Aguilar-Quesada *et al.* 2007; Dantzer *et al.* 1999; Murcia *et al.* 1997; Trucco *et al.* 1998). The higher DNA damage induction could increase the number of tumours, whereas the attenuated NF-κB-mediated inflammatory response slows tumour progression.

The AOM-induced DNA damage should be addressed in further experiments. Especially, the role of PARP-1 in BER and HRR is of interest. DNA repair defects should be examined with BER and HRR repair assays and the concomitant DNA damage induction via neutral and alkaline comet assay. TUNEL analysis of colon sections would be suitable to study cell death induction and confirm the sensitivity of animals lacking both PARP-1 and MGMT towards AOM. Furthermore, AOM/DSS-induced CRC formation should be compared to PARP-1-deficient animals treated with 1 mg/kg bw AOM or 3 mg/kg bw AOM and two 1 % DSS cycles.

Interestingly, study of AOM/DSS-induced CRC formation in DKO animals revealed a higher sensitivity of DKO animals to AOM-induced tumours in line with a slower progression of tumours. The slower

tumour progression is attributable to the weakened inflammatory response in absence of PARP-1, which was demonstrated in the previous parts of this work.

### 5.4.3 DKO ANIMALS ARE SENSITIVE TO AOM/DSS-INDUCED COLITIS

Mini endoscopic assessment of the colitis severity after the first DSS cycle revealed a slightly higher MEICS in DKO animals (10.8) compared to MGMT k.o. (8.9) (**Figure 52**). A direct comparison to WT and PARP-1$^{-/-}$ animals was not possible as colitis severity in these genotypes was only investigated at higher AOM doses. The MEICS of WT (1.5) and PARP-1 (0.8) animals challenged with 10 mg/kg bw AOM and 1 % DSS was much lower. These findings differ from the initial expectation that the colitis severity and tumour formation might be lower in animals lacking both repair enzymes. The stronger acute colitis is likely attributable to the higher cyto- and genotoxic effects of AOM in animals lacking PARP-1, thereby leading to increased cell death induction cell death (Murcia *et al.* 1997; Trucco *et al.* 1998).

Besides the already mentioned analysis of DNA damage induction and DNA repair capacity in DKO animals, the cell death induction during the first DSS cycle should be studied so strengthen the data. The inflammatory response in DKO and MGMT$^{-/-}$ after the first DSS cycle should be compared to PARP-1-deficient animals. Importantly, the chronic inflammatory response in PARP-1 k.o., MGMT-deficient and DKO animals must be compared to make a certain conclusion about the chronic inflammatory response which drives tumour promotion.

## 5.5 CONCLUSION AND PERSPECTIVES

This work bears significant implications for the role of PARP-1 in the aetiology colitis-associated CRC. Absence of PARP-1 is associated with a sensitivity to NOC-induced DNA damage and an attenuated NF-κB-mediated inflammatory response. This results in a decreased tumour formation in PARP-1-deficient animals challenged with the AOM/DSS protocol compared to WT animals. MGMT is responsible for the repair of NOC-induced $O^6$-MeG DNA adducts, a critical lesion driving colorectal carcinogenesis. PARP-$1^{-/-}$/MGMT$^{-/-}$ animals display a higher number of induced tumours compared to animals deficient for MGMT only but show a slower tumour progression. The latter is likely to be a result of the attenuated inflammatory response in absence of PARP-1. In conclusion, PARP-1 is crucial an efficient DNA repair and, moreover, facilitates tumour progression due to its role as co-activator of NF-κB.

Future studies should on one hand examine the DDR/DNA repair in PARP-$1^{-/-}$ animals and compare genotoxic endpoints to WT animals. On the other hand, the inflammatory response could be investigated in greater detail with a focus on the PARP-1-dependent activation of NF-κB and target genes. The chronic inflammatory response is of particular interest as it critically influences the promotion and progression of tumours. Analysis of AOM-induced cell death and DNA damage in DKO animals should be further analysed and compared to WT, PARP-$1^{-/-}$ and MGMT-deficient mice. Both points can be compared to human CRC or patients suffering from inflammatory bowel disease. COX-inhibitors are in use to decrease the risk for CRC in patients with chronic inflammatory diseases like inflammatory bowel disease (Chan *et al.* 2008; Flossmann, Rothwell 2007; Rostom *et al.* 2007) and, moreover, enhance overall survival in CRC patients whose tumours overexpress COX-2 (Chan *et al.* 2009). Here, PARP inhibitors bear the potential to inhibit not only downstream targets of the inflammatory response but attenuate the activation of the inflammatory master key regulator NF-κB.

# 6 REFERENCES

Aaltonen, L. A.; Peltomaki, P.; Leach, F. S.; Sistonen, P.; Pylkkanen, L.; Mecklin, J. P.; Jarvinen, H.; Powell, S. M.; Jen, J.; Hamilton, S. R. (1993): Clues to the pathogenesis of familial colorectal cancer. In: *Science (New York, N.Y.)* 260 (5109), S. 812–816.

Aas, Per Arne; Otterlei, Marit; Falnes, Pal O.; Vagbo, Cathrine B.; Skorpen, Frank; Akbari, Mansour; Sundheim, Ottar; Bjoras, Magnar; Slupphaug, Geir; Seeberg, Erling; Krokan, Hans E. (2003): Human and bacterial oxidative demethylases repair alkylation damage in both RNA and DNA. In: *Nature* 421 (6925), S. 859–863. DOI: 10.1038/nature01363.

Abdelaziz, N.; Colombo, F.; Mercier, I.; Calderone, A. (2001): Nitric oxide attenuates the expression of transforming growth factor-beta(3) mRNA in rat cardiac fibroblasts via destabilization. In: *Hypertension (Dallas, Tex. : 1979)* 38 (2), S. 261–266.

Adler, Adam S.; Kawahara, Tiara L. A.; Segal, Eran; Chang, Howard Y. (2008): Reversal of aging by NFkappaB blockade. In: *Cell cycle (Georgetown, Tex.)* 7 (5), S. 556–559. DOI: 10.4161/cc.7.5.5490.

Adler, Adam S.; Sinha, Saurabh; Kawahara, Tiara L. A.; Zhang, Jennifer Y.; Segal, Eran; Chang, Howard Y. (2007): Motif module map reveals enforcement of aging by continual NF-kappaB activity. In: *Genes & development* 21 (24), S. 3244–3257. DOI: 10.1101/gad.1588507.

Aguilar-Quesada, Rocio; Munoz-Gamez, Jose Antonio; Martin-Oliva, David; Peralta, Andreina; Valenzuela, Maria Teresa; Matinez-Romero, Ruben; Quiles-Perez, Rosa; Menissier-de Murcia, Josiane; Murcia, Gilbert de; Ruiz de Almodovar, Mariano; Oliver, F. Javier (2007): Interaction between ATM and PARP-1 in response to DNA damage and sensitization of ATM deficient cells through PARP inhibition. In: *BMC molecular biology* 8, S. 29. DOI: 10.1186/1471-2199-8-29.

Ahel, Ivan; Ahel, Dragana; Matsusaka, Takahiro; Clark, Allison J.; Pines, Jonathon; Boulton, Simon J.; West, Stephen C. (2008): Poly(ADP-ribose)-binding zinc finger motifs in DNA repair/checkpoint proteins. In: *Nature* 451 (7174), S. 81–85. DOI: 10.1038/nature06420.

Alano, Conrad C.; Ying, Weihai; Swanson, Raymond A. (2004): Poly(ADP-ribose) polymerase-1-mediated cell death in astrocytes requires NAD+ depletion and mitochondrial permeability transition. In: *The Journal of biological chemistry* 279 (18), S. 18895–18902. DOI: 10.1074/jbc.M313329200.

Alberts, Bruce (2002): Molecular biology of the cell. 4th ed / Bruce Alberts … [et al.]. New York: Garland Science.

Ali, Ammar A. E.; Timinszky, Gyula; Arribas-Bosacoma, Raquel; Kozlowski, Marek; Hassa, Paul O.; Hassler, Markus; Ladurner, Andreas G.; Pearl, Laurence H.; Oliver, Antony W. (2012): The zinc-finger domains of PARP1 cooperate to recognize DNA strand breaks. In: *Nature structural & molecular biology* 19 (7), S. 685–692. DOI: 10.1038/nsmb.2335.

Al-Salihi, Mazin A.; Terrece Pearman, A.; Doan, Thao; Reichert, Ethan C.; Rosenberg, Daniel W.; Prescott, Stephen M.; Stafforini, Diana M.; Topham, Matthew K. (2009): Transgenic expression of

cyclooxygenase-2 in mouse intestine epithelium is insufficient to initiate tumorigenesis but promotes tumor progression. In: *Cancer letters* 273 (2), S. 225–232. DOI: 10.1016/j.canlet.2008.08.012.

Alshammari, Atika Hazzaa; Shalaby, Manal Aly; Alanazi, Mohammad Saud; Saeed, Hesham Mahmoud (2014): Novel Mutations of the PARP-1 Gene Associated with Colorectal Cancer in the Saudi Population. In: *Asian Pacific Journal of Cancer Prevention* 15 (8), S. 3667–3673. DOI: 10.7314/APJCP.2014.15.8.3667.

Althaus, F. R. (1992): Poly ADP-ribosylation: a histone shuttle mechanism in DNA excision repair. In: *Journal of cell science* 102 (Pt 4), S. 663–670.

Althaus, F. R.; Richter, C. (1987): ADP-ribosylation of proteins. Enzymology and biological significance. In: *Molecular biology, biochemistry, and biophysics* 37, S. 1–237.

Altmeyer, Matthias; Messner, Simon; Hassa, Paul O.; Fey, Monika; Hottiger, Michael O. (2009): Molecular mechanism of poly(ADP-ribosyl)ation by PARP1 and identification of lysine residues as ADP-ribose acceptor sites. In: *Nucleic acids research* 37 (11), S. 3723–3738. DOI: 10.1093/nar/gkp229.

Alvarez-Gonzalez, R.; Mendoza-Alvarez, H. (1995): Dissection of ADP-ribose polymer synthesis into individual steps of initiation, elongation, and branching. In: *Biochimie* 77 (6), S. 403–407. DOI: 10.1016/0300-9084(96)88153-3.

Ame, Jean-Christophe; Spenlehauer, Catherine; Murcia, Gilbert de (2004): The PARP superfamily. In: *BioEssays : news and reviews in molecular, cellular and developmental biology* 26 (8), S. 882–893. DOI: 10.1002/bies.20085.

Andersson, Ulf; Tracey, Kevin J. (2011): HMGB1 is a therapeutic target for sterile inflammation and infection. In: *Annual review of immunology* 29, S. 139–162. DOI: 10.1146/annurev-immunol-030409-101323.

Andrabi, Shaida A.; Dawson, Ted M.; Dawson, Valina L. (2008): Mitochondrial and nuclear cross talk in cell death: parthanatos. In: *Annals of the New York Academy of Sciences* 1147, S. 233–241. DOI: 10.1196/annals.1427.014.

Andrabi, Shaida A.; Kim, No Soo; Yu, Seong-Woon; Wang, Hongmin; Koh, David W.; Sasaki, Masayuki; Klaus, Judith A.; Otsuka, Takashi; Zhang, Zhizheng; Koehler, Raymond C.; Hurn, Patricia D.; POIRIER, Guy G.; Dawson, Valina L.; Dawson, Ted M. (2006): Poly(ADP-ribose) (PAR) polymer is a death signal. In: *Proceedings of the National Academy of Sciences of the United States of America* 103 (48), S. 18308–18313. DOI: 10.1073/pnas.0606526103.

Aravind, L. (2001): The WWE domain: a common interaction module in protein ubiquitination and ADP ribosylation. In: *Trends in biochemical sciences* 26 (5), S. 273–275.

Atkin, W. S.; Edwards, R.; Wardle, J.; Northover, J. M.; Sutton, S.; Hart, A. R.; Williams, C. B.; Cuzick, J. (2001): Design of a multicentre randomised trial to evaluate flexible sigmoidoscopy in colorectal cancer screening. In: *Journal of medical screening* 8 (3), S. 137–144.

Audebert, Marc; Salles, Bernard; Calsou, Patrick (2004): Involvement of poly(ADP-ribose) polymerase-1 and XRCC1/DNA ligase III in an alternative route for DNA double-strand breaks rejoining. In: *The Journal of biological chemistry* 279 (53), S. 55117–55126. DOI: 10.1074/jbc.M404524200.

Austyn, J. M.; Gordon, S. (1981): F4/80, a monoclonal antibody directed specifically against the mouse macrophage. In: *European journal of immunology* 11 (10), S. 805–815. DOI: 10.1002/eji.1830111013.

Becker, C.; Fantini, M. C.; Neurath, M. F. (2006a): High resolution colonoscopy in live mice. In: *Nature protocols* 1 (6), S. 2900–2904. DOI: 10.1038/nprot.2006.446.

Becker, Christoph; Fantini, Massimo C.; Neurath, Markus F. (2006b): TGF-beta as a T cell regulator in colitis and colon cancer. In: *Cytokine & growth factor reviews* 17 (1-2), S. 97–106. DOI: 10.1016/j.cytogfr.2005.09.004.

Beneke, R.; Geisen, C.; Zevnik, B.; Bauch, T.; Muller, W. U.; Kupper, J. H.; Moroy, T. (2000): DNA excision repair and DNA damage-induced apoptosis are linked to Poly(ADP-ribosyl)ation but have different requirements for p53. In: *Molecular and cellular biology* 20 (18), S. 6695–6703.

Beneke, Sascha (2012): Regulation of chromatin structure by poly(ADP-ribosyl)ation. In: *Frontiers in genetics* 3, S. 169. DOI: 10.3389/fgene.2012.00169.

Beneke, Sascha; Cohausz, Odile; Malanga, Maria; Boukamp, Petra; Althaus, Felix; Burkle, Alexander (2008): Rapid regulation of telomere length is mediated by poly(ADP-ribose) polymerase-1. In: *Nucleic acids research* 36 (19), S. 6309–6317. DOI: 10.1093/nar/gkn615.

Benson, Victoria S.; Patnick, Julietta; Davies, Anna K.; Nadel, Marion R.; Smith, Robert A.; Atkin, Wendy S. (2008): Colorectal cancer screening: a comparison of 35 initiatives in 17 countries. In: *International journal of cancer* 122 (6), S. 1357–1367. DOI: 10.1002/ijc.23273.

Beranek, D. T. (1990): Distribution of methyl and ethyl adducts following alkylation with monofunctional alkylating agents. In: *Mutation research* 231 (1), S. 11–30.

Berger, N. A.; Berger, S. J. (1986): Metabolic consequences of DNA damage: the role of poly (ADP-ribose) polymerase as mediator of the suicide response. In: *Basic life sciences* 38, S. 357–363.

Bird, Adrian (2002): DNA methylation patterns and epigenetic memory. In: *Genes & development* 16 (1), S. 6–21. DOI: 10.1101/gad.947102.

Bissahoyo, Anika; Pearsall, R. Scott; Hanlon, Kathleen; Amann, Vicky; Hicks, Donna; Godfrey, Virginia L.; Threadgill, David W. (2005): Azoxymethane is a genetic background-dependent colorectal tumor initiator and promoter in mice: effects of dose, route, and diet. In: *Toxicological sciences : an official journal of the Society of Toxicology* 88 (2), S. 340–345. DOI: 10.1093/toxsci/kfi313.

Blasco, Maria A. (2005): Telomeres and human disease: ageing, cancer and beyond. In: *Nature reviews. Genetics* 6 (8), S. 611–622. DOI: 10.1038/nrg1656.

Boehler, Christian; Gauthier, Laurent R.; Mortusewicz, Oliver; Biard, Denis S.; Saliou, Jean-Michel; Bresson, Anne; Sanglier-Cianferani, Sarah; Smith, Susan; Schreiber, Valerie; Boussin,

Francois; Dantzer, Francoise (2011): Poly(ADP-ribose) polymerase 3 (PARP3), a newcomer in cellular response to DNA damage and mitotic progression. In: *Proceedings of the National Academy of Sciences of the United States of America* 108 (7), S. 2783–2788. DOI: 10.1073/pnas.1016574108.

Boucher, M. J.; Morisset, J.; Vachon, P. H.; Reed, J. C.; Laine, J.; Rivard, N. (2000): MEK/ERK signaling pathway regulates the expression of Bcl-2, Bcl-X(L), and Mcl-1 and promotes survival of human pancreatic cancer cells. In: *Journal of cellular biochemistry* 79 (3), S. 355–369.

Branzei, Dana; Foiani, Marco (2005): The DNA damage response during DNA replication. In: *Current opinion in cell biology* 17 (6), S. 568–575. DOI: 10.1016/j.ceb.2005.09.003.

Branzei, Dana; Foiani, Marco (2007): Interplay of replication checkpoints and repair proteins at stalled replication forks. In: *DNA repair* 6 (7), S. 994–1003. DOI: 10.1016/j.dnarep.2007.02.018.

Braun, Carie Ann; Anderson, Cindy Miller (2007): Pathophysiology. Functional alterations in human health. Philadelphia: Lippincott Williams & Wilkins.

Bryant, Helen E.; Petermann, Eva; Schultz, Niklas; Jemth, Ann-Sofie; Loseva, Olga; Issaeva, Natalia; Johansson, Fredrik; Fernandez, Serena; McGlynn, Peter; Helleday, Thomas (2009): PARP is activated at stalled forks to mediate Mre11-dependent replication restart and recombination. In: *The EMBO journal* 28 (17), S. 2601–2615. DOI: 10.1038/emboj.2009.206.

Bryant, Helen E.; Schultz, Niklas; Thomas, Huw D.; Parker, Kayan M.; Flower, Dan; Lopez, Elena; Kyle, Suzanne; Meuth, Mark; Curtin, Nicola J.; Helleday, Thomas (2005): Specific killing of BRCA2-deficient tumours with inhibitors of poly(ADP-ribose) polymerase. In: *Nature* 434 (7035), S. 913–917. DOI: 10.1038/nature03443.

Bugni, J. M.; Meira, L. B.; Samson, L. D. (2009): Alkylation-induced colon tumorigenesis in mice deficient in the Mgmt and Msh6 proteins. In: *Oncogene* 28 (5), S. 734–741. DOI: 10.1038/onc.2008.426.

Burkart, V.; Wang, Z. Q.; Radons, J.; Heller, B.; Herceg, Z.; Stingl, L.; Wagner, E. F.; Kolb, H. (1999): Mice lacking the poly(ADP-ribose) polymerase gene are resistant to pancreatic beta-cell destruction and diabetes development induced by streptozocin. In: *Nature medicine* 5 (3), S. 314–319. DOI: 10.1038/6535.

Bürkle, Alexander (2005): Poly(ADP-ribose). The most elaborate metabolite of NAD+. In: *The FEBS journal* 272 (18), S. 4576–4589. DOI: 10.1111/j.1742-4658.2005.04864.x.

Caldecott, K. W.; Aoufouchi, S.; Johnson, P.; Shall, S. (1996): XRCC1 polypeptide interacts with DNA polymerase beta and possibly poly (ADP-ribose) polymerase, and DNA ligase III is a novel molecular 'nick-sensor' in vitro. In: *Nucleic acids research* 24 (22), S. 4387–4394.

Calvo, Jennifer A.; Meira, Lisiane B.; Lee, Chun-Yue I.; Moroski-Erkul, Catherine A.; Abolhassani, Nona; Taghizadeh, Koli; Eichinger, Lindsey W.; Muthupalani, Sureshkumar; Nordstrand, Line M.; Klungland, Arne; Samson, Leona D. (2012): DNA repair is indispensable for survival after acute inflammation. In: *The Journal of clinical investigation* 122 (7), S. 2680–2689. DOI: 10.1172/JCI63338.

Canudas, Silvia; Houghtaling, Benjamin R.; Kim, Ju Youn; Dynek, Jasmin N.; Chang, William G.; Smith, Susan (2007): Protein requirements for sister telomere association in human cells. In: *The EMBO journal* 26 (23), S. 4867–4878. DOI: 10.1038/sj.emboj.7601903.

Capoa, A. de; Febbo, F. R.; Giovannelli, F.; Niveleau, A.; Zardo, G.; Marenzi, S.; Caiafa, P. (1999): Reduced levels of poly(ADP-ribosyl)ation result in chromatin compaction and hypermethylation as shown by cell-by-cell computer-assisted quantitative analysis. In: *FASEB journal : official publication of the Federation of American Societies for Experimental Biology* 13 (1), S. 89–93.

Carson, Dennis A.; Carrera, Carlos J.; Wasson, D.Bruce; Yamanaka, Hisashi (1988): Programmed cell death and adenine deoxynucleotide metabolism in human lymphocytes. In: *Advances in Enzyme Regulation* 27, S. 395–404. DOI: 10.1016/0065-2571(88)90028-3.

Casas-Selves, Matias; Kim, Jihye; Zhang, Zhiyong; Helfrich, Barbara A.; Gao, Dexiang; Porter, Christopher C.; Scarborough, Hannah A.; Bunn, Paul A., JR; Chan, Daniel C.; Tan, Aik Choon; DeGregori, James (2012): Tankyrase and the canonical Wnt pathway protect lung cancer cells from EGFR inhibition. In: *Cancer research* 72 (16), S. 4154–4164. DOI: 10.1158/0008-5472.CAN-11-2848.

Celona, Barbara; Weiner, Assaf; Di Felice, Francesca; Mancuso, Francesco M.; Cesarini, Elisa; Rossi, Riccardo L.; Gregory, Lorna; Baban, Dilair; Rossetti, Grazisa; Grianti, Paolo; Pagani, Massimiliano; Bonaldi, Tiziana; Ragoussis, Jiannis; Friedman, Nir; Camilloni, Giorgio; Bianchi, Marco E.; Agresti, Alessandra (2011): Substantial histone reduction modulates genomewide nucleosomal occupancy and global transcriptional output. In: *PLoS biology* 9 (6), e1001086. DOI: 10.1371/journal.pbio.1001086.

Chambon, P.; Weill, J. D.; Mandel, P. (1963): Nicotinamide mononucleotide activation of a new DNA-dependent polyadenylic acid synthesizing nuclear enzyme. In: *Biochemical and Biophysical Research Communications* 11 (1), S. 39–43. DOI: 10.1016/0006-291X(63)90024-X.

Chan, Andrew T.; Giovannucci, Edward L.; Meyerhardt, Jeffrey A.; Schernhammer, Eva S.; Wu, Kana; Fuchs, Charles S. (2008): Aspirin dose and duration of use and risk of colorectal cancer in men. In: *Gastroenterology* 134 (1), S. 21–28. DOI: 10.1053/j.gastro.2007.09.035.

Chan, Andrew T.; Ogino, Shuji; Fuchs, Charles S. (2009): Aspirin use and survival after diagnosis of colorectal cancer. In: *JAMA* 302 (6), S. 649–658. DOI: 10.1001/jama.2009.1112.

Chan, Annie On-On; Broaddus, Russell R.; Houlihan, Patrick S.; Issa, Jean-Pierre J.; Hamilton, Stanley R.; Rashid, Asif (2002): CpG Island Methylation in Aberrant Crypt Foci of the Colorectum. In: *The American Journal of Pathology* 160 (5), S. 1823–1830. DOI: 10.1016/S0002-9440(10)61128-5.

Chang, Paul; Coughlin, Margaret; Mitchison, Timothy J. (2005): Tankyrase-1 polymerization of poly(ADP-ribose) is required for spindle structure and function. In: *Nature cell biology* 7 (11), S. 1133–1139. DOI: 10.1038/ncb1322.

Chen, Jiezhong; Huang, Xu-Feng (2009): The signal pathways in azoxymethane-induced colon cancer and preventive implications. In: *Cancer biology & therapy* 8 (14), S. 1313–1317.

Chen, N.; Nomura, M.; She, Q. B.; Ma, W. Y.; Bode, A. M.; Wang, L.; Flavell, R. A.; Dong, Z. (2001): Suppression of skin tumorigenesis in c-Jun NH(2)-terminal kinase-2-deficient mice. In: *Cancer research* 61 (10), S. 3908–3912.

Chevanne, Marta; Calia, Corinne; Zampieri, Michele; Cecchinelli, Barbara; Caldini, Riccardo; Monti, Daniela; Bucci, Laura; Franceschi, Claudio; Caiafa, Paola (2007): Oxidative DNA damage repair and parp 1 and parp 2 expression in Epstein-Barr virus-immortalized B lymphocyte cells from young subjects, old subjects, and centenarians. In: *Rejuvenation research* 10 (2), S. 191–204. DOI: 10.1089/rej.2006.0514.

Chiang, Y. Jeffrey; Hsiao, Susan J.; Yver, Dena; Cushman, Samuel W.; Tessarollo, Lino; Smith, Susan; Hodes, Richard J. (2008): Tankyrase 1 and tankyrase 2 are essential but redundant for mouse embryonic development. In: *PloS one* 3 (7), S. e2639. DOI: 10.1371/journal.pone.0002639.

Chiarugi, Alberto; Dolle, Christian; Felici, Roberta; Ziegler, Mathias (2012): The NAD metabolome--a key determinant of cancer cell biology. In: *Nature reviews. Cancer* 12 (11), S. 741–752. DOI: 10.1038/nrc3340.

Chichlowski, Maciej; Westwood, Greg S.; Abraham, Soman N.; Hale, Laura P. (2010): Role of mast cells in inflammatory bowel disease and inflammation-associated colorectal neoplasia in IL-10-deficient mice. In: *PloS one* 5 (8), e12220. DOI: 10.1371/journal.pone.0012220.

Chiu, Ling-Ya; Ho, Feng-Ming; Shiah, Shine-Gwo; Chang, Yung; Lin, Wan-Wan (2011): Oxidative stress initiates DNA damager MNNG-induced poly(ADP-ribose)polymerase-1-dependent parthanatos cell death. In: *Biochemical Pharmacology* 81 (3), S. 459–470. DOI: 10.1016/j.bcp.2010.10.016.

Choi, Jinkuk; Southworth, Lucinda K.; Sarin, Kavita Y.; Venteicher, Andrew S.; Ma, Wenxiu; Chang, Woody; Cheung, Peggie; Jun, Sohee; Artandi, Maja K.; Shah, Naman; Kim, Stuart K.; Artandi, Steven E. (2008): TERT promotes epithelial proliferation through transcriptional control of a Myc- and Wnt-related developmental program. In: *PLoS genetics* 4 (1), e10. DOI: 10.1371/journal.pgen.0040010.

Christmann, Markus; Kaina, Bernd (2013): Transcriptional regulation of human DNA repair genes following genotoxic stress: trigger mechanisms, inducible responses and genotoxic adaptation. In: *Nucleic acids research* 41 (18), S. 8403–8420. DOI: 10.1093/nar/gkt635.

Christmann, Markus; Tomicic, Maja T.; Roos, Wynand P.; Kaina, Bernd (2003): Mechanisms of human DNA repair: an update. In: *Toxicology* 193 (1-2), S. 3–34.

Chulada, P. C.; Thompson, M. B.; Mahler, J. F.; Doyle, C. M.; Gaul, B. W.; Lee, C.; Tiano, H. F.; Morham, S. G.; Smithies, O.; Langenbach, R. (2000): Genetic disruption of Ptgs-1, as well as Ptgs-2, reduces intestinal tumorigenesis in Min mice. In: *Cancer research* 60 (17), S. 4705–4708.

Clevers, Hans (2006): Wnt/beta-catenin signaling in development and disease. In: *Cell* 127 (3), S. 469–480. DOI: 10.1016/j.cell.2006.10.018.

Confer, Nils F.; Kumari, Sunitha R.; Alvarez-Gonzalez, Rafael (2004): Biochemical association of poly(ADP-ribose) polymerase-1 and its apoptotic peptide fragments with DNA polymerase beta. In: *Chemistry & biodiversity* 1 (10), S. 1476–1486. DOI: 10.1002/cbdv.200490108.

Cooper, Geoffrey M. (1992): Elements of human cancer. Boston: Jones and Bartlett Publishers.

Cooper, H. S.; Murthy, S.; Kido, K.; Yoshitake, H.; Flanigan, A. (2000): Dysplasia and cancer in the dextran sulfate sodium mouse colitis model. Relevance to colitis-associated neoplasia in the human: a study of histopathology, B-catenin and p53 expression and the role of inflammation. In: *Carcinogenesis* 21 (4), S. 757–768.

Coquelle, Nicolas; Glover, J. N. Mark (2012): PARP pairs up to PARsylate. In: *Nature structural & molecular biology* 19 (7), S. 660–661. DOI: 10.1038/nsmb.2306.

Cottet, F.; Blanche, H.; Verasdonck, P.; Le Gall, I.; Schachter, F.; Burkle, A.; Muiras, M. L. (2000): New polymorphisms in the human poly(ADP-ribose) polymerase-1 coding sequence: lack of association with longevity or with increased cellular poly(ADP-ribosyl)ation capacity. In: *Journal of molecular medicine (Berlin, Germany)* 78 (8), S. 431–440.

Cunningham, David; Atkin, Wendy; Lenz, Heinz-Josef; Lynch, Henry T.; Minsky, Bruce; Nordlinger, Bernard; Starling, Naureen (2010): Colorectal cancer. In: *Lancet (London, England)* 375 (9719), S. 1030–1047. DOI: 10.1016/S0140-6736(10)60353-4.

Cunningham, J. M.; Christensen, E. R.; Tester, D. J.; Kim, C. Y.; Roche, P. C.; Burgart, L. J.; Thibodeau, S. N. (1998): Hypermethylation of the hMLH1 promoter in colon cancer with microsatellite instability. In: *Cancer research* 58 (15), S. 3455–3460.

D'Amours, D.; Desnoyers, S.; D'Silva, I.; Poirier, G. G. (1999): Poly(ADP-ribosyl)ation reactions in the regulation of nuclear functions. In: *The Biochemical journal* 342 (Pt 2), S. 249–268.

Daniels, Douglas S.; Woo, Tammy T.; Luu, Kieu X.; Noll, David M.; Clarke, Neil D.; Pegg, Anthony E.; Tainer, John A. (2004): DNA binding and nucleotide flipping by the human DNA repair protein AGT. In: *Nature structural & molecular biology* 11 (8), S. 714–720. DOI: 10.1038/nsmb791.

Dantzer, F.; Schreiber, V.; Niedergang, C.; Trucco, C.; Flatter, E.; La Rubia, G. de; Oliver, J.; Rolli, V.; Menissier-de Murcia, J.; Murcia, G. de (1999): Involvement of poly(ADP-ribose) polymerase in base excision repair. In: *Biochimie* 81 (1-2), S. 69–75.

David, Karen Kate; Andrabi, Shaida Ahmad; Dawson, Ted Murray; Dawson, Valina Lynn (2009): Parthanatos, a messenger of death. In: *Frontiers in bioscience (Landmark edition)* 14, S. 1116–1128.

Davidson, David; Wang, Yunzhe; Aloyz, Raquel; Panasci, Lawrence (2013): The PARP inhibitor ABT-888 synergizes irinotecan treatment of colon cancer cell lines. In: *Investigational new drugs* 31 (2), S. 461–468. DOI: 10.1007/s10637-012-9886-7.

Delker, D. A.; McKnight, S. J. 3rd; Rosenberg, D. W. (1998): The role of alcohol dehydrogenase in the metabolism of the colon carcinogen methylazoxymethanol. In: *Toxicological sciences : an official journal of the Society of Toxicology* 45 (1), S. 66–71. DOI: 10.1006/toxs.1998.2499.

Deschner, E. E.; Long, F. C. (1977): Colonic neoplasms in mice produced with six injections of 1,2-dimethylhydrazine. In: *Oncology* 34 (6), S. 255–257.

Di d'Adda Fagagna, F.; Hande, M. P.; Tong, W. M.; Lansdorp, P. M.; Wang, Z. Q.; Jackson, S. P. (1999): Functions of poly(ADP-ribose) polymerase in controlling telomere length and chromosomal stability. In: *Nature genetics* 23 (1), S. 76–80. DOI: 10.1038/12680.

Ditsworth, Dara; Zong, Wei-Xing; Thompson, Craig B. (2007): Activation of poly(ADP)-ribose polymerase (PARP-1) induces release of the pro-inflammatory mediator HMGB1 from the nucleus. In: *The Journal of biological chemistry* 282 (24), S. 17845–17854. DOI: 10.1074/jbc.M701465200.

Doly, J.; Mandel, P. (1967): Demonstration of the biosynthesis in vivo of a compound polymer, polyadenosine diphosphoribose in the nucleus of the liver of chickens. In: *Comptes rendus hebdomadaires des seances de l'Academie des sciences. Serie D: Sciences naturelles* 264 (23), S. 2687–2690.

Drablos, Finn; Feyzi, Emadoldin; Aas, Per Arne; Vaagbo, Cathrine B.; Kavli, Bodil; Bratlie, Marit S.; Pena-Diaz, Javier; Otterlei, Marit; Slupphaug, Geir; Krokan, Hans E. (2004): Alkylation damage in DNA and RNA--repair mechanisms and medical significance. In: *DNA repair* 3 (11), S. 1389–1407. DOI: 10.1016/j.dnarep.2004.05.004.

DuBois, R. N.; Abramson, S. B.; Crofford, L.; Gupta, R. A.; Simon, L. S.; Van De Putte, L B; Lipsky, P. E. (1998): Cyclooxygenase in biology and disease. In: *FASEB journal : official publication of the Federation of American Societies for Experimental Biology* 12 (12), S. 1063–1073.

DUKES, C. E. (1959): The etiology of cancer of the colon and rectum. In: *Diseases of the colon and rectum* 2 (1), S. 27–32.

Duncan, Tod; Trewick, Sarah C.; Koivisto, Pertti; Bates, Paul A.; Lindahl, Tomas; Sedgwick, Barbara (2002): Reversal of DNA alkylation damage by two human dioxygenases. In: *Proceedings of the National Academy of Sciences of the United States of America* 99 (26), S. 16660–16665. DOI: 10.1073/pnas.262589799.

Eaden, J. A.; Abrams, K. R.; Mayberry, J. F. (2001): The risk of colorectal cancer in ulcerative colitis: a meta-analysis. In: *Gut* 48 (4), S. 526–535.

Eberhart, C. E.; Coffey, R. J.; Radhika, A.; Giardiello, F. M.; Ferrenbach, S.; DuBois, R. N. (1994): Up-regulation of cyclooxygenase 2 gene expression in human colorectal adenomas and adenocarcinomas. In: *Gastroenterology* 107 (4), S. 1183–1188.

Ebrahimkhani, Mohammad R.; Daneshmand, Ali; Mazumder, Aprotim; Allocca, Mariacarmela; Calvo, Jennifer A.; Abolhassani, Nona; Jhun, Iny; Muthupalani, Sureshkumar; Ayata, Cenk; Samson, Leona D. (2014): Aag-initiated base excision repair promotes ischemia reperfusion injury in liver, brain, and kidney. In: *Proceedings of the National Academy of Sciences of the United States of America* 111 (45), S. 86. DOI: 10.1073/pnas.1413582111.

Engle, S. J.; Hoying, J. B.; Boivin, G. P.; Ormsby, I.; Gartside, P. S.; Doetschman, T. (1999): Transforming growth factor beta1 suppresses nonmetastatic colon cancer at an early stage of tumorigenesis. In: *Cancer research* 59 (14), S. 3379–3386.

Espejel, Silvia; Klatt, Peter; Menissier-de Murcia, Josiane; Martin-Caballero, Juan; Flores, Juana M.; Taccioli, Guillermo; Murcia, Gilbert de; Blasco, Maria A. (2004): Impact of telomerase ablation on organismal viability, aging, and tumorigenesis in mice lacking the DNA repair proteins PARP-1, Ku86, or DNA-PKcs. In: *The Journal of cell biology* 167 (4), S. 627–638. DOI: 10.1083/jcb.200407178.

Esteller, M.; Toyota, M.; Sanchez-Cespedes, M.; Capella, G.; Peinado, M. A.; Watkins, D. N.; Issa, J. P.; Sidransky, D.; Baylin, S. B.; Herman, J. G. (2000): Inactivation of the DNA repair gene O6-methylguanine-DNA methyltransferase by promoter hypermethylation is associated with G to A mutations in K-ras in colorectal tumorigenesis. In: *Cancer research* 60 (9), S. 2368–2371.

Ethier, Chantal; Labelle, Yves; POIRIER, Guy G. (2007): PARP-1-induced cell death through inhibition of the MEK/ERK pathway in MNNG-treated HeLa cells. In: *Apoptosis : an international journal on programmed cell death* 12 (11), S. 2037–2049. DOI: 10.1007/s10495-007-0127-z.

Ethier, Chantal; Tardif, Maxime; Arul, Laura; POIRIER, Guy G. (2012): PARP-1 modulation of mTOR signaling in response to a DNA alkylating agent. In: *PloS one* 7 (10), e47978. DOI: 10.1371/journal.pone.0047978.

Eustermann, Sebastian; Brockmann, Christoph; Mehrotra, Pawan Vinod; Yang, Ji-Chun; Loakes, David; West, Stephen C.; Ahel, Ivan; Neuhaus, David (2010): Solution structures of the two PBZ domains from human APLF and their interaction with poly(ADP-ribose). In: *Nature structural & molecular biology* 17 (2), S. 241–243. DOI: 10.1038/nsmb.1747.

Fahrer, Jörg; Frisch, Janina; Nagel, Georg; Kraus, Alexander; Dörsam, Bastian; Thomas, Adam D.; Reißig, Sonja; Waisman, Ari; Kaina, Bernd (2015): DNA repair by MGMT, but not AAG, causes a threshold in alkylation-induced colorectal carcinogenesis. In: *Carcinogenesis* 36 (10), S. 1235–1244. DOI: 10.1093/carcin/bgv114.

Fahrer, Jörg; Kaina, Bernd (2013): O6-methylguanine-DNA methyltransferase in the defense against N-nitroso compounds and colorectal cancer. In: *Carcinogenesis* 34 (11), S. 2435–2442. DOI: 10.1093/carcin/bgt275.

Fahrer, Jörg; Kaina, Bernd (2016): Impact of DNA repair on the dose-response of colorectal cancer formation induced by dietary carcinogens. In: *Food and chemical toxicology : an international journal published for the British Industrial Biological Research Association. DOI:* 10.1016/j.fct.2016.09.029.

Fahrer, Jörg; Kranaster, Ramon; Altmeyer, Matthias; Marx, Andreas; Burkle, Alexander (2007): Quantitative analysis of the binding affinity of poly(ADP-ribose) to specific binding proteins as a function of chain length. In: *Nucleic acids research* 35 (21), e143. DOI: 10.1093/nar/gkm944.

Fahrer, Jörg; Popp, Oliver; Malanga, Maria; Beneke, Sascha; Markovitz, David M.; Ferrando-May, Elisa; Burkle, Alexander; Kappes, Ferdinand (2010): High-affinity interaction of poly(ADP-ribose)

and the human DEK oncoprotein depends upon chain length. In: *Biochemistry* 49 (33), S. 7119–7130. DOI: 10.1021/bi1004365.

Fearon, E. R.; Vogelstein, B. (1990): A genetic model for colorectal tumorigenesis. In: *Cell* 61 (5), S. 759–767.

Fearon, Eric R. (2011): Molecular genetics of colorectal cancer. In: *Annual review of pathology* 6, S. 479–507. DOI: 10.1146/annurev-pathol-011110-130235.

Feinberg, A.; Zedeck, M. S. (1980): Production of a highly reactive alkylating agent from the organospecific carcinogen methylazoxymethanol by alcohol dehydrogenase. In: *Cancer research* 40 (12), S. 4446–4450.

Ferlay, Jacques; Soerjomataram, Isabelle; Dikshit, Rajesh; Eser, Sultan; Mathers, Colin; Rebelo, Marise; Parkin, Donald Maxwell; Forman, David; Bray, Freddie (2015): Cancer incidence and mortality worldwide: sources, methods and major patterns in GLOBOCAN 2012. In: *International journal of cancer* 136 (5), E359-86. DOI: 10.1002/ijc.29210.

Fiala, E. S. (1977): Investigations into the metabolism and mode of action of the colon carcinogens 1,2-dimethylhydrazine and azoxymethane. In: *Cancer* 40 (5 Suppl), S. 2436–2445.

Fiala, E. S.; Caswell, N.; Sohn, O. S.; Felder, M. R.; McCoy, G. D.; Weisburger, J. H. (1984): Non-alcohol dehydrogenase-mediated metabolism of methylazoxymethanol in the deer mouse, Peromyscus maniculatus. In: *Cancer research* 44 (7), S. 2885–2891.

Fitzgerald, D. C.; Meade, K. G.; McEvoy, A. N.; Lillis, L.; Murphy, E. P.; MacHugh, D. E.; Baird, A. W. (2007): Tumour necrosis factor-alpha (TNF-alpha) increases nuclear factor kappaB (NFkappaB) activity in and interleukin-8 (IL-8) release from bovine mammary epithelial cells. In: *Veterinary immunology and immunopathology* 116 (1-2), S. 59–68. DOI: 10.1016/j.vetimm.2006.12.008.

Flohr, Claudia; Bürkle, Alexander; Radicella, J. Pablo; Epe, Bernd (2003): Poly(ADP-ribosyl)ation accelerates DNA repair in a pathway dependent on Cockayne syndrome B protein. In: *Nucleic acids research* 31 (18), S. 5332–5337.

Flossmann, Enrico; Rothwell, Peter M. (2007): Effect of aspirin on long-term risk of colorectal cancer. Consistent evidence from randomised and observational studies. In: *The Lancet* 369 (9573), S. 1603–1613. DOI: 10.1016/S0140-6736(07)60747-8.

Formentini, Laura; Macchiarulo, Antonio; Cipriani, Giulia; Camaioni, Emidio; Rapizzi, Elena; Pellicciari, Roberto; Moroni, Flavio; Chiarugi, Alberto (2009): Poly(ADP-ribose) catabolism triggers AMP-dependent mitochondrial energy failure. In: *The Journal of biological chemistry* 284 (26), S. 17668–17676. DOI: 10.1074/jbc.M109.002931.

Frederick, Joshua P.; Liberati, Nicole T.; Waddell, David S.; Shi, Yigong; Wang, Xiao-Fan (2004): Transforming growth factor beta-mediated transcriptional repression of c-myc is dependent on direct binding of Smad3 to a novel repressive Smad binding element. In: *Molecular and cellular biology* 24 (6), S. 2546–2559.

Freund, Adam; Orjalo, Arturo V.; Desprez, Pierre-Yves; Campisi, Judith (2010): Inflammatory networks during cellular senescence: causes and consequences. In: *Trends in molecular medicine* 16 (5), S. 238–246. DOI: 10.1016/j.molmed.2010.03.003.

Fried, Michael; Manns, Michael P.; Rogler, Gerhard; Luescher, Thomas; Steffel, Jan (Hg.) (2013): Magen-Darm-Trakt. Berlin: Springer (Springer-Lehrbuch). Online verfügbar unter http://dx.doi.org/10.1007/978-3-642-29434-1.

Fu, Dragony; Calvo, Jennifer A.; Samson, Leona D. (2012): Balancing repair and tolerance of DNA damage caused by alkylating agents. In: *Nature reviews. Cancer* 12 (2), S. 104–120. DOI: 10.1038/nrc3185.

Gagne, Jean-Philippe; Isabelle, Maxim; Lo, Ken Sin; Bourassa, Sylvie; Hendzel, Michael J.; Dawson, Valina L.; Dawson, Ted M.; POIRIER, Guy G. (2008): Proteome-wide identification of poly(ADP-ribose) binding proteins and poly(ADP-ribose)-associated protein complexes. In: *Nucleic acids research* 36 (22), S. 6959–6976. DOI: 10.1093/nar/gkn771.

Gamble, Matthew J.; Fisher, Robert P. (2007): SET and PARP1 remove DEK from chromatin to permit access by the transcription machinery. In: *Nature structural & molecular biology* 14 (6), S. 548–555. DOI: 10.1038/nsmb1248.

Garcia, Samuel; Bodano, Ana; Gonzalez, Antonio; Forteza, Jeronimo; Gomez-Reino, Juan J.; Conde, Carmen (2006): Partial protection against collagen antibody-induced arthritis in PARP-1 deficient mice. In: *Arthritis research & therapy* 8 (1), R14. DOI: 10.1186/ar1865.

Garinis, George A.; van der Horst, Gijsbertus T J; Vijg, Jan; Hoeijmakers, Jan H. J. (2008): DNA damage and ageing: new-age ideas for an age-old problem. In: *Nature cell biology* 10 (11), S. 1241–1247. DOI: 10.1038/ncb1108-1241.

Gerken, Thomas; Girard, Christophe A.; Tung, Yi-Chun Loraine; Webby, Celia J.; Saudek, Vladimir; Hewitson, Kirsty S.; Yeo, Giles S. H.; McDonough, Michael A.; Cunliffe, Sharon; McNeill, Luke A.; Galvanovskis, Juris; Rorsman, Patrik; Robins, Peter; Prieur, Xavier; Coll, Anthony P.; Ma, Marcella; Jovanovic, Zorica; Farooqi, I. Sadaf; Sedgwick, Barbara; Barroso, Ines; Lindahl, Tomas; Ponting, Chris P.; Ashcroft, Frances M.; O'Rahilly, Stephen; Schofield, Christopher J. (2007): The obesity-associated FTO gene encodes a 2-oxoglutarate-dependent nucleic acid demethylase. In: *Science (New York, N.Y.)* 318 (5855), S. 1469–1472. DOI: 10.1126/science.1151710.

Germain, M.; Affar, E. B.; D'Amours, D.; Dixit, V. M.; Salvesen, G. S.; Poirier, G. G. (1999): Cleavage of automodified poly(ADP-ribose) polymerase during apoptosis. Evidence for involvement of caspase-7. In: *The Journal of biological chemistry* 274 (40), S. 28379–28384.

Gerson, S. L.; Trey, J. E.; Miller, K.; Berger, N. A. (1986): Comparison of O6-alkylguanine-DNA alkyltransferase activity based on cellular DNA content in human, rat and mouse tissues. In: *Carcinogenesis* 7 (5), S. 745–749.

Giavara, Sabrina; Kosmidou, Effie; Hande, M. Prakash; Bianchi, Marco E.; Morgan, Alan; Di d'Adda Fagagna, Fabrizio; Jackson, Stephen P. (2005): Yeast Nhp6A/B and mammalian Hmgb1

facilitate the maintenance of genome stability. In: *Current biology : CB* 15 (1), S. 68–72. DOI: 10.1016/j.cub.2004.12.065.

Gibson, Bryan A.; Kraus, W. Lee (2012): New insights into the molecular and cellular functions of poly(ADP-ribose) and PARPs. In: *Nature reviews. Molecular cell biology* 13 (7), S. 411–424. DOI: 10.1038/nrm3376.

Giles, Rachel H.; van Es, Johan H.; Clevers, Hans (2003): Caught up in a Wnt storm: Wnt signaling in cancer. In: *Biochimica et biophysica acta* 1653 (1), S. 1–24.

Gilmore, Thomas; Gapuzan, Maria-Emily; Kalaitzidis, Demetrios; Starczynowski, Daniel (2002): Rel/NF-κB/IκB signal transduction in the generation and treatment of human cancer. In: *Cancer letters* 181 (1), S. 1–9. DOI: 10.1016/S0304-3835(01)00795-9.

Gilsing, Anne M. J.; Fransen, Fiona; Kok, Theo M. de; Goldbohm, Alexandra R.; Schouten, Leo J.; Bruine, Adriaan P. de; van Engeland, Manon; van den Brandt, Piet A; de Goeij, Anton F P M; Weijenberg, Matty P. (2013): Dietary heme iron and the risk of colorectal cancer with specific mutations in KRAS and APC. In: *Carcinogenesis* 34 (12), S. 2757–2766. DOI: 10.1093/carcin/bgt290.

Giovannucci, Edward (2002): Modifiable risk factors for colon cancer. In: *Gastroenterology clinics of North America* 31 (4), S. 925–943.

Glassner, B. J.; Weeda, G.; Allan, J. M.; Broekhof, J. L.; Carls, N. H.; Donker, I.; Engelward, B. P.; Hampson, R. J.; Hersmus, R.; Hickman, M. J.; Roth, R. B.; Warren, H. B.; Wu, M. M.; Hoeijmakers, J. H.; Samson, L. D. (1999): DNA repair methyltransferase (Mgmt) knockout mice are sensitive to the lethal effects of chemotherapeutic alkylating agents. In: *Mutagenesis* 14 (3), S. 339–347.

Gomez, Marla; Wu, Jun; Schreiber, Valerie; Dunlap, John; Dantzer, Francoise; Wang, Yisong; Liu, Yie (2006): PARP1 Is a TRF2-associated poly(ADP-ribose)polymerase and protects eroded telomeres. In: *Molecular biology of the cell* 17 (4), S. 1686–1696. DOI: 10.1091/mbc.E05-07-0672.

Gomez-Lazaro, M.; Fernandez-Gomez, F. J.; Jordan, J. (2004): p53: twenty five years understanding the mechanism of genome protection. In: *Journal of physiology and biochemistry* 60 (4), S. 287–307.

Gonzalez, Carlos A. (2006): The European Prospective Investigation into Cancer and Nutrition (EPIC). In: *PHN* 9 (1a). DOI: 10.1079/PHN2005934.

Goran tek (2014): Layers of the Gastrointestinal Tract. Online verfügbar unter https://commons.wikimedia.org/w/index.php?curid=31413106, zuletzt aktualisiert am 02.03.2014, zuletzt geprüft am 20.10.2016.

Gordon, Kelly J.; Blobe, Gerard C. (2008): Role of transforming growth factor-beta superfamily signaling pathways in human disease. In: *Biochimica et biophysica acta* 1782 (4), S. 197–228. DOI: 10.1016/j.bbadis.2008.01.006.

Grafstrom, R. C.; Pegg, A. E.; Trump, B. F.; Harris, C. C. (1984): O6-alkylguanine-DNA alkyltransferase activity in normal human tissues and cells. In: *Cancer research* 44 (7), S. 2855–2857.

Grasso, P.; Creasey, M. (1969): Carcinoma of the colon in a rat. In: *European Journal of Cancer (1965)* 5 (4), S. 415–419. DOI: 10.1016/0014-2964(69)90054-1.

Green, Douglas R.; Ferguson, Thomas; Zitvogel, Laurence; Kroemer, Guido (2009): Immunogenic and tolerogenic cell death. In: *Nature reviews. Immunology* 9 (5), S. 353–363. DOI: 10.1038/nri2545.

Greten, Florian R.; Eckmann, Lars; Greten, Tim F.; Park, Jin Mo; Li, Zhi-Wei; Egan, Laurence J.; Kagnoff, Martin F.; Karin, Michael (2004): IKKbeta links inflammation and tumorigenesis in a mouse model of colitis-associated cancer. In: *Cell* 118 (3), S. 285–296. DOI: 10.1016/j.cell.2004.07.013.

Guastafierro, Tiziana; Cecchinelli, Barbara; Zampieri, Michele; Reale, Anna; Riggio, Giuseppe; Sthandier, Olga; Zupi, Gabriella; Calabrese, Lilia; Caiafa, Paola (2008): CCCTC-binding factor activates PARP-1 affecting DNA methylation machinery. In: *The Journal of biological chemistry* 283 (32), S. 21873–21880. DOI: 10.1074/jbc.M801170200.

Guengerich, F. Peter; Fang, Qingming; Liu, Liping; Hachey, David L.; Pegg, Anthony E. (2003): O6-alkylguanine-DNA alkyltransferase: low pKa and high reactivity of cysteine 145. In: *Biochemistry* 42 (37), S. 10965–10970. DOI: 10.1021/bi034937z.

Ha, H. C.; Snyder, S. H. (1999): Poly(ADP-ribose) polymerase is a mediator of necrotic cell death by ATP depletion. In: *Proceedings of the National Academy of Sciences of the United States of America* 96 (24), S. 13978–13982.

Haddad, M.; Rhinn, H.; Bloquel, C.; Coqueran, B.; Szabo, C.; Plotkine, M.; Scherman, D.; Margaill, I. (2006): Anti-inflammatory effects of PJ34, a poly(ADP-ribose) polymerase inhibitor, in transient focal cerebral ischemia in mice. In: *British journal of pharmacology* 149 (1), S. 23–30. DOI: 10.1038/sj.bjp.0706837.

Haince, Jean-Francois; Kozlov, Sergei; Dawson, Valina L.; Dawson, Ted M.; Hendzel, Michael J.; Lavin, Martin F.; POIRIER, Guy G. (2007): Ataxia telangiectasia mutated (ATM) signaling network is modulated by a novel poly(ADP-ribose)-dependent pathway in the early response to DNA-damaging agents. In: *The Journal of biological chemistry* 282 (22), S. 16441–16453. DOI: 10.1074/jbc.M608406200.

Haince, Jean-Francois; McDonald, Darin; Rodrigue, Amelie; Dery, Ugo; Masson, Jean-Yves; Hendzel, Michael J.; POIRIER, Guy G. (2008): PARP1-dependent kinetics of recruitment of MRE11 and NBS1 proteins to multiple DNA damage sites. In: *The Journal of biological chemistry* 283 (2), S. 1197–1208. DOI: 10.1074/jbc.M706734200.

Hakme, Antoinette; Wong, Heng-Kuan; Dantzer, Francoise; Schreiber, Valerie (2008): The expanding field of poly(ADP-ribosyl)ation reactions. 'Protein Modifications: Beyond the Usual Suspects' Review Series. In: *EMBO reports* 9 (11), S. 1094–1100. DOI: 10.1038/embor.2008.191.

Hall, P. A.; Levison, D. A.; Woods, A. L.; Yu, C. C.; Kellock, D. B.; Watkins, J. A.; Barnes, D. M.; Gillett, C. E.; Camplejohn, R.; Dover, R. (1990): Proliferating cell nuclear antigen (PCNA) immunolocalization in paraffin sections: an index of cell proliferation with evidence of deregulated

expression in some neoplasms. In: *The Journal of pathology* 162 (4), S. 285–294. DOI: 10.1002/path.1711620403.

Hamilton, W.; Round, A.; Sharp, D.; Peters, T. J. (2005): Clinical features of colorectal cancer before diagnosis: a population-based case-control study. In: *British journal of cancer* 93 (4), S. 399–405. DOI: 10.1038/sj.bjc.6602714.

Hanahan, Douglas; Weinberg, Robert A. (2011): Hallmarks of cancer: the next generation. In: *Cell* 144 (5), S. 646–674. DOI: 10.1016/j.cell.2011.02.013.

Hargrave, Barbara Y.; Tiangco, David A.; Lattanzio, Frank A.; Beebe, Stephen J. (2003): Cocaine, not morphine, causes the generation of reactive oxygen species and activation of NF-kappaB in transiently cotransfected heart cells. In: *Cardiovascular toxicology* 3 (2), S. 141–151.

Harris, Helena Erlandsson; Andersson, Ulf; Pisetsky, David S. (2012): HMGB1: a multifunctional alarmin driving autoimmune and inflammatory disease. In: *Nature reviews. Rheumatology* 8 (4), S. 195–202. DOI: 10.1038/nrrheum.2011.222.

Hassa, P. O.; Covic, M.; Hasan, S.; Imhof, R.; Hottiger, M. O. (2001): The enzymatic and DNA binding activity of PARP-1 are not required for NF-kappa B coactivator function. In: *The Journal of biological chemistry* 276 (49), S. 45588–45597. DOI: 10.1074/jbc.M106528200.

Hassa, P. O.; Hottiger, M. O. (2002): The functional role of poly(ADP-ribose)polymerase 1 as novel coactivator of NF-kappaB in inflammatory disorders. In: *Cellular and molecular life sciences : CMLS* 59 (9), S. 1534–1553.

Hassa, Paul O.; Buerki, Christine; Lombardi, Cornelia; Imhof, Ralph; Hottiger, Michael O. (2003): Transcriptional coactivation of nuclear factor-kappaB-dependent gene expression by p300 is regulated by poly(ADP)-ribose polymerase-1. In: *The Journal of biological chemistry* 278 (46), S. 45145–45153. DOI: 10.1074/jbc.M307957200.

Hata, Kazunori; Andoh, Akira; Shimada, Mitsue; Fujino, Sanae; Bamba, Shigeki; Araki, Yoshio; Okuno, Takafumi; Fujiyama, Yoshihide; Bamba, Tadao (2002): IL-17 stimulates inflammatory responses via NF-kappaB and MAP kinase pathways in human colonic myofibroblasts. In: *American journal of physiology. Gastrointestinal and liver physiology* 282 (6), G1035-44. DOI: 10.1152/ajpgi.00494.2001.

Hayden, Matthew S.; Ghosh, Sankar (2008): Shared principles in NF-kappaB signaling. In: *Cell* 132 (3), S. 344–362. DOI: 10.1016/j.cell.2008.01.020.

He, T. C.; Sparks, A. B.; Rago, C.; Hermeking, H.; Zawel, L.; da Costa, L. T.; Morin, P. J.; Vogelstein, B.; Kinzler, K. W. (1998): Identification of c-MYC as a target of the APC pathway. In: *Science (New York, N.Y.)* 281 (5382), S. 1509–1512.

Hecht, S. S. (1999): DNA adduct formation from tobacco-specific N-nitrosamines. In: *Mutation research* 424 (1-2), S. 127–142.

Hegan, Denise Campisi; Lu, Yuhong; Stachelek, Gregory C.; Crosby, Meredith E.; Bindra, Ranjit S.; Glazer, Peter M. (2010): Inhibition of poly(ADP-ribose) polymerase down-regulates BRCA1 and

RAD51 in a pathway mediated by E2F4 and p130. In: *Proceedings of the National Academy of Sciences of the United States of America* 107 (5), S. 2201–2206. DOI: 10.1073/pnas.0904783107.

Helleday, Thomas (2011): The underlying mechanism for the PARP and BRCA synthetic lethality: clearing up the misunderstandings. In: *Molecular oncology* 5 (4), S. 387–393. DOI: 10.1016/j.molonc.2011.07.001.

Herfarth, K. K.; Brent, T. P.; Danam, R. P.; Remack, J. S.; Kodner, I. J.; Wells, S. A., JR; Goodfellow, P. J. (1999): A specific CpG methylation pattern of the MGMT promoter region associated with reduced MGMT expression in primary colorectal cancers. In: *Molecular carcinogenesis* 24 (2), S. 90–98.

Herron, Deborah C.; Shank, Ronald C. (1979): Quantitative high-pressure liquid chromatographic analysis of methylated purines in DNA of rats treated with chemical carcinogens. In: *Analytical Biochemistry* 100 (1), S. 58–63. DOI: 10.1016/0003-2697(79)90109-X.

Hoesel, Bastian; Schmid, Johannes A. (2013): The complexity of NF-kappaB signaling in inflammation and cancer. In: *Molecular cancer* 12, S. 86. DOI: 10.1186/1476-4598-12-86.

Hoffman, D.; Tao, Z.; Liu, H. (2008): Domain C of human PARP-1.

Hofseth, Lorne J.; Khan, Mohammed A.; Ambrose, Mark; Nikolayeva, Olga; Xu-Welliver, Meng; Kartalou, Maria; Hussain, S. Perwez; Roth, Richard B.; Zhou, Xiaoling; Mechanic, Leah E.; Zurer, Irit; Rotter, Varda; Samson, Leona D.; Harris, Curtis C. (2003): The adaptive imbalance in base excision-repair enzymes generates microsatellite instability in chronic inflammation. In: *The Journal of clinical investigation* 112 (12), S. 1887–1894. DOI: 10.1172/JCI19757.

Hori, O.; Brett, J.; Slattery, T.; Cao, R.; Zhang, J.; Chen, J. X.; Nagashima, M.; Lundh, E. R.; Vijay, S.; Nitecki, D.; Morser, J.; Stern, D.; Schmidt, A. M. (1995): The Receptor for Advanced Glycation End Products (RAGE) Is a Cellular Binding Site for Amphoterin. MEDIATION OF NEURITE OUTGROWTH AND CO-EXPRESSION OF RAGE AND AMPHOTERIN IN THE DEVELOPING NERVOUS SYSTEM. In: *Journal of Biological Chemistry* 270 (43), S. 25752–25761. DOI: 10.1074/jbc.270.43.25752.

Hottiger, M. O.; Altmeyer, M. (2009): Poly(ADP-ribose) polymerase 1 at the crossroad of metabolic stress and inflammation in aging.

Hottiger, Michael O.; Hassa, Paul O.; Luscher, Bernhard; Schuler, Herwig; Koch-Nolte, Friedrich (2010): Toward a unified nomenclature for mammalian ADP-ribosyltransferases. In: *Trends in biochemical sciences* 35 (4), S. 208–219. DOI: 10.1016/j.tibs.2009.12.003.

Hsiao, Susan J.; Smith, Susan (2008): Tankyrase function at telomeres, spindle poles, and beyond. In: *Biochimie* 90 (1), S. 83–92. DOI: 10.1016/j.biochi.2007.07.012.

Huambachano, Orlando; Herrera, Fatima; Rancourt, Ann; Satoh, Masahiko S. (2011): Double-stranded DNA binding domain of poly(ADP-ribose) polymerase-1 and molecular insight into the regulation of its activity. In: *The Journal of biological chemistry* 286 (9), S. 7149–7160. DOI: 10.1074/jbc.M110.175190.

Huang, J. C.; Hsu, D. S.; Kazantsev, A.; Sancar, A. (1994): Substrate spectrum of human excinuclease: repair of abasic sites, methylated bases, mismatches, and bulky adducts. In: *Proceedings of the National Academy of Sciences of the United States of America* 91 (25), S. 12213–12217.

Huang, Jin; Xie, Yangchun; Sun, Xiaofang; Zeh, Herbert J. 3rd; Kang, Rui; Lotze, Michael T.; Tang, Daolin (2015): DAMPs, ageing, and cancer: The 'DAMP Hypothesis'. In: *Ageing research reviews* 24 (Pt A), S. 3–16. DOI: 10.1016/j.arr.2014.10.004.

Huang, S.; Pettaway, C. A.; Uehara, H.; Bucana, C. D.; Fidler, I. J. (2001): Blockade of NF-kappaB activity in human prostate cancer cells is associated with suppression of angiogenesis, invasion, and metastasis. In: *Oncogene* 20 (31), S. 4188–4197. DOI: 10.1038/sj.onc.1204535.

Huang, Shih-Min A.; Mishina, Yuji M.; Liu, Shanming; Cheung, Atwood; Stegmeier, Frank; Michaud, Gregory A.; Charlat, Olga; Wiellette, Elizabeth; Zhang, Yue; Wiessner, Stephanie; Hild, Marc; Shi, Xiaoying; Wilson, Christopher J.; Mickanin, Craig; Myer, Vic; Fazal, Aleem; Tomlinson, Ronald; Serluca, Fabrizio; Shao, Wenlin; Cheng, Hong; Shultz, Michael; Rau, Christina; Schirle, Markus; Schlegl, Judith; Ghidelli, Sonja; Fawell, Stephen; Lu, Chris; Curtis, Daniel; Kirschner, Marc W.; Lengauer, Christoph; Finan, Peter M.; Tallarico, John A.; Bouwmeester, Tewis; Porter, Jeffery A.; Bauer, Andreas; Cong, Feng (2009): Tankyrase inhibition stabilizes axin and antagonizes Wnt signalling. In: *Nature* 461 (7264), S. 614–620. DOI: 10.1038/nature08356.

Huletsky, A.; Murcia, G. de; Muller, S.; Hengartner, M.; Menard, L.; Lamarre, D.; Poirier, G. G. (1989): The effect of poly(ADP-ribosyl)ation on native and H1-depleted chromatin. A role of poly(ADP-ribosyl)ation on core nucleosome structure. In: *The Journal of biological chemistry* 264 (15), S. 8878–8886.

Idogawa, Masashi; Masutani, Mitsuko; Shitashige, Miki; Honda, Kazufumi; Tokino, Takashi; Shinomura, Yasuhisa; Imai, Kohzoh; Hirohashi, Setsuo; Yamada, Tesshi (2007): Ku70 and poly(ADP-ribose) polymerase-1 competitively regulate beta-catenin and T-cell factor-4-mediated gene transactivation: possible linkage of DNA damage recognition and Wnt signaling. In: *Cancer research* 67 (3), S. 911–918. DOI: 10.1158/0008-5472.CAN-06-2360.

Idogawa, Masashi; Yamada, Tesshi; Honda, Kazufumi; Sato, Satoshi; Imai, Kohzoh; Hirohashi, Setsuo (2005): Poly(ADP-ribose) polymerase-1 is a component of the oncogenic T-cell factor-4/beta-catenin complex. In: *Gastroenterology* 128 (7), S. 1919–1936.

Iliakis, George (2009): Backup pathways of NHEJ in cells of higher eukaryotes: cell cycle dependence. In: *Radiotherapy and oncology : journal of the European Society for Therapeutic Radiology and Oncology* 92 (3), S. 310–315. DOI: 10.1016/j.radonc.2009.06.024.

Ionov, Y.; Peinado, M. A.; Malkhosyan, S.; Shibata, D.; Perucho, M. (1993): Ubiquitous somatic mutations in simple repeated sequences reveal a new mechanism for colonic carcinogenesis. In: *Nature* 363 (6429), S. 558–561. DOI: 10.1038/363558a0.

Isogai, Shin; Kanno, Shin-Ichiro; Ariyoshi, Mariko; Tochio, Hidehito; Ito, Yutaka; Yasui, Akira; Shirakawa, Masahiro (2010): Solution structure of a zinc-finger domain that binds to poly-ADP-ribose.

In: *Genes to cells : devoted to molecular & cellular mechanisms* 15 (2), S. 101–110. DOI: 10.1111/j.1365-2443.2009.01369.x.

Issa, Jean-Pierre (2004): CpG island methylator phenotype in cancer. In: *Nature reviews. Cancer* 4 (12), S. 988–993. DOI: 10.1038/nrc1507.

Itzkowitz, Steven H.; Harpaz, Noam (2004): Diagnosis and management of dysplasia in patients with inflammatory bowel diseases. In: *Gastroenterology* 126 (6), S. 1634–1648.

Iyer, Ravi R.; Pluciennik, Anna; Burdett, Vickers; Modrich, Paul L. (2006): DNA mismatch repair: functions and mechanisms. In: *Chemical reviews* 106 (2), S. 302–323. DOI: 10.1021/cr0404794.

Jackson, Petra; Pedersen, Lourdes M.; Kyjovska, Zdenka O.; Jacobsen, Nicklas R.; Saber, Anne T.; Hougaard, Karin S.; Vogel, Ulla; Wallin, Håkan (2013): Validation of freezing tissues and cells for analysis of DNA strand break levels by comet assay. In: *Mutagenesis* 28 (6), S. 699–707. DOI: 10.1093/mutage/get049.

Jacobson, Elaine L.; Jacobson, Myron K. (1976): Pyridine nucleotide levels as a function of growth in normal and transformed 3T3 cells. In: *Archives of Biochemistry and Biophysics* 175 (2), S. 627–634. DOI: 10.1016/0003-9861(76)90553-1.

Janeway, Charles (2005): Immunobiology. The immune system in health and disease / Charles A. Janeway, Jr.. [et al.]. 6th ed. New York, London: Garland Science.

Jijon, H. B.; Churchill, T.; Malfair, D.; Wessler, A.; Jewell, L. D.; Parsons, H. G.; Madsen, K. L. (2000): Inhibition of poly(ADP-ribose) polymerase attenuates inflammation in a model of chronic colitis. In: *American journal of physiology. Gastrointestinal and liver physiology* 279 (3), S. 51.

Jones, Rebecca M.; Petermann, Eva (2012): Replication fork dynamics and the DNA damage response. In: *The Biochemical journal* 443 (1), S. 13–26. DOI: 10.1042/BJ20112100.

Joosen, Annemiek M C P; Kuhnle, Gunter G. C.; Aspinall, Sue M.; Barrow, Timothy M.; Lecommandeur, Emmanuelle; Azqueta, Amaya; Collins, Andrew R.; Bingham, Sheila A. (2009): Effect of processed and red meat on endogenous nitrosation and DNA damage. In: *Carcinogenesis* 30 (8), S. 1402–1407. DOI: 10.1093/carcin/bgp130.

Juarez-Salinas, H.; Levi, V.; Jacobson, E. L.; Jacobson, M. K. (1982): Poly(ADP-ribose) has a branched structure in vivo. In: *The Journal of biological chemistry* 257 (2), S. 607–609.

Juarez-Salinas, H.; Sims, J. L.; Jacobson, M. K. (1979): Poly(ADP-ribose) levels in carcinogen-treated cells. In: *Nature* 282 (5740), S. 740–741.

Juarez-Salinas, Hector; Mendoza-Alvarez, Hilda; Levi, Viktorya; Jacobson, Myron K.; Jacobson, Elaine L. (1983): Simultaneous determination of linear and branched residues in poly(ADP-ribose). In: *Analytical Biochemistry* 131 (2), S. 410–418. DOI: 10.1016/0003-2697(83)90192-6.

Kaina, Bernd; Christmann, Markus; Naumann, Steffen; Roos, Wynand P. (2007): MGMT: key node in the battle against genotoxicity, carcinogenicity and apoptosis induced by alkylating agents. In: *DNA repair* 6 (8), S. 1079–1099. DOI: 10.1016/j.dnarep.2007.03.008.

Kanai, M.; Uchida, M.; Hanai, S.; Uematsu, N.; Uchida, K.; Miwa, M. (2000): Poly(ADP-ribose) polymerase localizes to the centrosomes and chromosomes. In: *Biochemical and Biophysical Research Communications* 278 (2), S. 385–389. DOI: 10.1006/bbrc.2000.3801.

Kanai, Masayuki; Tong, Wei-Min; Sugihara, Eiji; Wang, Zhao-Qi; Fukasawa, Kenji; Miwa, Masanao (2003): Involvement of poly(ADP-Ribose) polymerase 1 and poly(ADP-Ribosyl)ation in regulation of centrosome function. In: *Molecular and cellular biology* 23 (7), S. 2451–2462.

Kanai, Masayuki; Tong, Wei-Min; Wang, Zhao-Qi; Miwa, Masanao (2007): Haploinsufficiency of poly(ADP-ribose) polymerase-1-mediated poly(ADP-ribosyl)ation for centrosome duplication. In: *Biochemical and Biophysical Research Communications* 359 (3), S. 426–430. DOI: 10.1016/j.bbrc.2007.05.108.

Kandala, Prabodh K.; Wright, Stephen E.; Srivastava, Sanjay K. (2012): Blocking epidermal growth factor receptor activation by 3,3'-diindolylmethane suppresses ovarian tumor growth in vitro and in vivo. In: *The Journal of pharmacology and experimental therapeutics* 341 (1), S. 24–32. DOI: 10.1124/jpet.111.188706.

Kang, R.; Tang, D.; Schapiro, N. E.; Loux, T.; Livesey, K. M.; Billiar, T. R.; Wang, H.; van Houten, B.; Lotze, M. T.; Zeh, H. J. (2014): The HMGB1/RAGE inflammatory pathway promotes pancreatic tumor growth by regulating mitochondrial bioenergetics. In: *Oncogene* 33 (5), S. 567–577. DOI: 10.1038/onc.2012.631.

Kappes, F.; Fahrer, J.; Khodadoust, M. S.; Tabbert, A.; Strasser, C.; Mor-Vaknin, N.; Moreno-Villanueva, M.; Burkle, A.; Markovitz, D. M.; Ferrando-May, E. (2008): DEK is a poly(ADP-ribose) acceptor in apoptosis and mediates resistance to genotoxic stress. In: *Molecular and cellular biology* 28 (10), S. 3245–3257. DOI: 10.1128/MCB.01921-07.

Karran, P.; Bignami, M. (1994): DNA damage tolerance, mismatch repair and genome instability. In: *BioEssays : news and reviews in molecular, cellular and developmental biology* 16 (11), S. 833–839. DOI: 10.1002/bies.950161110.

Karras, Georgios I.; Kustatscher, Georg; Buhecha, Heeran R.; Allen, Mark D.; Pugieux, Celine; Sait, Fiona; Bycroft, Mark; Ladurner, Andreas G. (2005): The macro domain is an ADP-ribose binding module. In: *The EMBO journal* 24 (11), S. 1911–1920. DOI: 10.1038/sj.emboj.7600664.

Kawahara, Tiara L. A.; Michishita, Eriko; Adler, Adam S.; Damian, Mara; Berber, Elisabeth; Lin, Meihong; McCord, Ron A.; Ongaigui, Kristine C. L.; Boxer, Lisa D.; Chang, Howard Y.; Chua, Katrin F. (2009): SIRT6 links histone H3 lysine 9 deacetylation to NF-kappaB-dependent gene expression and organismal life span. In: *Cell* 136 (1), S. 62–74. DOI: 10.1016/j.cell.2008.10.052.

Kim, Hak-Su; Kim, Myung-Jin; Kim, Eun Ju; Yang, Young; Lee, Myeong-Sok; Lim, Jong-Seok (2012): Berberine-induced AMPK activation inhibits the metastatic potential of melanoma cells via reduction of ERK activity and COX-2 protein expression. In: *Biochemical Pharmacology* 83 (3), S. 385–394. DOI: 10.1016/j.bcp.2011.11.008.

Kim, Hyun Soo; Kundu, Joydeb Kumar; Lee, Jeong-Sang; Oh, Tae-Young; Na, Hye-Kyung; Surh, Young-Joon (2008): Chemopreventive effects of the standardized extract (DA-9601) of Artemisia

asiatica on azoxymethane-initiated and dextran sulfate sodium-promoted mouse colon carcinogenesis. In: *Nutrition and cancer* 60 Suppl 1, S. 90–97. DOI: 10.1080/01635580802404170.

Kim, Mi Young; Mauro, Steven; Gevry, Nicolas; Lis, John T.; Kraus, W. Lee (2004): NAD+-dependent modulation of chromatin structure and transcription by nucleosome binding properties of PARP-1. In: *Cell* 119 (6), S. 803–814. DOI: 10.1016/j.cell.2004.11.002.

Kim, Mi Young; Zhang, Tong; Kraus, W. Lee (2005): Poly(ADP-ribosyl)ation by PARP-1: 'PAR-laying' NAD+ into a nuclear signal. In: *Genes & development* 19 (17), S. 1951–1967. DOI: 10.1101/gad.1331805.

King, Brenee S.; Cooper, Karen L.; Liu, Ke Jian; Hudson, Laurie G. (2012): Poly(ADP-ribose) contributes to an association between poly(ADP-ribose) polymerase-1 and xeroderma pigmentosum complementation group A in nucleotide excision repair. In: *The Journal of biological chemistry* 287 (47), S. 39824–39833. DOI: 10.1074/jbc.M112.393504.

Klune, JR; Dhupar, R.; Cardinal, J.; Billiar, T. R.; Tsung, A. (2008): HMGB1: endogenous danger signaling. In: *Molecular medicine (Cambridge, Mass.)* 14 (7-8), S. 476–484. DOI: 10.2119/2008-00034.Klune.

Knoepfler, Paul S. (2007): Myc goes global: new tricks for an old oncogene. In: *Cancer research* 67 (11), S. 5061–5063. DOI: 10.1158/0008-5472.CAN-07-0426.

Kobaek-Larsen, M.; Thorup, I.; Diederichsen, A.; Fenger, C.; Hoitinga, M. R. (2000): Review of colorectal cancer and its metastases in rodent models: comparative aspects with those in humans. In: *Comparative medicine* 50 (1), S. 16–26.

Koesters, R.; Hans, M. A.; Benner, A.; Prosst, R.; Boehm, J.; Gahlen, J.; Doeberitz, M. K. (2001): Predominant mutation of codon 41 of the beta-catenin proto-oncogene in rat colon tumors induced by 1,2-dimethylhydrazine using a complete carcinogenic protocol. In: *Carcinogenesis* 22 (11), S. 1885–1890.

Koh, David W.; Dawson, Ted M.; Dawson, Valina L. (2005): Mediation of cell death by poly(ADP-ribose) polymerase-1. In: *Pharmacological research* 52 (1), S. 5–14. DOI: 10.1016/j.phrs.2005.02.011.

Kohno, Hiroyuki; Suzuki, Rikako; Curini, Massimo; Epifano, Francesco; Maltese, Federica; Gonzales, Sylvia Prieto; Tanaka, Takuji (2006): Dietary administration with prenyloxycoumarins, auraptene and collinin, inhibits colitis-related colon carcinogenesis in mice. In: *International journal of cancer* 118 (12), S. 2936–2942. DOI: 10.1002/ijc.21719.

Kohno, Michiaki; Tanimura, Susumu; Ozaki, Kei-ichi (2011): Targeting the Extracellular Signal-Regulated Kinase Pathway in Cancer Therapy. In: *Biol. Pharm. Bull.* 34 (12), S. 1781–1784. DOI: 10.1248/bpb.34.1781.

Korkmaz, Ahmet; Kurt, Bulent; Yildirim, Ibrahim; Basal, Seref; Topal, Turgut; Sadir, Serdar; Oter, Sukru (2008): Effects of poly(ADP-ribose) polymerase inhibition in bladder damage caused by

cyclophosphamide in rats. In: *Experimental biology and medicine (Maywood, N.J.)* 233 (3), S. 338–343. DOI: 10.3181/0706-RM-151.

Kraus, W. Lee (2008): Transcriptional control by PARP-1: chromatin modulation, enhancer-binding, coregulation, and insulation. In: *Current opinion in cell biology* 20 (3), S. 294–302. DOI: 10.1016/j.ceb.2008.03.006.

Krietsch, Jana; Rouleau, Michele; Pic, Emilie; Ethier, Chantal; Dawson, Ted M.; Dawson, Valina L.; Masson, Jean-Yves; POIRIER, Guy G.; Gagne, Jean-Philippe (2013): Reprogramming cellular events by poly(ADP-ribose)-binding proteins. In: *Molecular aspects of medicine* 34 (6), S. 1066–1087. DOI: 10.1016/j.mam.2012.12.005.

Krishnakumar, Raga; Kraus, W. Lee (2010a): PARP-1 regulates chromatin structure and transcription through a KDM5B-dependent pathway. In: *Molecular cell* 39 (5), S. 736–749. DOI: 10.1016/j.molcel.2010.08.014.

Krishnakumar, Raga; Kraus, W. Lee (2010b): The PARP side of the nucleus: molecular actions, physiological outcomes, and clinical targets. In: *Molecular cell* 39 (1), S. 8–24. DOI: 10.1016/j.molcel.2010.06.017.

Kubben, F. J.; Peeters-Haesevoets, A.; Engels, L. G.; Baeten, C. G.; Schutte, B.; Arends, J. W.; Stockbrugger, R. W.; Blijham, G. H. (1994): Proliferating cell nuclear antigen (PCNA): a new marker to study human colonic cell proliferation. In: *Gut* 35 (4), S. 530–535.

Kuhnle, Gunter G. C.; Story, Giles W.; Reda, Torsten; Mani, Ali R.; Moore, Kevin P.; Lunn, Joanne C.; Bingham, Sheila A. (2007): Diet-induced endogenous formation of nitroso compounds in the GI tract. In: *Free radical biology & medicine* 43 (7), S. 1040–1047. DOI: 10.1016/j.freeradbiomed.2007.03.011.

Kulkarni, A. B.; Huh, C. G.; Becker, D.; Geiser, A.; Lyght, M.; Flanders, K. C.; Roberts, A. B.; Sporn, M. B.; Ward, J. M.; Karlsson, S. (1993): Transforming growth factor beta 1 null mutation in mice causes excessive inflammatory response and early death. In: *Proceedings of the National Academy of Sciences of the United States of America* 90 (2), S. 770–774.

Kumari, S. R.; Mendoza-Alvarez, H.; Alvarez-Gonzalez, R. (1998): Functional interactions of p53 with poly(ADP-ribose) polymerase (PARP) during apoptosis following DNA damage: covalent poly(ADP-ribosyl)ation of p53 by exogenous PARP and noncovalent binding of p53 to the M(r) 85,000 proteolytic fragment. In: *Cancer research* 58 (22), S. 5075–5078.

Kummar, Shivaani; Chen, Alice; Ji, Jiuping; Zhang, Yiping; Reid, Joel M.; Ames, Matthew; Jia, Lee; Weil, Marcie; Speranza, Giovanna; Murgo, Anthony J.; Kinders, Robert; Wang, Lihua; Parchment, Ralph E.; Carter, John; Stotler, Howard; Rubinstein, Larry; Hollingshead, Melinda; Melillo, Giovanni; Pommier, Yves; Bonner, William; Tomaszewski, Joseph E.; Doroshow, James H. (2011): Phase I study of PARP inhibitor ABT-888 in combination with topotecan in adults with refractory solid tumors and lymphomas. In: *Cancer research* 71 (17), S. 5626–5634. DOI: 10.1158/0008-5472.CAN-11-1227.

Kummar, Shivaani; Ji, Jiuping; Morgan, Robert; Lenz, Heinz-Josef; Puhalla, Shannon L.; Belani, Chandra P.; Gandara, David R.; Allen, Deborah; Kiesel, Brian; Beumer, Jan H.; Newman, Edward M.; Rubinstein, Larry; Chen, Alice; Zhang, Yiping; Wang, Lihua; Kinders, Robert J.; Parchment, Ralph E.; Tomaszewski, Joseph E.; Doroshow, James H. (2012): A phase I study of veliparib in combination with metronomic cyclophosphamide in adults with refractory solid tumors and lymphomas. In: *Clinical cancer research : an official journal of the American Association for Cancer Research* 18 (6), S. 1726–1734. DOI: 10.1158/1078-0432.CCR-11-2821.

Kuo, Linda J.; Yang, Li-Xi (2008): Gamma-H2AX - a novel biomarker for DNA double-strand breaks. In: *In vivo (Athens, Greece)* 22 (3), S. 305–309.

Kurowski, Michal A.; Bhagwat, Ashok S.; Papaj, Grzegorz; Bujnicki, Janusz M. (2003): Phylogenomic identification of five new human homologs of the DNA repair enzyme AlkB. In: *BMC genomics* 4 (1), S. 48. DOI: 10.1186/1471-2164-4-48.

Kuwano, Takashi; Nakao, Shintaro; Yamamoto, Hidetaka; Tsuneyoshi, Masazumi; Yamamoto, Tomoya; Kuwano, Michihiko; Ono, Mayumi (2004): Cyclooxygenase 2 is a key enzyme for inflammatory cytokine-induced angiogenesis. In: *FASEB journal : official publication of the Federation of American Societies for Experimental Biology* 18 (2), S. 300–310. DOI: 10.1096/fj.03-0473com.

Lai, L.; Alaverdi, N.; Maltais, L.; Morse, H. C. 3rd (1998): Mouse cell surface antigens: nomenclature and immunophenotyping. In: *Journal of immunology (Baltimore, Md. : 1950)* 160 (8), S. 3861–3868.

Lange, Sabine S.; Mitchell, David L.; Vasquez, Karen M. (2008): High mobility group protein B1 enhances DNA repair and chromatin modification after DNA damage. In: *Proceedings of the National Academy of Sciences of the United States of America* 105 (30), S. 10320–10325. DOI: 10.1073/pnas.0803181105.

Langelier, Marie-France; Planck, Jamie L.; Roy, Swati; Pascal, John M. (2012): Structural basis for DNA damage-dependent poly(ADP-ribosyl)ation by human PARP-1. In: *Science (New York, N.Y.)* 336 (6082), S. 728–732. DOI: 10.1126/science.1216338.

Langelier, Marie-France; Ruhl, Donald D.; Planck, Jamie L.; Kraus, W. Lee; Pascal, John M. (2010): The Zn3 domain of human poly(ADP-ribose) polymerase-1 (PARP-1) functions in both DNA-dependent poly(ADP-ribose) synthesis activity and chromatin compaction. In: *The Journal of biological chemistry* 285 (24), S. 18877–18887. DOI: 10.1074/jbc.M110.105668.

Langelier, Marie-France; Servent, Kristin M.; Rogers, Elizabeth E.; Pascal, John M. (2008): A third zinc-binding domain of human poly(ADP-ribose) polymerase-1 coordinates DNA-dependent enzyme activation. In: *The Journal of biological chemistry* 283 (7), S. 4105–4114. DOI: 10.1074/jbc.M708558200.

LAQUEUR, G. L. (1964): CARCINOGENIC EFFECTS OF CYCAD MEAL AND CYCASIN, METHYLAZOXYMETHANOL GLYCOSIDE, IN RATS AND EFFECTS OF CYCASIN IN GERMFREE RATS. In: *Federation proceedings* 23, S. 1386–1388.

Larmonier, Claire B.; Shehab, Kareem W.; Laubitz, Daniel; Jamwal, Deepa R.; Ghishan, Fayez K.; Kiela, Pawel R. (2016): Transcriptional Reprogramming and Resistance to Colonic Mucosal Injury in Poly(ADP-ribose) Polymerase 1 (PARP1)-deficient Mice. In: *The Journal of biological chemistry* 291 (17), S. 8918–8930. DOI: 10.1074/jbc.M116.714386.

Laroui, Hamed; Ingersoll, Sarah A.; Liu, Hong Chun; Baker, Mark T.; Ayyadurai, Saravanan; Charania, Moiz A.; Laroui, Famina; Yan, Yutao; Sitaraman, Shanthi V.; Merlin, Didier (2012): Dextran sodium sulfate (DSS) induces colitis in mice by forming nano-lipocomplexes with medium-chain-length fatty acids in the colon. In: *PloS one* 7 (3), e32084. DOI: 10.1371/journal.pone.0032084.

Lau, Ted; Chan, Emily; Callow, Marinella; Waaler, Jo; Boggs, Jason; Blake, Robert A.; Magnuson, Steven; Sambrone, Amy; Schutten, Melissa; Firestein, Ron; Machon, Ondrej; Korinek, Vladimir; Choo, Edna; Diaz, Dolores; Merchant, Mark; Polakis, Paul; Holsworth, Daniel D.; Krauss, Stefan; Costa, Mike (2013): A novel tankyrase small-molecule inhibitor suppresses APC mutation-driven colorectal tumor growth. In: *Cancer research* 73 (10), S. 3132–3144. DOI: 10.1158/0008-5472.CAN-12-4562.

Lees, N. P.; Harrison, K. L.; Hall, C. N.; Margison, G. P.; Povey, A. C. (2007): Human colorectal mucosal O6-alkylguanine DNA-alkyltransferase activity and DNA-N7-methylguanine levels in colorectal adenoma cases and matched referents. In: *Gut* 56 (3), S. 380–384. DOI: 10.1136/gut.2006.097899.

Lees, Nicholas P.; Harrison, Kathryn L.; Hill, Elizabeth; Hall, C. Nicholas; Povey, Andrew C.; Margison, Geoffrey P. (2002): Heterogeneity of O(6)-alkylguanine-DNA alkyltransferase activity in colorectal cancer: implications for treatment. In: *Oncology* 63 (4), S. 393–397.

Leichman, Lawrence; Groshen, Susan; O'Neil, Bert H.; Messersmith, Wells; Berlin, Jordan; Chan, Emily; Leichman, Cynthia G.; Cohen, Steven J.; Cohen, Deirdre; Lenz, Heinz-Josef; Gold, Philip; Boman, Bruce; Fielding, Anitra; Locker, Gershon; Cason, Ronald C.; Hamilton, Stan R.; Hochster, Howard S. (2016): Phase II Study of Olaparib (AZD-2281) After Standard Systemic Therapies for Disseminated Colorectal Cancer. In: *The oncologist* 21 (2), S. 172–177. DOI: 10.1634/theoncologist.2015-0319.

Lengauer, C.; Kinzler, K. W.; Vogelstein, B. (1998): Genetic instabilities in human cancers. In: *Nature* 396 (6712), S. 643–649. DOI: 10.1038/25292.

Leppard, John B.; Dong, Zhiwan; Mackey, Zachary B.; Tomkinson, Alan E. (2003): Physical and functional interaction between DNA ligase IIIalpha and poly(ADP-Ribose) polymerase 1 in DNA single-strand break repair. In: *Molecular and cellular biology* 23 (16), S. 5919–5927.

Lewin, Michelle H.; Bailey, Nina; Bandaletova, Tanya; Bowman, Richard; Cross, Amanda J.; Pollock, Jim; Shuker, David E. G.; Bingham, Sheila A. (2006): Red meat enhances the colonic formation of the DNA adduct O6-carboxymethyl guanine: implications for colorectal cancer risk. In: *Cancer research* 66 (3), S. 1859–1865. DOI: 10.1158/0008-5472.CAN-05-2237.

Lijinsky, W. (1999): N-Nitroso compounds in the diet. In: *Mutation research* 443 (1-2), S. 129–138.

Lind, Guro E.; Thorstensen, Lin; Lovig, Tone; Meling, Gunn I.; Hamelin, Richard; Rognum, Torleiv O.; Esteller, Manel; Lothe, Ragnhild A. (2004): A CpG island hypermethylation profile of primary colorectal carcinomas and colon cancer cell lines. In: *Molecular cancer* 3, S. 28. DOI: 10.1186/1476-4598-3-28.

Lindahl, T. (1993): Instability and decay of the primary structure of DNA. In: *Nature* 362 (6422), S. 709–715. DOI: 10.1038/362709a0.

Linkermann, Andreas; Stockwell, Brent R.; Krautwald, Stefan; Anders, Hans-Joachim (2014): Regulated cell death and inflammation: an auto-amplification loop causes organ failure. In: *Nature reviews. Immunology* 14 (11), S. 759–767. DOI: 10.1038/nri3743.

Lips, J.; Kaina, B. (2001): Repair of O(6)-methylguanine is not affected by thymine base pairing and the presence of MMR proteins. In: *Mutation research* 487 (1-2), S. 59–66.

Litman, Gary W.; Cannon, John P.; Dishaw, Larry J. (2005): Reconstructing immune phylogeny: new perspectives. In: *Nature reviews. Immunology* 5 (11), S. 866–879. DOI: 10.1038/nri1712.

Liu, Dan; O'Connor, Matthew S.; Qin, Jun; Songyang, Zhou (2004): Telosome, a mammalian telomere-associated complex formed by multiple telomeric proteins. In: *The Journal of biological chemistry* 279 (49), S. 51338–51342. DOI: 10.1074/jbc.M409293200.

Livak, K. J.; Schmittgen, T. D. (2001): Analysis of relative gene expression data using real-time quantitative PCR and the 2(-Delta Delta C(T)) Method. In: *Methods (San Diego, Calif.)* 25 (4), S. 402–408. DOI: 10.1006/meth.2001.1262.

Llor, Xavier; Pons, Elisenda; Xicola, Rosa M.; Castells, Antoni; Alenda, Cristina; Pinol, Virginia; Andreu, Montserrat; Castellvi-Bel, Sergi; Paya, Artemio; Jover, Rodrigo; Bessa, Xavier; Giros, Anna; Roca, Anna; Gassull, Miquel A. (2005): Differential features of colorectal cancers fulfilling Amsterdam criteria without involvement of the mutator pathway. In: *Clinical cancer research : an official journal of the American Association for Cancer Research* 11 (20), S. 7304–7310. DOI: 10.1158/1078-0432.CCR-05-0965.

Loeffler, Paul A.; Cuneo, Matthew J.; Mueller, Geoffrey A.; DeRose, Eugene F.; Gabel, Scott A.; London, Robert E. (2011): Structural studies of the PARP-1 BRCT domain. In: *BMC structural biology* 11, S. 37. DOI: 10.1186/1472-6807-11-37.

Lombard, David B.; Chua, Katrin F.; Mostoslavsky, Raul; Franco, Sonia; Gostissa, Monica; Alt, Frederick W. (2005): DNA repair, genome stability, and aging. In: *Cell* 120 (4), S. 497–512. DOI: 10.1016/j.cell.2005.01.028.

Lonskaya, Irina; Potaman, Vladimir N.; Shlyakhtenko, Luda S.; Oussatcheva, Elena A.; Lyubchenko, Yuri L.; Soldatenkov, Viatcheslav A. (2005): Regulation of poly(ADP-ribose) polymerase-1 by DNA structure-specific binding. In: *The Journal of biological chemistry* 280 (17), S. 17076–17083. DOI: 10.1074/jbc.M413483200.

Lothe, R. A.; Peltomaki, P.; Meling, G. I.; Aaltonen, L. A.; Nystrom-Lahti, M.; Pylkkanen, L.; Heimdal, K.; Andersen, T. I.; Moller, P.; Rognum, T. O. (1993): Genomic instability in colorectal

cancer: relationship to clinicopathological variables and family history. In: *Cancer research* 53 (24), S. 5849–5852.

Lotze, Michael T.; Tracey, Kevin J. (2005): High-mobility group box 1 protein (HMGB1): nuclear weapon in the immune arsenal. In: *Nature reviews. Immunology* 5 (4), S. 331–342. DOI: 10.1038/nri1594.

Luan, Zheng-Gang; Zhang, Hao; Yang, Ping-Ting; Ma, Xiao-Chun; Zhang, Cheng; Guo, Ren-Xuan (2010): HMGB1 activates nuclear factor-kappaB signaling by RAGE and increases the production of TNF-alpha in human umbilical vein endothelial cells. In: *Immunobiology* 215 (12), S. 956–962. DOI: 10.1016/j.imbio.2009.11.001.

Luca, P. de; Moretti, A.; Sabato, S.; Siniscalco Gigliano, G. (1980): The ubiquity of cycasin in cycads. In: *Phytochemistry* 19 (10), S. 2230–2231. DOI: 10.1016/S0031-9422(00)82239-6.

Lundberg, Jon O.; Weitzberg, Eddie (2013): Biology of nitrogen oxides in the gastrointestinal tract. In: *Gut* 62 (4), S. 616–629. DOI: 10.1136/gutjnl-2011-301649.

Luo, Guangjo; Hershko, Dan D.; Robb, Bruce W.; Wray, Curtis J.; Hasselgren, Per-Olof (2003): IL-1beta stimulates IL-6 production in cultured skeletal muscle cells through activation of MAP kinase signaling pathway and NF-kappa B. In: *American journal of physiology. Regulatory, integrative and comparative physiology* 284 (5), S. 54. DOI: 10.1152/ajpregu.00490.2002.

Lupo, Barbara; Trusolino, Livio (2014): Inhibition of poly(ADP-ribosyl)ation in cancer: old and new paradigms revisited. In: *Biochimica et biophysica acta* 1846 (1), S. 201–215. DOI: 10.1016/j.bbcan.2014.07.004.

Lynch, Henry T.; Lynch, Jane F.; Lynch, Patrick M.; Attard, Thomas (2008): Hereditary colorectal cancer syndromes: molecular genetics, genetic counseling, diagnosis and management. In: *Familial cancer* 7 (1), S. 27–39. DOI: 10.1007/s10689-007-9165-5.

Malanga, M. (1998): Poly(ADP-ribose) Binds to Specific Domains of p53 and Alters Its DNA Binding Functions. In: *Journal of Biological Chemistry* 273 (19), S. 11839–11843. DOI: 10.1074/jbc.273.19.11839.

Malanga, Maria; Althaus, Felix R. (2005): The role of poly(ADP-ribose) in the DNA damage signaling network. In: *Biochemistry and cell biology = Biochimie et biologie cellulaire* 83 (3), S. 354–364. DOI: 10.1139/o05-038.

Maltzman, T.; Whittington, J.; Driggers, L.; Stephens, J.; Ahnen, D. (1997): AOM-induced mouse colon tumors do not express full-length APC protein. In: *Carcinogenesis* 18 (12), S. 2435–2439.

Mandir, A. S.; Przedborski, S.; Jackson-Lewis, V.; Wang, Z. Q.; Simbulan-Rosenthal, C. M.; Smulson, M. E.; Hoffman, B. E.; Guastella, D. B.; Dawson, V. L.; Dawson, T. M. (1999): Poly(ADP-ribose) polymerase activation mediates 1-methyl-4-phenyl-1, 2,3,6-tetrahydropyridine (MPTP)-induced parkinsonism. In: *Proceedings of the National Academy of Sciences of the United States of America* 96 (10), S. 5774–5779.

Mangerich, Aswin; Bürkle, Alexander (2011): How to kill tumor cells with inhibitors of poly(ADP-ribosyl)ation. In: *International journal of cancer* 128 (2), S. 251–265. DOI: 10.1002/ijc.25683.

Mangerich, Aswin; Bürkle, Alexander (2012): Pleiotropic cellular functions of PARP1 in longevity and aging: genome maintenance meets inflammation. In: *Oxidative medicine and cellular longevity* 2012, S. 321653. DOI: 10.1155/2012/321653.

Margison, Geoffrey P.; Santibanez-Koref, Mauro F. (2002): O6-alkylguanine-DNA alkyltransferase: role in carcinogenesis and chemotherapy. In: *BioEssays : news and reviews in molecular, cellular and developmental biology* 24 (3), S. 255–266. DOI: 10.1002/bies.10063.

Markowitz, Sanford D.; Bertagnolli, Monica M. (2009): Molecular origins of cancer: Molecular basis of colorectal cancer. In: *The New England journal of medicine* 361 (25), S. 2449–2460. DOI: 10.1056/NEJMra0804588.

Markowitz, Sanford D.; Dawson, Dawn M.; Willis, Joseph; Willson, James K. V. (2002): Focus on colon cancer. In: *Cancer cell* 1 (3), S. 233–236.

Marsischky, G. T.; Wilson, B. A.; Collier, R. J. (1995): Role of glutamic acid 988 of human poly-ADP-ribose polymerase in polymer formation. Evidence for active site similarities to the ADP-ribosylating toxins. In: *The Journal of biological chemistry* 270 (7), S. 3247–3254.

Martello, Rita; Mangerich, Aswin; Sass, Sabine; Dedon, Peter C.; Bürkle, Alexander (2013): Quantification of cellular poly(ADP-ribosyl)ation by stable isotope dilution mass spectrometry reveals tissue- and drug-dependent stress response dynamics. In: *ACS chemical biology* 8 (7), S. 1567–1575. DOI: 10.1021/cb400170b.

Masson, M.; Niedergang, C.; Schreiber, V.; Muller, S.; Menissier-de Murcia, J.; Murcia, G. de (1998): XRCC1 is specifically associated with poly(ADP-ribose) polymerase and negatively regulates its activity following DNA damage. In: *Molecular and cellular biology* 18 (6), S. 3563–3571.

Masutani, M.; Suzuki, H.; Kamada, N.; Watanabe, M.; Ueda, O.; Nozaki, T.; Jishage, K.; Watanabe, T.; Sugimoto, T.; Nakagama, H.; Ochiya, T.; Sugimura, T. (1999): Poly(ADP-ribose) polymerase gene disruption conferred mice resistant to streptozotocin-induced diabetes. In: *Proceedings of the National Academy of Sciences of the United States of America* 96 (5), S. 2301–2304.

Matsumoto, H.; Higa, H. H. (1966): Studies on methylazoxymethanol, the aglycone of cycasin: methylation of nucleic acids in vitro. In: *The Biochemical journal* 98 (2), 20C-22C.

Matsumura, Shunji; Oue, Naohide; Ito, Reiko; Nakayama, Hirofumi; Kitadai, Yasuhiko; Yokozaki, Hiroshi; Chayama, Kazuaki; Yasui, Wataru (2003): The promoter methylation status of the DNA repair gene O6-methylguanine-DNA methyltransferase in ulcerative colitis. In: *Virchows Archiv : an international journal of pathology* 443 (4), S. 518–523. DOI: 10.1007/s00428-003-0877-0.

Matzinger, Polly (2002): The danger model: a renewed sense of self. In: *Science (New York, N.Y.)* 296 (5566), S. 301–305. DOI: 10.1126/science.1071059.

Mauchley, David C.; Lynge, Dana C.; Langdale, Lorrie A.; Stelzner, Matthias G.; Mock, Charles N.; Billingsley, Kevin G. (2005): Clinical utility and cost-effectiveness of routine preoperative computed tomography scanning in patients with colon cancer. In: *American journal of surgery* 189 (5), S. 512. DOI: 10.1016/j.amjsurg.2005.01.027.

Medzhitov, Ruslan (2007): Recognition of microorganisms and activation of the immune response. In: *Nature* 449 (7164), S. 819–826. DOI: 10.1038/nature06246.

Megnin-Chanet, Frederique; Bollet, Marc A.; Hall, Janet (2010): Targeting poly(ADP-ribose) polymerase activity for cancer therapy. In: *Cellular and molecular life sciences : CMLS* 67 (21), S. 3649–3662. DOI: 10.1007/s00018-010-0490-8.

Meira, Lisiane B.; Bugni, James M.; Green, Stephanie L.; Lee, Chung-Wei; Pang, Bo; Borenshtein, Diana; Rickman, Barry H.; Rogers, Arlin B.; Moroski-Erkul, Catherine A.; McFaline, Jose L.; Schauer, David B.; Dedon, Peter C.; Fox, James G.; Samson, Leona D. (2008): DNA damage induced by chronic inflammation contributes to colon carcinogenesis in mice. In: *The Journal of clinical investigation* 118 (7), S. 2516–2525. DOI: 10.1172/JCI35073.

Mendoza-Alvarez, H.; Alvarez-Gonzalez, R. (1993): Poly(ADP-ribose) polymerase is a catalytic dimer and the automodification reaction is intermolecular. In: *The Journal of biological chemistry* 268 (30), S. 22575–22580.

Mendoza-Alvarez, H.; Alvarez-Gonzalez, R. (1999): Biochemical characterization of mono(ADP-ribosyl)ated poly(ADP-ribose) polymerase. In: *Biochemistry* 38 (13), S. 3948–3953. DOI: 10.1021/bi982148p.

Mendoza-Alvarez, H.; Alvarez-Gonzalez, R. (2001): Regulation of p53 sequence-specific DNA-binding by covalent poly(ADP-ribosyl)ation. In: *The Journal of biological chemistry* 276 (39), S. 36425–36430. DOI: 10.1074/jbc.M105215200.

Menissier de Murcia, Josiane; Ricoul, Michelle; Tartier, Laurence; Niedergang, Claude; Huber, Aline; Dantzer, Francoise; Schreiber, Valerie; Ame, Jean-Christophe; Dierich, Andree; LeMeur, Marianne; Sabatier, Laure; Chambon, Pierre; Murcia, Gilbert de (2003): Functional interaction between PARP-1 and PARP-2 in chromosome stability and embryonic development in mouse. In: *The EMBO journal* 22 (9), S. 2255–2263. DOI: 10.1093/emboj/cdg206.

Meyer, Ralph G.; Meyer-Ficca, Mirella L.; Whatcott, Clifford J.; Jacobson, Elaine L.; Jacobson, Myron K. (2007): Two small enzyme isoforms mediate mammalian mitochondrial poly(ADP-ribose) glycohydrolase (PARG) activity. In: *Experimental cell research* 313 (13), S. 2920–2936. DOI: 10.1016/j.yexcr.2007.03.043.

Meyer-Ficca, Mirella L.; Meyer, Ralph G.; Coyle, Donna L.; Jacobson, Elaine L.; Jacobson, Myron K. (2004): Human poly(ADP-ribose) glycohydrolase is expressed in alternative splice variants yielding isoforms that localize to different cell compartments. In: *Experimental cell research* 297 (2), S. 521–532. DOI: 10.1016/j.yexcr.2004.03.050.

Mikami, T.; Mitomi, H.; Hara, A.; Yanagisawa, N.; Yoshida, T.; Tsuruta, O.; Okayasu, I. (2000): Decreased expression of CD44, alpha-catenin, and deleted colon carcinoma and altered expression of

beta-catenin in ulcerative colitis-associated dysplasia and carcinoma, as compared with sporadic colon neoplasms. In: *Cancer* 89 (4), S. 733–740.

Min, Ahrum; Im, Seock-Ah; Yoon, Young-Kwang; Song, Sang-Hyun; Nam, Hyun-Jin; Hur, Hyung-Seok; Kim, Hwang-Phill; Lee, Kyung-Hun; Han, Sae-Won; Oh, Do-Youn; Kim, Tae-You; O'Connor, Mark J.; Kim, Woo-Ho; Bang, Yung-Jue (2013): RAD51C-deficient cancer cells are highly sensitive to the PARP inhibitor olaparib. In: *Molecular cancer therapeutics* 12 (6), S. 865–877. DOI: 10.1158/1535-7163.MCT-12-0950.

Minamoto, T.; Buschmann, T.; Habelhah, H.; Matusevich, E.; Tahara, H.; Boerresen-Dale, A. L.; Harris, C.; Sidransky, D.; Ronai, Z. (2001): Distinct pattern of p53 phosphorylation in human tumors. In: *Oncogene* 20 (26), S. 3341–3347. DOI: 10.1038/sj.onc.1204458.

Miossec, Pierre; Korn, Thomas; Kuchroo, Vijay K. (2009): Interleukin-17 and type 17 helper T cells. In: *The New England journal of medicine* 361 (9), S. 888–898. DOI: 10.1056/NEJMra0707449.

Miwa, M.; Saikawa, N.; Yamaizumi, Z.; Nishimura, S.; Sugimura, T. (1979): Structure of poly(adenosine diphosphate ribose): identification of 2'-1''-ribosyl-2''-(or 3''-)(1'''-ribosyl)adenosine-5',5'',5'''-tris(phosphate) as a branch linkage. In: *Proceedings of the National Academy of Sciences of the United States of America* 76 (2), S. 595–599.

Miwa, M.; Sugimura, T. (1982): Structure of poly(adenosine diphosphate ribose). In: *Princess Takamatsu symposia* 12, S. 205–212.

Morin, P. J.; Sparks, A. B.; Korinek, V.; Barker, N.; Clevers, H.; Vogelstein, B.; Kinzler, K. W. (1997): Activation of beta-catenin-Tcf signaling in colon cancer by mutations in beta-catenin or APC. In: *Science (New York, N.Y.)* 275 (5307), S. 1787–1790.

Morrone, Seamus; Cheng, Zhihong; Moon, Randall T.; Cong, Feng; Xu, Wenqing (2012): Crystal structure of a Tankyrase-Axin complex and its implications for Axin turnover and Tankyrase substrate recruitment. In: *Proceedings of the National Academy of Sciences of the United States of America* 109 (5), S. 1500–1505. DOI: 10.1073/pnas.1116618109.

Morteau, O.; Morham, S. G.; Sellon, R.; Dieleman, L. A.; Langenbach, R.; Smithies, O.; Sartor, R. B. (2000): Impaired mucosal defense to acute colonic injury in mice lacking cyclooxygenase-1 or cyclooxygenase-2. In: *The Journal of clinical investigation* 105 (4), S. 469–478. DOI: 10.1172/JCI6899.

Moskalev, Alexey; Shaposhnikov, Mikhail (2011): Pharmacological inhibition of NF-kappaB prolongs lifespan of Drosophila melanogaster. In: *Aging* 3 (4), S. 391–394.

Murcia, J. M. de; Niedergang, C.; Trucco, C.; Ricoul, M.; Dutrillaux, B.; Mark, M.; Oliver, F. J.; Masson, M.; Dierich, A.; LeMeur, M.; Walztinger, C.; Chambon, P.; Murcia, G. de (1997): Requirement of poly(ADP-ribose) polymerase in recovery from DNA damage in mice and in cells. In: *Proceedings of the National Academy of Sciences of the United States of America* 94 (14), S. 7303–7307.

Nagasaka, Takeshi; Goel, Ajay; Notohara, Kenji; Takahata, Takaomi; Sasamoto, Hiromi; Uchida, Takuyuki; Nishida, Naoshi; Tanaka, Noriaki; Boland, Clement Richard; Matsubara, Nagahide (2008): Methylation pattern of the O6-methylguanine-DNA methyltransferase gene in colon during

progressive colorectal tumorigenesis. In: *International journal of cancer* 122 (11), S. 2429–2436. DOI: 10.1002/ijc.23398.

NAGASAWA, H. T.; SHIROTA, FRANCES N.; MATSUMOTO, HIROMU (1972): Decomposition of Methylazoxymethanol, the Aglycone of Cycasin, in D2O. In: *Nature* 236 (5344), S. 234–235. DOI: 10.1038/236234a0.

Nambiar, Prashant R.; Giardina, Charles; Guda, Kishore; Aizu, Wataru; Raja, Rajiv; Rosenberg, Daniel W. (2002): Role of the alternating reading frame (P19)-p53 pathway in an in vivo murine colon tumor model. In: *Cancer research* 62 (13), S. 3667–3674.

Naura, A. S.; Datta, R.; Hans, C. P.; Zerfaoui, M.; Rezk, B. M.; Errami, Y.; Oumouna, M.; Matrougui, K.; Boulares, A. H. (2009): Reciprocal regulation of iNOS and PARP-1 during allergen-induced eosinophilia. In: *The European respiratory journal* 33 (2), S. 252–262. DOI: 10.1183/09031936.00089008.

Neufert, Clemens; Becker, Christoph; Neurath, Markus F. (2007): An inducible mouse model of colon carcinogenesis for the analysis of sporadic and inflammation-driven tumor progression. In: *Nature protocols* 2 (8), S. 1998–2004. DOI: 10.1038/nprot.2007.279.

Neuvonen, Maarit; Ahola, Tero (2009): Differential activities of cellular and viral macro domain proteins in binding of ADP-ribose metabolites. In: *Journal of molecular biology* 385 (1), S. 212–225. DOI: 10.1016/j.jmb.2008.10.045.

Niere, M.; Mashimo, M.; Agledal, L.; Dolle, C.; Kasamatsu, A.; Kato, J.; Moss, J.; Ziegler, M. (2012): ADP-ribosylhydrolase 3 (ARH3), Not Poly(ADP-ribose) Glycohydrolase (PARG) Isoforms, Is Responsible for Degradation of Mitochondrial Matrix-associated Poly(ADP-ribose). In: *Journal of Biological Chemistry* 287 (20), S. 16088–16102. DOI: 10.1074/jbc.M112.349183.

Niere, Marc; Kernstock, Stefan; Koch-Nolte, Friedrich; Ziegler, Mathias (2008): Functional localization of two poly(ADP-ribose)-degrading enzymes to the mitochondrial matrix. In: *Molecular and cellular biology* 28 (2), S. 814–824. DOI: 10.1128/MCB.01766-07.

Nishizuka, Y.; Ueda, K.; Nakazawa, K.; Hayaishi, O. (1967): Studies on the polymer of adenosine diphosphate ribose. I. Enzymic formation from nicotinamide adenine dinuclotide in mammalian nuclei. In: *The Journal of biological chemistry* 242 (13), S. 3164–3171.

Noffsinger, Amy E. (2009): Serrated polyps and colorectal cancer: new pathway to malignancy. In: *Annual review of pathology* 4, S. 343–364. DOI: 10.1146/annurev.pathol.4.110807.092317.

Noren Hooten, Nicole; Kompaniez, Kari; Barnes, Janice; Lohani, Althaf; Evans, Michele K. (2011): Poly(ADP-ribose) polymerase 1 (PARP-1) binds to 8-oxoguanine-DNA glycosylase (OGG1). In: *The Journal of biological chemistry* 286 (52), S. 44679–44690. DOI: 10.1074/jbc.M111.255869.

Nosho, Katsuhiko; Yamamoto, Hiroyuki; Mikami, Masashi; Taniguchi, Hiroaki; Takahashi, Taiga; Adachi, Yasushi; Imamura, Akimichi; Imai, Kohzoh; Shinomura, Yasuhisa (2006): Overexpression of poly(ADP-ribose) polymerase-1 (PARP-1) in the early stage of colorectal carcinogenesis. In: *European journal of cancer (Oxford, England : 1990)* 42 (14), S. 2374–2381. DOI: 10.1016/j.ejca.2006.01.061.

Notman, J.; Tan, Q. H.; Zedeck, M. S. (1982): Inhibition of methylazoxymethanol-induced intestinal tumors in the rat by pyrazole with paradoxical effects on skin and kidney. In: *Cancer research* 42 (5), S. 1774–1780.

Nowsheen, Somaira; Cooper, Tiffiny; Bonner, James A.; LoBuglio, Albert F.; Yang, Eddy S. (2012): HER2 overexpression renders human breast cancers sensitive to PARP inhibition independently of any defect in homologous recombination DNA repair. In: *Cancer research* 72 (18), S. 4796–4806. DOI: 10.1158/0008-5472.CAN-12-1287.

Nusinow, Dmitri A.; Hernandez-Munoz, Inmaculada; Fazzio, Thomas G.; Shah, Girish M.; Kraus, W. Lee; Panning, Barbara (2007): Poly(ADP-ribose) polymerase 1 is inhibited by a histone H2A variant, MacroH2A, and contributes to silencing of the inactive X chromosome. In: *The Journal of biological chemistry* 282 (17), S. 12851–12859. DOI: 10.1074/jbc.M610502200.

Oberoi, Jasmeen; Richards, Mark W.; Crumpler, Simon; Brown, Nathan; Blagg, Julian; Bayliss, Richard (2010): Structural basis of poly(ADP-ribose) recognition by the multizinc binding domain of checkpoint with forkhead-associated and RING Domains (CHFR). In: *The Journal of biological chemistry* 285 (50), S. 39348–39358. DOI: 10.1074/jbc.M110.159855.

Oei, S. L.; Griesenbeck, J.; Schweiger, M. (1997): The role of poly(ADP-ribosyl)ation. In: *Reviews of physiology, biochemistry and pharmacology* 131, S. 127–173.

Oei, S. L.; Griesenbeck, J.; Schweiger, M.; Ziegler, M. (1998a): Regulation of RNA polymerase II-dependent transcription by poly(ADP-ribosyl)ation of transcription factors. In: *The Journal of biological chemistry* 273 (48), S. 31644–31647.

Oei, S. L.; Griesenbeck, J.; Ziegler, M.; Schweiger, M. (1998b): A novel function of poly(ADP-ribosyl)ation: silencing of RNA polymerase II-dependent transcription. In: *Biochemistry* 37 (6), S. 1465–1469. DOI: 10.1021/bi9727390.

Ohanna, Mickael; Giuliano, Sandy; Bonet, Caroline; Imbert, Veronique; Hofman, Veronique; Zangari, Josephine; Bille, Karine; Robert, Caroline; Bressac-de Paillerets, Brigitte; Hofman, Paul; Rocchi, Stephane; Peyron, Jean-Francois; Lacour, Jean-Philippe; Ballotti, Robert; Bertolotto, Corine (2011): Senescent cells develop a PARP-1 and nuclear factor-{kappa}B-associated secretome (PNAS). In: *Genes & development* 25 (12), S. 1245–1261. DOI: 10.1101/gad.625811.

Okayasu, I.; Hatakeyama, S.; Yamada, M.; Ohkusa, T.; Inagaki, Y.; Nakaya, R. (1990): A novel method in the induction of reliable experimental acute and chronic ulcerative colitis in mice. In: *Gastroenterology* 98 (3), S. 694–702.

Oliver, F. J.; Menissier-de Murcia, J.; Nacci, C.; Decker, P.; Andriantsitohaina, R.; Muller, S.; La Rubia, G. de; Stoclet, J. C.; Murcia, G. de (1999): Resistance to endotoxic shock as a consequence of defective NF-kappaB activation in poly (ADP-ribose) polymerase-1 deficient mice. In: *The EMBO journal* 18 (16), S. 4446–4454. DOI: 10.1093/emboj/18.16.4446.

Oshima, M.; Dinchuk, J. E.; Kargman, S. L.; Oshima, H.; Hancock, B.; Kwong, E.; Trzaskos, J. M.; Evans, J. F.; Taketo, M. M. (1996): Suppression of intestinal polyposis in Apc delta716 knockout mice by inhibition of cyclooxygenase 2 (COX-2). In: *Cell* 87 (5), S. 803–809.

O'Toole, S. M.; Pegg, A. E.; Swenberg, J. A. (1993): Repair of O6-methylguanine and O4-methylthymidine in F344 rat liver following treatment with 1,2-dimethylhydrazine and O6-benzylguanine. In: *Cancer research* 53 (17), S. 3895–3898.

Ouararhni, Khalid; Hadj-Slimane, Reda; Ait-Si-Ali, Slimane; Robin, Philippe; Mietton, Flore; Harel-Bellan, Annick; Dimitrov, Stefan; Hamiche, Ali (2006): The histone variant mH2A1.1 interferes with transcription by down-regulating PARP-1 enzymatic activity. In: *Genes & development* 20 (23), S. 3324–3336. DOI: 10.1101/gad.396106.

Pacher, Pal; Szabo, Csaba (2007): Role of poly(ADP-ribose) polymerase 1 (PARP-1) in cardiovascular diseases: the therapeutic potential of PARP inhibitors. In: *Cardiovascular drug reviews* 25 (3), S. 235–260. DOI: 10.1111/j.1527-3466.2007.00018.x.

Pancer, Zeev; Cooper, Max D. (2006): The evolution of adaptive immunity. In: *Annual review of immunology* 24, S. 497–518. DOI: 10.1146/annurev.immunol.24.021605.090542.

Paradisi, Andrea; Maisse, Carine; Coissieux, Marie-May; Gadot, Nicolas; Lepinasse, Florian; Delloye-Bourgeois, Celine; Delcros, Jean-Guy; Svrcek, Magali; Neufert, Clemens; Flejou, Jean-Francois; Scoazec, Jean-Yves; Mehlen, Patrick (2009): Netrin-1 up-regulation in inflammatory bowel diseases is required for colorectal cancer progression. In: *Proceedings of the National Academy of Sciences of the United States of America* 106 (40), S. 17146–17151. DOI: 10.1073/pnas.0901767106.

Park, Jong Sung; Svetkauskaite, Daiva; He, Qianbin; Kim, Jae-Yeol; Strassheim, Derek; Ishizaka, Akitoshi; Abraham, Edward (2004): Involvement of toll-like receptors 2 and 4 in cellular activation by high mobility group box 1 protein. In: *The Journal of biological chemistry* 279 (9), S. 7370–7377. DOI: 10.1074/jbc.M306793200.

Patel, Anand G.; Lorenzo, Silvana B. de; Flatten, Karen S.; POIRIER, Guy G.; Kaufmann, Scott H. (2012): Failure of iniparib to inhibit poly(ADP-Ribose) polymerase in vitro. In: *Clinical cancer research : an official journal of the American Association for Cancer Research* 18 (6), S. 1655–1662. DOI: 10.1158/1078-0432.CCR-11-2890.

Patel, Anand G.; Sarkaria, Jann N.; Kaufmann, Scott H. (2011): Nonhomologous end joining drives poly(ADP-ribose) polymerase (PARP) inhibitor lethality in homologous recombination-deficient cells. In: *Proceedings of the National Academy of Sciences of the United States of America* 108 (8), S. 3406–3411. DOI: 10.1073/pnas.1013715108.

Peltomaki, Paivi (2003): Role of DNA mismatch repair defects in the pathogenesis of human cancer. In: *Journal of clinical oncology : official journal of the American Society of Clinical Oncology* 21 (6), S. 1174–1179.

Petesch, Steven J.; Lis, John T. (2008): Rapid, Transcription-Independent Loss of Nucleosomes over a Large Chromatin Domain at Hsp70 Loci. In: *Cell* 134 (1), S. 74–84. DOI: 10.1016/j.cell.2008.05.029.

Petrucco, Stefania; Percudani, Riccardo (2008): Structural recognition of DNA by poly(ADP-ribose)polymerase-like zinc finger families. In: *The FEBS journal* 275 (5), S. 883–893. DOI: 10.1111/j.1742-4658.2008.06259.x.

Pieper, A. A.; Brat, D. J.; Krug, D. K.; Watkins, C. C.; Gupta, A.; Blackshaw, S.; Verma, A.; Wang, Z. Q.; Snyder, S. H. (1999): Poly(ADP-ribose) polymerase-deficient mice are protected from streptozotocin-induced diabetes. In: *Proceedings of the National Academy of Sciences of the United States of America* 96 (6), S. 3059–3064.

Pignone, Michael; Rich, Melissa; Teutsch, Steven M.; Berg, Alfred O.; Lohr, Kathleen N. (2002): Screening for colorectal cancer in adults at average risk: a summary of the evidence for the U.S. Preventive Services Task Force. In: *Annals of internal medicine* 137 (2), S. 132–141.

Pines, Alex; Vrouwe, Mischa G.; Marteijn, Jurgen A.; Typas, Dimitris; Luijsterburg, Martijn S.; Cansoy, Medine; Hensbergen, Paul; Deelder, Andre; Groot, Anton de; Matsumoto, Syota; Sugasawa, Kaoru; Thoma, Nicolas; Vermeulen, Wim; Vrieling, Harry; Mullenders, Leon (2012): PARP1 promotes nucleotide excision repair through DDB2 stabilization and recruitment of ALC1. In: *The Journal of cell biology* 199 (2), S. 235–249. DOI: 10.1083/jcb.201112132.

Pion, Emmanuelle; Bombarda, Elisa; Stiegler, Patrick; Ullmann, G. Matthias; Mely, Yves; Murcia, Gilbert de; Gerard, Dominique (2003): Poly(ADP-ribose) polymerase-1 dimerizes at a 5' recessed DNA end in vitro: a fluorescence study. In: *Biochemistry* 42 (42), S. 12409–12417. DOI: 10.1021/bi0344432.

Pleschke, J. M.; Kleczkowska, H. E.; Strohm, M.; Althaus, F. R. (2000): Poly(ADP-ribose) binds to specific domains in DNA damage checkpoint proteins. In: *The Journal of biological chemistry* 275 (52), S. 40974–40980. DOI: 10.1074/jbc.M006520200.

Povey, A. C.; Hall, C. N.; Cooper, D. P.; O'Connor, P. J.; Margison, G. P. (2000): Determinants ofO6-alkylguanine-DNA alkyltransferase activity in normal and tumour tissue from human colon and rectum. In: *Int. J. Cancer* 85 (1), S. 68–72. DOI: 10.1002/(SICI)1097-0215(20000101)85:1<68::AID-IJC12>3.0.CO;2-0.

Preuss, I.; Eberhagen, I.; Haas, S.; Eibl, R. H.; Kaufmann, M.; Minckwitz, G. von; Kaina, B. (1995): O6-methylguanine-DNA methyltransferase activity in breast and brain tumors. In: *International journal of cancer* 61 (3), S. 321–326.

Racz, Boglarka; Hanto, Katalin; Tapodi, Antal; Solti, Izabella; Kalman, Nikoletta; Jakus, Peter; Kovacs, Krisztina; Debreceni, Balazs; Gallyas, Ferenc, JR; Sumegi, Balazs (2010): Regulation of MKP-1 expression and MAPK activation by PARP-1 in oxidative stress: a new mechanism for the cytoplasmic effect of PARP-1 activation. In: *Free radical biology & medicine* 49 (12), S. 1978–1988. DOI: 10.1016/j.freeradbiomed.2010.09.026.

Ray Chaudhuri, Arnab; Hashimoto, Yoshitami; Herrador, Raquel; Neelsen, Kai J.; Fachinetti, Daniele; Bermejo, Rodrigo; Cocito, Andrea; Costanzo, Vincenzo; Lopes, Massimo (2012): Topoisomerase I poisoning results in PARP-mediated replication fork reversal. In: *Nature structural & molecular biology* 19 (4), S. 417–423. DOI: 10.1038/nsmb.2258.

Reale, Anna; Matteis, Giovanna De; Galleazzi, Giada; Zampieri, Michele; Caiafa, Paola (2005): Modulation of DNMT1 activity by ADP-ribose polymers. In: *Oncogene* 24 (1), S. 13–19. DOI: 10.1038/sj.onc.1208005.

Reddy, B. S.; Weisburger, J. H.; Narisawa, T.; Wynder, E. L. (1974): Colon carcinogenesis in germ-free rats with 1,2-dimethylhydrazine and N-methyl-n'-nitro-N-nitrosoguanidine. In: *Cancer research* 34 (9), S. 2368–2372.

Reeder, R. H.; Ueda, K.; Honjo, T.; Nishizuka, Y.; Hayaishi, O. (1967): Studies on the polymer of adenosine diphosphate ribose. II. Characterization of the polymer. In: *The Journal of biological chemistry* 242 (13), S. 3172–3179.

Reinhardt, H. Christian; Schumacher, Bjorn (2012): The p53 network: cellular and systemic DNA damage responses in aging and cancer. In: *Trends in genetics : TIG* 28 (3), S. 128–136. DOI: 10.1016/j.tig.2011.12.002.

Renard, Patricia; Zachary, Marie-Denise; Bougelet, Catherine; Mirault, Marc-Edouard; Haegeman, Guy; Remacle, José; Raes, Martine (1997): Effects of antioxidant enzyme modulations on interleukin-1-induced nuclear factor kappa B Activation. In: *Biochemical Pharmacology* 53 (2), S. 149–160. DOI: 10.1016/S0006-2952(96)00645-4.

Robertis, Mariangela de; Massi, Emanuela; Poeta, Maria Luana; Carotti, Simone; Morini, Sergio; Cecchetelli, Loredana; Signori, Emanuela; Fazio, Vito Michele (2011): The AOM/DSS murine model for the study of colon carcinogenesis: From pathways to diagnosis and therapy studies. In: *Journal of carcinogenesis* 10, S. 9. DOI: 10.4103/1477-3163.78279.

Rogakou, E. P.; Nieves-Neira, W.; Boon, C.; Pommier, Y.; Bonner, W. M. (2000): Initiation of DNA fragmentation during apoptosis induces phosphorylation of H2AX histone at serine 139. In: *The Journal of biological chemistry* 275 (13), S. 9390–9395.

Romer, Lin; Klein, Christian; Dehner, Alexander; Kessler, Horst; Buchner, Johannes (2006): p53--a natural cancer killer: structural insights and therapeutic concepts. In: *Angewandte Chemie (International ed. in English)* 45 (39), S. 6440–6460. DOI: 10.1002/anie.200600611.

Roon, Alexander C. von; Reese, George; Teare, Julian; Constantinides, Vasilis; Darzi, Ara W.; Tekkis, Paris P. (2007): The risk of cancer in patients with Crohn's disease. In: *Diseases of the colon and rectum* 50 (6), S. 839–855. DOI: 10.1007/s10350-006-0848-z.

Roos, Wynand P.; Kaina, Bernd (2006): DNA damage-induced cell death by apoptosis. In: *Trends in molecular medicine* 12 (9), S. 440–450. DOI: 10.1016/j.molmed.2006.07.007.

Roos, Wynand P.; Kaina, Bernd (2013): DNA damage-induced cell death: from specific DNA lesions to the DNA damage response and apoptosis. In: *Cancer letters* 332 (2), S. 237–248. DOI: 10.1016/j.canlet.2012.01.007.

Rossi, Marie L.; Ghosh, Avik K.; Bohr, Vilhelm A. (2010): Roles of Werner syndrome protein in protection of genome integrity. In: *DNA repair* 9 (3), S. 331–344. DOI: 10.1016/j.dnarep.2009.12.011.

Rostom, Alaa; Dube, Catherine; Lewin, Gabriela; Tsertsvadze, Alexander; Barrowman, Nicholas; Code, Catherine; Sampson, Margaret; Moher, David (2007): Nonsteroidal anti-inflammatory drugs and cyclooxygenase-2 inhibitors for primary prevention of colorectal cancer: a systematic review

prepared for the U.S. Preventive Services Task Force. In: *Annals of internal medicine* 146 (5), S. 376–389.

Rovetto, M. J.; Lamberton, W. F.; Neely, J. R. (1975): Mechanisms of glycolytic inhibition in ischemic rat hearts. In: *Circulation research* 37 (6), S. 742–751.

Rovillain, E.; Mansfield, L.; Caetano, C.; Alvarez-Fernandez, M.; Caballero, O. L.; Medema, R. H.; Hummerich, H.; Jat, P. S. (2011): Activation of nuclear factor-kappa B signalling promotes cellular senescence. In: *Oncogene* 30 (20), S. 2356–2366. DOI: 10.1038/onc.2010.611.

Rowell, John P.; Simpson, Kathryn L.; Stott, Katherine; Watson, Matthew; Thomas, Jean O. (2012): HMGB1-facilitated p53 DNA binding occurs via HMG-Box/p53 transactivation domain interaction, regulated by the acidic tail. In: *Structure (London, England : 1993)* 20 (12), S. 2014–2024. DOI: 10.1016/j.str.2012.09.004.

Ruf, A.; Mennissier de Murcia, J.; Murcia, G. de; Schulz, G. E. (1996): Structure of the catalytic fragment of poly(AD-ribose) polymerase from chicken. In: *Proceedings of the National Academy of Sciences of the United States of America* 93 (15), S. 7481–7485.

Ruf, A.; Murcia, G. de; Schulz, G. E. (1998): Inhibitor and NAD+ binding to poly(ADP-ribose) polymerase as derived from crystal structures and homology modeling. In: *Biochemistry* 37 (11), S. 3893–3900. DOI: 10.1021/bi972383s.

Ruscetti, T.; Lehnert, B. E.; Halbrook, J.; Le Trong, H.; Hoekstra, M. F.; Chen, D. J.; Peterson, S. R. (1998): Stimulation of the DNA-dependent protein kinase by poly(ADP-ribose) polymerase. In: *The Journal of biological chemistry* 273 (23), S. 14461–14467.

Sakumi, K.; Shiraishi, A.; Shimizu, S.; Tsuzuki, T.; Ishikawa, T.; Sekiguchi, M. (1997): Methylnitrosourea-induced tumorigenesis in MGMT gene knockout mice. In: *Cancer research* 57 (12), S. 2415–2418.

Sameer, Aga Syed (2013): Colorectal cancer: molecular mutations and polymorphisms. In: *Frontiers in oncology* 3, S. 114. DOI: 10.3389/fonc.2013.00114.

Samper, Enrique; Goytisolo, Fermín A.; Murcia, Josiane Ménissier-de; González-Suárez, Eva; Cigudosa, Juan C.; Murcia, Gilbert de; Blasco, María A. (2001): Normal telomere length and chromosomal end capping in poly(ADP-ribose) polymerase–deficient mice and primary cells despite increased chromosomal instability. In: *J Cell Biol* 154 (1), S. 49–60. DOI: 10.1083/jcb.200103049.

Sanchez-Fidalgo, Susana; Villegas, Isabel; Martin, Antonio; Sanchez-Hidalgo, Marina; La Alarcon de Lastra, Catalina (2007): PARP inhibition reduces acute colonic inflammation in rats. In: *European journal of pharmacology* 563 (1-3), S. 216–223. DOI: 10.1016/j.ejphar.2007.01.070.

Saxena, Alka; Saffery, Richard; Wong, Lee H.; Kalitsis, Paul; Choo, K. H. Andy (2002a): Centromere proteins Cenpa, Cenpb, and Bub3 interact with poly(ADP-ribose) polymerase-1 protein and are poly(ADP-ribosyl)ated. In: *The Journal of biological chemistry* 277 (30), S. 26921–26926. DOI: 10.1074/jbc.M200620200.

Saxena, Alka; Wong, Lee H.; Kalitsis, Paul; Earle, Elizabeth; Shaffer, Lisa G.; Choo, K. H. Andy (2002b): Poly(ADP-ribose) polymerase 2 localizes to mammalian active centromeres and interacts with PARP-1, Cenpa, Cenpb and Bub3, but not Cenpc. In: *Human molecular genetics* 11 (19), S. 2319–2329.

Schipler, Agnes; Iliakis, George (2013): DNA double-strand-break complexity levels and their possible contributions to the probability for error-prone processing and repair pathway choice. In: *Nucleic acids research* 41 (16), S. 7589–7605. DOI: 10.1093/nar/gkt556.

Schoental, R. (1973): The mechanisms of action of the carcinogenic nitroso and related compounds. In: *British journal of cancer* 28 (5), S. 436–439.

Scholey, Jonathan M.; Brust-Mascher, Ingrid; Mogilner, Alex (2003): Cell division. In: *Nature* 422 (6933), S. 746–752. DOI: 10.1038/nature01599.

Schothorst, R. C.; Somers, H. H. J. (2005): Determination of N-nitrosodiethanolamine in cosmetic products by LC-MS-MS. In: *Analytical and bioanalytical chemistry* 381 (3), S. 681–685. DOI: 10.1007/s00216-004-2914-5.

Schultheisz, Heather L.; Szymczyna, Blair R.; Williamson, James R. (2009): Enzymatic Synthesis and Structural Characterization of 13 C, 15 N-Poly(ADP-ribose). In: *J. Am. Chem. Soc.* 131 (40), S. 14571–14578. DOI: 10.1021/ja903155s.

Senthong, Pattama; Millington, Christopher L.; Wilkinson, Oliver J.; Marriott, Andrew S.; Watson, Amanda J.; Reamtong, Onrapak; Eyers, Claire E.; Williams, David M.; Margison, Geoffrey P.; Povey, Andrew C. (2013): The nitrosated bile acid DNA lesion O6-carboxymethylguanine is a substrate for the human DNA repair protein O6-methylguanine-DNA methyltransferase. In: *Nucleic acids research* 41 (5), S. 3047–3055. DOI: 10.1093/nar/gks1476.

Seril, Darren N.; Liao, Jie; Yang, Guang-Yu (2007): Colorectal carcinoma development in inducible nitric oxide synthase-deficient mice with dextran sulfate sodium-induced ulcerative colitis. In: *Molecular carcinogenesis* 46 (5), S. 341–353. DOI: 10.1002/mc.20282.

Shank, R. C.; Magee, P. N. (1967): Similarities between the biochemical actions of cycasin and dimethylnitrosamine. In: *Biochem. J.* 105 (2), S. 521–527. DOI: 10.1042/bj1050521.

Sharp, C.; Warren, A.; Oshima, T.; Williams, L.; Li, J. H.; Alexander, J. S. (2001): Poly ADP ribose-polymerase inhibitors prevent the upregulation of ICAM-1 and E-selectin in response to Th1 cytokine stimulation. In: *Inflammation* 25 (3), S. 157–163.

Shieh, W. M.; Amé, J. C.; Wilson, M. V.; Wang, Z. Q.; Koh, D. W.; Jacobson, M. K.; Jacobson, E. L. (1998): Poly(ADP-ribose) polymerase null mouse cells synthesize ADP-ribose polymers. In: *The Journal of biological chemistry* 273 (46), S. 30069–30072.

Shiio, Yuzuru; Donohoe, Sam; Yi, Eugene C.; Goodlett, David R.; Aebersold, Ruedi; Eisenman, Robert N. (2002): Quantitative proteomic analysis of Myc oncoprotein function. In: *The EMBO journal* 21 (19), S. 5088–5096.

Shintani, N.; Nakajima, T.; Nakakubo, H.; Nagai, H.; Kagitani, Y.; Takizawa, H.; Asakura, H. (1997): Intravenous immunoglobulin (IVIG) treatment of experimental colitis induced by dextran sulfate sodium in rats. In: *Clinical and experimental immunology* 108 (2), S. 340–345.

Shiokawa, Motoko; Masutani, Mitsuko; Fujihara, Hisako; Ueki, Keisuke; Nishikawa, Ryo; Sugimura, Takashi; Kubo, Harumi; Nakagama, Hitoshi (2005): Genetic alteration of poly(ADP-ribose) polymerase-1 in human germ cell tumors. In: *Japanese journal of clinical oncology* 35 (2), S. 97–102. DOI: 10.1093/jjco/hyi028.

Shrivastav, Meena; Haro, Leyma P. de; Nickoloff, Jac A. (2008): Regulation of DNA double-strand break repair pathway choice. In: *Cell research* 18 (1), S. 134–147. DOI: 10.1038/cr.2007.111.

Shrivastav, Nidhi; Li, Deyu; Essigmann, John M. (2010): Chemical biology of mutagenesis and DNA repair: cellular responses to DNA alkylation. In: *Carcinogenesis* 31 (1), S. 59–70. DOI: 10.1093/carcin/bgp262.

Shuker, D. E.; Margison, G. P. (1997): Nitrosated glycine derivatives as a potential source of O6-methylguanine in DNA. In: *Cancer research* 57 (3), S. 366–369.

Simonin, F.; Poch, O.; Delarue, M.; Murcia, G. de (1993): Identification of potential active-site residues in the human poly(ADP-ribose) polymerase. In: *The Journal of biological chemistry* 268 (12), S. 8529–8535.

Sinicrope, Frank A.; Gill, Sharlene (2004): Role of cyclooxygenase-2 in colorectal cancer. In: *Cancer metastasis reviews* 23 (1-2), S. 63–75.

Slattery, Martha L.; Lundgreen, Abbie; Bondurant, Kristina L.; Wolff, Roger K. (2011): Interferon-signaling pathway: associations with colon and rectal cancer risk and subsequent survival. In: *Carcinogenesis* 32 (11), S. 1660–1667. DOI: 10.1093/carcin/bgr189.

Smith-Garvin, Jennifer E.; Koretzky, Gary A.; Jordan, Martha S. (2009): T cell activation. In: *Annual review of immunology* 27, S. 591–619. DOI: 10.1146/annurev.immunol.021908.132706.

Sobin, L. H.; Fleming, I. D. (1997): TNM Classification of Malignant Tumors, fifth edition (1997). Union Internationale Contre le Cancer and the American Joint Committee on Cancer. In: *Cancer* 80 (9), S. 1803–1804.

Sohn, O. S.; Fiala, E. S.; Requeijo, S. P.; Weisburger, J. H.; Gonzalez, F. J. (2001): Differential effects of CYP2E1 status on the metabolic activation of the colon carcinogens azoxymethane and methylazoxymethanol. In: *Cancer research* 61 (23), S. 8435–8440.

Sohn, Ock Soon; Ishizaki, Hiroyuki; Yang, Chung S.; Fiala, Emerich S. (1991): Metabolism of azoxymethane, methylazoxymethanol and N -nitrosodimethylamine by cytochrome P450IIE1. In: *Carcinogenesis* 12 (1), S. 127–131. DOI: 10.1093/carcin/12.1.127.

Soni, Aashish; Siemann, Maria; Grabos, Martha; Murmann, Tamara; Pantelias, Gabriel E.; Iliakis, George (2014): Requirement for Parp-1 and DNA ligases 1 or 3 but not of Xrcc1 in chromosomal translocation formation by backup end joining. In: *Nucleic acids research* 42 (10), S. 6380–6392. DOI: 10.1093/nar/gku298.

Southan, Garry J.; Szabo, Csaba (2003): Poly(ADP-ribose) polymerase inhibitors. In: *Current medicinal chemistry* 10 (4), S. 321–340.

Spagnolo, Laura; Barbeau, Jody; Curtin, Nicola J.; Morris, Edward P.; Pearl, Laurence H. (2012): Visualization of a DNA-PK/PARP1 complex. In: *Nucleic acids research* 40 (9), S. 4168–4177. DOI: 10.1093/nar/gkr1231.

Standring, Susan; Ananad, Neel (Hg.) (2016): Gray's anatomy. The anatomical basis of clinical practice ; [get full access and more at ExpertConsult.com]. 41. ed. Philadelphia, Pa.: Elsevier (Recommended shelving classification Anatomy).

Stanilov, N. S.; Dobreva, Z. G.; Stanilova, S. A. (2014): Higher TNF-Alpha Production Detected in Colorectal Cancer Patients Monocytes. In: *Biotechnology & Biotechnological Equipment* 26 (sup1), S. 107–110. DOI: 10.5504/50YRTIMB.2011.0020.

Stilmann, Michael; Hinz, Michael; Arslan, Seda Col; Zimmer, Anja; Schreiber, Valerie; Scheidereit, Claus (2009): A nuclear poly(ADP-ribose)-dependent signalosome confers DNA damage-induced IkappaB kinase activation. In: *Molecular cell* 36 (3), S. 365–378. DOI: 10.1016/j.molcel.2009.09.032.

Strom, Cecilia E.; Johansson, Fredrik; Uhlen, Mathias; Szigyarto, Cristina Al-Khalili; Erixon, Klaus; Helleday, Thomas (2011): Poly (ADP-ribose) polymerase (PARP) is not involved in base excision repair but PARP inhibition traps a single-strand intermediate. In: *Nucleic acids research* 39 (8), S. 3166–3175. DOI: 10.1093/nar/gkq1241.

Stvrtinová, V.; Jakubovsky, Jan; Hulin, Ivan (1995): Inflammation and fever. [Place of publication not identified]: Academic Electronic Press; Computing Centre, Slovak Academy of Sciences, Slovakia online.

Sugimura, T. (2000): Nutrition and dietary carcinogens. In: *Carcinogenesis* 21 (3), S. 387–395.

Sugimura, T.; Fujimura, S. (1967): Biosynthesis of ADP ribose polymer from NAD with nuclear enzymes. In: *Tanpakushitsu kakusan koso. Protein, nucleic acid, enzyme* 12 (12), S. 1059–1068.

Sulzyc-Bielicka, Violetta; Domagala, Pawel; Hybiak, Jolanta; Majewicz-Broda, Anna; Safranow, Krzysztof; Domagala, Wenecjanusz (2012): Colorectal cancers differ in respect of PARP-1 protein expression. In: *Polish journal of pathology : official journal of the Polish Society of Pathologists* 63 (2), S. 87–92.

Suzui, M.; Yoshimi, N.; Ushijima, T.; Hirose, Y.; Makita, H.; Wang, A.; Kawamori, T.; Tanaka, T.; Mori, H.; Nagao, M. (1995): No involvement of Ki-ras or p53 gene mutations in colitis-associated rat colon tumors induced by 1-hydroxyanthraquinone and methylazoxymethanol acetate. In: *Molecular carcinogenesis* 12 (4), S. 193–197.

Suzuki, Rikako; Kohno, Hiroyuki; Sugie, Shigeyuki; Nakagama, Hitoshi; Tanaka, Takuji (2006): Strain differences in the susceptibility to azoxymethane and dextran sodium sulfate-induced colon carcinogenesis in mice. In: *Carcinogenesis* 27 (1), S. 162–169. DOI: 10.1093/carcin/bgi205.

Suzuki, Rikako; Miyamoto, Shingo; Yasui, Yumiko; Sugie, Shigeyuki; Tanaka, Takuji (2007): Global gene expression analysis of the mouse colonic mucosa treated with azoxymethane and dextran sodium sulfate. In: *BMC cancer* 7, S. 84. DOI: 10.1186/1471-2407-7-84.

Svec, Jiri; Ergang, Peter; Mandys, Vaclav; Kment, Milan; Pacha, Jiri (2010): Expression profiles of proliferative and antiapoptotic genes in sporadic and colitis-related mouse colon cancer models. In: *International journal of experimental pathology* 91 (1), S. 44–53. DOI: 10.1111/j.1365-2613.2009.00698.x.

Szanto, Arpad; Hellebrand, Eva E.; Bognar, Zita; Tucsek, Zsuzsanna; Szabo, Aliz; Gallyas, Ferenc, JR; Sumegi, Balazs; Varbiro, Gabor (2009): PARP-1 inhibition-induced activation of PI-3-kinase-Akt pathway promotes resistance to taxol. In: *Biochemical Pharmacology* 77 (8), S. 1348–1357. DOI: 10.1016/j.bcp.2009.01.008.

Takahashi, M.; Mutoh, M.; Kawamori, T.; Sugimura, T.; Wakabayashi, K. (2000a): Altered expression of beta-catenin, inducible nitric oxide synthase and cyclooxygenase-2 in azoxymethane-induced rat colon carcinogenesis. In: *Carcinogenesis* 21 (7), S. 1319–1327.

Takahashi, M.; Nakatsugi, S.; Sugimura, T.; Wakabayashi, K. (2000b): Frequent mutations of the beta-catenin gene in mouse colon tumors induced by azoxymethane. In: *Carcinogenesis* 21 (6), S. 1117–1120.

Takahashi, Mami; Wakabayashi, Keiji (2004): Gene mutations and altered gene expression in azoxymethane-induced colon carcinogenesis in rodents. In: *Cancer science* 95 (6), S. 475–480.

Takesue, F.; Korenaga, D.; Yao, T.; Kabashima, A.; Sugimachi, K. (2001): Development of colonic neoplasms and expressions of p53 and p21 proteins in experimental colitis of mice induced by dextran sulfate sodium. In: *Journal of experimental & clinical cancer research : CR* 20 (3), S. 413–418.

Takizawa, Hideaki; Shintani, Nahoko; Natsui, Masaaki; Sasakawa, Tetsuya; Nakakubo, Hiroshi; Nakajima, Tsunetaka; Asakura, Hitoshi (2004): Activated Immunocompetent Cells in Rat Colitis Mucosa Induced by Dextran Sulfate Sodium and Not Complete but Partial Suppression of Colitis by FK506. In: *Digestion* 56 (3), S. 259–264. DOI: 10.1159/000201253.

Tanaka, Takuji; Kohno, Hiroyuki; Suzuki, Rikako; Yamada, Yasuhiro; Sugie, Shigeyuki; Mori, Hideki (2003): A novel inflammation-related mouse colon carcinogenesis model induced by azoxymethane and dextran sodium sulfate. In: *Cancer science* 94 (11), S. 965–973.

Tanaka, Takuji; Suzuki, Rikako; Kohno, Hiroyuki; Sugie, Shigeyuki; Takahashi, Mami; Wakabayashi, Keiji (2005): Colonic adenocarcinomas rapidly induced by the combined treatment with 2-amino-1-methyl-6-phenylimidazo4,5-bpyridine and dextran sodium sulfate in male ICR mice possess beta-catenin gene mutations and increases immunoreactivity for beta-catenin, cyclooxygenase-2 and inducible nitric oxide synthase. In: *Carcinogenesis* 26 (1), S. 229–238. DOI: 10.1093/carcin/bgh292.

Tang, Daolin; Kang, Rui; Zeh, Herbert J. 3rd; Lotze, Michael T. (2011): High-mobility group box 1, oxidative stress, and disease. In: *Antioxidants & redox signaling* 14 (7), S. 1315–1335. DOI: 10.1089/ars.2010.3356.

Tang, Daolin; Shi, Yongzhong; Kang, Rui; Li, Tong; Xiao, Weimin; Wang, Haichao; Xiao, Xianzhong (2007): Hydrogen peroxide stimulates macrophages and monocytes to actively release HMGB1. In: *Journal of leukocyte biology* 81 (3), S. 741–747. DOI: 10.1189/jlb.0806540.

Thorn, Mari; Finnstrom, Niklas; Lundgren, Stefan; Rane, Anders; Loof, Lars (2005): Cytochromes P450 and MDR1 mRNA expression along the human gastrointestinal tract. In: *British journal of clinical pharmacology* 60 (1), S. 54–60. DOI: 10.1111/j.1365-2125.2005.02389.x.

Thorslund, Tina; Kobbe, Cayetano von; Harrigan, Jeanine A.; Indig, Fred E.; Christiansen, Mette; Stevnsner, Tinna; Bohr, Vilhelm A. (2005): Cooperation of the Cockayne syndrome group B protein and poly(ADP-ribose) polymerase 1 in the response to oxidative stress. In: *Molecular and cellular biology* 25 (17), S. 7625–7636. DOI: 10.1128/MCB.25.17.7625-7636.2005.

Thurnherr, N.; Deschner, E. E.; Stonehill, E. H.; Lipkin, M. (1973): Induction of adenocarcinomas of the colon in mice by weekly injections of 1,2-dimethylhydrazine. In: *Cancer research* 33 (5), S. 940–945.

Tian, Jane; Avalos, Ana Maria; Mao, Su-Yau; Chen, Bo; Senthil, Kannaki; Wu, Herren; Parroche, Peggy; Drabic, Stacey; Golenbock, Douglas; Sirois, Cherilyn; Hua, Jing; An, Ling Ling; Audoly, Laurent; La Rosa, Greg; Bierhaus, Angelika; Naworth, Peter; Marshak-Rothstein, Ann; Crow, Mary K.; Fitzgerald, Katherine A.; Latz, Eicke; Kiener, Peter A.; Coyle, Anthony J. (2007): Toll-like receptor 9-dependent activation by DNA-containing immune complexes is mediated by HMGB1 and RAGE. In: *Nature immunology* 8 (5), S. 487–496. DOI: 10.1038/ni1457.

Tilstra, Jeremy S.; Clauson, Cheryl L.; Niedernhofer, Laura J.; Robbins, Paul D. (2011): NF-kappaB in Aging and Disease. In: *Aging and disease* 2 (6), S. 449–465.

Tong, W. M.; Cortes, U.; Wang, Z. Q. (2001): Poly(ADP-ribose) polymerase: a guardian angel protecting the genome and suppressing tumorigenesis. In: *Biochimica et biophysica acta* 1552 (1), S. 27–37.

Trewick, Sarah C.; Henshaw, Timothy F.; Hausinger, Robert P.; Lindahl, Tomas; Sedgwick, Barbara (2002): Oxidative demethylation by Escherichia coli AlkB directly reverts DNA base damage. In: *Nature* 419 (6903), S. 174–178. DOI: 10.1038/nature00908.

Trucco, C.; Oliver, F. J.; Murcia, G. de; Menissier-de Murcia, J. (1998): DNA repair defect in poly(ADP-ribose) polymerase-deficient cell lines. In: *Nucleic acids research* 26 (11), S. 2644–2649.

Tsujii, M.; DuBois, R. N. (1995): Alterations in cellular adhesion and apoptosis in epithelial cells overexpressing prostaglandin endoperoxide synthase 2. In: *Cell* 83 (3), S. 493–501.

Tulin, Alexei; Spradling, Allan (2003): Chromatin loosening by poly(ADP)-ribose polymerase (PARP) at Drosophila puff loci. In: *Science (New York, N.Y.)* 299 (5606), S. 560–562. DOI: 10.1126/science.1078764.

U.S. National Institutes of Health: clinicaltrials.gov. National Institutes of Health, 9000 Rockville Pike, Bethesda, Maryland 20892. Online verfügbar unter https://clinicaltrials.gov, zuletzt geprüft am 24.06.2016.

Ullrich, O.; Diestel, A.; Eyupoglu, I. Y.; Nitsch, R. (2001): Regulation of microglial expression of integrins by poly(ADP-ribose) polymerase-1. In: *Nature cell biology* 3 (12), S. 1035–1042. DOI: 10.1038/ncb1201-1035.

Umar, Asad; Boland, C. Richard; Terdiman, Jonathan P.; Syngal, Sapna; La Chapelle, Albert de; Ruschoff, Josef; Fishel, Richard; Lindor, Noralane M.; Burgart, Lawrence J.; Hamelin, Richard; Hamilton, Stanley R.; Hiatt, Robert A.; Jass, Jeremy; Lindblom, Annika; Lynch, Henry T.; Peltomaki, Paivi; Ramsey, Scott D.; Rodriguez-Bigas, Miguel A.; Vasen, Hans F. A.; Hawk, Ernest T.; Barrett, J. Carl; Freedman, Andrew N.; Srivastava, Sudhir (2004): Revised Bethesda Guidelines for hereditary nonpolyposis colorectal cancer (Lynch syndrome) and microsatellite instability. In: *Journal of the National Cancer Institute* 96 (4), S. 261–268.

Valencia, A.; Chardin, P.; Wittinghofer, A.; Sander, C. (1991): The ras protein family: evolutionary tree and role of conserved amino acids. In: *Biochemistry* 30 (19), S. 4637–4648.

Vilar, Eduardo; Bartnik, Catherine M.; Stenzel, Stephanie L.; Raskin, Leon; Ahn, Jaeil; Moreno, Victor; Mukherjee, Bhramar; Iniesta, Maria D.; Morgan, Meredith A.; Rennert, Gad; Gruber, Stephen B. (2011): MRE11 deficiency increases sensitivity to poly(ADP-ribose) polymerase inhibition in microsatellite unstable colorectal cancers. In: *Cancer research* 71 (7), S. 2632–2642. DOI: 10.1158/0008-5472.CAN-10-1120.

Vivona, A. A.; Shpitz, B.; Medline, A.; Bruce, W. R.; Hay, K.; Ward, M. A.; Stern, H. S.; Gallinger, S. (1993): K-ras mutations in aberrant crypt foci, adenomas and adenocarcinomas during azoxymethane-induced colon carcinogenesis. In: *Carcinogenesis* 14 (9), S. 1777–1781.

Vogel, S. de; Weijenberg, M. P.; Herman, J. G.; Wouters, K. A. D.; de Goeij, A F P M; van den Brandt, P A; Bruine, A. P. de; van Engeland, M. (2009): MGMT and MLH1 promoter methylation versus APC, KRAS and BRAF gene mutations in colorectal cancer: indications for distinct pathways and sequence of events. In: *Annals of oncology : official journal of the European Society for Medical Oncology* 20 (7), S. 1216–1222. DOI: 10.1093/annonc/mdn782.

Vogelstein, B.; Fearon, E. R.; Hamilton, S. R.; Kern, S. E.; Preisinger, A. C.; Leppert, M.; Nakamura, Y.; White, R.; Smits, A. M.; Bos, J. L. (1988): Genetic alterations during colorectal-tumor development. In: *The New England journal of medicine* 319 (9), S. 525–532. DOI: 10.1056/NEJM198809013190901.

Vogelstein, B.; Fearon, E. R.; Kern, S. E.; Hamilton, S. R.; Preisinger, A. C.; Nakamura, Y.; White, R. (1989): Allelotype of colorectal carcinomas. In: *Science (New York, N.Y.)* 244 (4901), S. 207–211.

Vogelstein, Bert; Kinzler, Kenneth W. (2002): The genetic basis of human cancer. 2nd ed. New York, London: McGraw-Hill Medical Publishing Division.

Wacker, David A.; Ruhl, Donald D.; Balagamwala, Ehsan H.; Hope, Kristine M.; Zhang, Tong; Kraus, W. Lee (2007): The DNA binding and catalytic domains of poly(ADP-ribose) polymerase 1 cooperate in the regulation of chromatin structure and transcription. In: *Molecular and cellular biology* 27 (21), S. 7475–7485. DOI: 10.1128/MCB.01314-07.

Wali, R. K. (1999): Inhibition of O6-methylguanine-DNA methyltransferase increases azoxymethane-induced colonic tumors in rats. In: *Carcinogenesis* 20 (12), S. 2355–2360. DOI: 10.1093/carcin/20.12.2355.

Wang, Chunfang; Jurk, Diana; Maddick, Mandy; Nelson, Glyn; Martin-Ruiz, Carmen; Zglinicki, Thomas von (2009a): DNA damage response and cellular senescence in tissues of aging mice. In: *Aging cell* 8 (3), S. 311–323. DOI: 10.1111/j.1474-9726.2009.00481.x.

Wang, D.; DuBois, R. N. (2010): The role of COX-2 in intestinal inflammation and colorectal cancer. In: *Oncogene* 29 (6), S. 781–788. DOI: 10.1038/onc.2009.421.

Wang, Dingzhi; Mann, Jason R.; DuBois, Raymond N. (2005): The role of prostaglandins and other eicosanoids in the gastrointestinal tract. In: *Gastroenterology* 128 (5), S. 1445–1461.

Wang, Jingxin; Jacob, Naduparambil K.; Ladner, Katherine J.; Beg, Amer; Perko, James D.; Tanner, Stephan M.; Liyanarachchi, Sandya; Fishel, Richard; Guttridge, Denis C. (2009b): RelA/p65 functions to maintain cellular senescence by regulating genomic stability and DNA repair. In: *EMBO reports* 10 (11), S. 1272–1278. DOI: 10.1038/embor.2009.197.

Wang, Minli; Wu, Weizhong; Wu, Wenqi; Rosidi, Bustanur; Zhang, Lihua; Wang, Huichen; Iliakis, George (2006): PARP-1 and Ku compete for repair of DNA double strand breaks by distinct NHEJ pathways. In: *Nucleic acids research* 34 (21), S. 6170–6182. DOI: 10.1093/nar/gkl840.

Wang, Q. S.; Papanikolaou, A.; Sabourin, C. L.; Rosenberg, D. W. (1998): Altered expression of cyclin D1 and cyclin-dependent kinase 4 in azoxymethane-induced mouse colon tumorigenesis. In: *Carcinogenesis* 19 (11), S. 2001–2006.

Wang, Xiao-Gan; Wang, Zhao-Qi; Tong, Wei-Min; Shen, Yan (2007): PARP1 Val762Ala polymorphism reduces enzymatic activity. In: *Biochemical and Biophysical Research Communications* 354 (1), S. 122–126. DOI: 10.1016/j.bbrc.2006.12.162.

Wang, Zhizhi; Michaud, Gregory A.; Cheng, Zhihong; Zhang, Yue; Hinds, Thomas R.; Fan, Erkang; Cong, Feng; Xu, Wenqing (2012): Recognition of the iso-ADP-ribose moiety in poly(ADP-ribose) by WWE domains suggests a general mechanism for poly(ADP-ribosyl)ation-dependent ubiquitination. In: *Genes & development* 26 (3), S. 235–240. DOI: 10.1101/gad.182618.111.

Watson, Alastair J. M.; Collins, Paul D. (2011): Colon cancer: a civilization disorder. In: *Digestive diseases (Basel, Switzerland)* 29 (2), S. 222–228. DOI: 10.1159/000323926.

Weaver, Alice N.; Yang, Eddy S. (2013): Beyond DNA Repair: Additional Functions of PARP-1 in Cancer. In: *Frontiers in oncology* 3, S. 290. DOI: 10.3389/fonc.2013.00290.

Wesierska-Gadek, J.; Bugajska-Schretter, A.; Cerni, C. (1996a): ADP-ribosylation of p53 tumor suppressor protein: mutant but not wild-type p53 is modified. In: *Journal of cellular biochemistry* 62 (1), S. 90–101. DOI: 10.1002/(SICI)1097-4644(199607)62:1<90::AID-JCB10>3.0.CO;2-J.

Wesierska-Gadek, J.; Schmid, G.; Cerni, C. (1996b): ADP-ribosylation of wild-type p53 in vitro: binding of p53 protein to specific p53 consensus sequence prevents its modification. In: *Biochemical and Biophysical Research Communications* 224 (1), S. 96–102. DOI: 10.1006/bbrc.1996.0990.

Wesierska-Gadek, Jozefa; Wojciechowski, Jacek; Schmid, Gerald (2003a): Central and carboxy-terminal regions of human p53 protein are essential for interaction and complex formation with PARP-1. In: *Journal of cellular biochemistry* 89 (2), S. 220–232. DOI: 10.1002/jcb.10521.

Wesierska-Gadek, Jozefa; Wojciechowski, Jacek; Schmid, Gerald (2003b): Phosphorylation regulates the interaction and complex formation between wt p53 protein and PARP-1. In: *Journal of cellular biochemistry* 89 (6), S. 1260–1284. DOI: 10.1002/jcb.10569.

Weston, Victoria J.; Oldreive, Ceri E.; Skowronska, Anna; Oscier, David G.; Pratt, Guy; Dyer, Martin J. S.; Smith, Graeme; Powell, Judy E.; Rudzki, Zbigniew; Kearns, Pamela; Moss, Paul A. H.; Taylor, A. Malcolm R.; Stankovic, Tatjana (2010): The PARP inhibitor olaparib induces significant killing of ATM-deficient lymphoid tumor cells in vitro and in vivo. In: *Blood* 116 (22), S. 4578–4587. DOI: 10.1182/blood-2010-01-265769.

Wirtz, Stefan; Nagel, Georg; Eshkind, Leonid; Neurath, Markus F.; Samson, Leona D.; Kaina, Bernd (2010): Both base excision repair and O6-methylguanine-DNA methyltransferase protect against methylation-induced colon carcinogenesis. In: *Carcinogenesis* 31 (12), S. 2111–2117. DOI: 10.1093/carcin/bgq174.

Xu, J.; Jiang, Y.; Wang, J.; Shi, X.; Liu, Q.; Liu, Z.; Li, Y.; Scott, M. J.; Xiao, G.; Li, S.; Fan, L.; Billiar, T. R.; Wilson, M. A.; Fan, J. (2014): Macrophage endocytosis of high-mobility group box 1 triggers pyroptosis. In: *Cell death and differentiation* 21 (8), S. 1229–1239. DOI: 10.1038/cdd.2014.40.

Yang, C. S.; Yoo, J. S.; Ishizaki, H.; Hong, J. Y. (1990): Cytochrome P450IIE1: roles in nitrosamine metabolism and mechanisms of regulation. In: *Drug metabolism reviews* 22 (2-3), S. 147–159. DOI: 10.3109/03602539009041082.

Yang, Yang; Ikezoe, Takeyuki; Saito, Tsuyako; Kobayashi, Makoto; Koeffler, H. Phillip; Taguchi, Hirokuni (2004): Proteasome inhibitor PS-341 induces growth arrest and apoptosis of non-small cell lung cancer cells via the JNK/c-Jun/AP-1 signaling. In: *Cancer science* 95 (2), S. 176–180. DOI: 10.1111/j.1349-7006.2004.tb03200.x.

Yekkala, Krishna; Baudino, Troy A. (2007): Inhibition of intestinal polyposis with reduced angiogenesis in ApcMin/+ mice due to decreases in c-Myc expression. In: *Molecular cancer research : MCR* 5 (12), S. 1296–1303. DOI: 10.1158/1541-7786.MCR-07-0232.

Yelamos, Jose; Schreiber, Valerie; Dantzer, Francoise (2008): Toward specific functions of poly(ADP-ribose) polymerase-2. In: *Trends in molecular medicine* 14 (4), S. 169–178. DOI: 10.1016/j.molmed.2008.02.003.

Yoshioka, Ken-ichi; Yoshioka, Yoshiko; Hsieh, Peggy (2006): ATR kinase activation mediated by MutSalpha and MutLalpha in response to cytotoxic O6-methylguanine adducts. In: *Molecular cell* 22 (4), S. 501–510. DOI: 10.1016/j.molcel.2006.04.023.

Young, Lisa E.; Sanduja, Sandhya; Bemis-Standoli, Kristi; Pena, Edsel A.; Price, Robert L.; Dixon, Dan A. (2009): The mRNA binding proteins HuR and tristetraprolin regulate cyclooxygenase 2 expression during colon carcinogenesis. In: *Gastroenterology* 136 (5), S. 1669–1679. DOI: 10.1053/j.gastro.2009.01.010.

Yu, Hongping; Ma, Hongxia; Yin, Ming; Wei, Qingyi (2012): Association between PARP-1 V762A polymorphism and cancer susceptibility: a meta-analysis. In: *Genetic epidemiology* 36 (1), S. 56–65. DOI: 10.1002/gepi.20663.

Yu, Seong-Woon; Wang, Hongmin; Poitras, Marc F.; Coombs, Carmen; Bowers, William J.; Federoff, Howard J.; POIRIER, Guy G.; Dawson, Ted M.; Dawson, Valina L. (2002): Mediation of poly(ADP-ribose) polymerase-1-dependent cell death by apoptosis-inducing factor. In: *Science (New York, N.Y.)* 297 (5579), S. 259–263. DOI: 10.1126/science.1072221.

Zaidi, Nasir H.; Pretlow, Theresa P.; O'Riordan, Mary Ann; Dumenco, Luba L.; Allay, Esther; Gerson, Stanton L. (1995): Transgenic expression of human MGMT protects against azoxymethane-induced aberrant crypt foci and G to A mutations in the K- ras oncogene of mouse colon. In: *Carcinogenesis* 16 (3), S. 451–456. DOI: 10.1093/carcin/16.3.451.

Zampieri, Michele; Passananti, Claudio; Calabrese, Roberta; Perilli, Mariagrazia; Corbi, Nicoletta; Cave, Fabiana de; Guastafierro, Tiziana; Bacalini, Maria Giulia; Reale, Anna; Amicosante, Gianfranco; Calabrese, Lilia; Zlatanova, Jordanka; Caiafa, Paola (2009): Parp1 localizes within the Dnmt1 promoter and protects its unmethylated state by its enzymatic activity. In: *PloS one* 4 (3), e4717. DOI: 10.1371/journal.pone.0004717.

Zardo, G.; Marenzi, S.; Perilli, M.; Caiafa, P. (1999): Inhibition of poly(ADP-ribosyl)ation introduces an anomalous methylation pattern in transfected foreign DNA. In: *FASEB journal : official publication of the Federation of American Societies for Experimental Biology* 13 (12), S. 1518–1522.

Zaremba, T.; Ketzer, P.; Cole, M.; Coulthard, S.; Plummer, E. R.; Curtin, N. J. (2009): Poly(ADP-ribose) polymerase-1 polymorphisms, expression and activity in selected human tumour cell lines. In: *British journal of cancer* 101 (2), S. 256–262. DOI: 10.1038/sj.bjc.6605166.

Zhang, Qiuhong; Kang, Rui; Zeh, Herbert J. 3rd; Lotze, Michael T.; Tang, Daolin (2013): DAMPs and autophagy: cellular adaptation to injury and unscheduled cell death. In: *Autophagy* 9 (4), S. 451–458. DOI: 10.4161/auto.23691.

Zhang, Yue; Liu, Shanming; Mickanin, Craig; Feng, Yan; Charlat, Olga; Michaud, Gregory A.; Schirle, Markus; Shi, Xiaoying; Hild, Marc; Bauer, Andreas; Myer, Vic E.; Finan, Peter M.; Porter, Jeffery A.; Huang, Shih-Min A.; Cong, Feng (2011): RNF146 is a poly(ADP-ribose)-directed E3 ligase that regulates axin degradation and Wnt signalling. In: *Nature cell biology* 13 (5), S. 623–629. DOI: 10.1038/ncb2222.

Zheng, Y. W.; Bey, M.; Liu, H.; Felder, M. R. (1993): Molecular basis of the alcohol dehydrogenase-negative deer mouse. Evidence for deletion of the gene for class I enzyme and identification of a possible new enzyme class. In: *The Journal of biological chemistry* 268 (33), S. 24933–24939.

Zingarelli, B.; Salzman, A. L.; Szabo, C. (1998): Genetic disruption of poly (ADP-ribose) synthetase inhibits the expression of P-selectin and intercellular adhesion molecule-1 in myocardial ischemia/reperfusion injury. In: *Circulation research* 83 (1), S. 85–94.

Zingarelli, Basilia; O'Connor, Michael; Hake, Paul W. (2003): Inhibitors of poly (ADP-ribose) polymerase modulate signal transduction pathways in colitis. In: *European journal of pharmacology* 469 (1-3), S. 183–194. DOI: 10.1016/S0014-2999(03)01726-6.

Zobeck, Katie L.; Buckley, Martin S.; Zipfel, Warren R.; Lis, John T. (2010): Recruitment timing and dynamics of transcription factors at the Hsp70 loci in living cells. In: *Molecular cell* 40 (6), S. 965–975. DOI: 10.1016/j.molcel.2010.11.022.

Zong, Wei-Xing; Ditsworth, Dara; Bauer, Daniel E.; Wang, Zhao-Qi; Thompson, Craig B. (2004): Alkylating DNA damage stimulates a regulated form of necrotic cell death. In: *Genes & development* 18 (11), S. 1272–1282. DOI: 10.1101/gad.1199904.

# 7 APPENDIX

## 7.1 ABBREVIATIONS

AA ..... Amino acid
AAG ..... 3-alkyladenine DNA glycosylase
ACF ..... Aberrant crypt foci
ADH ..... Alcohol dehydrogenase
Ado ..... Adenosine
AIF ..... Apoptosis inducing factor
ALKBH ..... AlkB homologue
AOM ..... Azoxymethane
AP site ..... Apurinic/apurimidinic site
APC ..... Adenomatous polyposis coli
ARH3 ..... ADP ribosylhydrolase 3
ART ..... ADP-ribosyl transferase
ATM ..... Ataxia telangiectasia mutated
*BAX* ..... *BCL-2-associated X*
BER ..... Base excision repair
B-NHEJ ... Backup non-homologous end-joining
BSA ..... Bovine serum albumin fraction V
bw ..... Body weight
CBP ..... CREB-binding protein
CD ..... Catalytic domain
CD11b ..... Cluster differentiation molecule 11b
CD3 ..... Cluster of differentiation 3
*Cdk4* ..... Cyclin-dependent kinase 4
c-Myc ..... Myelocytomatosis oncogene
COX-2 ..... Cyclooxygenase-2
CpG ..... 5'-C-phosphate-G-3'
CRC ..... Colorectal cancer
CSB ..... Cockayne syndrome group B
CT ..... Computed tomography
CXCL2 ..... Chemokine (C-X-C motif) ligand 2
CXCR2 ..... C-X-C motif chemokine receptor 2
CYP2E1 ..... Cytochrome P450 2E1
DBD ..... DNA binding domain
DDB2 ..... DNA binding protein 2
dd$H_2O$ ..... Double-distilled water
DDR ..... DNA damage response
DKO ..... Double knock out
DMH ..... 1,2-dimethylhydrazine
DMSO ..... Dimethyl sulfoxide
DNA ..... Deoxyribonucleic acid
DNA-PKcs ..... DNA dependent protein kinase catalytic subunit
DNase ..... Deoxyribonuclease
DNAse ..... Deoxyribonuclease
DNMT ..... DNA methyltransferase
DSB ..... DNA double strand break
dsDNA ..... Double-stranded DNA
DSS ..... Dextran sodium sulfate
DTT ..... Dithiothreitol
EDTA ..... Ethylenediaminetetraacetic acid
EpCAM ..... Epithelial cell adhesion molecule
ERK ..... Extracellular-signal regulated kinases
EtOH ..... Ethanol
FAP ..... Familial adenomatous polyposis
GIT ..... Gastrointestinal tract
GSK-3β ..... Glycogen synthase kinase-3β
HCA ..... Heterocyclic aromatic amine
HD ..... Helical subdomain
HE stain ..... Haematoxylin and eosin stain
HMGB1 ..... High mobility group box 1
HNPCC ..... Hereditary non-polposis colorectal cancer
HRP ..... Horseradish peroxidase
HRR ..... Homologous recombination repair
*i.p.* ..... Intraperitoneal
IFNγ ..... Interferon gamma, Interferon-γ
IHC ..... Immunohistochemistry
IKK ..... IκB kinase
IL-1 ..... Interleukin-1
IL-1b ..... Interleukin-1 beta
IL-6 ..... Interleukin-6
IκB ..... Inhibitor of κB

JNK .....c-Jun N-terminal kinase
k.o. .....Knock out
LC-MS/MS ..... HPLC-coupled tandem mass spectrometry
LPO..... Lipid peroxidation
MAM .....Methylazoxymethanol
MAPK..... Mitogen-activated protein kinase
MEF ..... Mouse embryonic fibroblast
MEICS ..... Murine endoscopic index of colitis severity
MGMT.....$O^6$-methylguanin-DNA methyltransferase
MHC.....Major histocompatibility complex
MMR ..... DNA mismatch repair
MMS ..... Methylmethanesulfonate
MNU.....Methylnitrosurea
MPG.....*N*-methylpurine DNA glycosylase
*N*1-MeA..... *N*1-methyladenine
*N*3-MeA..... *N*3-methyladenine
*N*3-MeC .....*N*3-methylcytosine
*N*7-MeG ..... *N*7-methylguanine
$NAD^+$ ..... Nicotinamide adenine dinucleotide
NER ..... Nucleotide excision repair
NF-κB.....Nuclear factor 'kappa-light-chain-enhancer' of activated B-cells
NHEJ ..... Non-homologous end-joining
NMN..... Nicotinamide mononucleotide
NMNAT .....NMN adenyltransferase
NMR.....Nuclear magnetic resonance
NOC..... *N*-nitroso compound
NOS ..... Nitric oxide synthase
$O^6$-BG .....$O^6$-benzylguanine
$O^6$-CMG .....$O^6$-carboxymethylguanine
$O^6$-MeG.....$O^6$-methylguanine
PAH .....Polycyclic aromatic hydrocarbon
PAMP..Pathogen-associated molecular pattern
PAR .....Poly(ADP)ribose
PARG.....Poly(ADPribose) glycohydrolase
PARP .....Poly(ADP-ribose) polymerase
PARP-1.....Poly(ADP-ribose) polymerase-1
PARylation..... Poly(ADP-ribosly)ation
PBM ..... PAR binding motif
PBS..... Phosphate buffered saline
PBZ ..... PAR-binding zinc finger
PCNA .....Proliferating cell nuclear antigen
PCR.....Polymerase chain reaction
PEG 400 ..... Polyethylene glycol 400
PIPropidium iodide
PIKK Phosphatidyl inositol 3 like protein kinase
PMSF ..... Phenylmethylsulfonyl fluoride
PRR.....Pattern recognition receptor
$R_2$-Ado.....Diribosyladenosine
R-Ado .....Ribosyladenosine
RAGE....Receptors for advanced glycation end products
RNA.....Ribonucleic acid
RNAse A .....Ribonuclease A
RONS... Reactive oxygen and nitrogen species
ROS ..... Reactive oxygen species
RPA.....Replication protein A
RT .....Room temperature
SASP.....Senescence-associated secretory phenotype
SDS.....Sodium dodecyl sulfate
SDS-PAGE .....SDS-polyacrylamide gel electrophoresis
SNP.....Single-nucleotide polymorphism
SSB.....DNA single strand break
ssRNA..... Singe stranded RNA
TCF ..... T-cell factor
TEMED .....Tetramethylethylenediamine
*TGFBR2 Transforming growth factor β receptor II*
TGF-β.....Transforming grwoth factor-β
TLR .....Toll-like receptor
TMZ.....Temozolomide
TNB..... Trinitrobenzene sulfonic acid
TNF ..... Tumour necrosis factor
TNFα..... Tumor necrosis factor alpha
TNKS..... Tankyrase
UICC .... Union for International Cancer Control
WRN.....Werner syndrome RecQ like helicase

WT .....Wild type

XPA..... Xeroderma pigmentosus

γH2AX..... Phosphorylated histone H2AX

## 7.2 FIGURES

## 7.3 TABLES

[redacted]

[redacted]

[redacted]

| | |
|---|---|
| [redacted] | [redacted] |
| [redacted] | [redacted] |
| [redacted] | [redacted] |
| [redacted] | [redacted] |

[redacted]

---

| | |
|---|---|
| [redacted] | [redacted] |
| [redacted] | [redacted] |

- [redacted]
- [redacted]
- [redacted]

| | |
|---|---|
| [redacted] | [redacted] |

- [redacted]

[redacted]

[redacted]

- [redacted]

[redacted]

[redacted]

[redacted]

[redacted]

[redacted]